UW-Madison.
SSEC Publication No.99.09.R1a.

University of Wisconsin

FY99 Final Report

Engineering and Scientific Support for the National Polar-orbiting Operational Environmental Satellite System Airborne Sounder Testbed - Interferometer (NAST-I) Instrument

30 September 1999

Contract Information:

This is the final report for the University of Wisconsin proposal entitled, "Engineering and Scientific Support for the National Polar-orbiting Operational Environmental Satellite System Airborne Sounder Testbed - Interferometer (NAST-I) Instrument". This proposal was in response to NASA Langley Research Center Procurement Request Number GLD.2056 under Contract Number NAS1-99123. Principal Investigator on this University of Wisconsin proposal is Dr. Henry E. Revercomb, Senior Scientist, Space Science and Engineering Center, UW-Madison.

Project Description:

The proposed tasks and deliverables identified by the contract are outlined below as modified by the exceptions called out in the UW proposal.

Task 1: Analysis of NAST-I data along with SHIS & AERI data from the CAMEX-3 mission during August/September 1998 and analysis of NAST-I data along with either SHIS or HIS data from the WINTEX mission.

Deliverable: Contractor shall provide a report documenting the operational functionality of the NAST-I Instrument and a comparison of the spectra achieved from NAST-I, AERI, and SHIS (from selected flights mutually agreed upon by UW and LaRC) during the CAMEX-3 field experiment. Contractor shall also provide a comparison of the spectra achieved from NAST-I and either SHIS or HIS during at least five flights of the WINTEX field experiment in March 1999. Contractor shall furnish copies of at least two papers of the CAMEX or WINTEX data and analysis submitted to referenceable publications in trade journals or conference proceedings.

Task 2: Improvements to the NAST-I instrument

Deliverable: Contractor shall provide not more than 5 reports detailing their solutions to the problems identified above as requested by NASA LaRC through the period of instrument improvements at NASA LaRc.

Task 3: Weather Products Test Bed

Deliverable: Contractor shall provide meteorological sounding data products from selected data sets mutually agreed upon by UW and LaRC. Contractor shall also provide retrieval algorithms to process meteorological data.

Task 4: Algorithm Development

Deliverable: Contractor shall provide monthly technical status reports and a final report at the completion of this task. Contractor shall also provide the electronic code for the algorithms developed along with programmer and user documentation.

Deliverables by Task:

Task 1

Report documenting the operational functionality of NAST-I during CAMEX-3

1.NASTI Detector Nonlinearity Summary
URL: http://danspc.larc.nasa.gov/NAST/Talks/990225_Tobin/index.html
2.NASTI Validation: Comparison with HIS from Wallops 98
URL: http://danspc.larc.nasa.gov/NAST/val_his.html
3.NASTI Validation: Comparison with AERI from Wallops 98 :
URL: http://danspc.larc.nasa.gov/NAST/val_aeri.html
4.Data Processing Summary
URL: http://tyler.ssec.wisc.edu/~bobk/camex3/proc_status.html
5.Radiance Product Quicklooks
URL: http://cimss.ssec.wisc.edu/nast/camex3/camex3_index.html

Comparison of spectra from NAST-I, AERI, & SHIS over Andros Island during CAMEX-3.

1.Comparison of SHIS and NAST-I data during CAMEX-3
URL: http://arm1.ssec.wisc.edu/~shis/Results/980913_NASTcomp/nast_comparison.html
2.NASTI comparison with calculations from CAMEX3
URL: http://danspc.larc.nasa.gov/NAST/val_calcs2.html
3.Comparison of Scanning HIS data with an LBLRTM calculation from CAMEX-3
URL: http://arm1.ssec.wisc.edu/~shis/Results/980913_LBLRTMcomp/shiscalc.html
4.Validation data from Andros Island (AERI, Sondes, GPS, ...)
URL: http://cimss.ssec.wisc.edu/camex3/camexiii.html

Comparison of spectra from NAST-I and SHIS during WINTEX

1.S-HIS/NAST-I Comparison from WINTEX
URL: http://arm1.ssec.wisc.edu/~shis/wintex/results/shisnastcomp.html
2.NASTI comparison with calculations from WINTEX:
- Case Description (URL: http://danspc.larc.nasa.gov/NAST/wintexa/wintexa.html)
- Comparison Summary (postscript file Wintex_NASTI_Obscalc.ps)

Papers submitted to trade journals or conferences concerning NAST-I performance.
(click here to see the list of papers)

Task 2

Specific recommendations made to LaRC for the operation of NAST-I (click here to view the recommendations)

Task 3

Meteorological sounding products from selected datasets as directed by the LaRC NAST-I Principal Investigator
URL: http://its.ssec.wisc.edu/nast/retrieval/products/

NAST-I radiance and validation datasets provided to LaRC to assist the Integrated Program Office (IPO) in their downselect for the CrIS contractor.
URL: http://danspc.larc.nasa.gov/NAST/).

Task 4

Retrieval algorithm development summary
URL: http://its.ssec.wisc.edu/nast/retrieval/description/

Retrieval algorithm delivery schedule
URL: http://its.ssec.wisc.edu/nast/retrieval/delivery/
NOTE -- delivery made to NASA-LaRC as per P.I. request, future / ongoing work declared. No general public release of retrieval code allowed, only delivery to NASA-LaRC permitted.

Accurate 3-D representation of NAST-I derived atmospheric parameters
URL: http://its.ssec.wisc.edu/nast/retrieval/3-D/

Summary

This web page represents the final report of the FY99 activities of the University of Wisconsin under contract to NASA Langley Research Center in support of the NAST-I instrument and data analysis. All required tasks were completed through the period of performance ending September 30, 1999.

Points of Contact:

Principal Investigator: hank.revercomb@ssec.wisc.edu

Program Manager: fred.best@ssec.wisc.edu

Final Report: robert.knuteson@ssec.wisc.edu

Last Updated: 9 November 1999

University of Wisconsin

FY99 Final Report

Engineering and Scientific Support for the National Polar-orbiting Operational Environmental Satellite System Airborne Sounder Testbed - Interferometer (NAST-I) Instrument

30 September 1999

Deliverables by Task:

Task 1

Report documenting the operational functionality of NAST-I during CAMEX-3

1.NASTI Detector Nonlinearity Summary
URL: http://danspc.larc.nasa.gov/NAST/Talks/990225_Tobin/index.html

NAST-I Detector Non-linearity

D. Tobin, H. Revercomb, R. Knuteson, V. Walden, H. Howell, D. Deslover, and C. Sisko
Space Science and Engineering Center, University of Wisconsin-Madison

W. Smith
LaRC, NASA

Outline:

- Introduction
- Characterization and correction:
  - Out-of-band response
  - Ground-based, downwelling spectra
  - In-flight, upwelling spectra
  - Reference calibration blackbodies
- Summary
- *Validation*

Introduction

- HgCdTe detector theory predicts
  $Q = c_1\Delta n + c_2(\Delta n)^2 + c_3(\Delta n)^3$
  where Q is the incident photon flux density and Δn is the photo-generated conduction band electron concentration. (Marion B. Reine, 1979)
- The measured signal, I_m, is proportional to Δn, and the corrected linear signal, I_c, is proportional to Q:
  $I_c = I_m + a_2(I_m)^2 + a_3(I_m)^3$
- Separating I_m into an AC interferogram, $f(x)$, and a DC offset, V, gives:
  $I_c = (f + V) + a_2(f + V)^2 + a_3(f + V)^3$

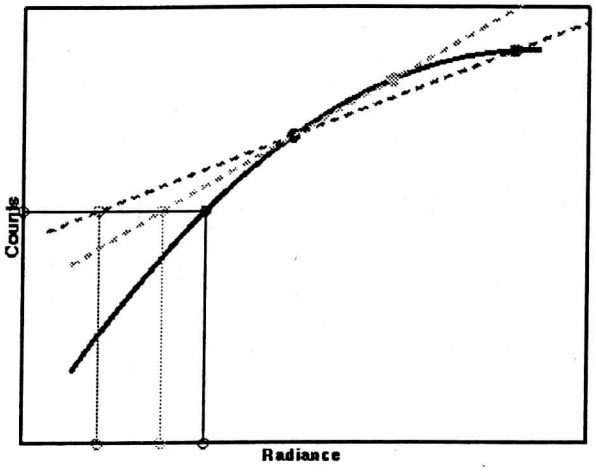

a_2 determined from

- Out of Band: $\widetilde{I_c} = 0 \rightarrow |a_n| = \widetilde{I_m}/\widetilde{I_m^n}$
- uplooking clear sky comparisons with AERI
- in-flight clear sky comparisons with HIS
- comparisons with external blackbodies

$$\rightarrow \widetilde{I_c} = (1 + 2a_2V + 3a_3V^2)\widetilde{f} + (a_2 + 3a_3V)\widetilde{f^2} + a_3\widetilde{f^3}$$

$$\rightarrow V = \frac{V_s}{e} + \frac{V_n}{e}\frac{k + 2r_{dw}}{\frac{B_n}{B_i}(t_{fw} + r_{fw} - r_{dw})}$$

Out-of-Band characterization

$$\mathcal{F}\{f(x)^2\} = \mathcal{F}\{f(x)\} \otimes \mathcal{F}\{f(x)\}$$

980729 data

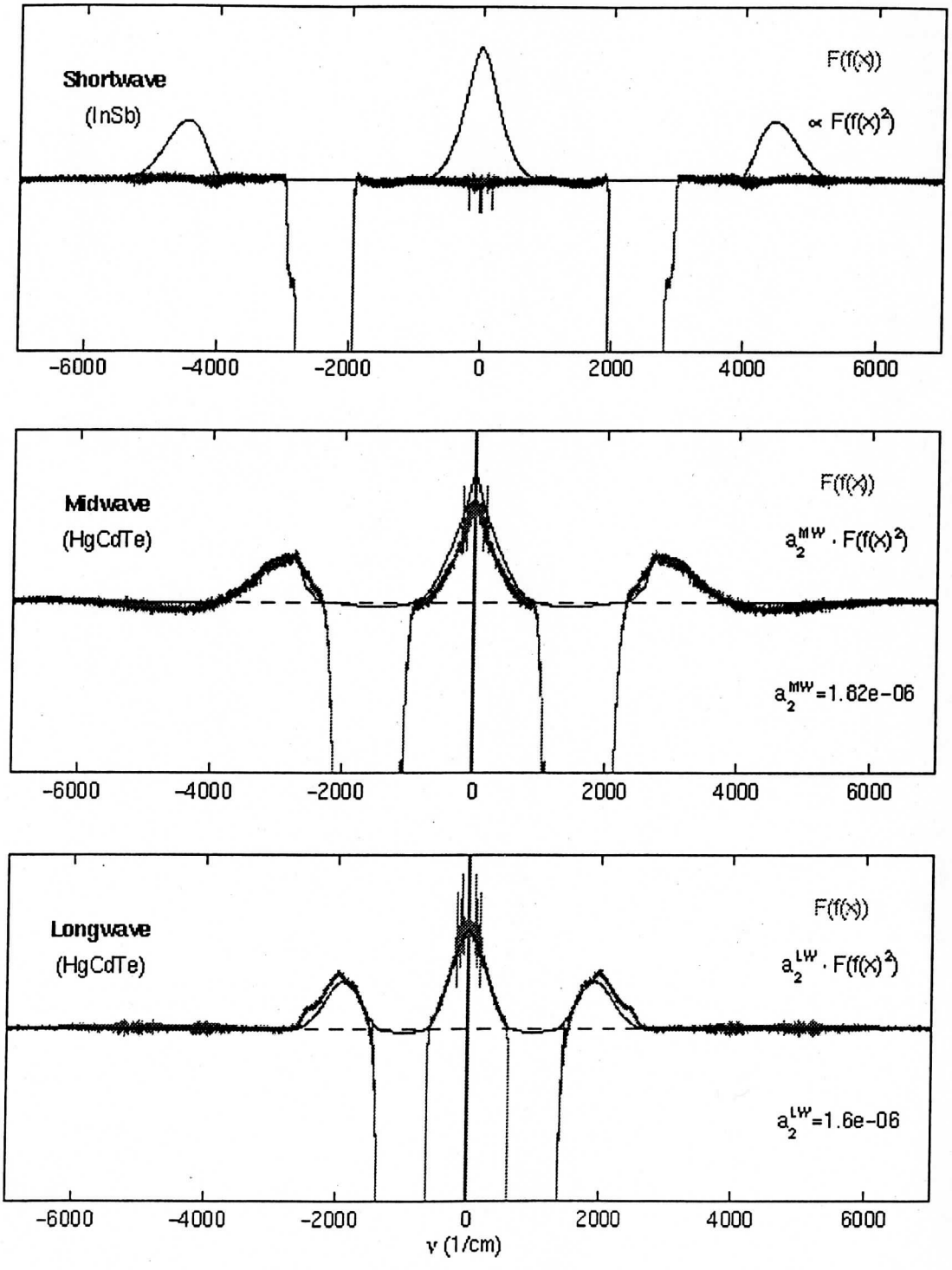

Ground-based Downwelling Spectra: AERI

Coincident downwelling NAST-I and AERI measurements: 26 June 1998 @ WFF

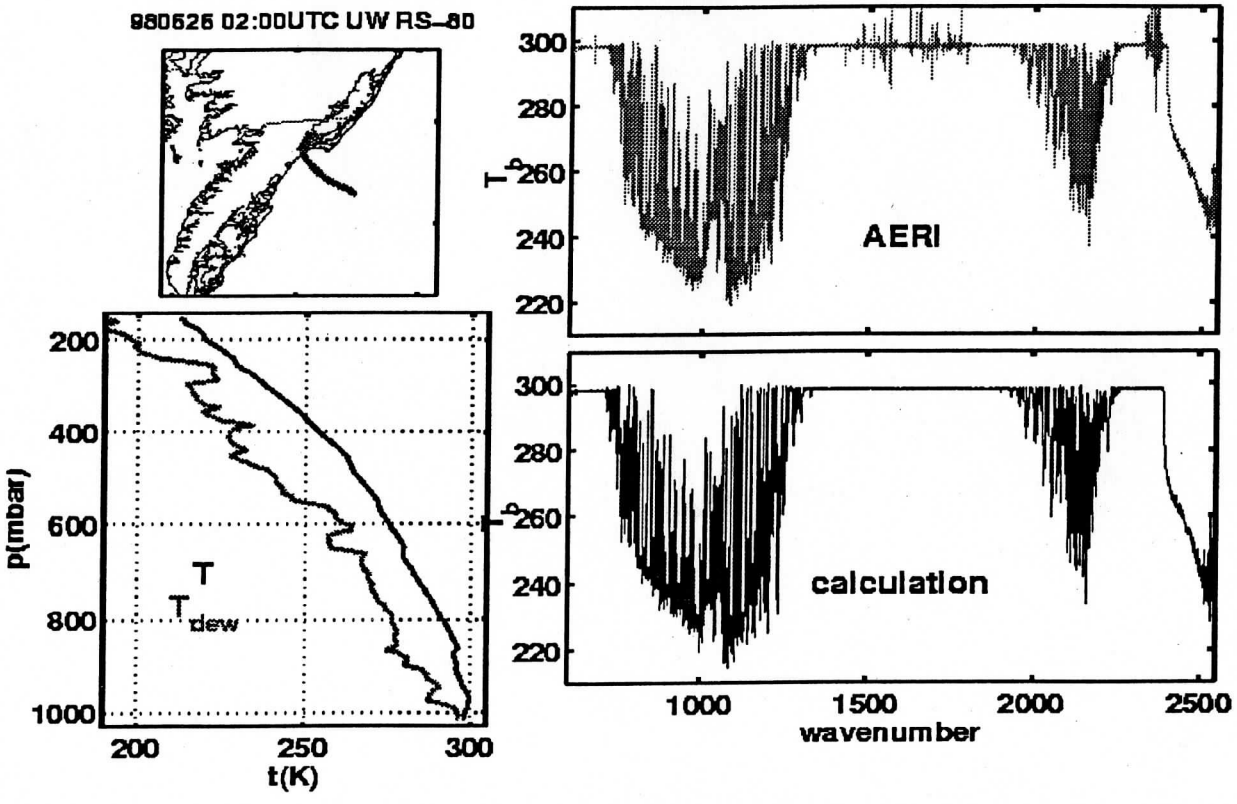

Ground-based Downwelling Spectra: AERI (cont.)

26 June 1998, 01:44-02:00 UTC at Wallops Island, VA.

NAST: T_{HBB} ≃333.0K, T_{AMB} ≃297.5K

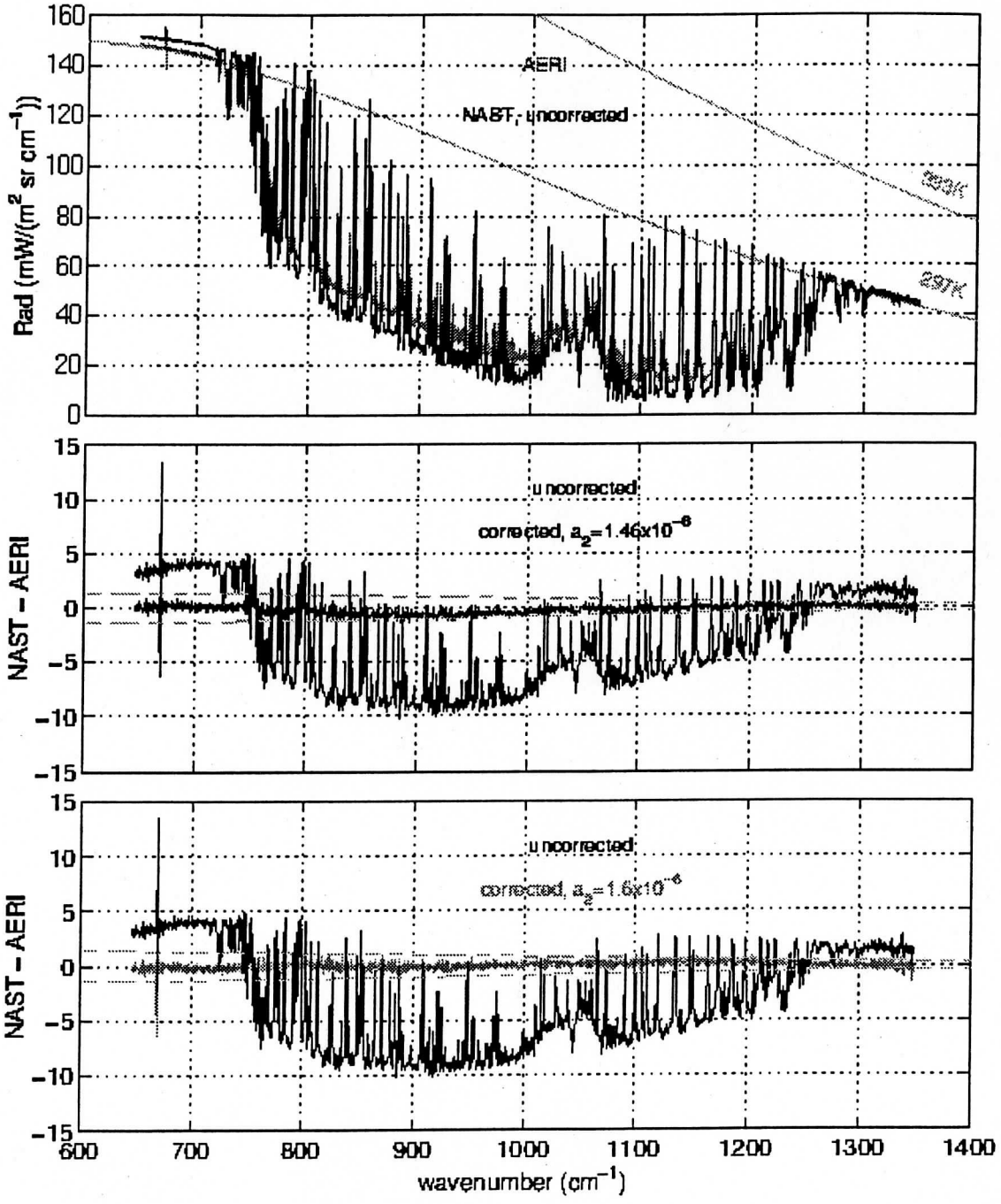

Ground-based Downwelling Spectra: AERI (cont.)

26 June 1998, 01:44-02:00 UTC at Wallops Island, VA.

NAST: T_{HBB} ≃333.0K, T_{AMB} ≃297.5K

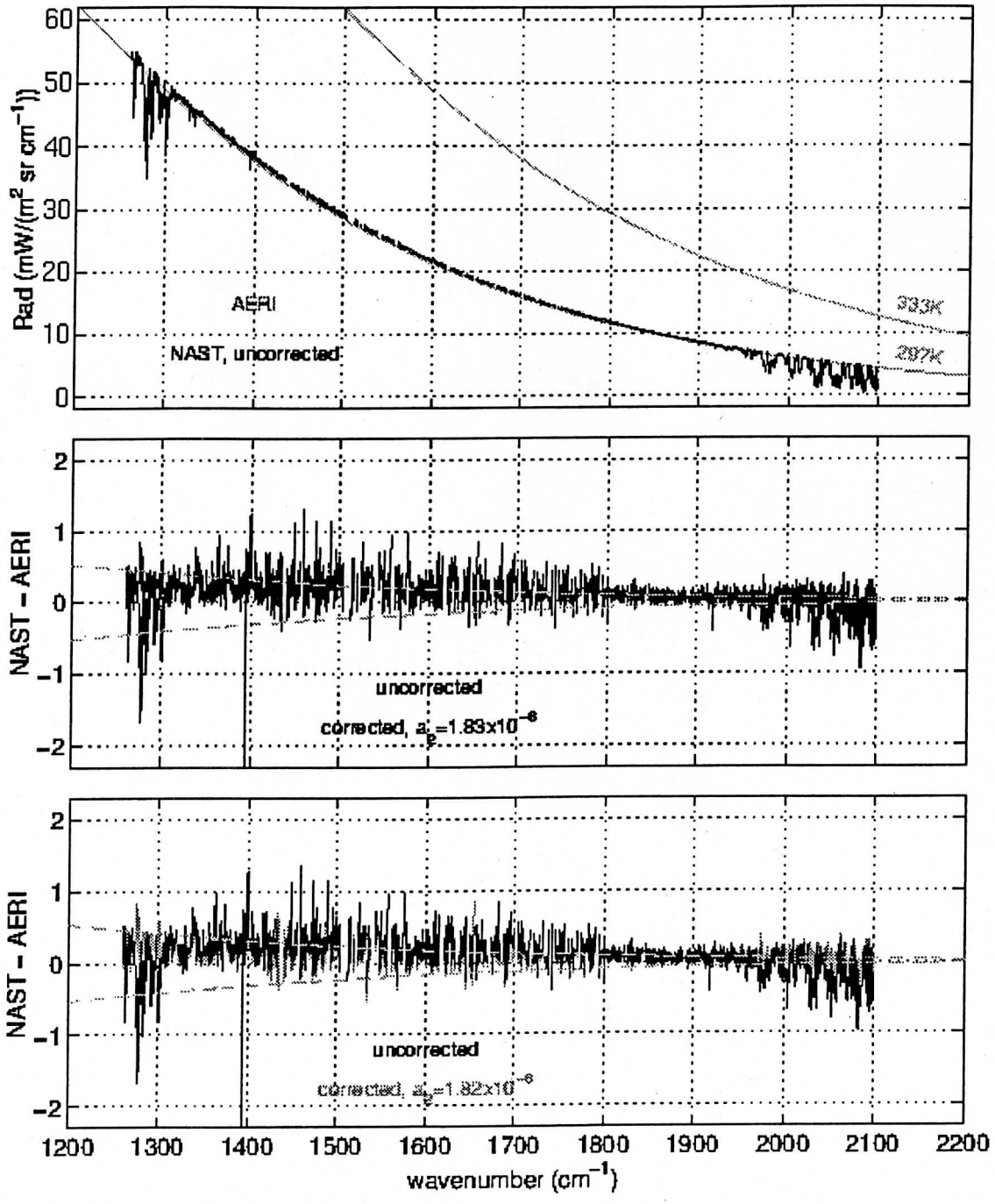

Ground-based Downwelling Spectra: AERI (cont.)

26 June 1998, 01:44-02:00 UTC at Wallops Island, VA.

NAST: $T_{HBB} \simeq 333.0$K, $T_{AMB} \simeq 297.5$K

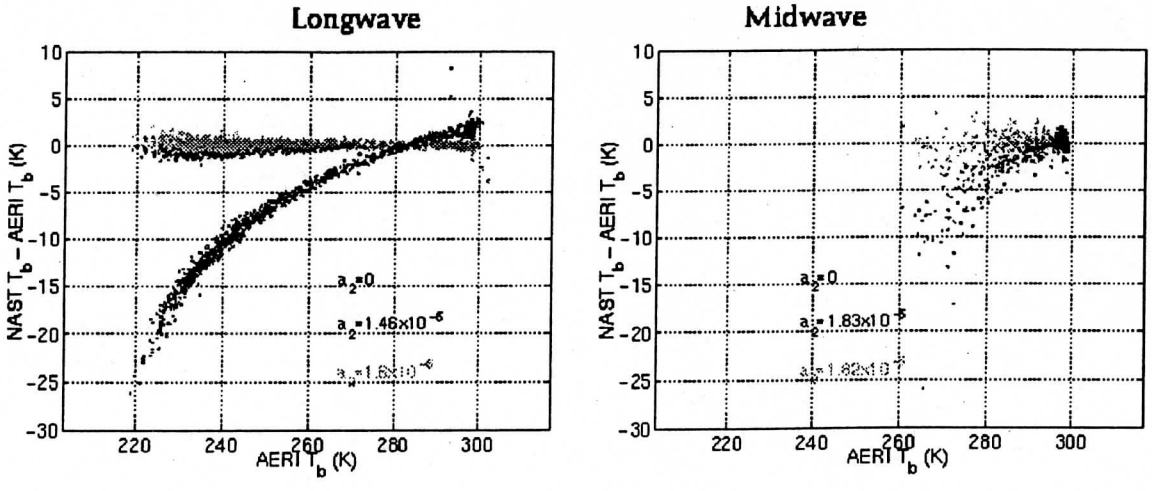

In-flight Upwelling Spectra: HIS

- NASTI and HIS on ER-2 (20 km) for Wallops '98 flights in June/July 1998
- clear sky time period over ocean on 7 July 1998, 13:00-13:05 UTC
- NASTI: $T_{HBB} \simeq 333.0$K, $T_{AMB} \simeq 263.5$K

GOES-8, channel 10, 11 July 1998, 14:15 UTC

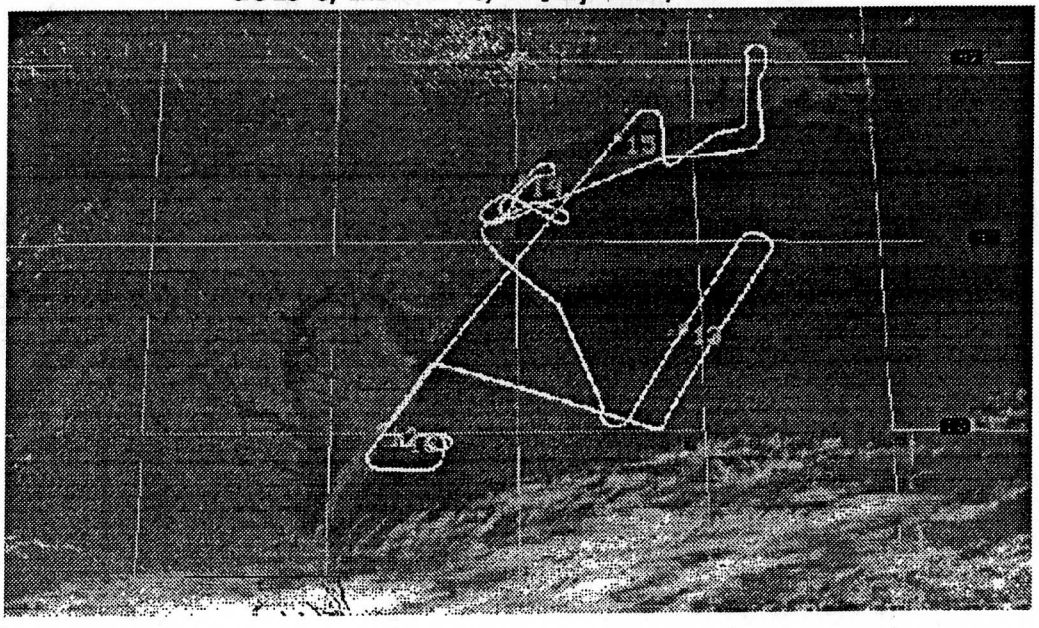

In-flight Upwelling Spectra: HIS (cont.)

11 July 1998, 13:00-13:05 UTC

NAST: $T_{HBB} \simeq 333.0$K, $T_{AMB} \simeq = 263.5$K

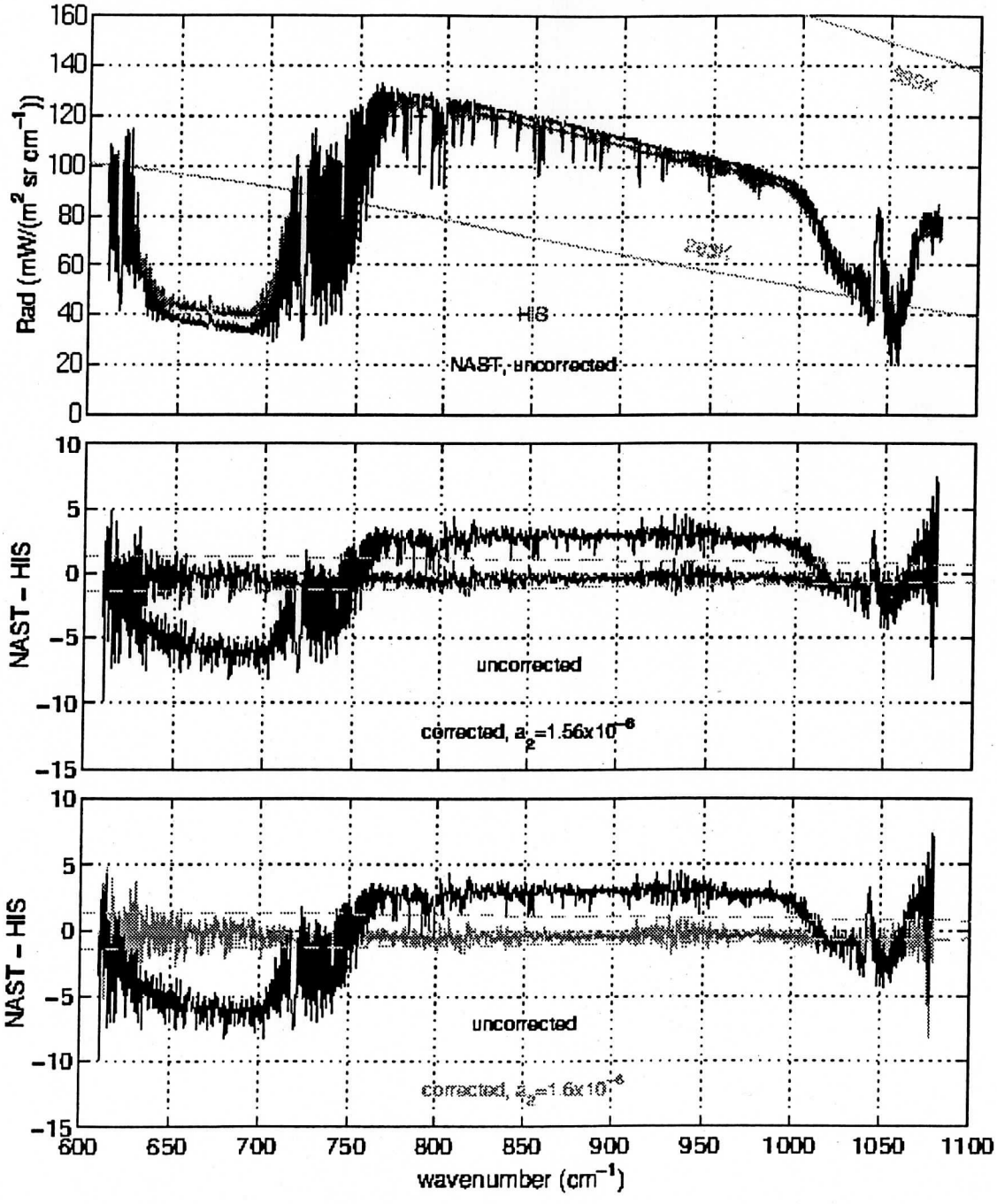

In-flight Upwelling Spectra: HIS (cont.)

11 July 1998, 13:00-13:05 UTC

NAST: $T_{HBB} \simeq 333.0$K, $T_{AMB} \simeq = 263.5$K

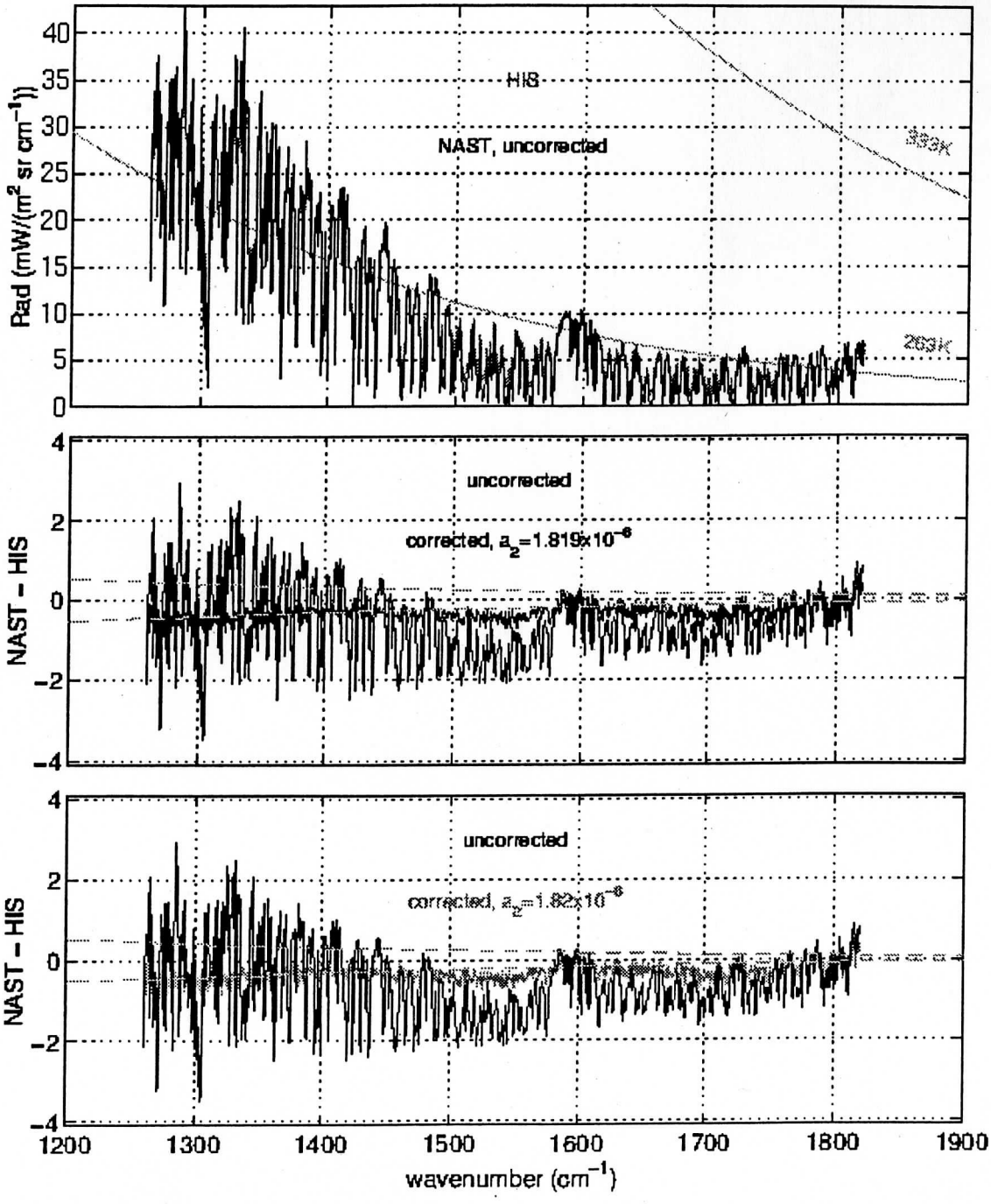

In-flight Upwelling Spectra: HIS (cont.)

11 July 1998, 13:00-13:05 UTC

NAST: $T_{HBB} \simeq 333.0$K, $T_{AMB} \simeq = 263.5$K

Longwave

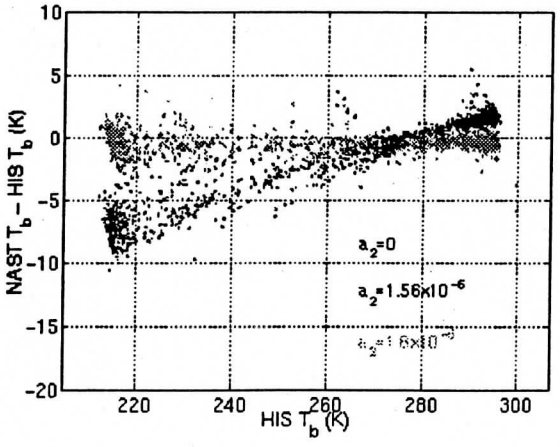

Midwave

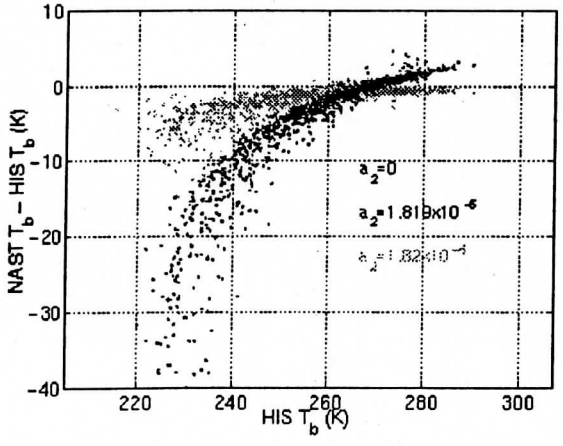

Reference Calibration Blackbody Data

Calibrated NAST-I spectra (w/o non-linearity correction) and Calculations:

October '98 LaRC data. Internal blackbodies @ ~298.5K and ~333.0K

External bodies: 333.00K (+60C), 313.27K (+40C), 295.84K, (ambient), 273.18K (ICE bath), ~77K (LN_2)

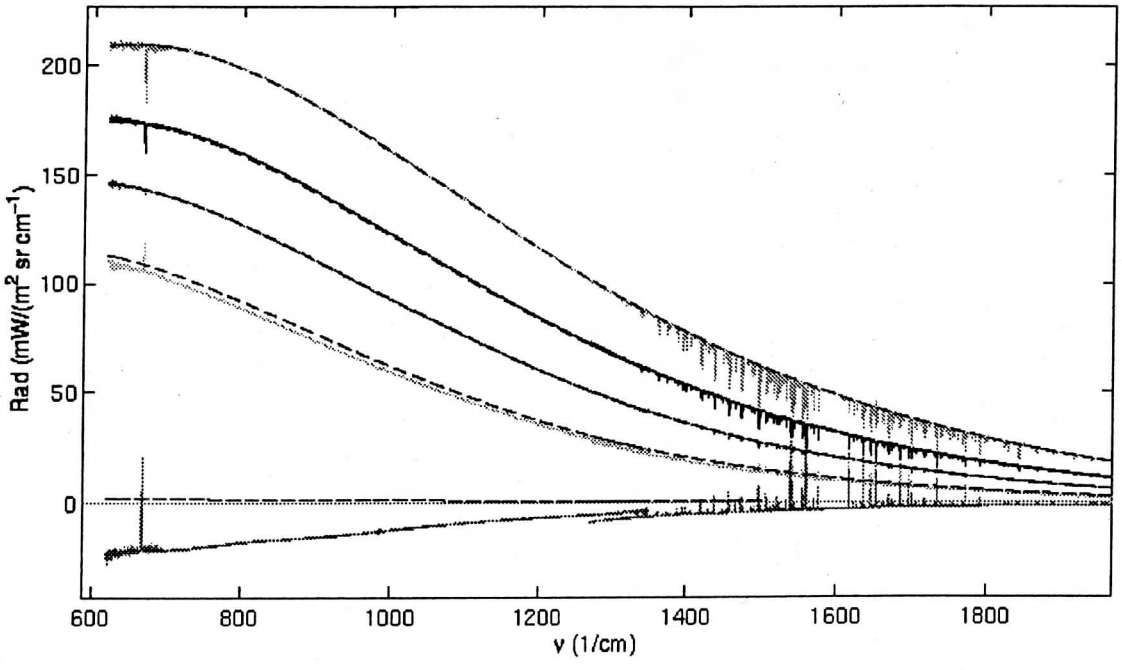

Reference Blackbody Data (cont.)

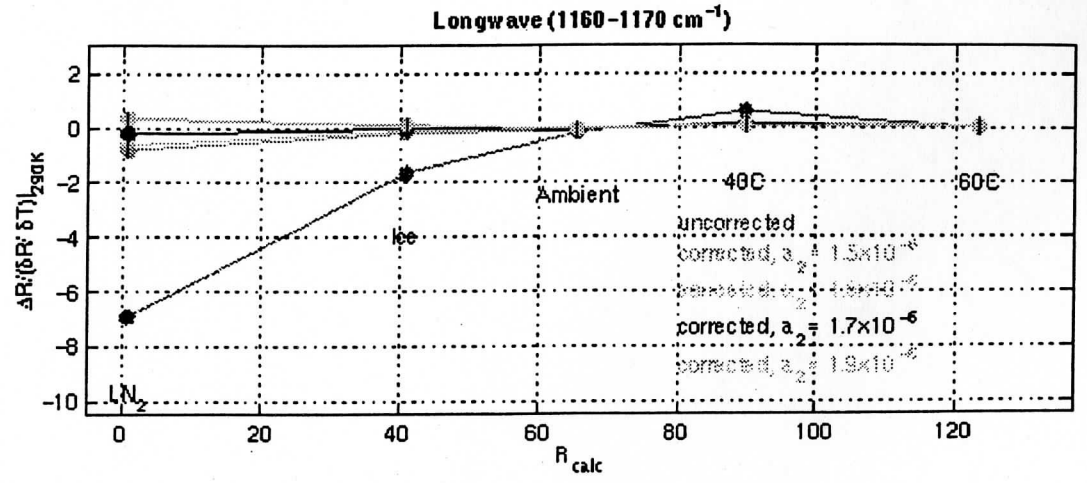

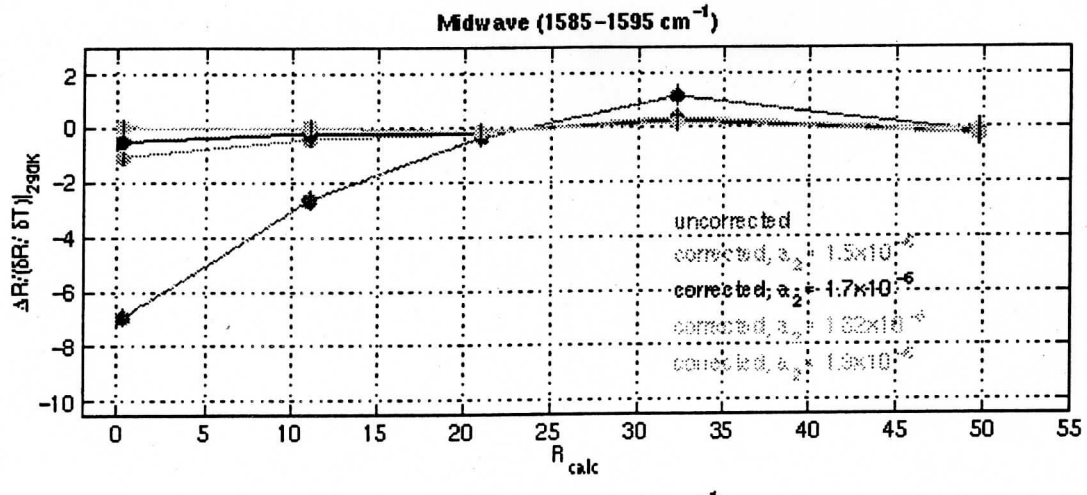

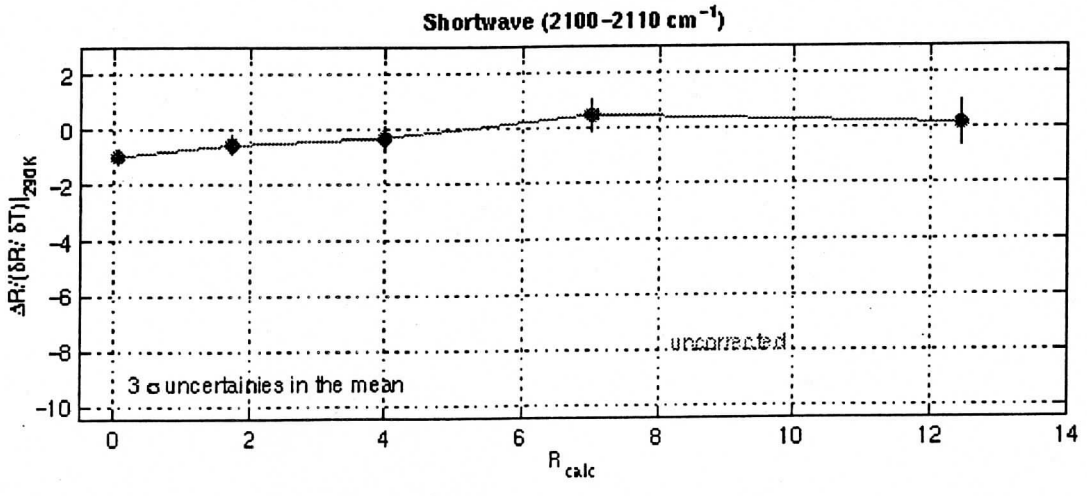

Summary

- AERI/HgCdTe detector nonlinearity correction algorithm adapted to NAST-I
- quadratic non-linearity coefficients, a_2 ($\times 10^6$) :

	Out-of-Band (ν_{HBB})		AERI (uplooking)	HIS (downlooking)	blackbodies
	$\nu < \nu_c$	$\nu > \nu_c$			
Longwave	1.67±0.06	1.82±0.05	1.46±0.05	1.56±0.05	1.65±0.15
Midwave †	1.20±0.09	1.67±0.08	1.83±0.15	1.82±0.05	1.75±0.15

†: determined with $a_3 = 0$.

- Final values of a_2: 1.60×10^{-6} (longwave) and 1.82×10^{-6} (midwave) with uncertainties of 5–10 %
- Uncertainty in in-flight radiances :

★ Reduce T_{HBB} from 333K to ~305K for future flights
↪ will reduce size of in-flight non-linearity signal and correction by a factor of ~2

- Remaining issues/tasks
  - ▷ repeat cal tests after/during WINTEX (March '99)
  - ▷ details of out-of-band response
    midwave: incorporate cubic non-linearity
  - ▷ validation
    - ○ clear sky calculations
    - ○ HIS/NAST-I clouded scenes from Wallops '98

Non-linearity Correction Uncertainty Estimate

Clear sky in-flight data from 980711, T_{AMB} =263.5K, T_{HBB} =333.0K

Longwave: $R_{1.60\times10^{-6}} - R_{1.70\times10^{-6}}$, Midwave: $R_{1.82\times10^{-6}} - R_{1.92\times10^{-6}}$

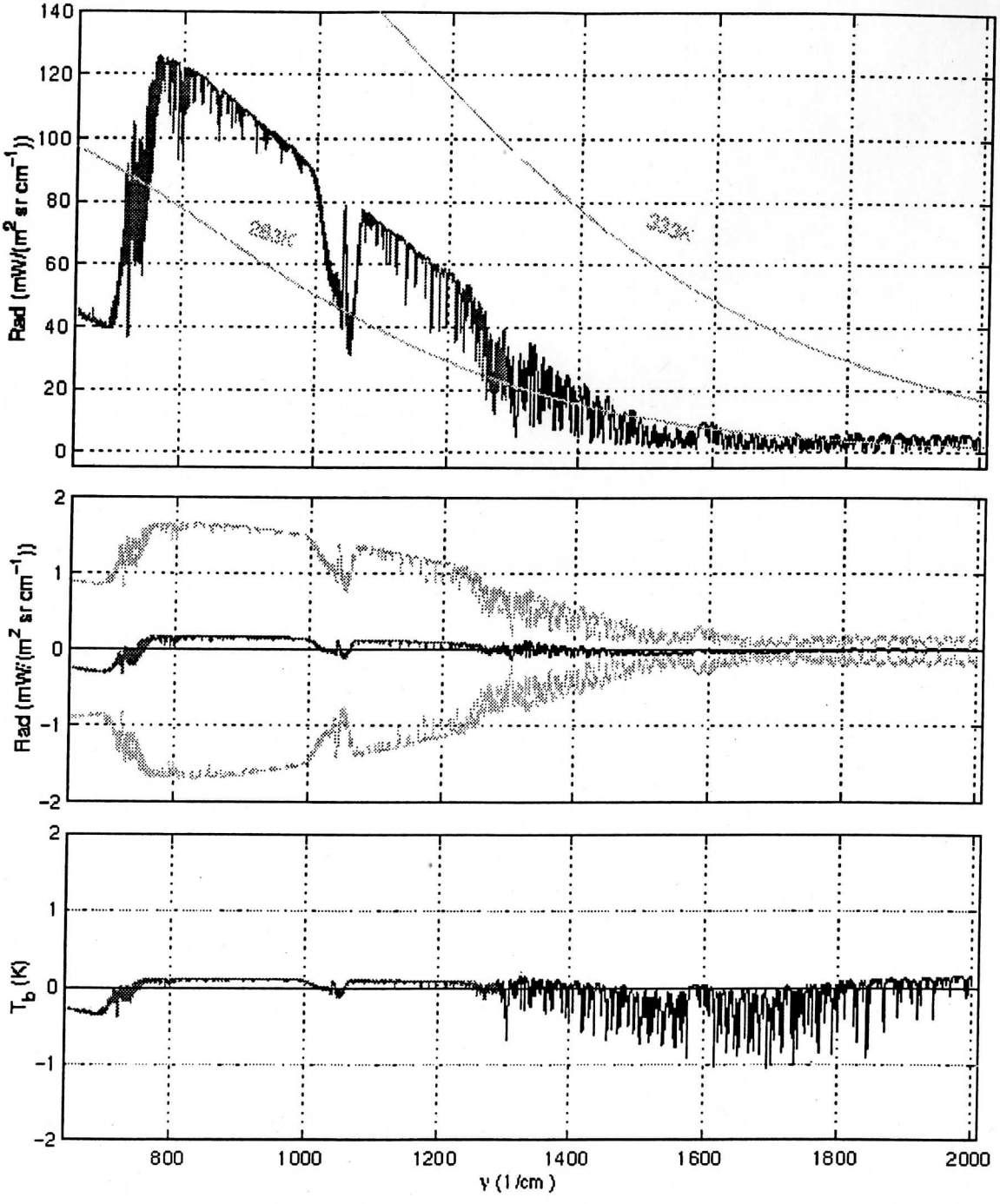

Out-of-Band characterization

$$\mathcal{F}\{f(x)^3\} = \mathcal{F}\{f(x)\} \otimes \mathcal{F}\{f(x)\} \otimes \mathcal{F}\{f(x)\}$$

980729 data

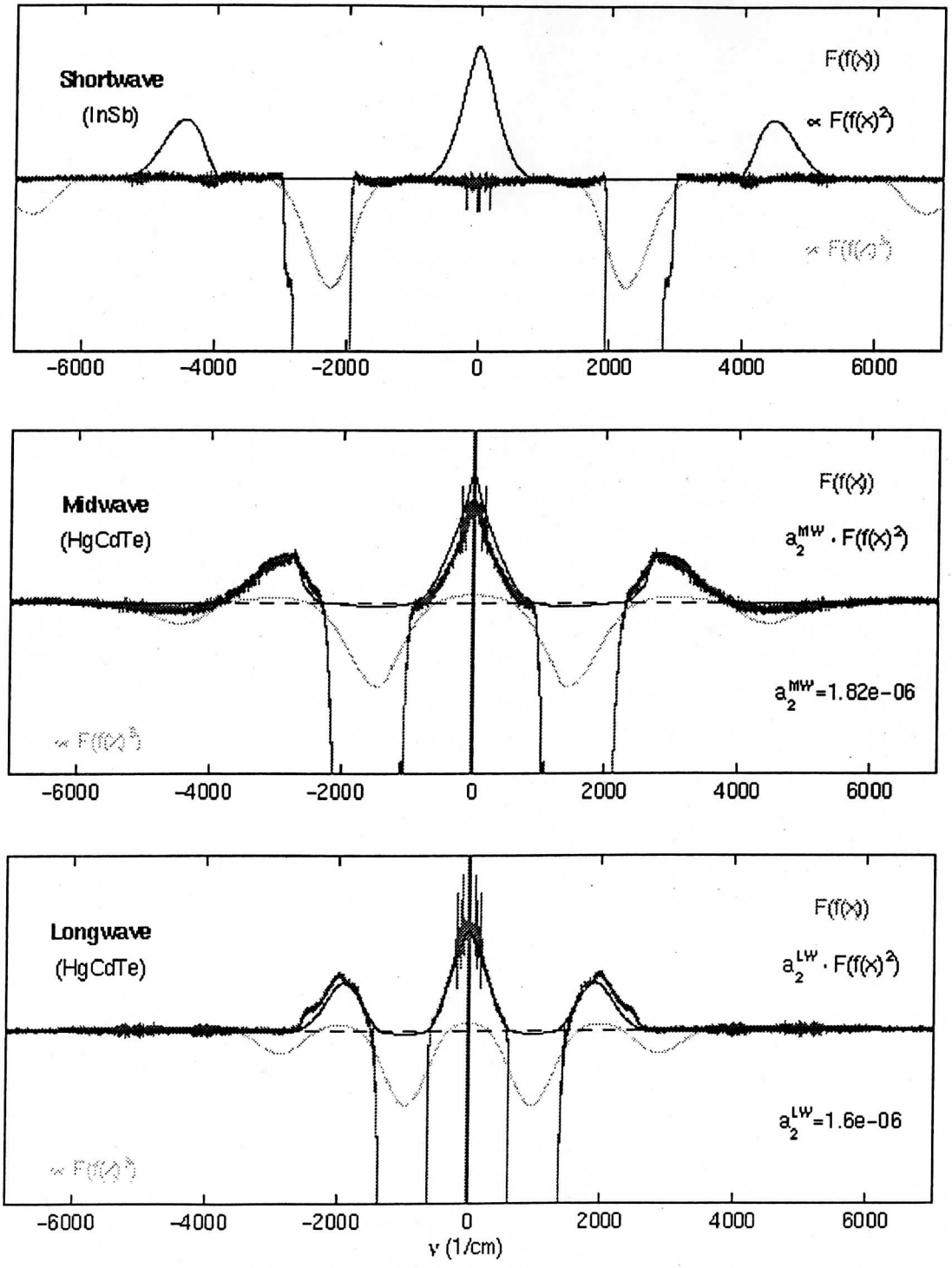

In-flight Upwelling Spectra: HIS

11 July 1998, 13:00-13:05 UTC. NAST:T_{HBB} ≃333.0K, T_{AMB} ≃=263.5K

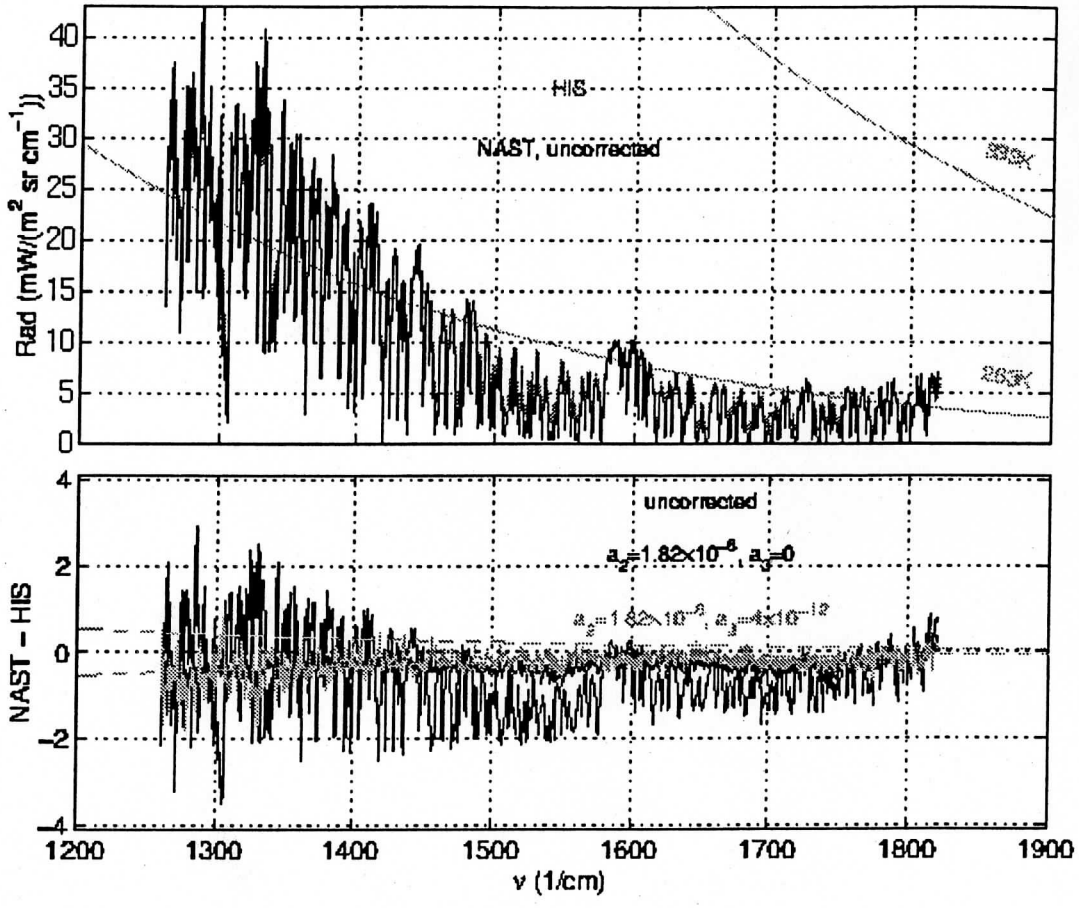

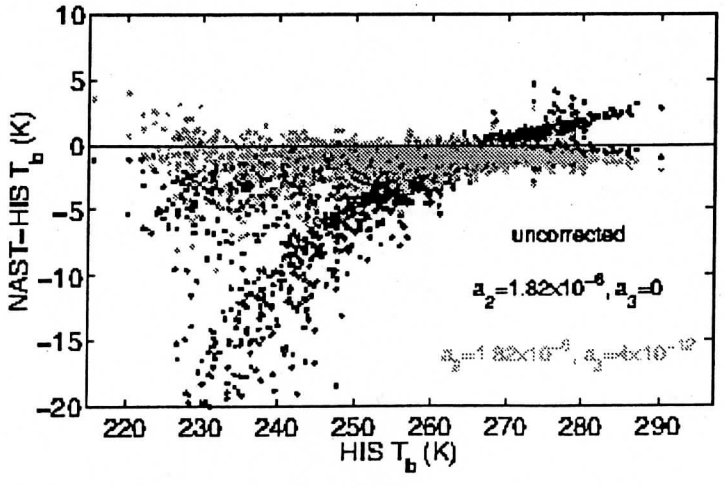

Validation

- clear-sky NAST-I observations compared to NAST-I fast model (*Strow et al.*) calculation
- nadir NAST-I spectra averaged from 23:47 to 23:50 UTC
- Vaisala RS-80 launched at 22:37 UTC
- calculation:PFAST/kCARTA w/ CKDv0, HI-TRAN'96+Toth, e_s=0.975, Kaiser Bessel apodization
- *http://danspc.larc.nasa.gov/NAST/val_calcs2.html*

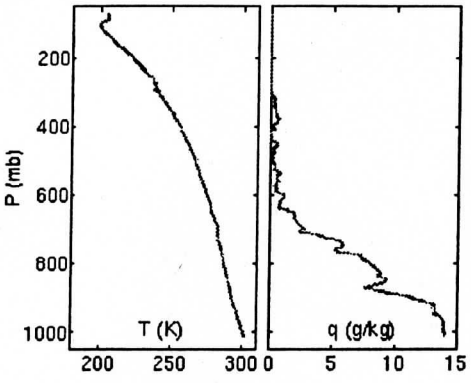

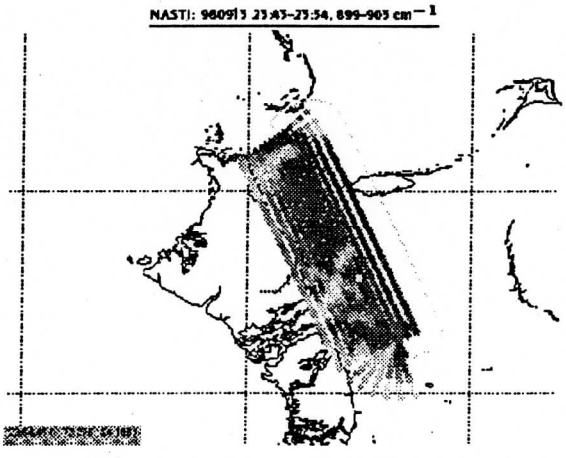

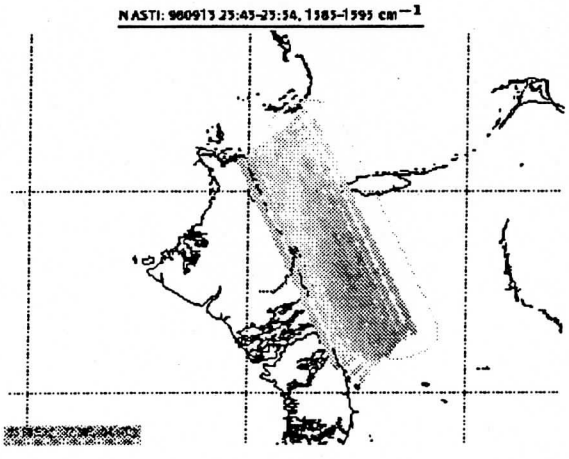

Validation (cont.)

Longwave: NAST-I and fast model calculation

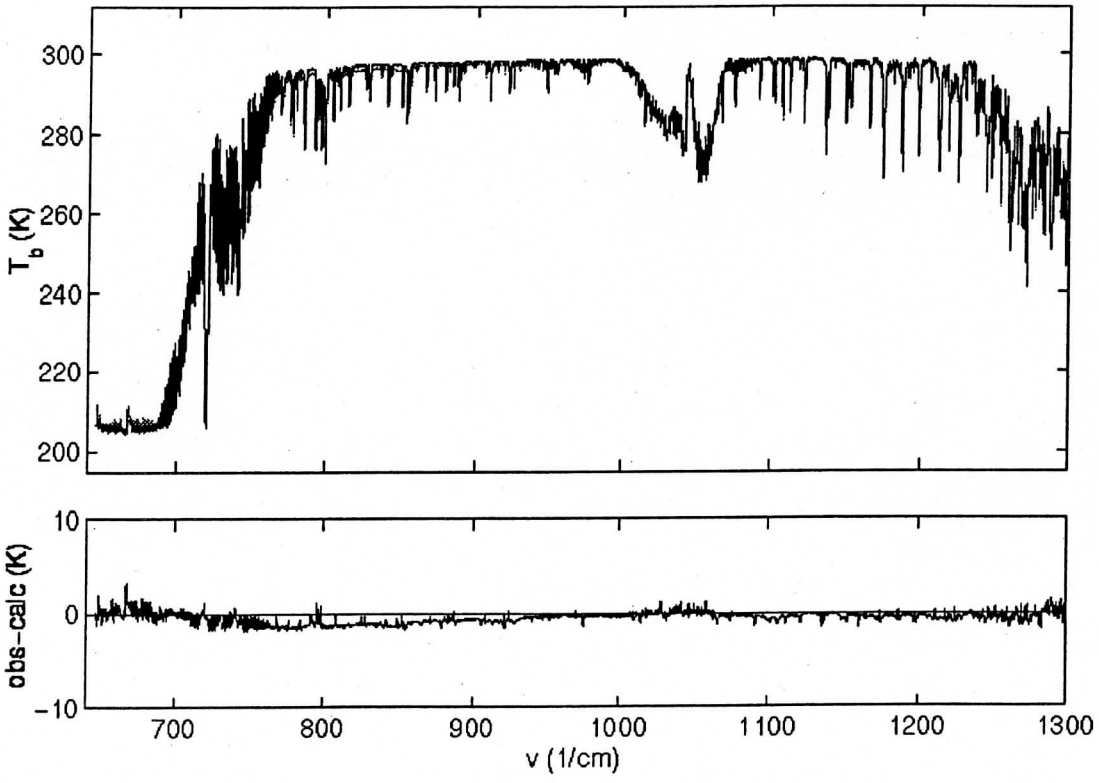

Validation (cont.)

Midwave: NAST-I and fast model calculation

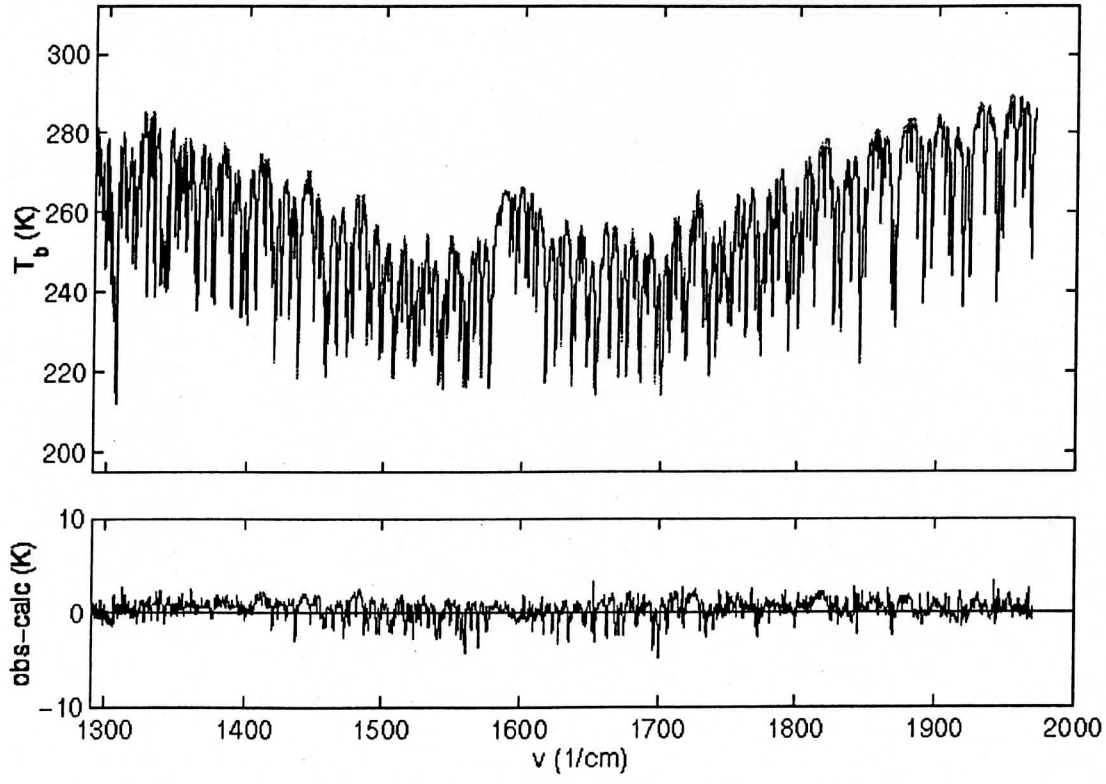

Validation (cont.)

Shortwave: NAST-I and fast model calculation

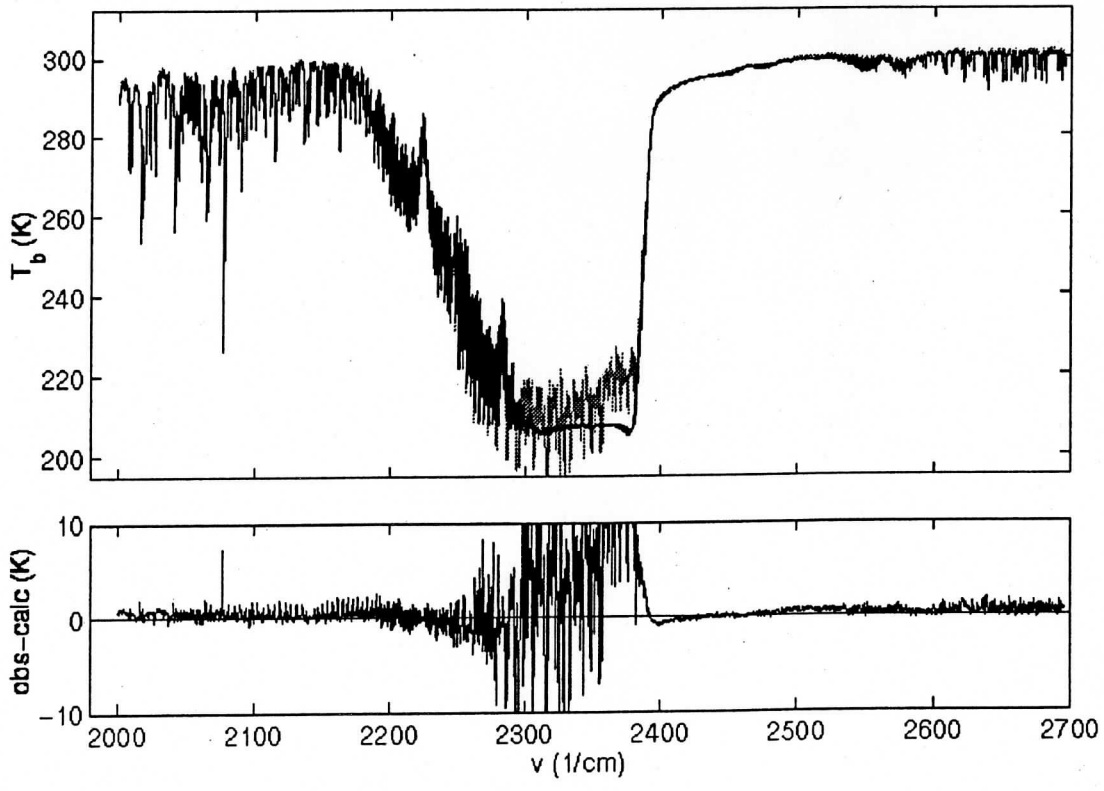

26

Postscript Viewers and Compression

Papers

Author	Title	Journal/Proceedings
Hank Revercomb, et al.	Recent results from two new aircraft-based Fourier transform interferometers: The Scanning High-resolution Interferometer Sounder and the NPOESS Atmospheric Sounder Testbed Interferometer	8th International Workshop on Atmospheric Science from Space using Fourier Transform Spectrometry (ASSFTS), Toulouse, France, 16-18 November 1998

Talks

Speaker	Affiliation	Lecture Date	Lecture Title	Audience
Dave Tobin	University of Wisconsin	25 Feb 1999		AIRS Science Team

[NAST Home]

University of Wisconsin

FY99 Final Report

Engineering and Scientific Support for the National Polar-orbiting Operational Environmental Satellite System Airborne Sounder Testbed - Interferometer (NAST-I) Instrument

30 September 1999

Deliverables by Task:

Task 1

Report documenting the operational functionality of NAST-I during CAMEX-3

2.NASTI Validation: Comparison with HIS from Wallops 98
URL: http://danspc.larc.nasa.gov/NAST/val_his.html

http://danspc.larc.nasa.gov/NAST/val_his.html

NASTI Validation: comparison with HIS spectra

This page presents a comparison of University of Wisconsin HIS and NASTI spectra taken during the Wallops '98 field campaign aboard the NASA ER-2 during a clear-sky time period over the Atlantic Ocean. The following figures show the flight track of the ER-2 along with GOES, HIS, and NASTI observations. Low-noise averaged spectra were produced from the nadir views of each instrument using data recorded between 13:00:00 and 13:05:45 UTC. (This time period is marked by the two black circles in the HIS map below.) This is an average of 48 individual HIS spectra and 28 individual nadir NASTI spectra.

GOES with ER-2 flight track
HIS surface Tbs:
NASTI surface Tbs:

The mean longwave spectrum for NAST and HIS (each reduced to HIS spectral resolution and Beer apodized) are shown here:
channel 3 :

Differences between the mean HIS and NASTI spectra (at HIS resolution and apodized):
Radiances :
Brightness temperatures :

And overlays of NASTI and HIS (at HIS resolution and apodized) :
710-810 cm^{-1} :
650-710 cm^{-1} :
724-740 cm^{-1}:
775-815 cm^{-1}:
867-885 cm^{-1} :
885-1065 cm^{-1}:

Last modified: Wed Dec 30 17:45:47 UTC 1998

29

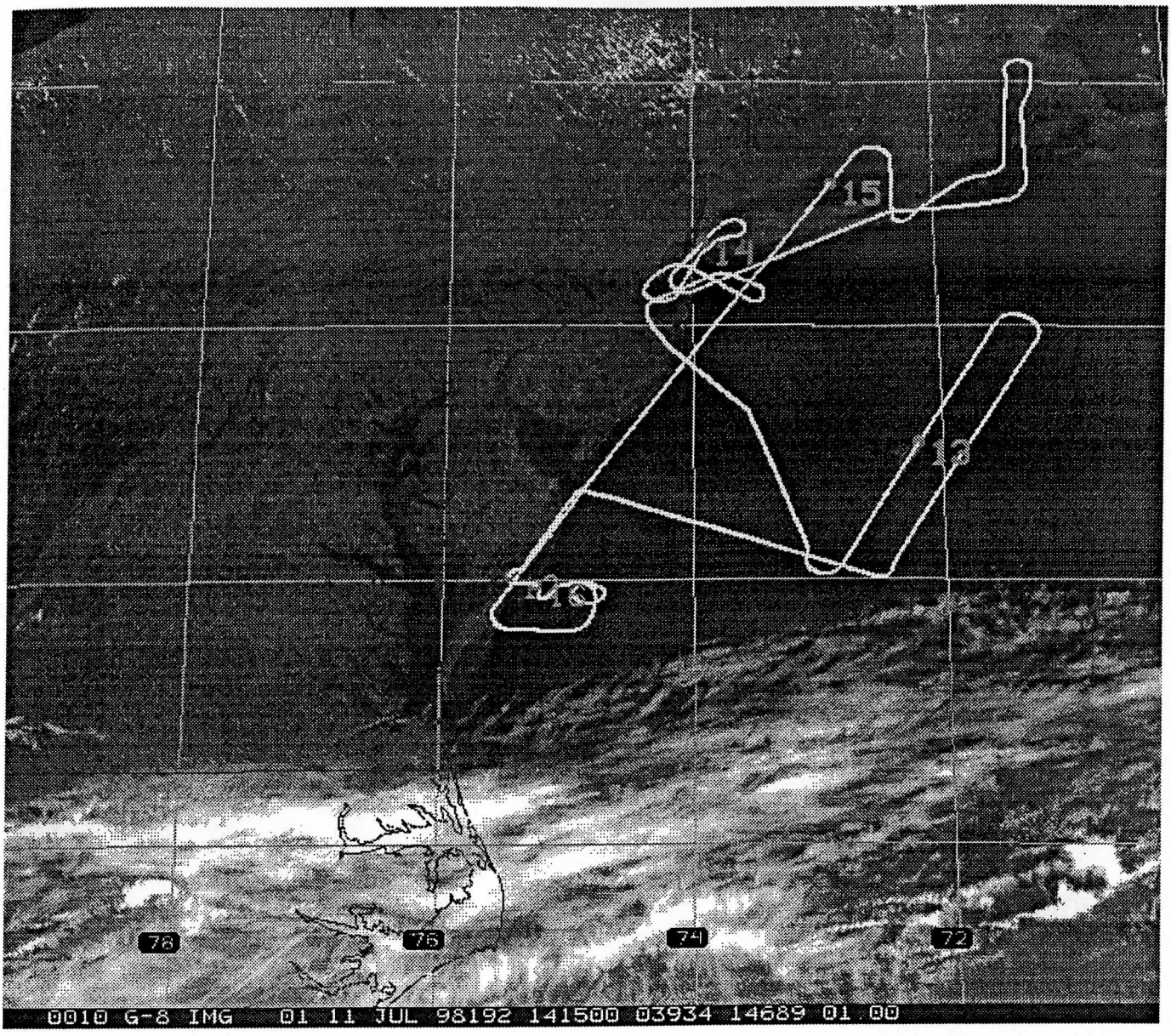
15
78
75
74
72
0010 G-8 IMG 01 11 JUL 98192 141500 03934 14689 01 00

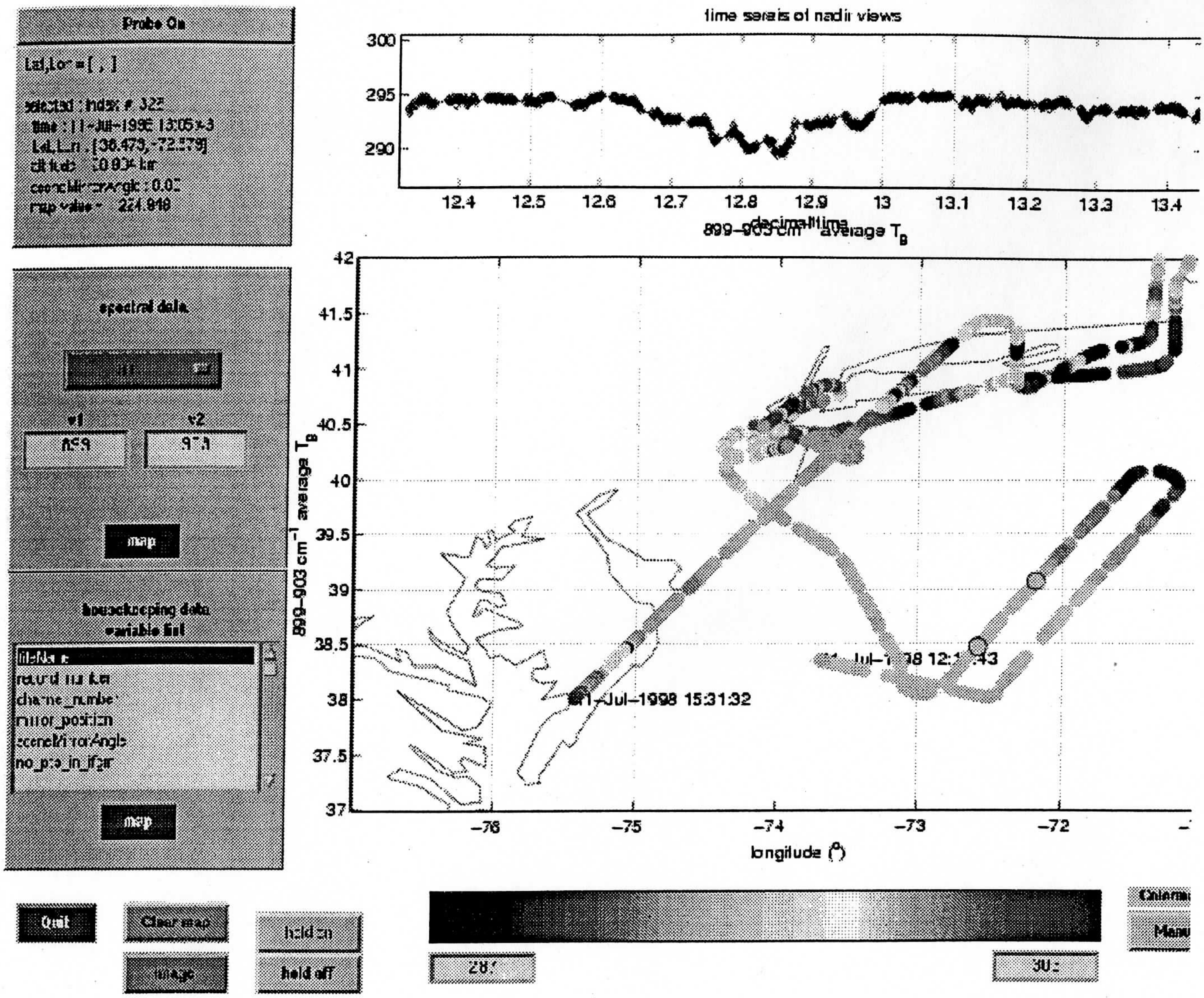
Probe On
time series of nadir views
decimal time
899–903 cm^{-1} average T_B
11-Jul-1998 15:31:32
longitude (°)
spectral data
v1
v2
map
housekeeping data variable list
fileName
record number
channel_number
mirror_position
sceneMirrorAngle
map
Quit
Clear map
image
hold on
hold off
Menu

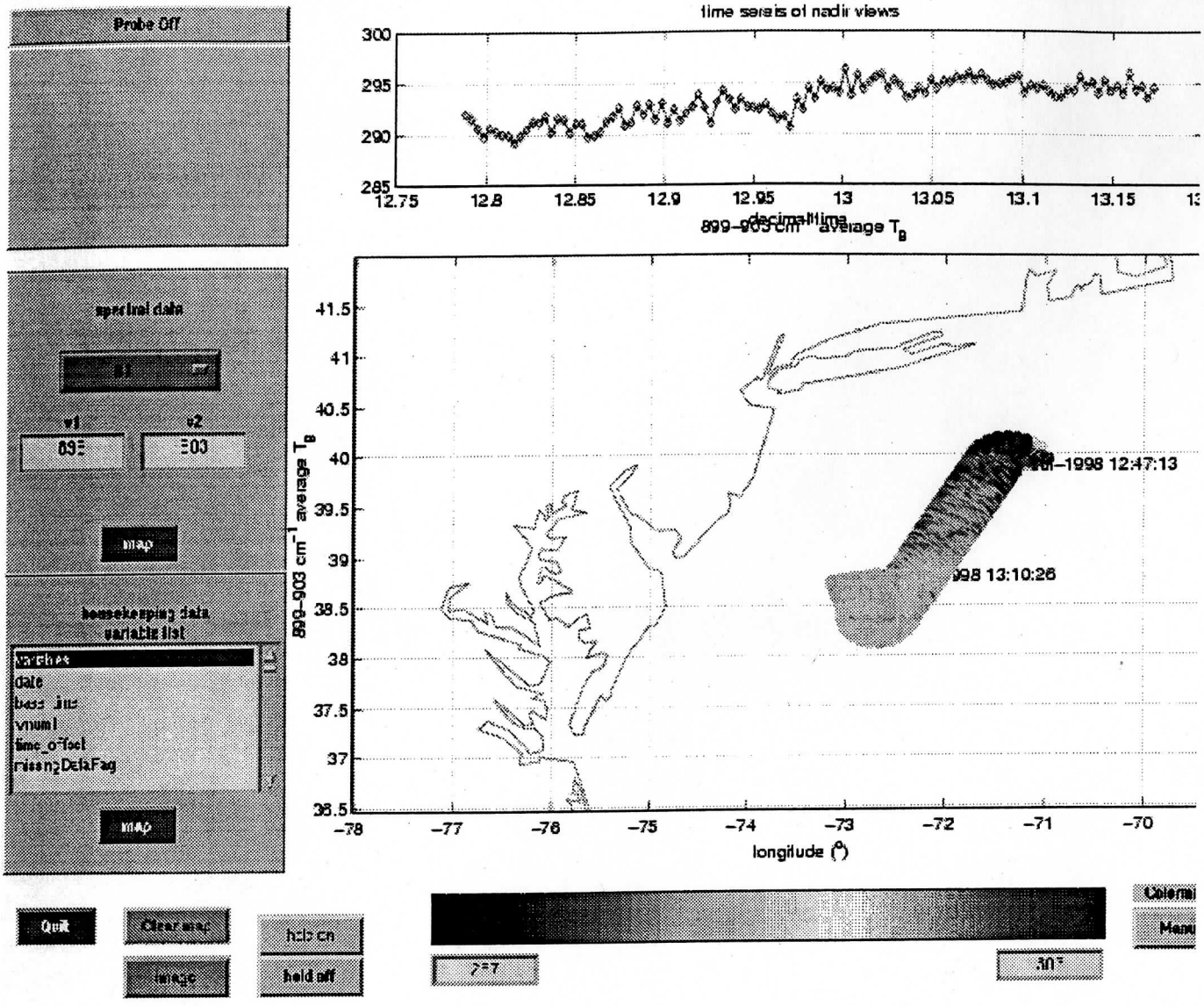
Probe Off
time series of nadir views
300
295
290
285
12.75
12.8
12.85
12.9
12.95
13
13.05
13.1
13.15
decimal time
899-903 cm⁻¹ average T_B
spectral data
v1
v2
map
housekeeping data
variable list
date
map
41.5
41
40.5
40
39.5
39
38.5
38
37.5
37
36.5
899-903 cm⁻¹ average T_B
-78
-77
-76
-75
-74
-73
-72
-71
-70
longitude (°)
1998 12:47:13
998 13:10:26
Quit
Clear image
hold on
hold off
30

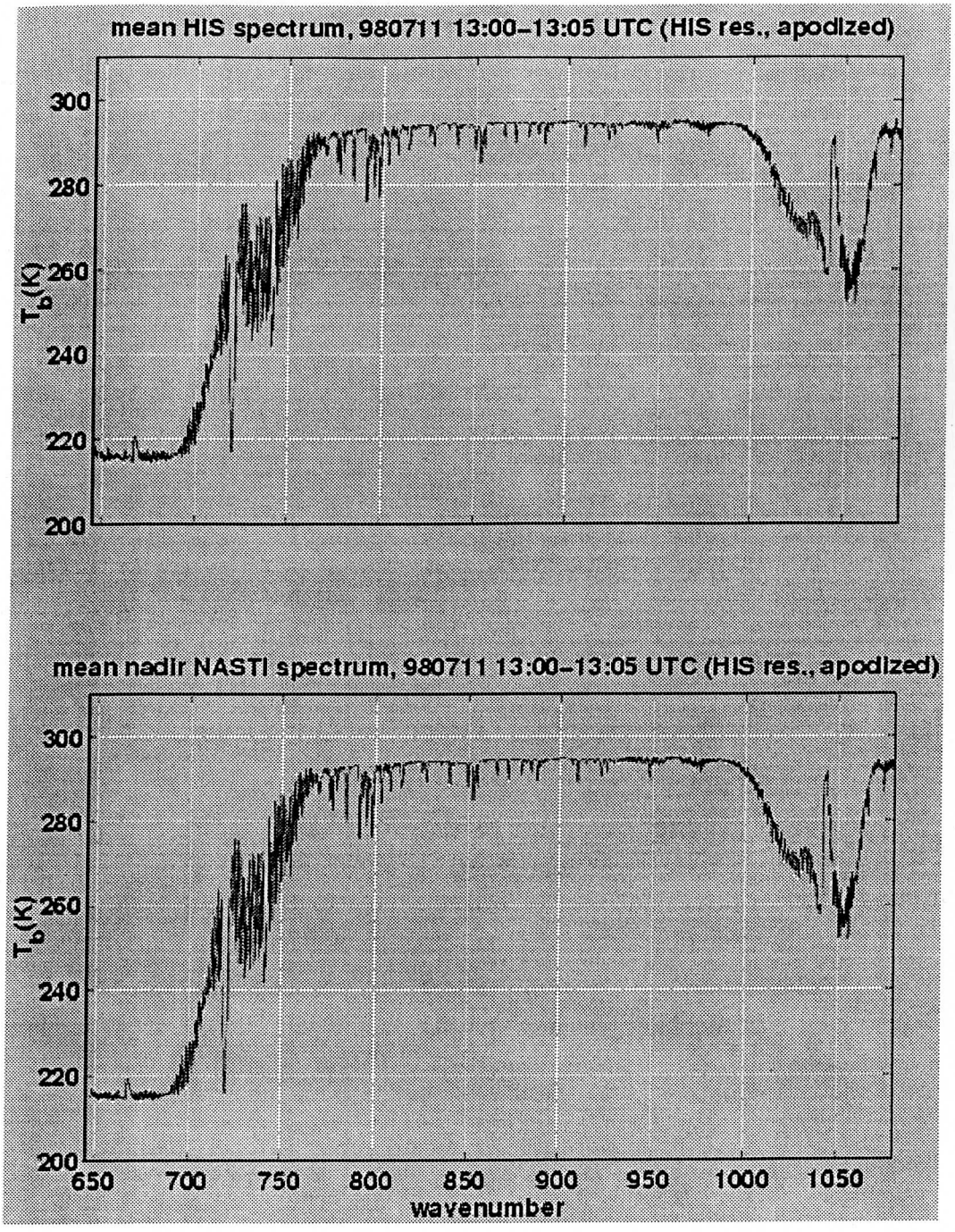
mean HIS spectrum, 980711 13:00–13:05 UTC (HIS res., apodized)
300
280
260
240
220
200
T_b(K)
mean nadir NASTI spectrum, 980711 13:00–13:05 UTC (HIS res., apodized)
300
280
260
240
220
200
T_b(K)
650
700
750
800
850
900
950
1000
1050
wavenumber

33

channel 3 mean radiances : HIS (blue) and NASTI (red) (HIS res., apodized)

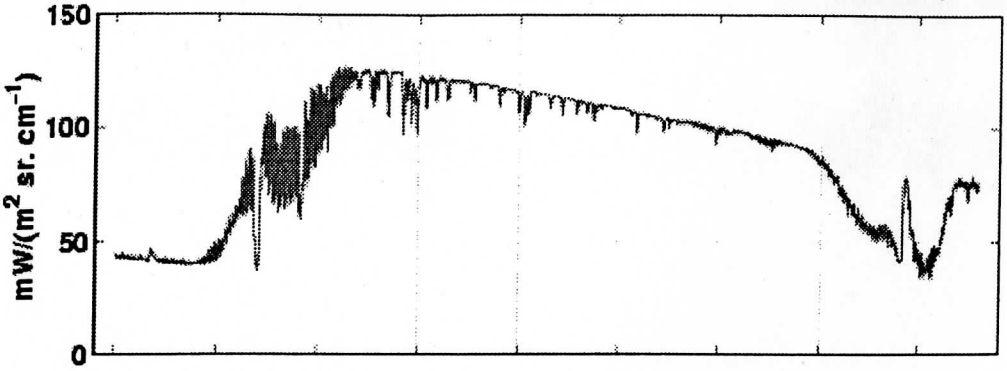

HIS – NASTI

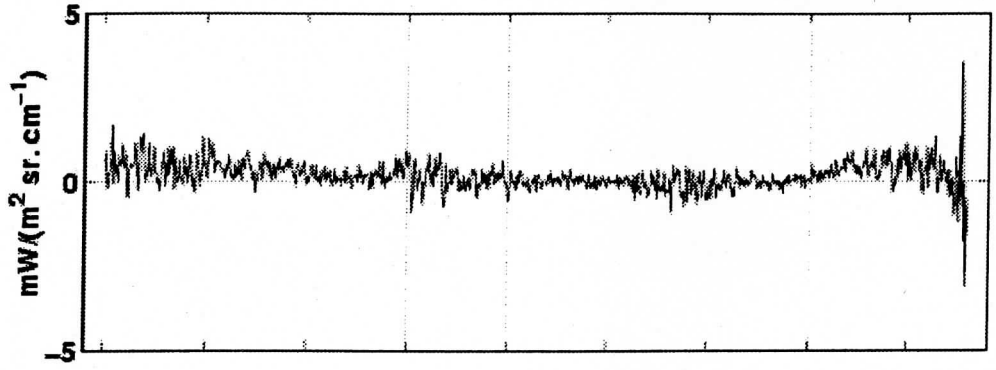

HIS (blue) and NASTI (red) uncertainty (HIS res., apodized)

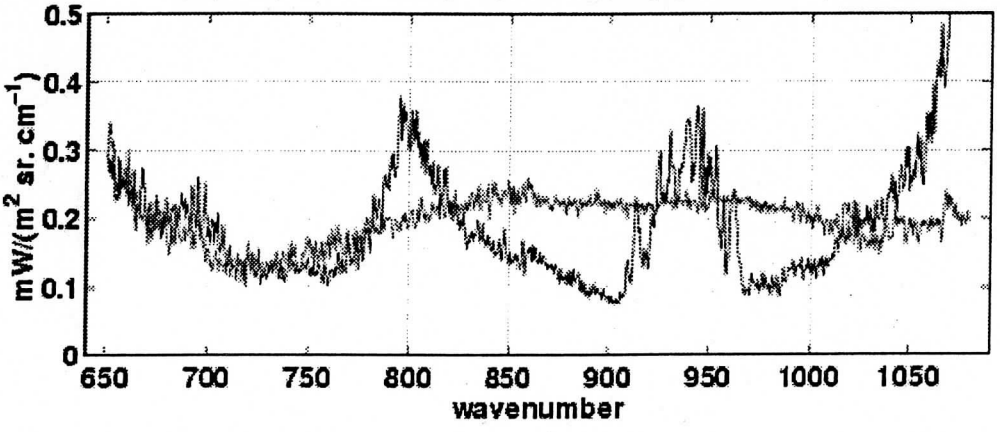

channel 3 mean T_b : HIS (blue) and NASTI (red) (HIS res., apodized)

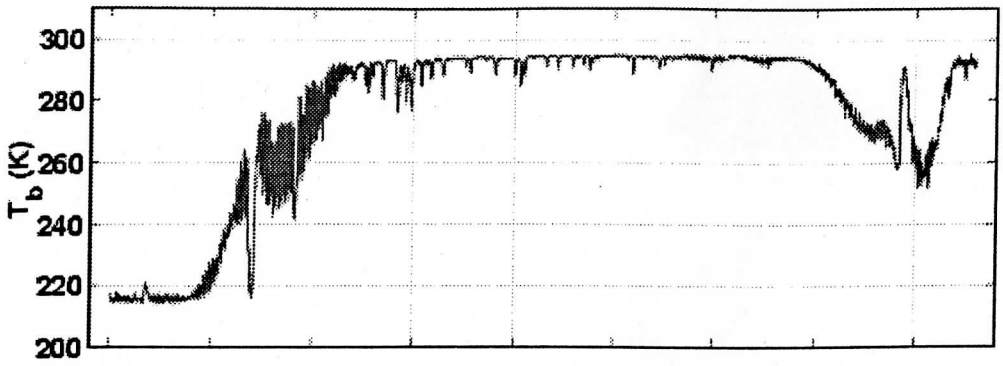

HIS – NASTI

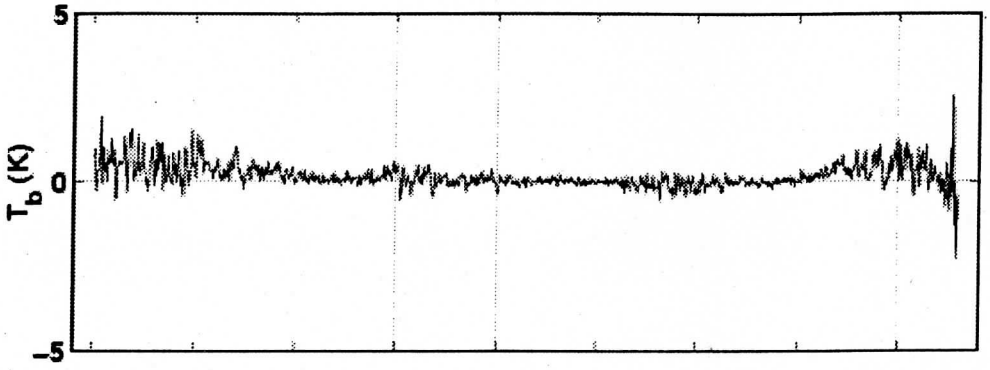

HIS (blue) and NASTI (red) uncertainty (HIS res., apodized)

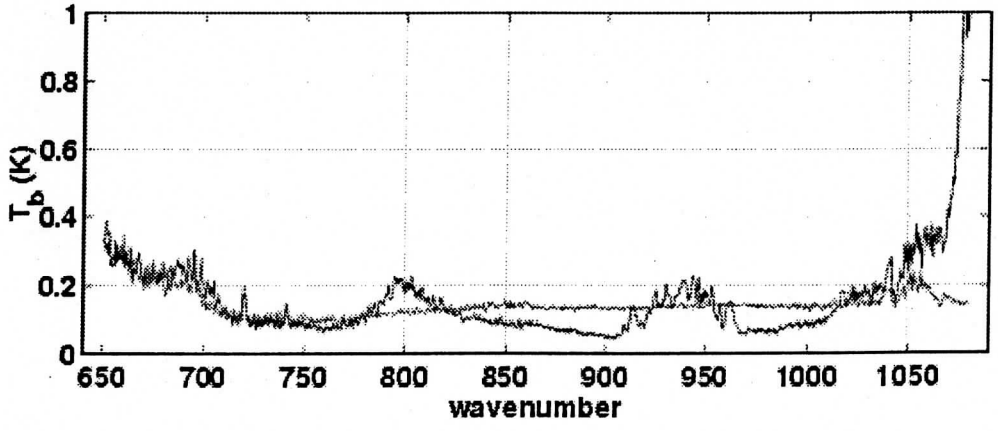

35

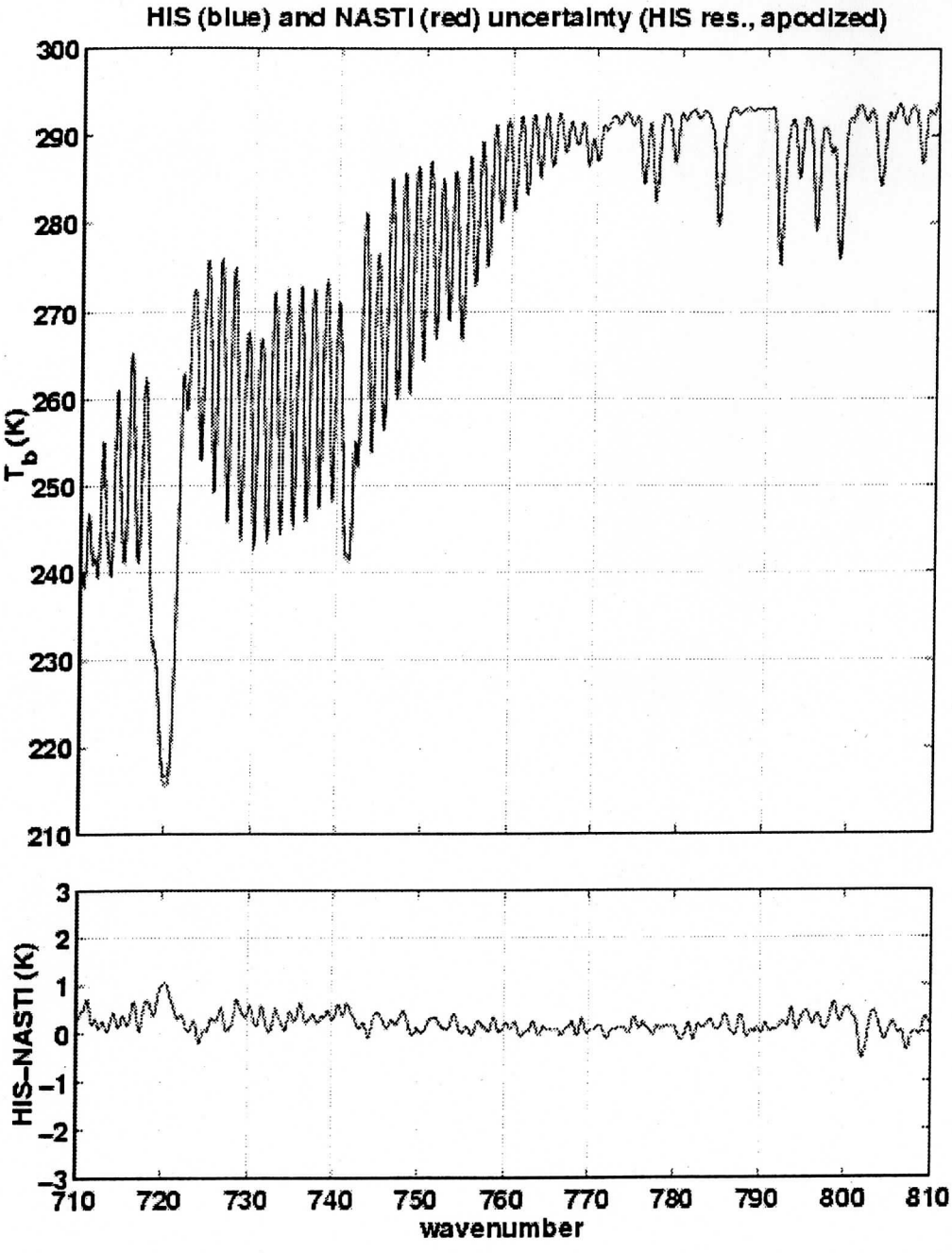
HIS (blue) and NASTI (red) uncertainty (HIS res., apodized)
T_b (K)
HIS–NASTI (K)
wavenumber
300
290
280
270
260
250
240
230
220
210
3
2
1
0
−1
−2
−3
710
720
730
740
750
760
770
780
790
800
810

36

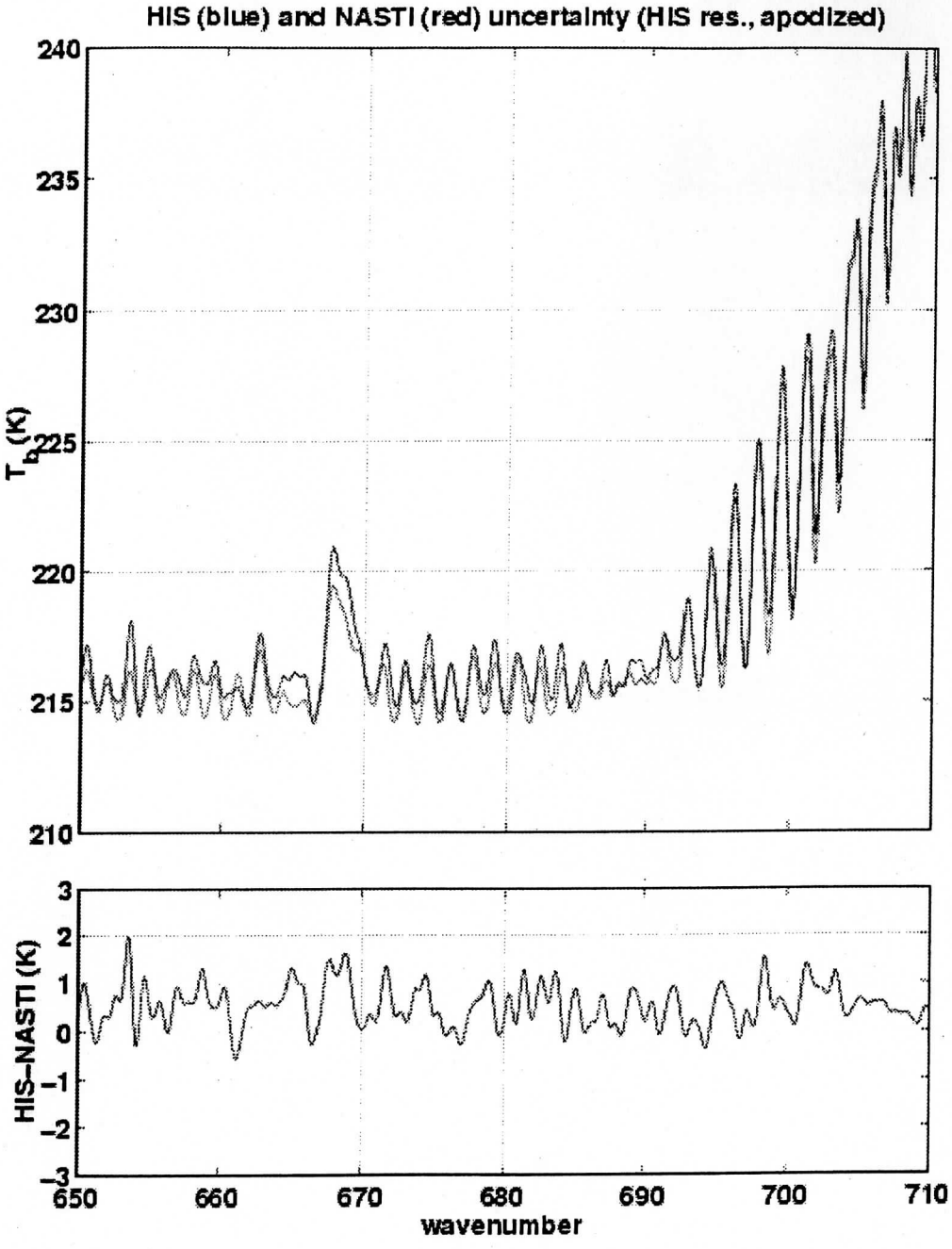
HIS (blue) and NASTI (red) uncertainty (HIS res., apodized)
240
235
230
225
220
215
210
T_b (K)
3
2
1
0
−1
−2
−3
HIS−NASTI (K)
650
660
670
680
690
700
710
wavenumber

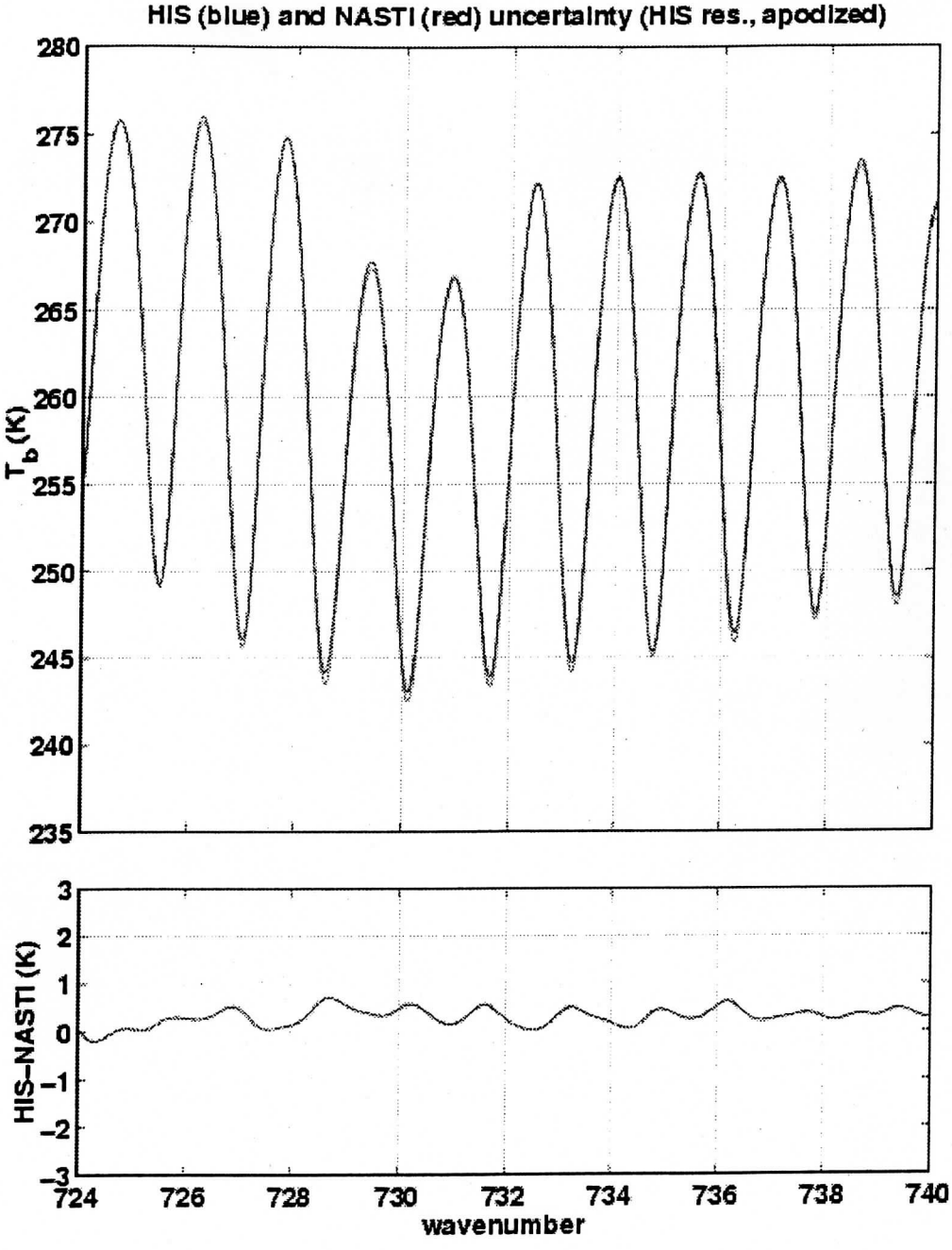
HIS (blue) and NASTI (red) uncertainty (HIS res., apodized)
T_b (K)
280
275
270
265
260
255
250
245
240
235
HIS–NASTI (K)
3
2
1
0
−1
−2
−3
724
726
728
730
732
734
736
738
740
wavenumber

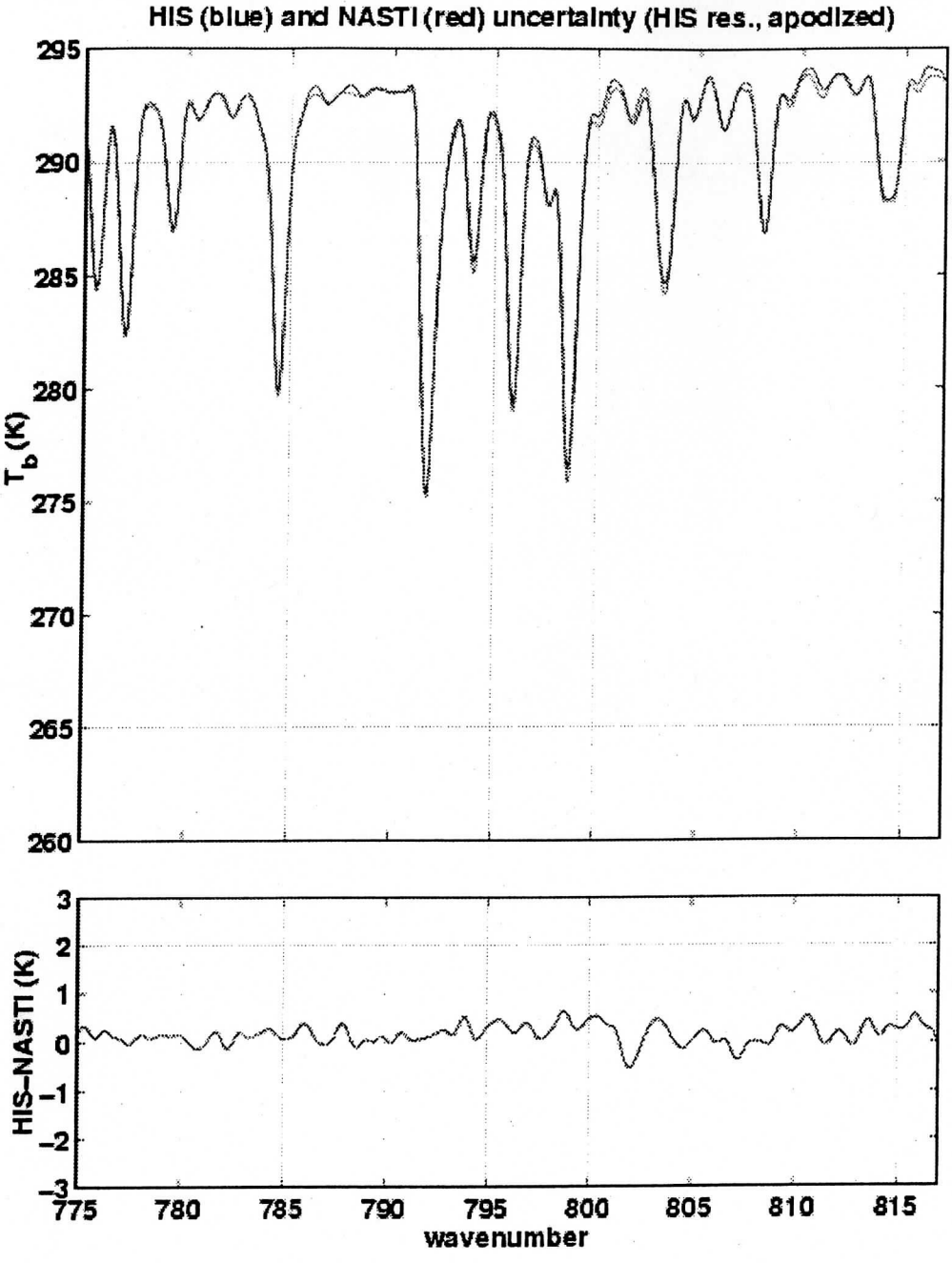
HIS (blue) and NASTI (red) uncertainty (HIS res., apodized)
295
290
285
280
275
270
265
260
T_b (K)
3
2
1
0
−1
−2
−3
HIS–NASTI (K)
775
780
785
790
795
800
805
810
815
wavenumber

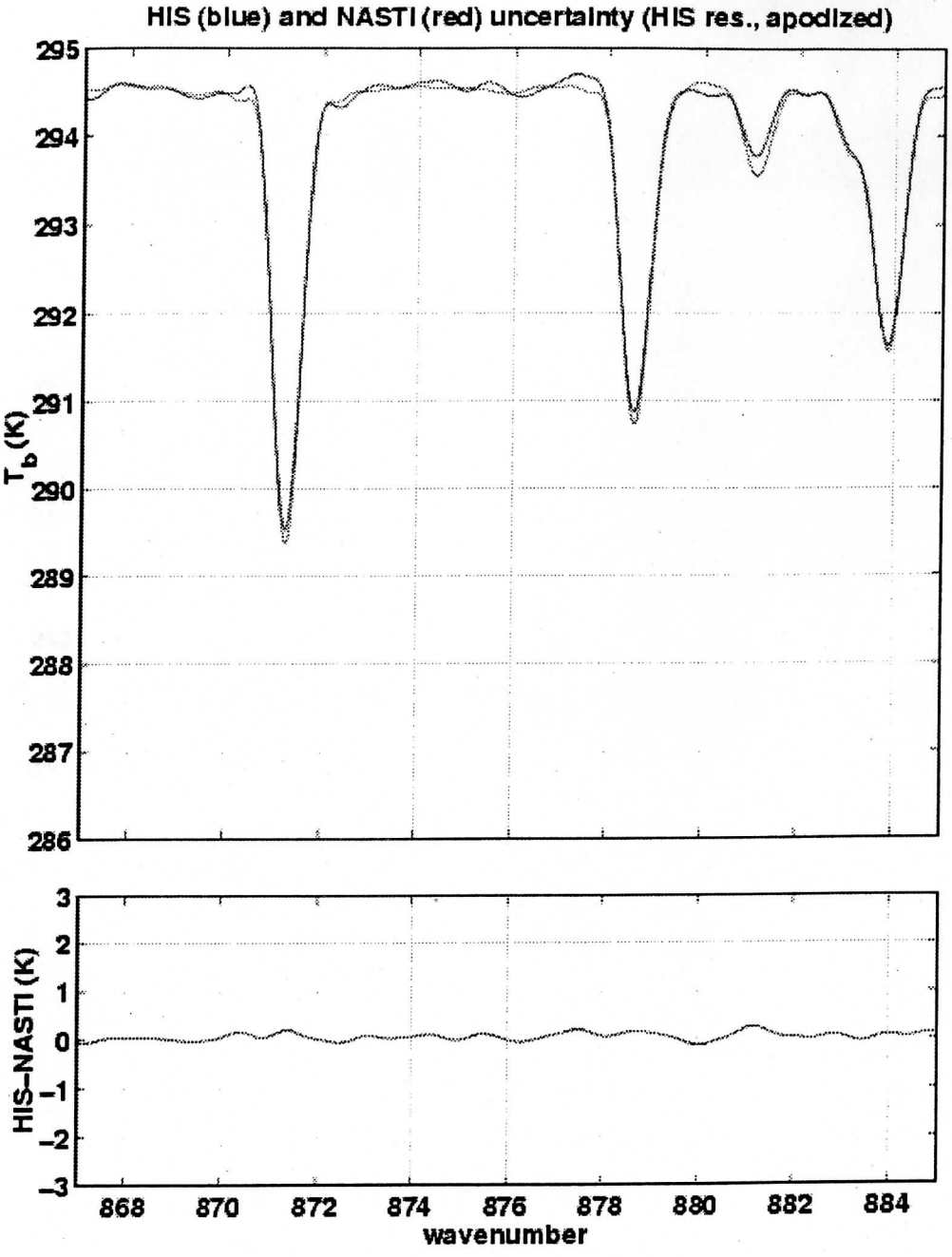
HIS (blue) and NASTI (red) uncertainty (HIS res., apodized)
295
294
293
292
291
290
289
288
287
286
T_b (K)
3
2
1
0
−1
−2
−3
HIS–NASTI (K)
868
870
872
874
876
878
880
882
884
wavenumber

40

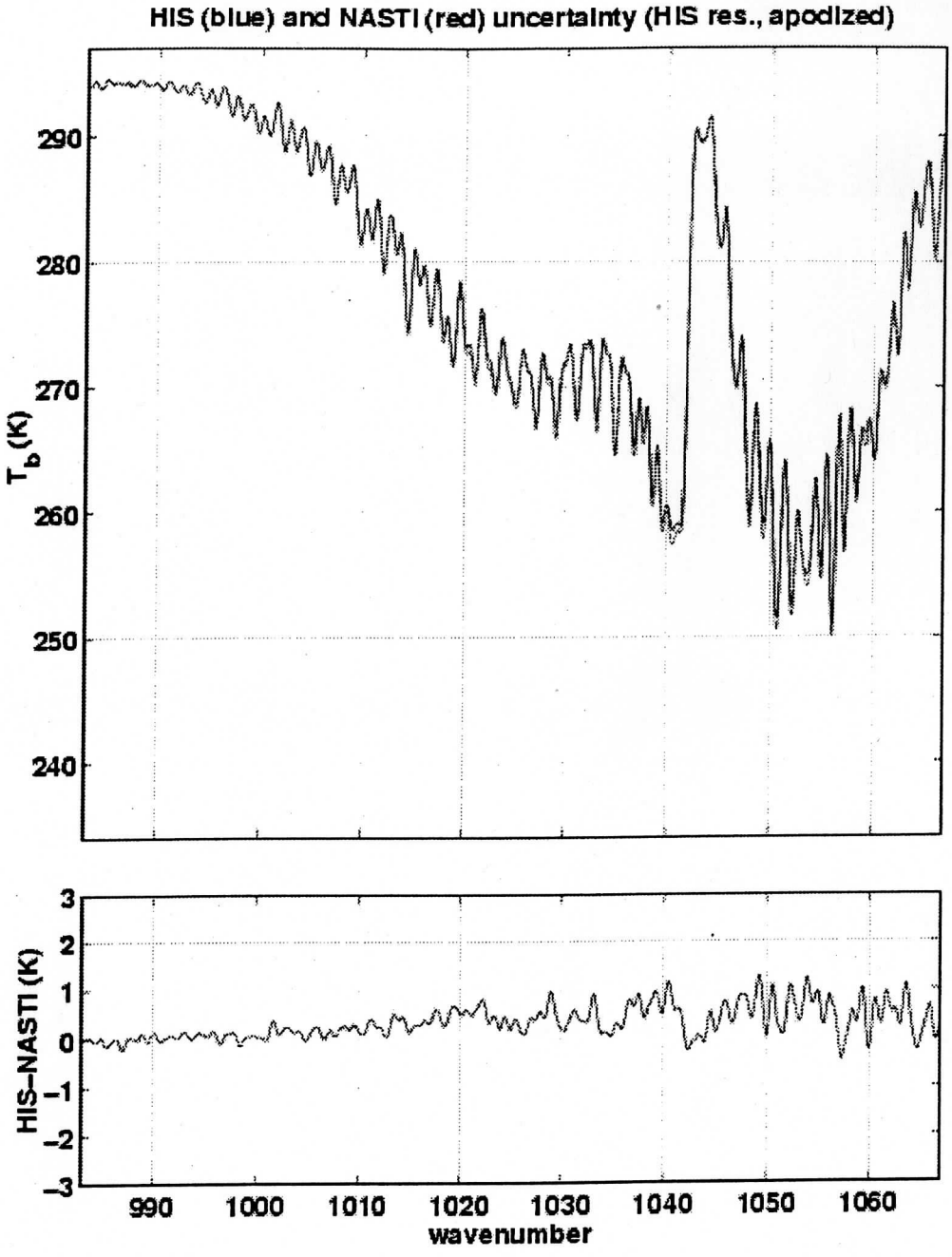
HIS (blue) and NASTI (red) uncertainty (HIS res., apodized)
290
280
270
260
250
240
T_b (K)
3
2
1
0
−1
−2
−3
HIS–NASTI (K)
990
1000
1010
1020
1030
1040
1050
1060
wavenumber

University of Wisconsin

FY99 Final Report

Engineering and Scientific Support for the National Polar-orbiting Operational Environmental Satellite System Airborne Sounder Testbed - Interferometer (NAST-I) Instrument

30 September 1999

Deliverables by Task:

Task 1

Report documenting the operational functionality of NAST-I during CAMEX-3

3.NASTI Validation: Comparison with AERI from Wallops 98 :
URL: http://danspc.larc.nasa.gov/NAST/val_aeri.html

42

NASTI Validation: comparison with uplooking AERI spectra

This page presents validation of the NASTI based on comparisons with the the University of Wisconsin AERI prototype instrument. During the Wallops '98 field campaign (at the Wallops Flight Facility in Wallops Island, Virginia), the NAST-I was placed next to the AERI and coincident uplooking spectra were recorded. The following figure shows the mean AERI and NASTI calibrated spectra measured on 980627 from 1:44:30 to 2:00:05 UTC (~10 pm local). This is an average of 71 individual nadir NASTI spectra and 3 nadir AERI spectra. The atmosphere was clear and stable during this time period. Also shown is a line-by-line calculation performed using LBLRTM and a Vaisala RS-80 radiosonde launched at 02:00:00 UTC from the same site. (In this figure and all others on this page, the NASTI spectra and calculation have been reduced to AERI spectral resolution.)

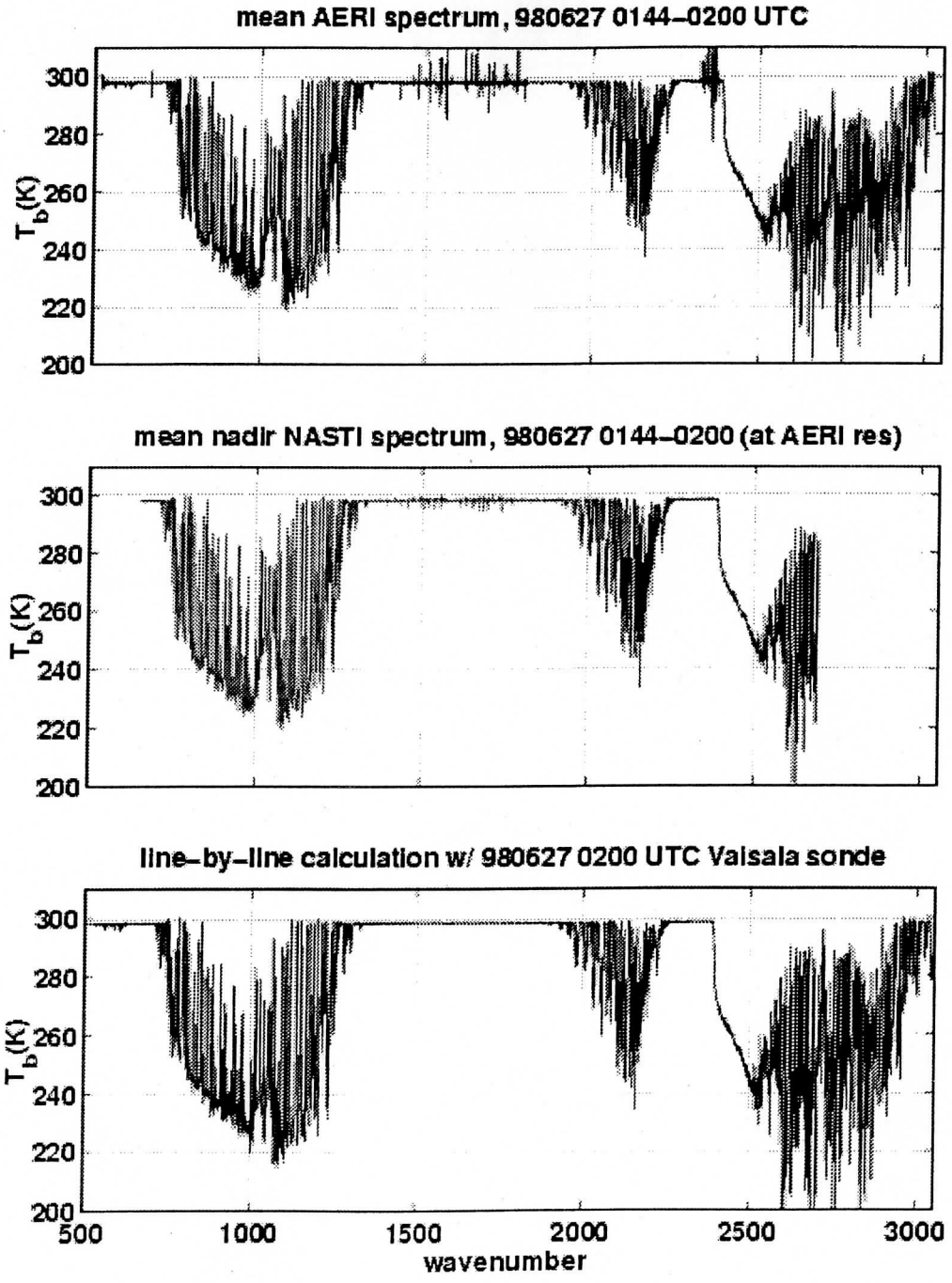

43

gif | gif (landscape) | eps | eps (landscape)

channel 1 only: gif | eps, channel 2 only: gif | eps, channel 3 only: gif | eps

The uncertainty in these mean spectra are shown in the following figures:

- AERI : gif | eps
- NASTI : gif | eps
- AERI and NASTI overlaid : gif | eps

The AERI/NASTI radiance differences:

- channel 1 (shortwave) : gif | eps
- channel 2 (midwave) : gif | eps
- channel 3 (longwave) : gif | eps

And the differences in brightness temperature:

- channel 1 (shortwave) : gif | eps
  - 2000-2070 cm^{-1}: gif | eps
  - 2170-2220 cm^{-1}: gif | eps
  - 2350-2450 cm^{-1}: gif | eps
- channel 2 (midwave) : gif | eps
- channel 3 (longwave) : gif | eps
  - 695-760 cm^{-1}: gif | eps
  - 780-900 cm^{-1}: gif | eps
  - 1100-1150 cm^{-1}: gif | eps

Last modified: Tue Dec 29 10:19:54 UTC 1998

Task 4

- Retrieval algorithm development summary
  URL: http://its.ssec.wisc.edu/nast/retrieval/description/

- Retrieval algorithm delivery schedule
  URL: http://its.ssec.wisc.edu/nast/retrieval/delivery/
  NOTE -- delivery made to NASA-LaRC as per P.I. request, future / ongoing work declared. No general public release of retrieval code allowed, only delivery to NASA-LaRC permitted.

- Accurate 3-D representation of NAST-I derived atmospheric parameters
  URL: http://its.ssec.wisc.edu/nast/retrieval/3-D/

Summary

This web page represents the final report of the FY99 activities of the University of Wisconsin under contract to NASA Langley Research Center in support of the NAST-I instrument and data analysis. All required tasks were completed through the period of performance ending September 30, 1999.

Points of Contact:

Principal Investigator: hank.revercomb@ssec.wisc.edu

Program Manager: fred.best@ssec.wisc.edu

Final Report: robert.knuteson@ssec.wisc.edu

Last Updated: 9 November 1999

---

mean AERI spectrum, 980627 0144–0200 UTC

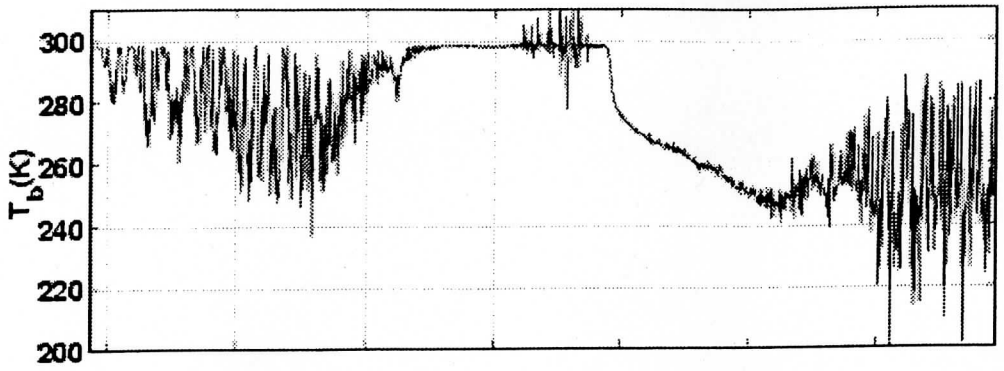

mean nadir NASTI spectrum, 980627 0144–0200 (at AERI res)

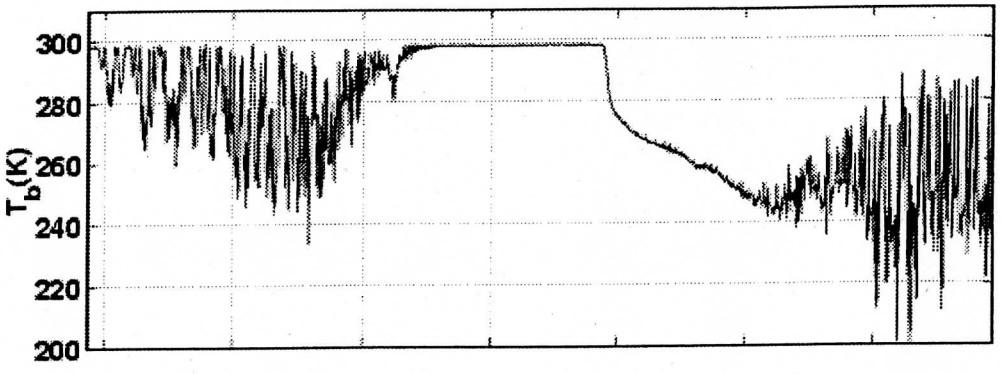

line–by–line calculation w/ 980627 0200 UTC Vaisala sonde

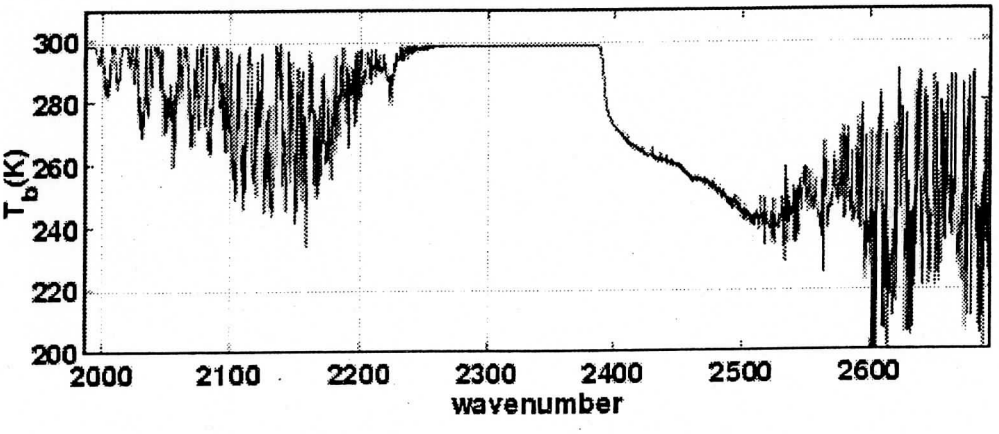

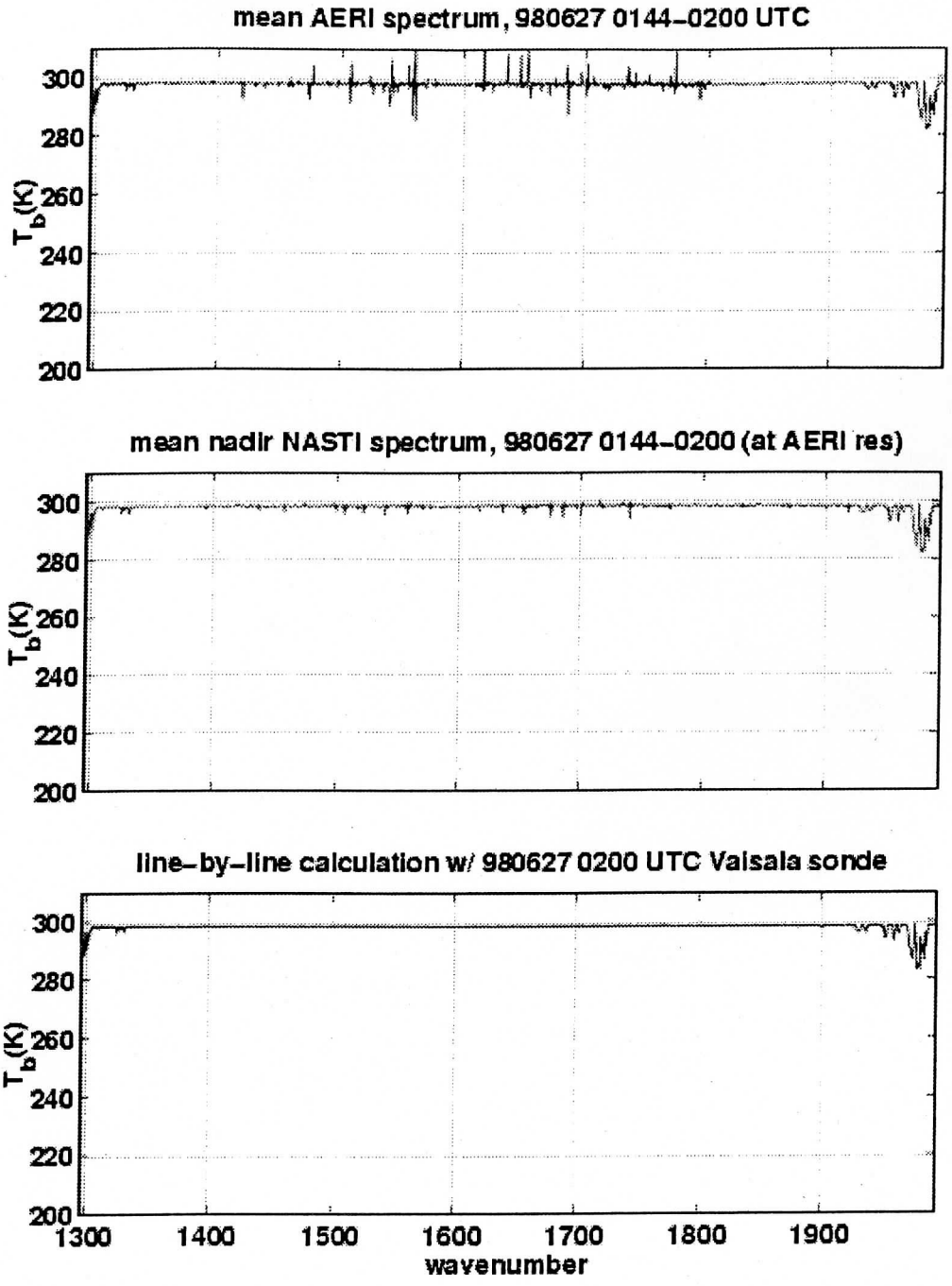
mean AERI spectrum, 980627 0144–0200 UTC
mean nadir NASTI spectrum, 980627 0144–0200 (at AERI res)
line–by–line calculation w/ 980627 0200 UTC Vaisala sonde
T_b(K)
300
280
260
240
220
200
1300
1400
1500
1600
1700
1800
1900
wavenumber

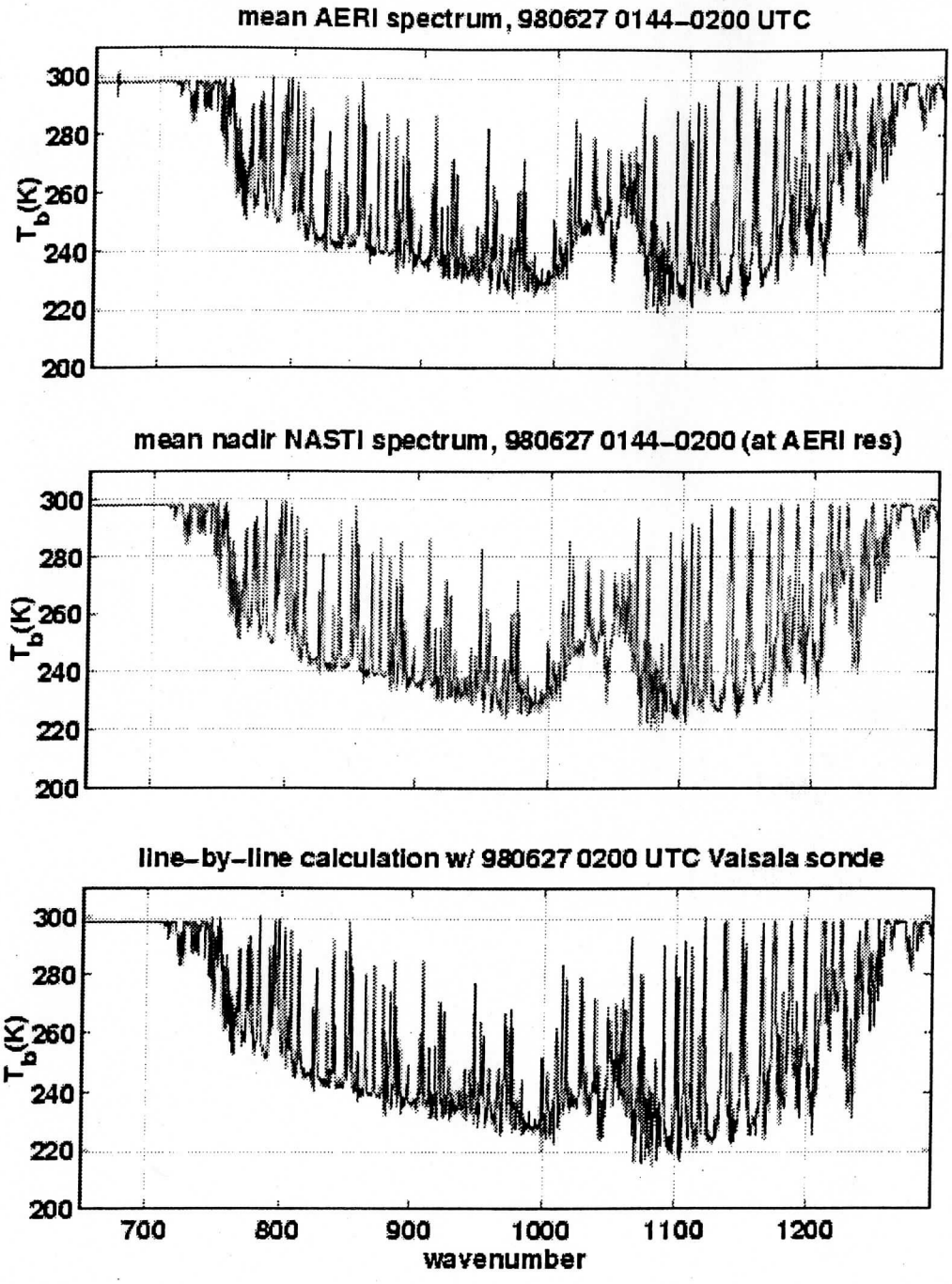
mean AERI spectrum, 980627 0144–0200 UTC
mean nadir NASTI spectrum, 980627 0144–0200 (at AERI res)
line–by–line calculation w/ 980627 0200 UTC Vaisala sonde
T_b(K)
300
280
260
240
220
200
700
800
900
1000
1100
1200
wavenumber

48

uncertainty in mean AERI spectrum

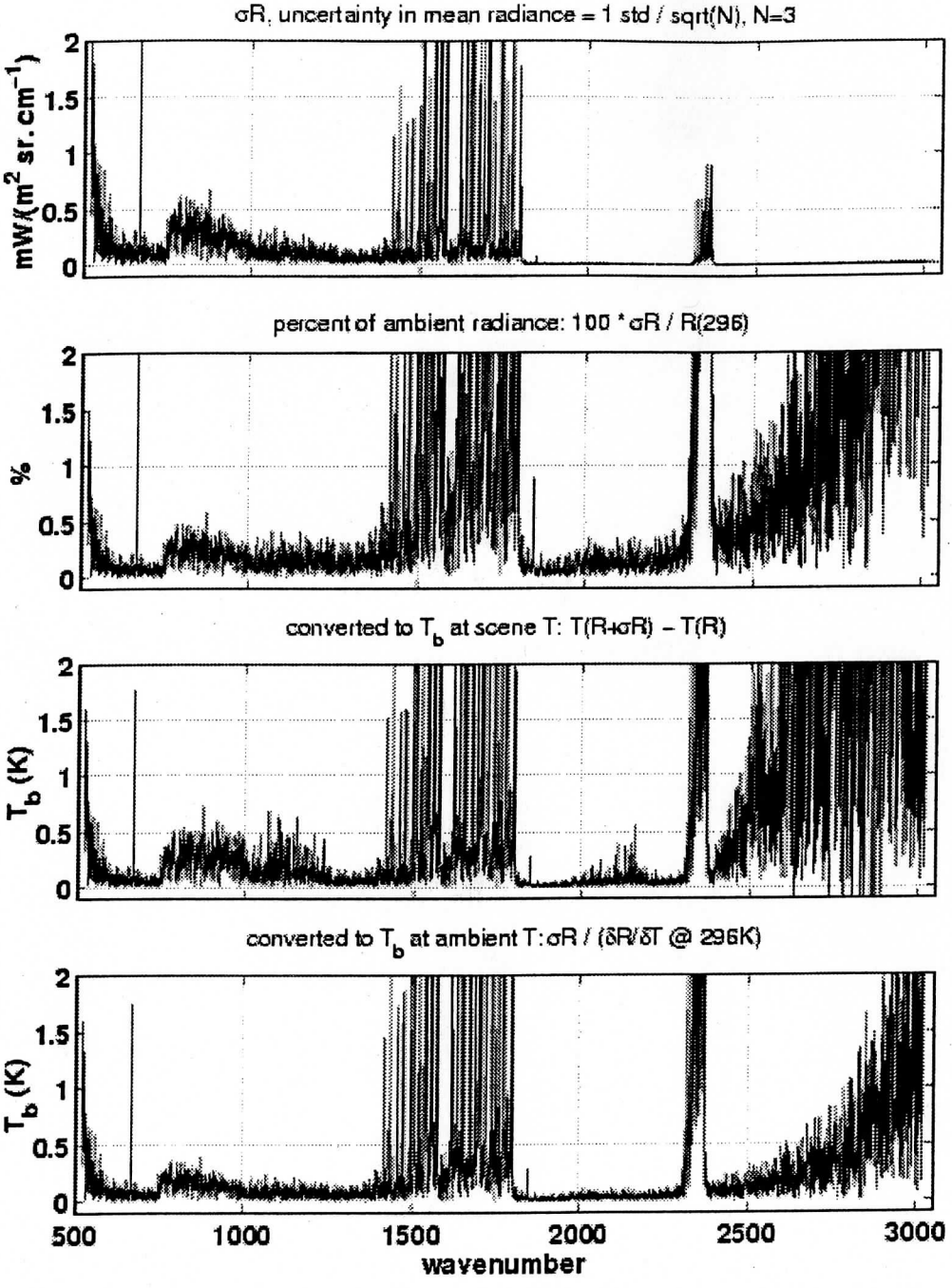

uncertainty in mean spectra: AERI (blue) and NASTI (red) at AERI res.

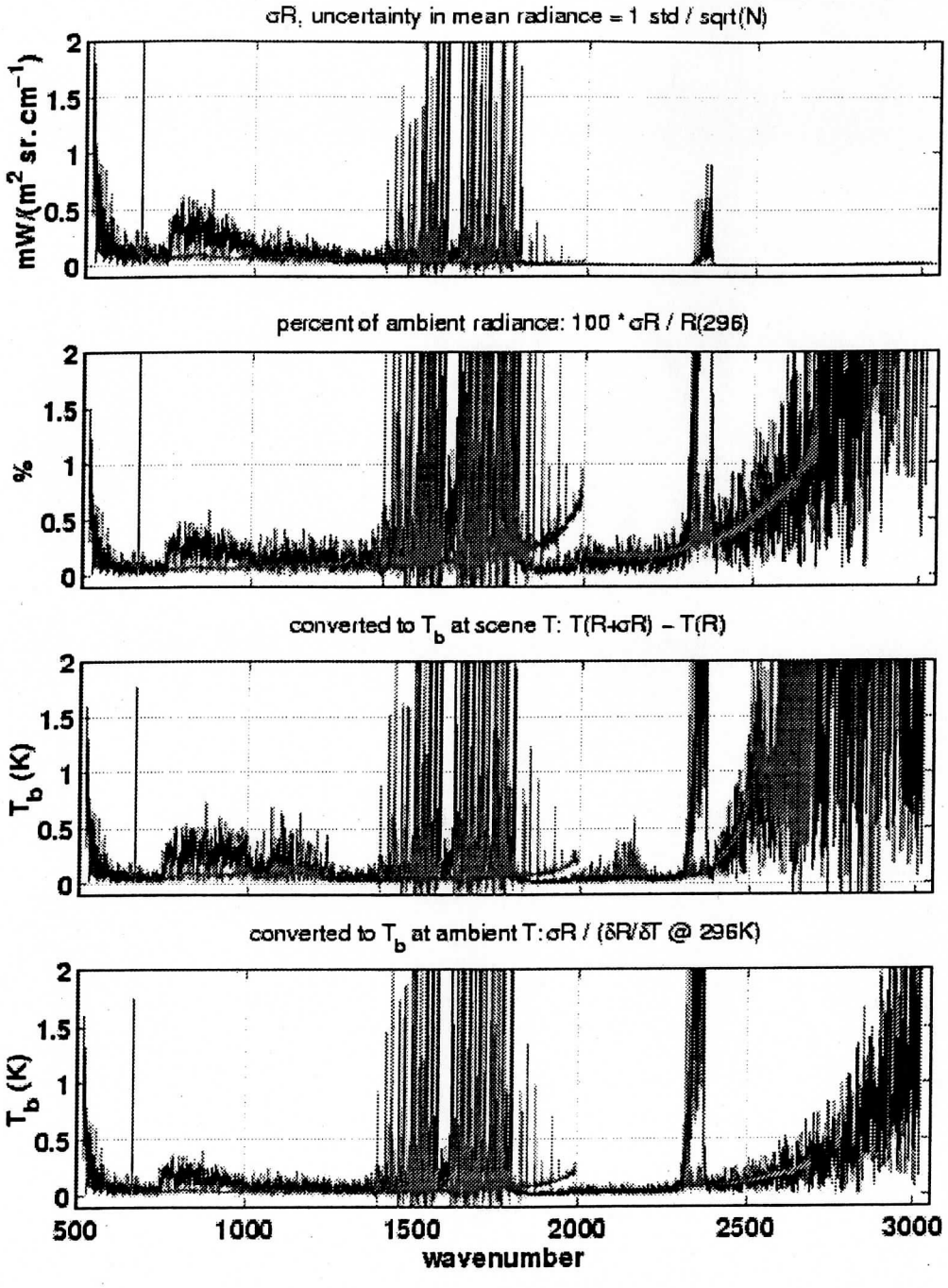

50

channel 1 mean radiances : AERI (blue), NASTI (red), and calculation (black) at AERI re

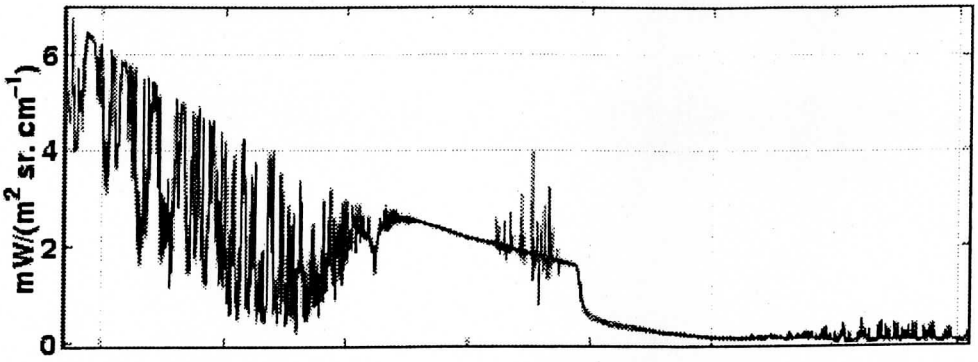

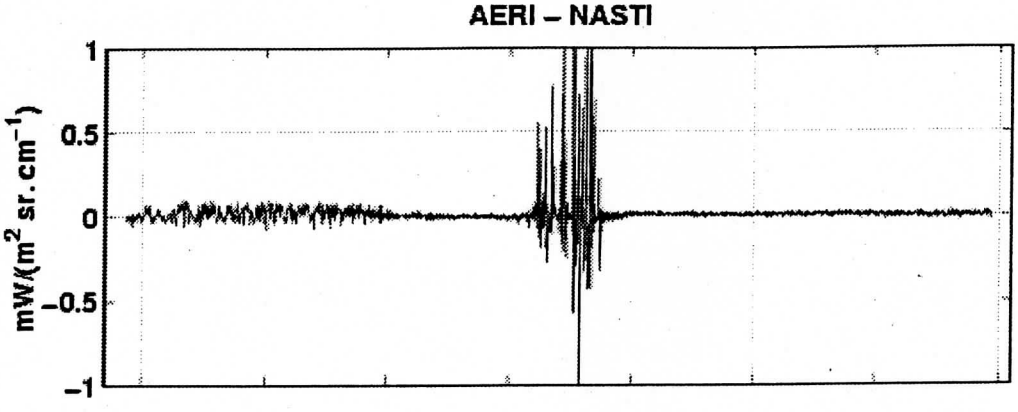

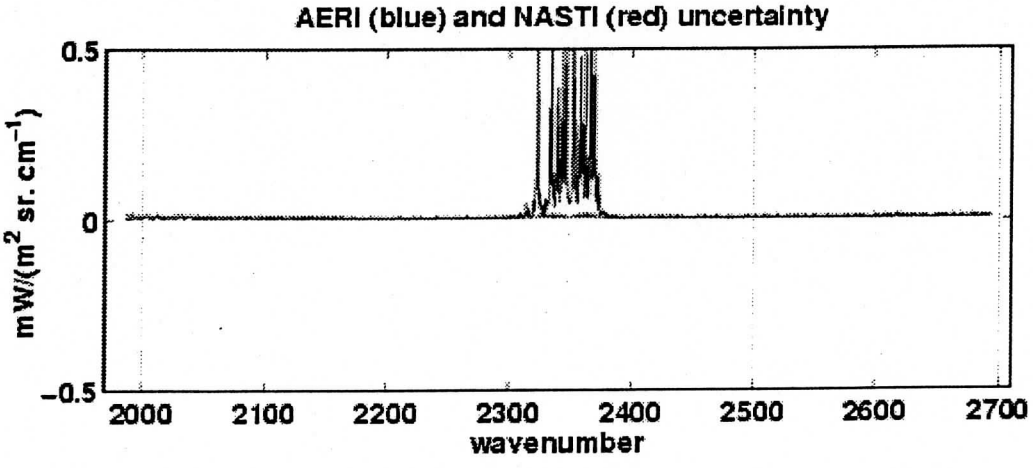

51

channel 2 mean radiances : AERI (blue), NASTI (red), and calculation (black) at AERI re

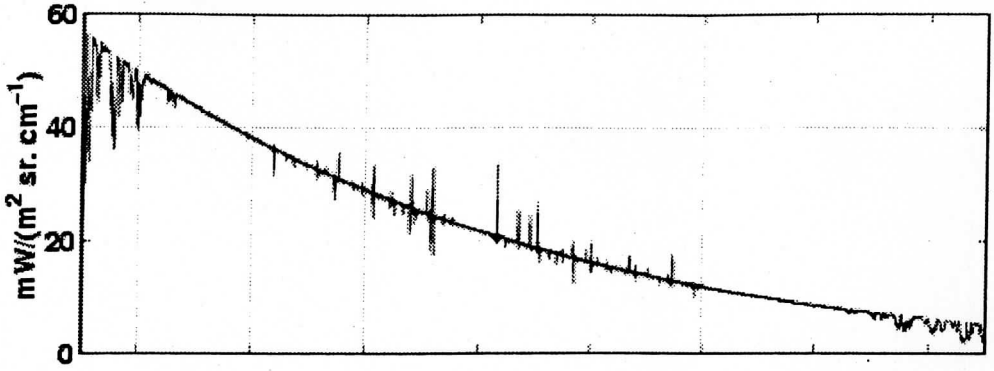

AERI – NASTI

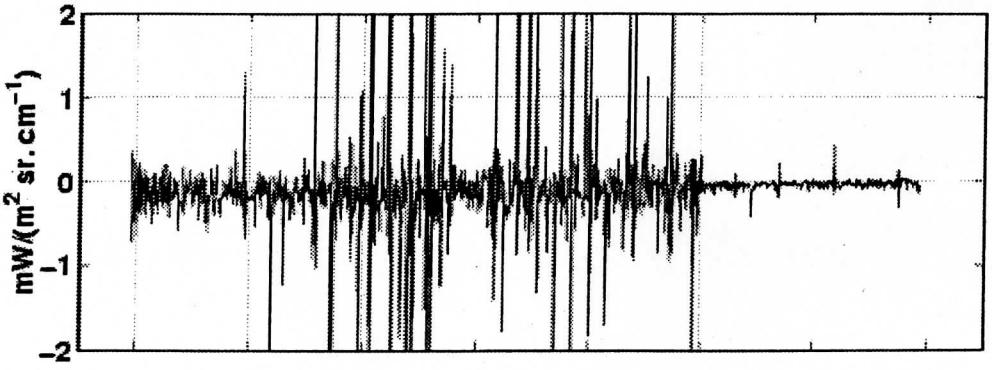

AERI (blue) and NASTI (red) uncertainty

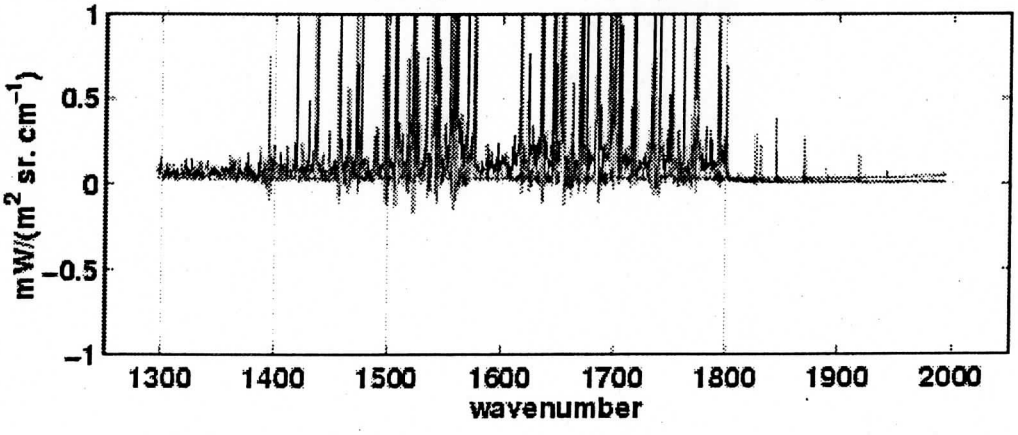

channel 3 mean radiances : AERI (blue), NASTI (red), and calculation (black) at AERI re

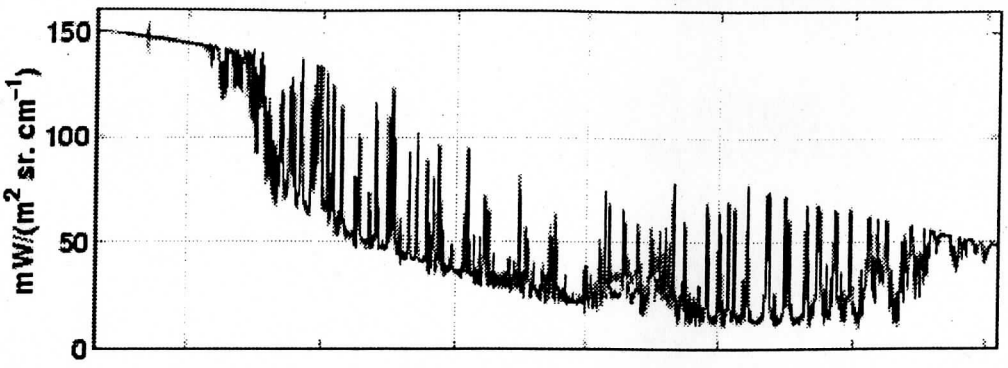

AERI – NASTI

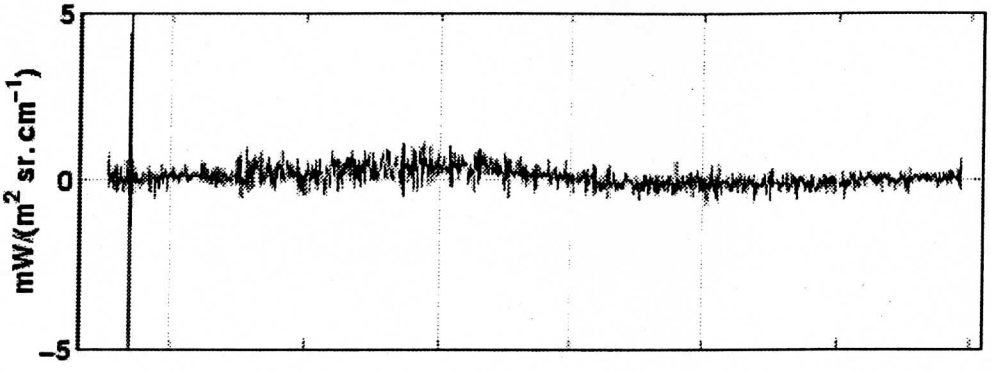

AERI (blue) and NASTI (red) uncertainty

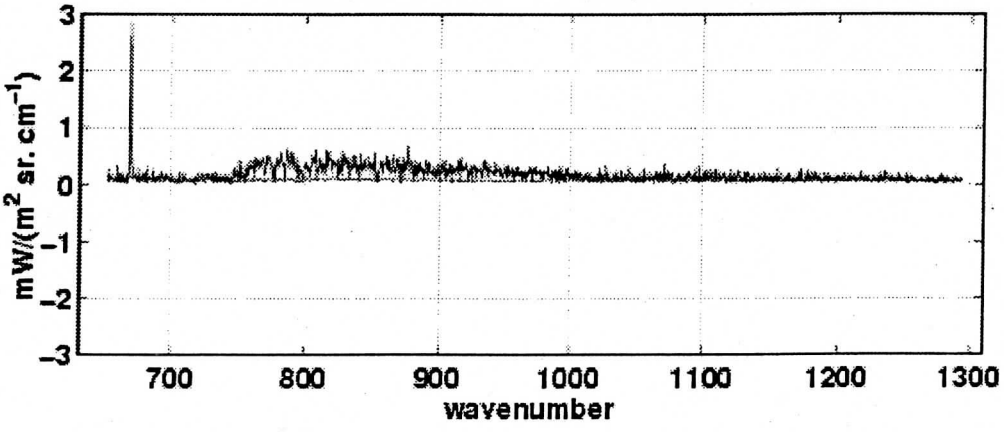

53

channel 1 mean T_b : AERI (blue), NASTI (red), and calculation (black) at AERI res

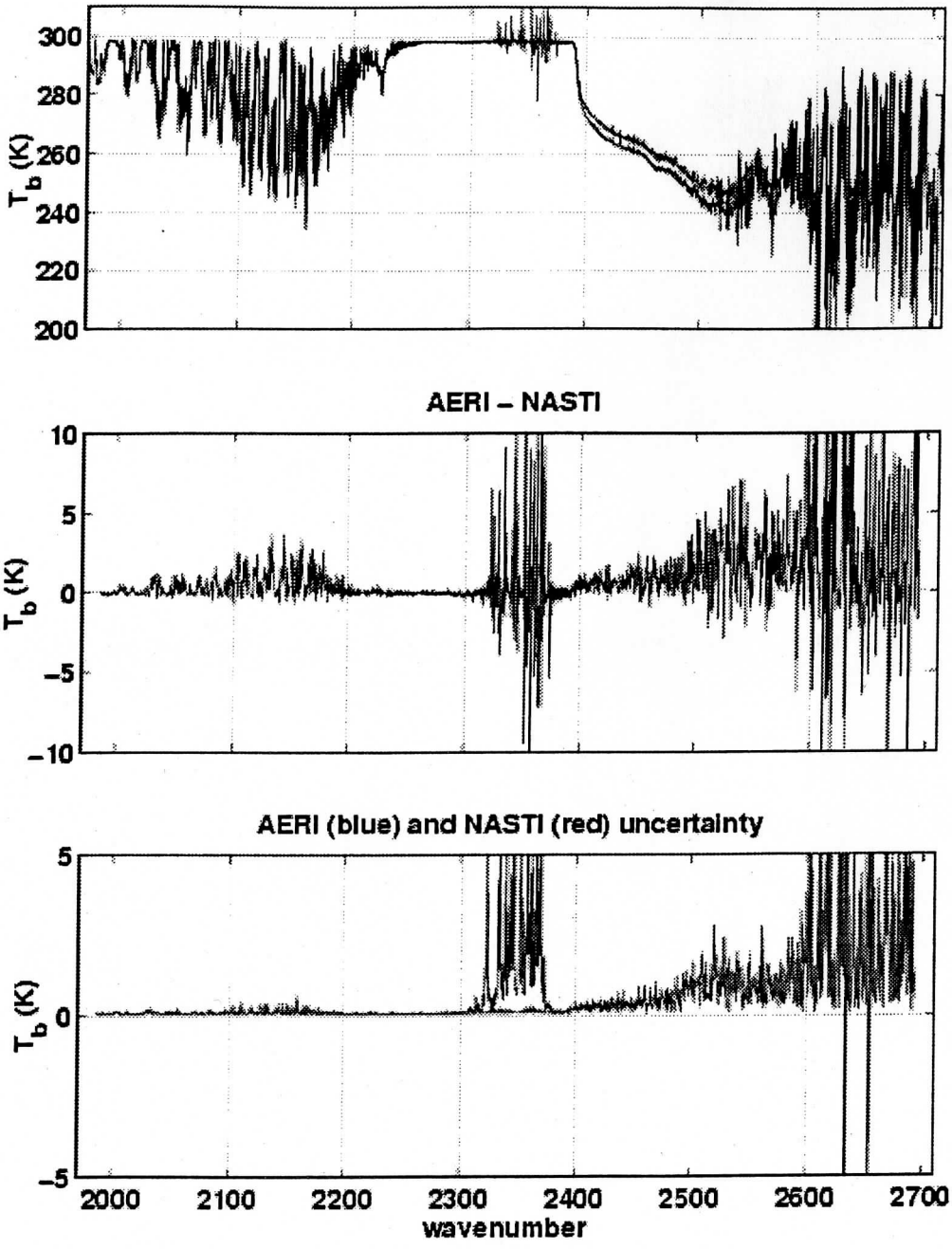

54

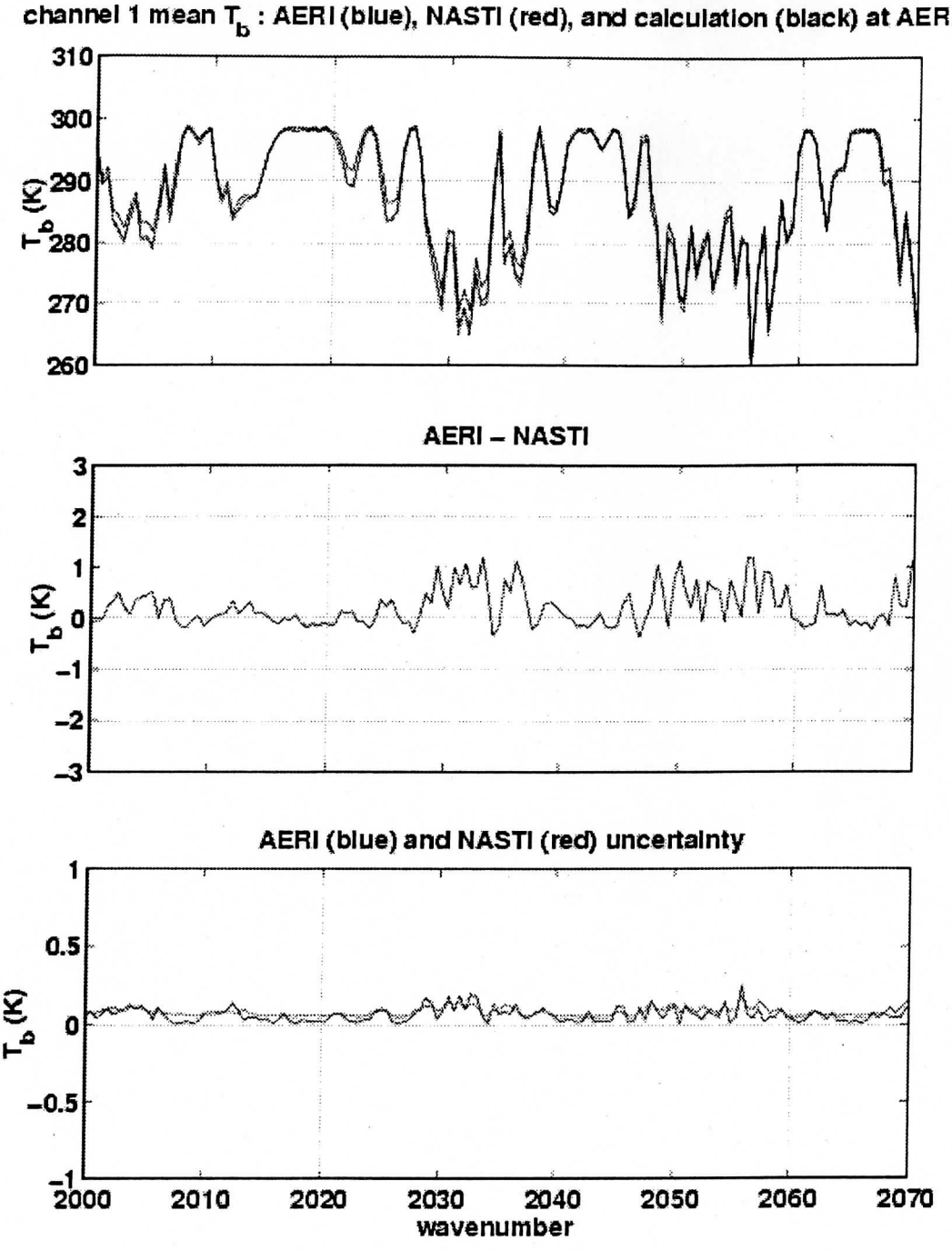
channel 1 mean T_b : AERI (blue), NASTI (red), and calculation (black) at AERI res
310
300
290
280
270
260
T_b (K)
AERI – NASTI
3
2
1
0
−1
−2
−3
T_b (K)
AERI (blue) and NASTI (red) uncertainty
1
0.5
0
−0.5
−1
T_b (K)
2000
2010
2020
2030
2040
2050
2060
2070
wavenumber

channel 1 mean T_b : AERI (blue), NASTI (red), and calculation (black) at AERI res

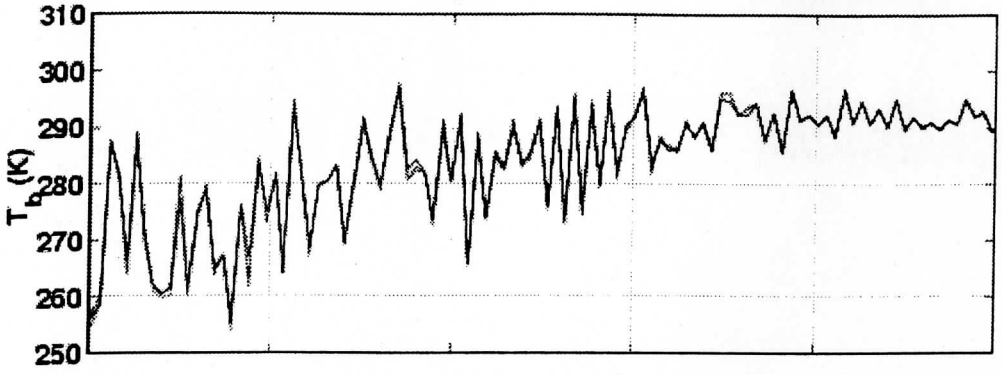

AERI – NASTI

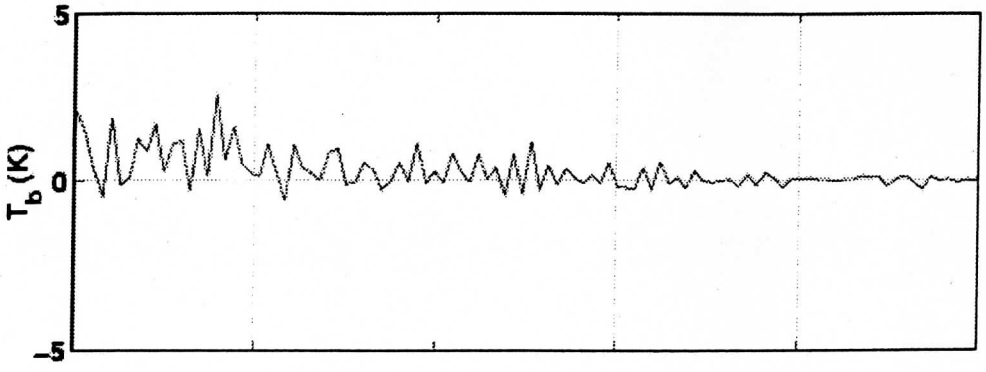

AERI (blue) and NASTI (red) uncertainty

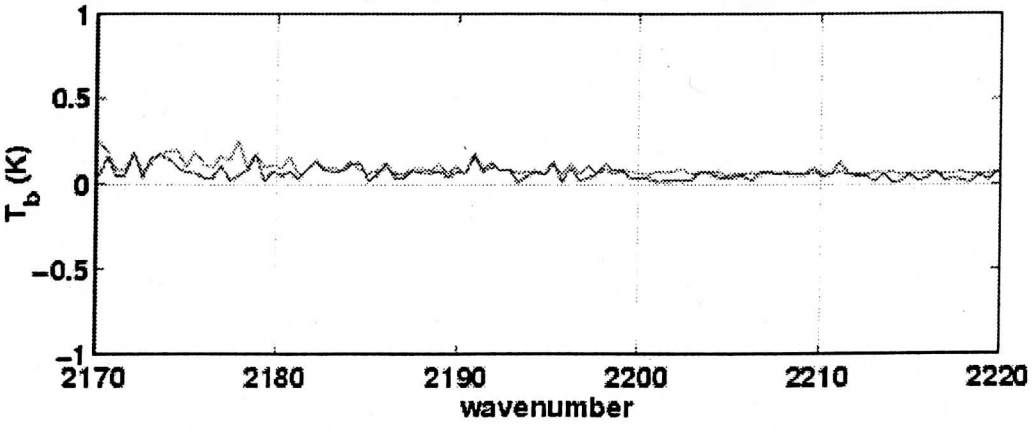

56

channel 1 mean T_b : AERI (blue), NASTI (red), and calculation (black) at AERI res

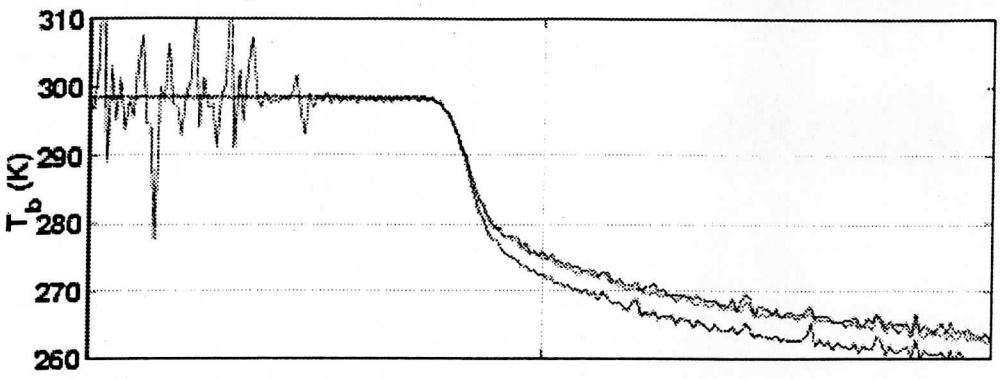

AERI – NASTI

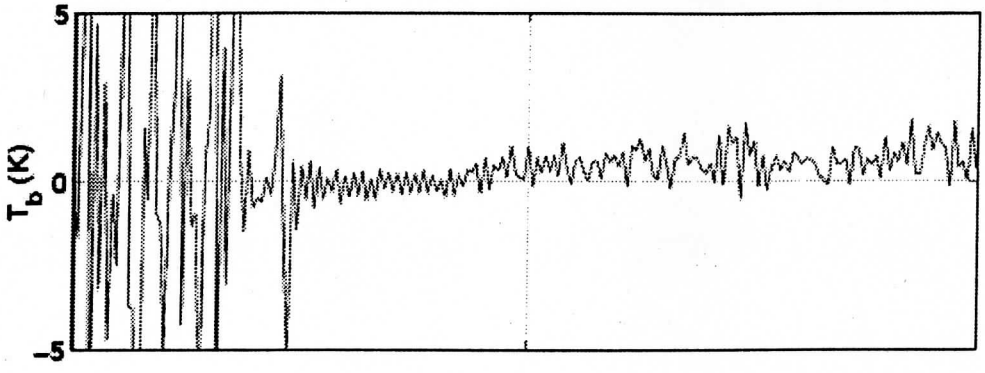

AERI (blue) and NASTI (red) uncertainty

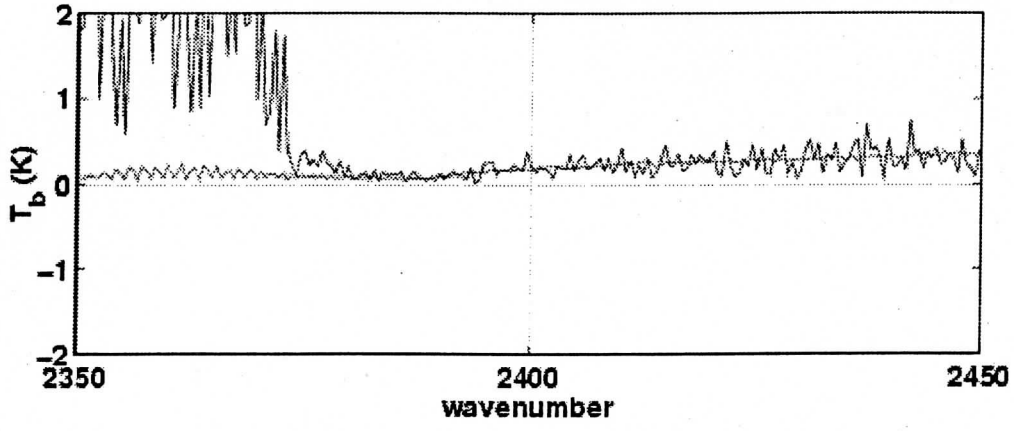

57

channel 2 mean T_b : AERI (blue), NASTI (red), and calculation (black) at AERI res

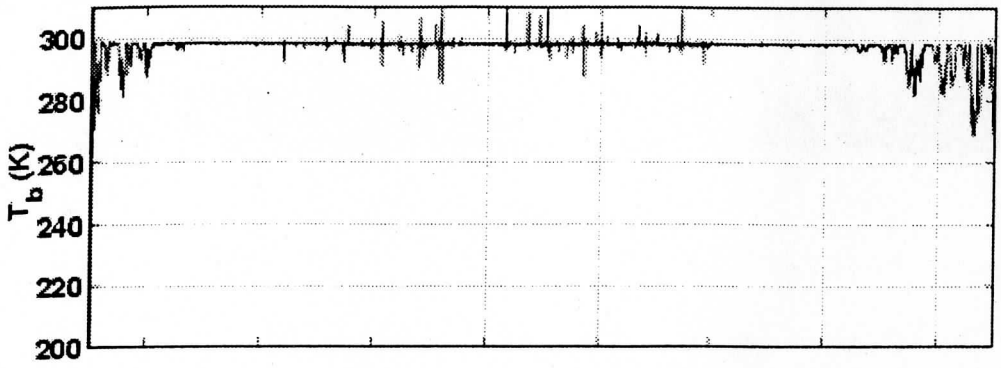

AERI – NASTI

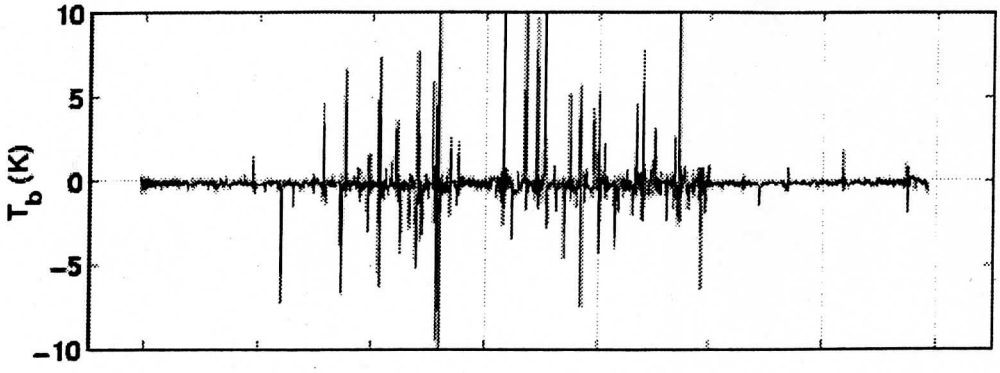

AERI (blue) and NASTI (red) uncertainty

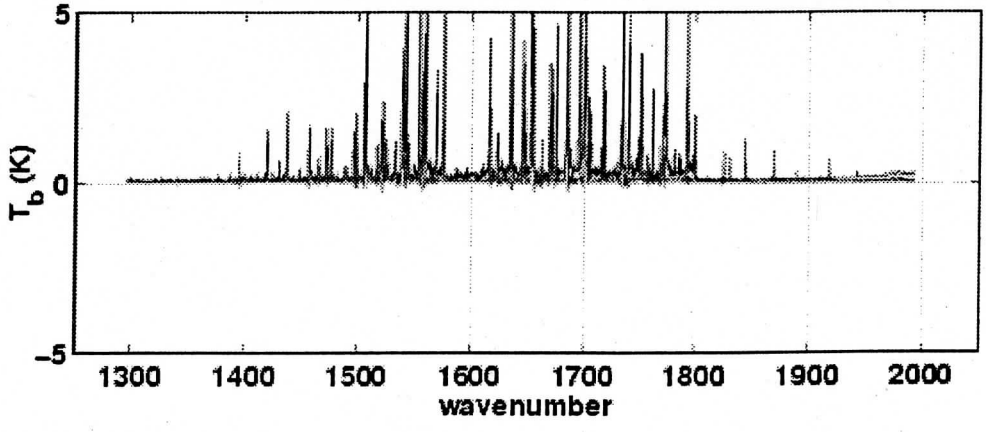

58

channel 3 mean T_b : AERI (blue), NASTI (red), and calculation (black) at AERI res

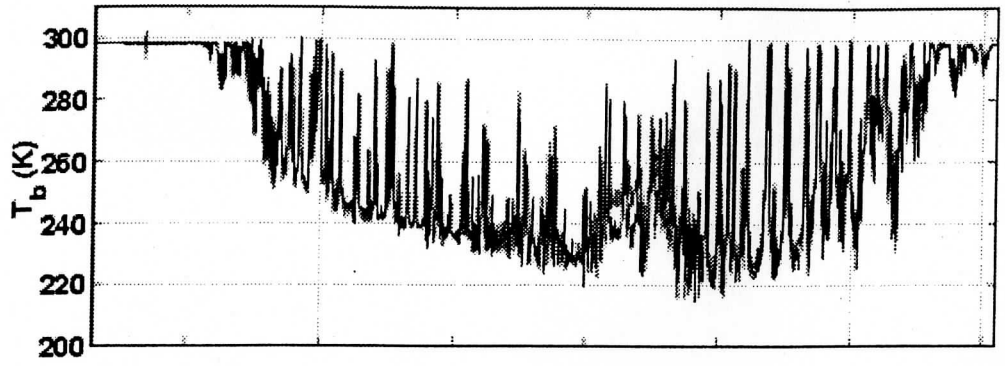

AERI – NASTI

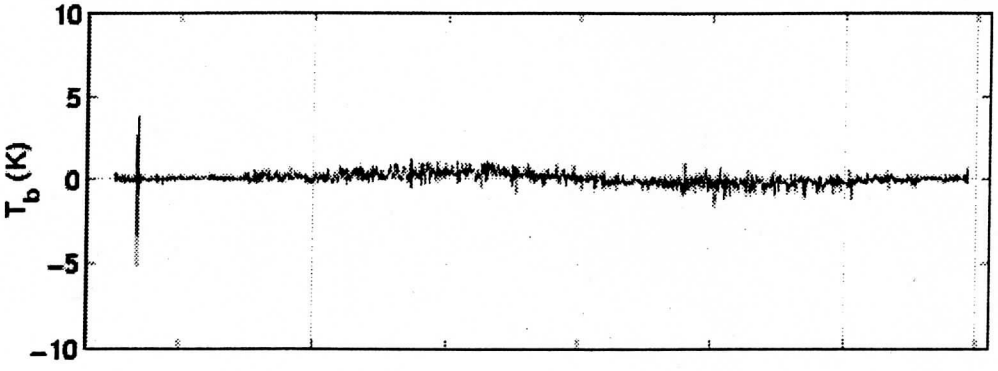

AERI (blue) and NASTI (red) uncertainty

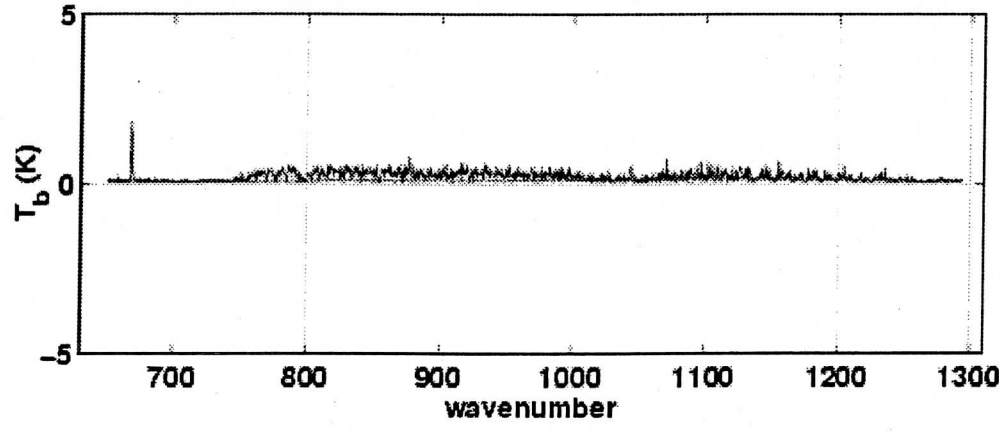

59

channel 3 mean T_b : AERI (blue), NASTI (red), and calculation (black) at AERI res

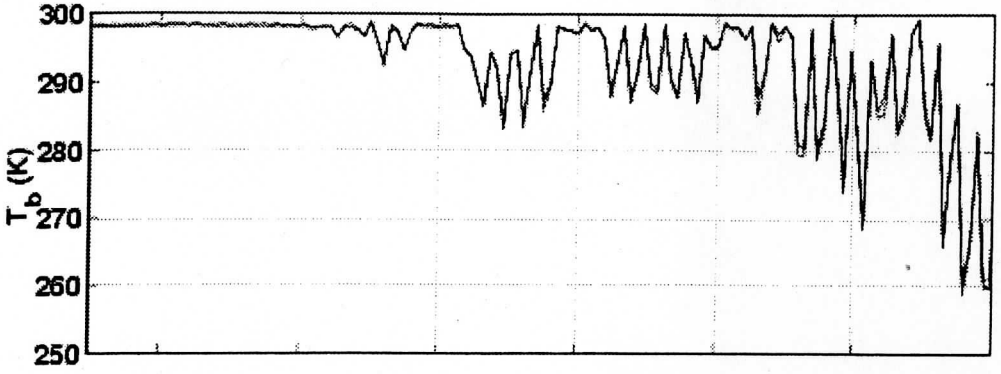

AERI – NASTI

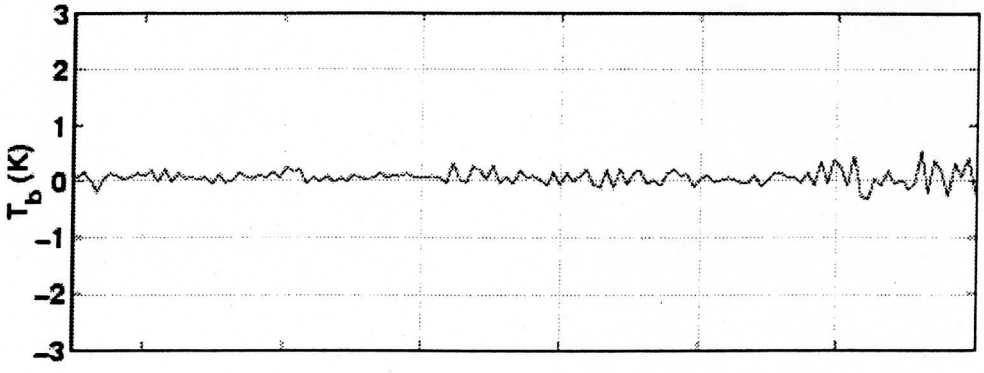

AERI (blue) and NASTI (red) uncertainty

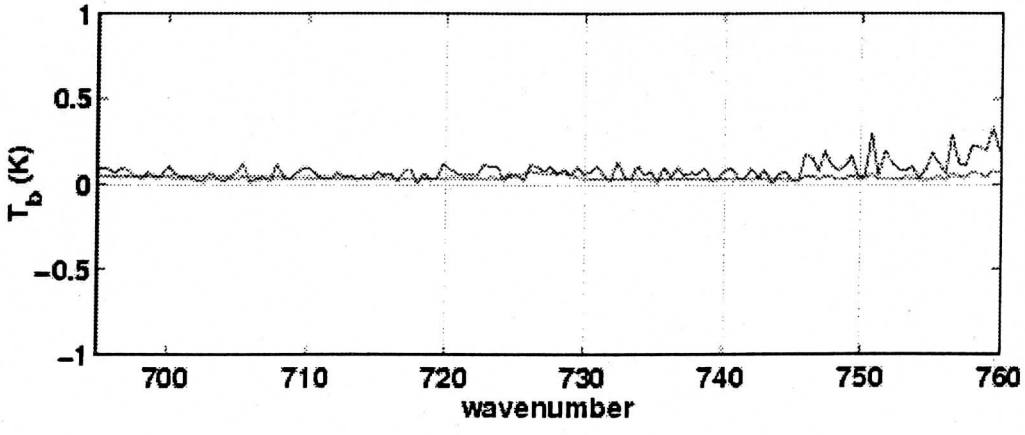

60

channel 3 mean T_b : AERI (blue), NASTI (red), and calculation (black) at AERI res

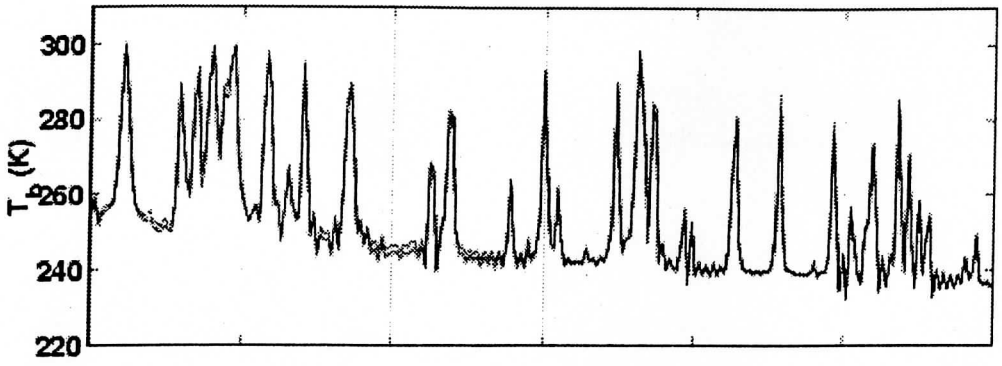

AERI – NASTI

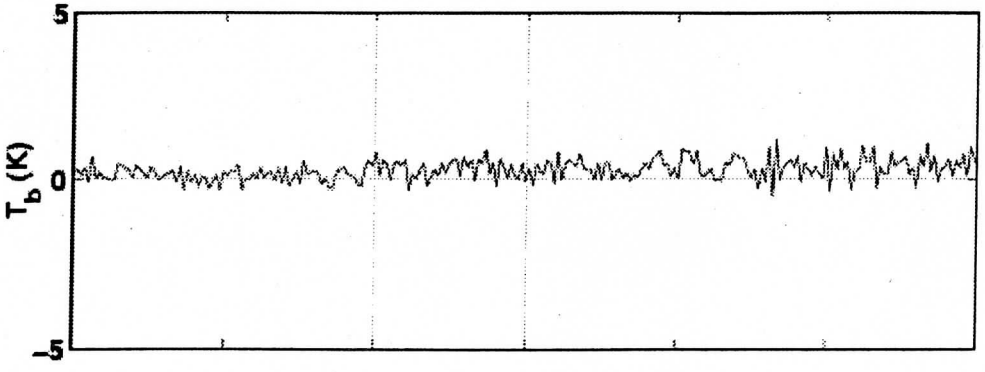

AERI (blue) and NASTI (red) uncertainty

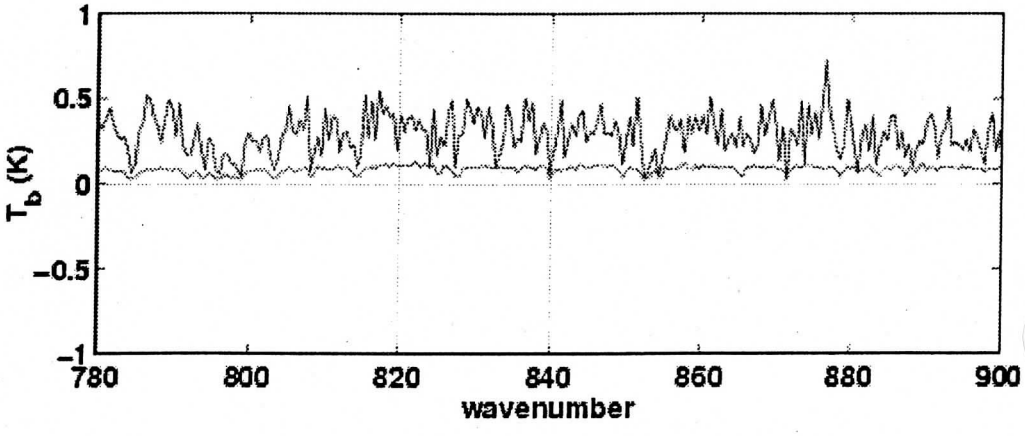

61

channel 3 mean T_b : AERI (blue), NASTI (red), and calculation (black) at AERI res

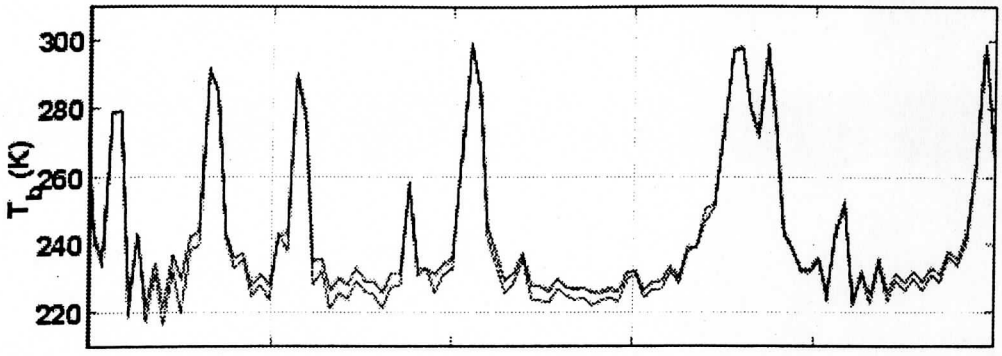

AERI – NASTI

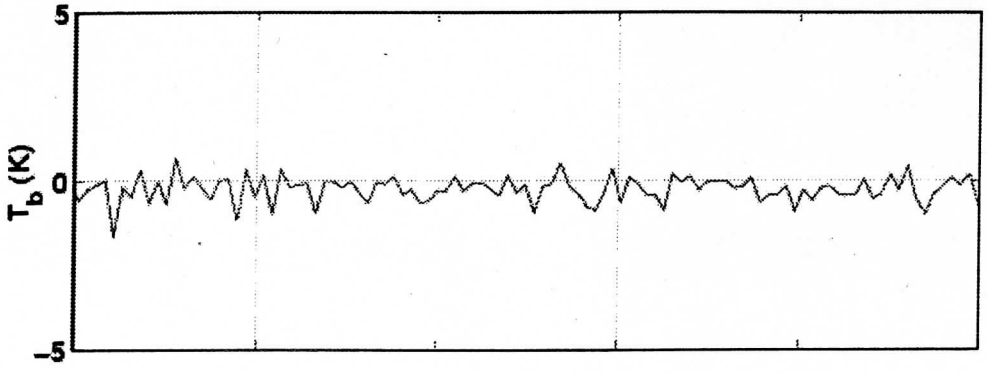

AERI (blue) and NASTI (red) uncertainty

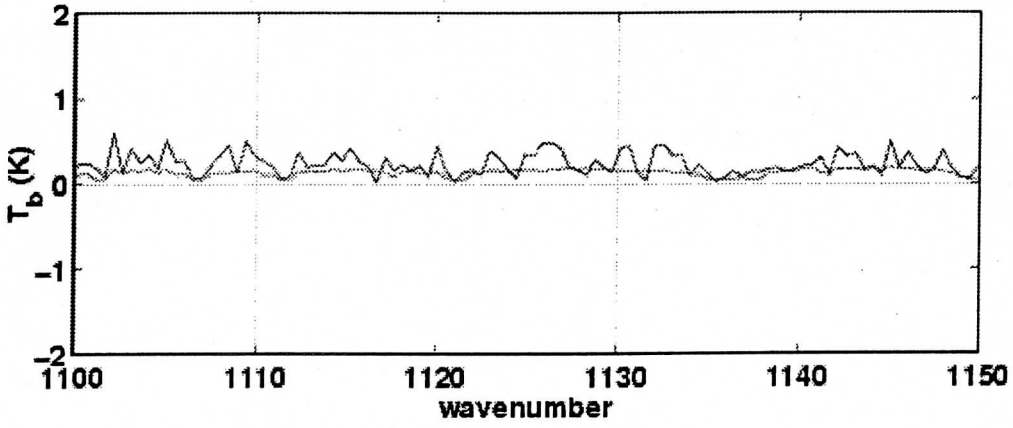

University of Wisconsin

FY99 Final Report

Engineering and Scientific Support for the National Polar-orbiting Operational Environmental Satellite System Airborne Sounder Testbed - Interferometer (NAST-I) Instrument

30 September 1999

Deliverables by Task:

Task 1

Report documenting the operational functionality of NAST-I during CAMEX-3

4.Data Processing Summary
URL: http://tyler.ssec.wisc.edu/~bobk/camex3/proc_status.html

Processing Status for NAST-I CAMEX3 Data: (Reload page to receive latest updates)

ER2 Sortie	Launch Date	Comment	Raw Data Archive	Calibration	QCed Radiances	3-Line-Smoothed (w/o tilt corr)	Tilt Corrected 3-Line-Smooth
98-105	980805	Ferry Flight	~NASTI-03,04	* 4/12/99 ROK NASTI-107	*6/2/99 ROK NASTI-180,181	*6/5/99 ROK NASTI-182	*7/9/99 ROK NASTI-183
98-106	980808	Instrument Failed No Data	NA	NA	NA	NA	NA
98-107	980813	TEFLUN-B and Andros Island	~NASTI-05,06	* 4/13/99 ROK NASTI-108	*5/28/99 ROK NASTI-176,177	*5/28/99 ROK NASTI-178	*7/13/99 ROK NASTI-179
98-108	980815	TEFULN-B and TRMM underfly	~NASTI-07	* 4/14/99 ROK	* 4/14/99 ROK NASTI-109,110	*5/27/99 ROK NASTI-174	*7/13/99 ROK NASTI-175
98-109	980823	H. Bonnie Eyewall and Andros Island	NASTI-08,09,10	6/7/99 ROK	6/7/99 ROK NASTI-184,185, NASTI-186,187	6/9/99 ROK NASTI-188,189	6/9/99 ROK NASTI-190,19
98-110	980824	H. Bonnie Eyewall	NASTI-11,12,13	*4/23/99 ROK	* 4/23/99 ROK NASTI-122,123	*5/26/99 ROK NASTI-170,171	*5/26/99 ROK NASTI-172,17
98-111	980826	H. Bonnie Landfall	NASTI-14,15,16	* 4/18/99 ROK	* 4/19/99 ROK NASTI-118,119,120	* 5/20/99 ROK NASTI-158,159	* 5/21/99 ROK NASTI-160,16
98-112	980829	ER-2 Abort No Data	NA	NA	NA	NA	NA
98-113	980830	H. Danielle	NASTI-19,20	4/24/99 ROK	4/24/99 ROK NASTI-124,125	5/21/99 ROK NASTI-162	5/21/99 ROK NASTI-163
98-114	980902	H. Earl	NASTI-25,26	4/25/99 ROK	4/25/99 ROK NASTI-126,127,128	5/22/99 ROK NASTI-168	5/25/99 ROK NASTI-169
98-115	980905	TEFLUN-B and TRMM underfly	NASTI-29,30	4/26/99 ROK	4/26/99 ROK NASTI-129	5/22/99 ROK NASTI-166	5/22/99 ROK NASTI-167
98-116	980908	TEFLUN-B	NASTI-32	4/27/99 ROK	4/27/99 ROK NASTI-130	5/22/99 ROK NASTI-164	5/22/99 ROK NASTI-165
98-117	980913	EOS Calibration / Validation	NASTI-34,35	4/28/99 ROK	4/28/99 ROK NASTI-131,132	4/28/99 ROK NASTI-137	5/19/99 ROK NASTI-142
98-118	980917	TEFLUN-B	NASTI-37,38	4/29/99 ROK	4/29/99 ROK NASTI-138,139	4/29/99 ROK NASTI-140	5/20/99 ROK NASTI-141
98-119	980921	H. Georges	NASTI-40,41,42	6/12/99 ROK	6/14/99 ROK NASTI-195,196 NASTI-197,198	6/15/99 ROK NASTI-201,202	6/15/99 ROK NASTI-199,20

98-120	980922	H. Georges Synoptic Inflow	NASTI-45,46,47	5/7/99 ROK	5/7/99 ROK NASTI-148,149,150	5/18/99 ROK NASTI-151,152	5/18/99 ROK NASTI-156,15
98-132	980923	Evacuation Flt.	NASTI-49	6/21/99 ROK	6/21/99 ROK NASTI-203	6/22/99 ROK NASTI-204	6/22/99 ROK NASTI-205
98-136	980925	H. Georges	NASTI-50,51,52	6/24/99 ROK	6/24/99 ROK NASTI-206,207 NASTI-208,209	6/24/99 ROK NASTI-210,211	6/25/99 ROK NASTI-212,21
98-137	980927	H. Georges Landfall	NASTI-53,54,55	6/28/99 ROK	6/28/99 ROK NASTI-214,215,217	6/28/99 ROK NASTI-216,220	7/1/99 ROK NASTI-218,21
98-138	980928	Ferry Flight	NASTI-56,57	7/7/99 ROK	7/7/99 ROK NASTI-221,222	7/8/99 ROK NASTI-223	7/9/99 ROK NASTI-224

* - HHMMSS time variable rounds to 99 minutes at the top of each hour.
~ - First three flights have excessive H2O inside instrument canister.
NA - Data Not Available

Processing Description

Last updated: 7/16/99 ROK

Contact: Robert Knuteson, robert.knuteson@ssec.wisc.edu, 608-263-7974

University of Wisconsin

FY99 Final Report

Engineering and Scientific Support for the National Polar-orbiting Operational Environmental Satellite System
Airborne Sounder Testbed - Interferometer (NAST-I) Instrument

30 September 1999

Deliverables by Task:

Task 1

Report documenting the operational functionality of NAST-I during CAMEX-3

5.Radiance Product Quicklooks
URL: http://cimss.ssec.wisc.edu/nast/camex3/camex3_index.html

66

NPOESS Aircraft Sounder Testbed - Interferometer

NAST-I Quicklooks (CAMEX-3)

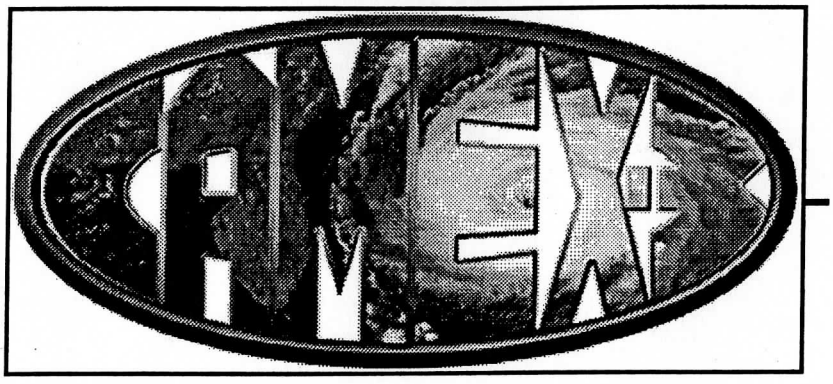

Missions completed to date (CAMEX-3):

- Sortie #98-105 **August 5, 1998** (Ferry Flight, DFRC to PAFB)
- Sortie #98-106 August 8, 1998 (Checkout and Andros Overflight) RAM chip failure (no data collected)
- Sortie #98-107 **August 13, 1998** (TEFLUN-B mission and Andros Overflight)
- Sortie #98-108 **August 15, 1998** (TEFLUN-B mission and TRMM underflight)
- Sortie #98-109 **August 23, 1998** (Hurricane Bonnie Eyewall mission and Andros Island overflight)
- Sortie #98-110 **August 24, 1998** (Hurricane Bonnie Eyewall Mission)
- Sortie #98-111 **August 26, 1998** (Hurricane Bonnie Landfall Mission)
- Sortie #98-112 August 29, 1998 (Hurricane Danielle mission) ER-2 abort (no data collected)
- Sortie #98-113 **August 30, 1998** (Hurricane Danielle mission) ER-2 short mission
- Sortie #98-114 **September 2, 1998** (Hurricane / Tropical Storm Earl mission)
- Sortie #98-115 **September 5, 1998** (TEFLUN-B mission and TRMM underflight)

67

- Sortie #98-116 **September 8, 1998** (TEFLUN-B mission)
- Sortie #98-117 **September 13, 1998** (EOS Calibration / Validation mission)
- Sortie #98-118 **September 17, 1998** (TEFLUN-B mission)
- Sortie #98-119 **September 21, 1998** (Hurricane Georges Eyewall mission)
- Sortie #98-120 **September 22, 1998** (Hurricane Georges Synoptic Inflow mission)
- Sortie #98-132 **September 23, 1998** relocation to Warner-Robbins AFB, GA
- Sortie #98-136 **September 25, 1998** (Hurricane Georges mission)
- Sortie #98-137 **September 27, 1998** (Hurricane Georges Landfall mission)
- Sortie #98-138 **September 28, 1998** (Ferry Flight, RAFB to DFRC)

Go to the NASA/MSFC CAMEX-3 home page for more information about the CAMEX-3 field experiment.

Mail questions and comments to the NAST Principal Investigator Dr. Bill Smith NASA/LaRC
bill.l.smith@larc.nasa.gov

go to [NAST main Work page]

go to [NAST Offical Home page]

last updated: Oct 18, 1999

University of Wisconsin

FY99 Final Report

Engineering and Scientific Support for the National Polar-orbiting Operational Environmental Satellite System Airborne Sounder Testbed - Interferometer (NAST-I) Instrument

30 September 1999

Deliverables by Task:

Task 1

Comparison of spectra from NAST-I, AERI, & SHIS over Andros Island during CAMEX-3.

1. Comparison of SHIS and NAST-I data during CAMEX-3
   URL: http://arm1.ssec.wisc.edu/~shis/Results/980913_NASTcomp/nast_comparison.html

69

Comparison of SHIS and NAST-I data during CAMEX-3

Sortie 98-416, 980914, 0100 - 0106 GMT

On 980913, NASA's ER-2 and DC-8 flew a combined mission over Andros Island. (see 9/13/1993 FLT under "Pick the date to use" at http://origin.ssec.wisc.edu/~tomw/camex/) The primary objective of the last few hours of these flights were to obtain data in clear skies conditions to support calibration and validation of the AIRS instrument. The NAST-I instrument flew aboard the ER-2, while the Scanning HIS instrument flew on the DC-8 at about 25,000 feet. The DC-8 flew at this altitude to allow the LASE instrument to view in both the nadir and zenith directions; this is the first time this was accomplished by the LASE team.

This was the maiden science mission for the Scanning HIS instrument, which measures spectral infrared radiance in 3 bands: longwave (LW) 600 - 1200 cm-1, midwave (MW) 1200-1800 cm-1, and shortwave (SW) 1800-2800 cm-1. The NAST-I instrument has similar spectral bands.

In addition to flying the NAST-I instrument, the ER-2 flew the MAMS instrument. The MAMS data from 01:00:00 to 01:08:00 on 980914 were used to identify a time for intercomparison of the NAST-I with the Scanning HIS.

SPECTRAL COMPARISON

The nadir views of both the NAST-I and S-HIS data were averaged over the time period of 01:00 to 01:02 for comparison.

SHIS mean spectrum for 01:00 - 01:02 (nadir view) [jpg ps]

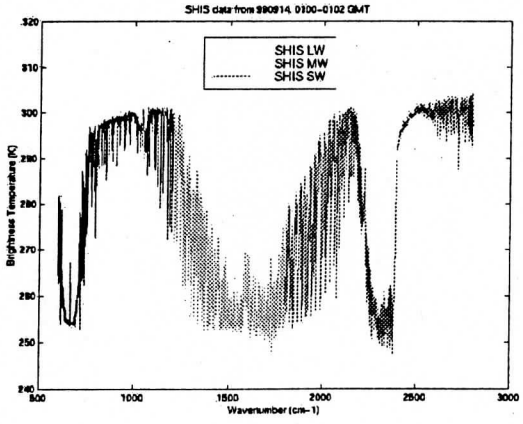

LW band comparison of NAST-I and S-HIS (800-830 cm-1) [jpg ps]

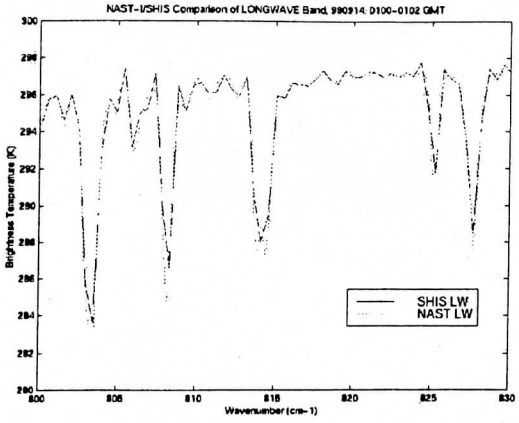

Note that the difference seen in the CO2 bands at 600 - 800 cm-1 and 2200 and 2400 cm-1, the ozone band around 1050 cm-1, and the water vapor band from 1200 - 1800 cm-1 are due to differences in the altitudes of the aircraft; the DC-8 flew at about 25000 ft, and the ER-2 at about 70000 ft.

IMAGES

Images were made from both instruments from 01:00 to 01:06. By comparing the Scanning HIS image with those from the MAMS and NAST-I, it is obvious that the DC-8 was leading the ER-2 along the flight track by about one minute, since the S-HIS begins to see the cloud at about 01:04:30, whereas the NAST-I sees it at about 01:05:30. Note that the NAST-I obtains 13 views between +/- 45 degrees, while the S-HIS takes 7 views at 6 degrees increments between +/- 18 degrees.

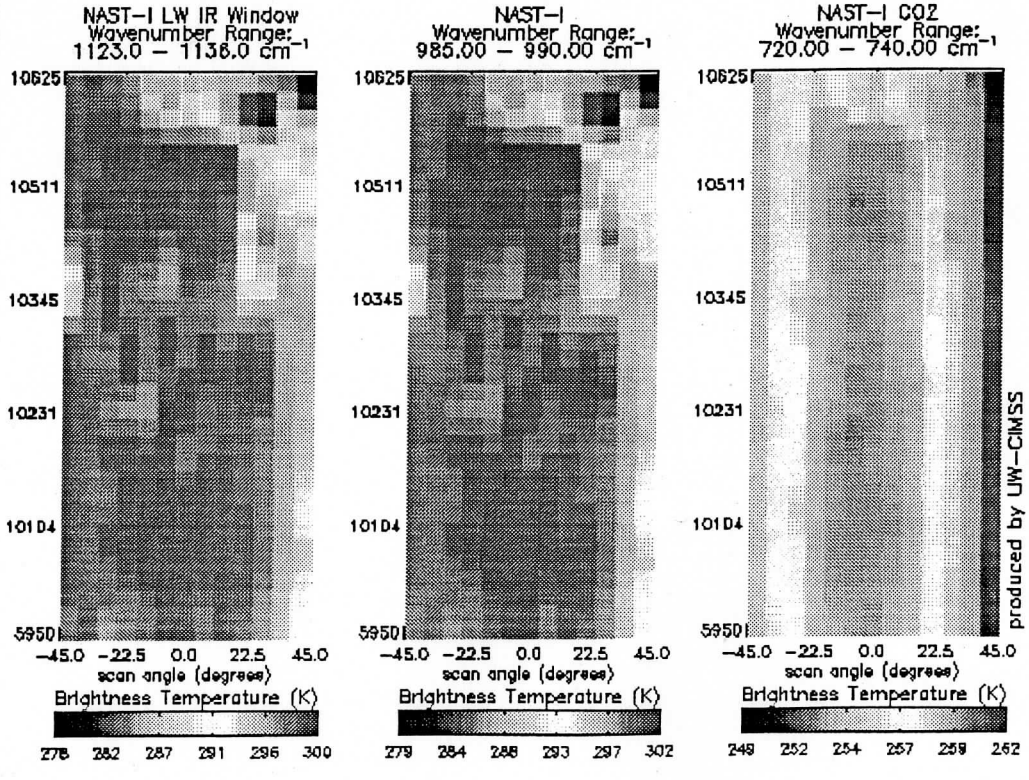

71

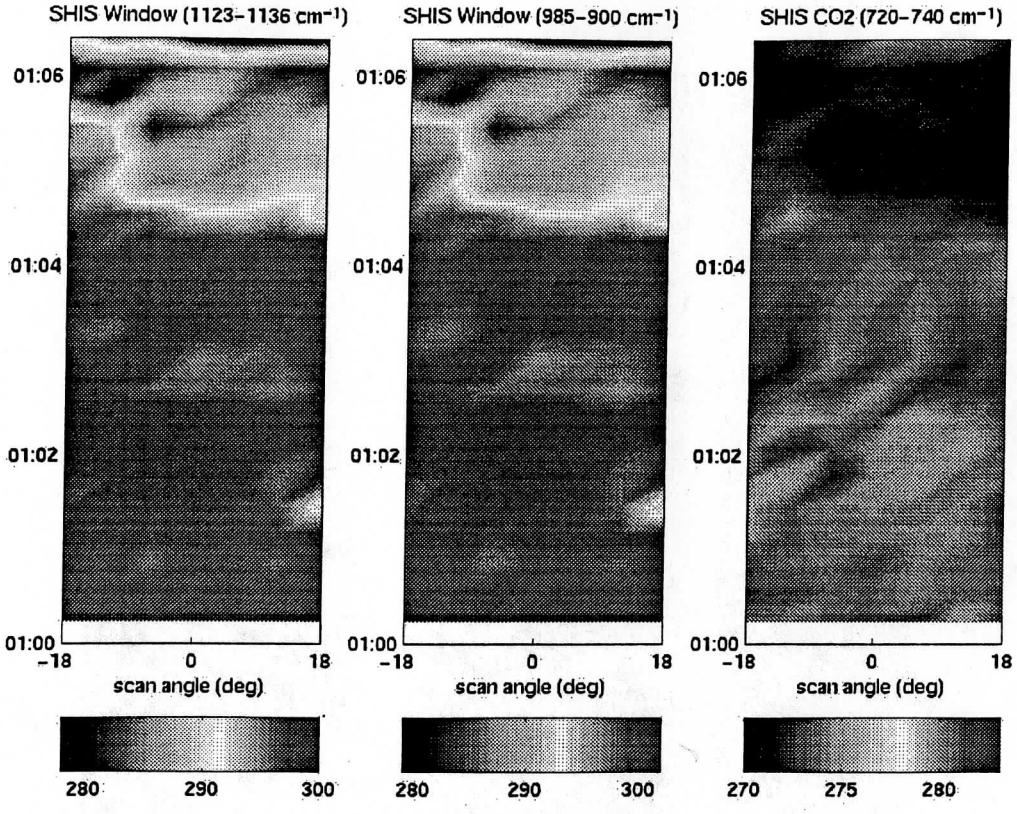

[jpg ps]

Matlab routines used for comparison

Questions? (Email Von P. Walden at U. Wisconsin)

72

MAMS CAMEX-3 QUICKLOOK 98/09/13 (Anthony.Guillory@MSFC.NASA.GOV) TRACK

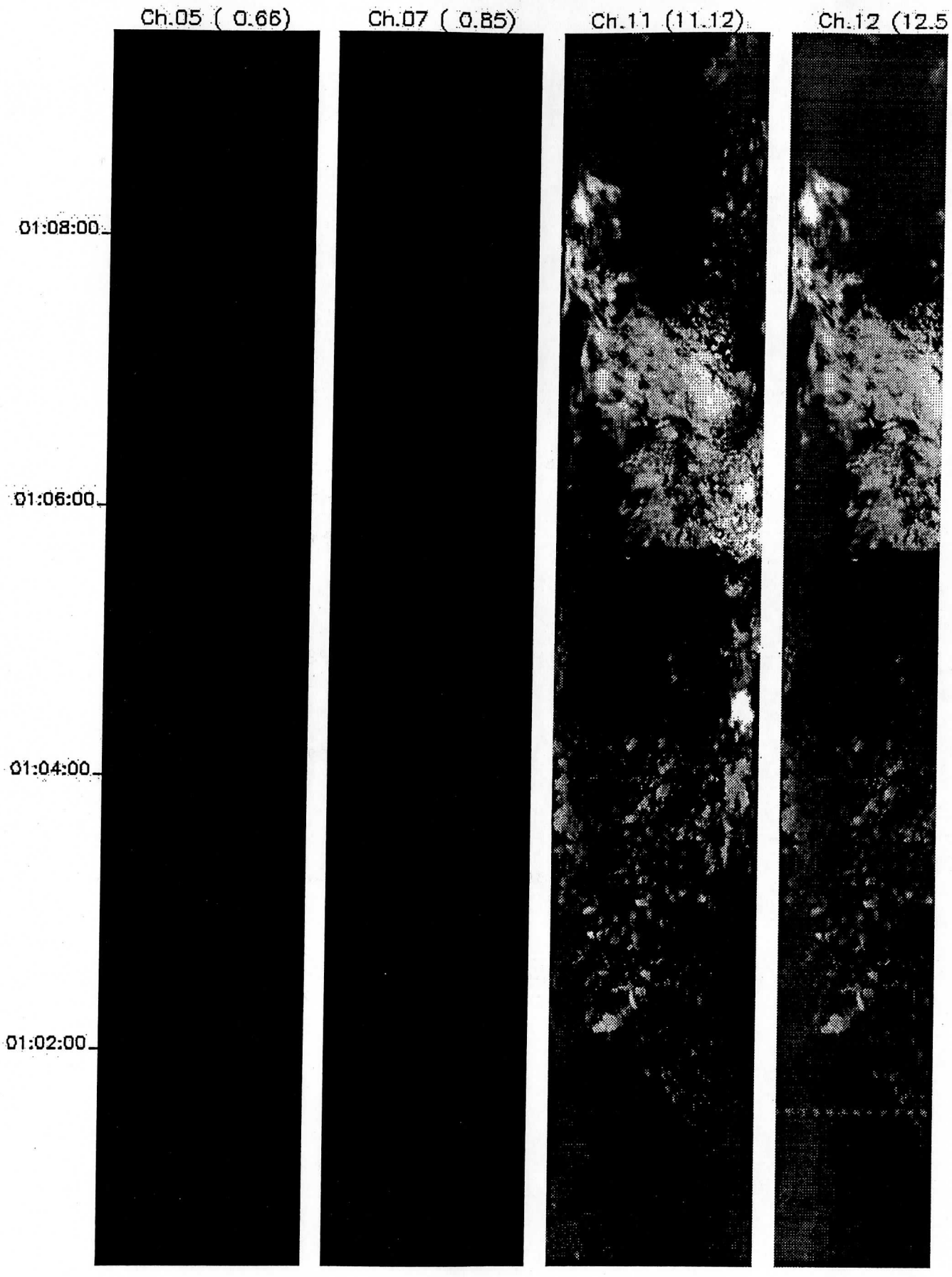

```
load /home/vonw/shis/data/sh980913/980416/cygbhei.mat
shis = data;
clear data;
N = 56;                              % Last nadir view to use.
btime = shis.timeHHMMSS(4);         % First nadir view
etime = shis.timeHHMMSS(N);

% Band 1
i1 = find(shis.wnum1 > 600 & shis.wnum1 < 1200);
wns1 = shis.wnum1(i1)+1.2*(15798/32768);          % Wavenumber scale is
mshis1 = mean(shis.Radiance(4:7:N,i1));
btshis1 = brittemp(wns1,mshis1');

% Band 2
i2 = find(shis.wnum1 > 1200 & shis.wnum1 < 1800);
wns2 = shis.wnum1(i2);
mshis2 = mean(shis.Radiance(4:7:N,i2));
btshis2 = brittemp(wns2,mshis2');

% Band 3
i3 = find(shis.wnum1 > 1800 & shis.wnum1 < 2800);
wns3 = shis.wnum1(i3)+0.2*(15798/32768);                % Wavenumber scal
mshis3 = mean(shis.Radiance(4:7:N,i3));
btshis3 = brittemp(wns3,mshis3');
clear shis;

% Band 3
nast = rd_netcdf('/home/vonw/nast/ni980913/980914c3_ass_0051_0105.nc');
ind = find(nast.timeHHMMSS >= btime & nast.timeHHMMSS <= etime & nast.s
i3 = find(nast.wnum1 > 600 & nast.wnum1 < 1260);
wnn3 = nast.wnum1(i3);
mnast3 = mean(nast.Radiance(ind,i3));
btnast3 = brittemp(wnn3,mnast3');
clear nast;

% SHIS data
figure
plot(wns1,btshis1,'b',wns2,btshis2,'g',wns3,btshis3,'r')
axis([500 3000 240 320])
xlabel('Wavenumber (cm-1)')
ylabel('Brightness Temperature (K)')
title('SHIS data from 980914, 0100-0102 GMT')
legend('SHIS LW','SHIS MW','SHIS SW',0)

print -dpsc shisdata.ps
print -djpeg shisdata.jpg

% Band 3 blowup
figure
plot(wns1,btshis1,'b',wnn3,btnast3,'c')
axis([800 830 280 300])
xlabel('Wavenumber (cm-1)')
ylabel('Brightness Temperature (K)')
```

```
title('NAST-I/SHIS Comparison of LONGWAVE Band, 980914, 0100-0102 GMT')
legend('SHIS LW','NAST LW',0)

print -dpsc nastshis_lwcomp.ps
print -djpeg nastshis_lwcomp.jpg
```

```
load cygbhei_1.mat
data1 = data;
clear data;

load cygbhei_2.mat
data2 = data;
clear data;

wn = data1.wnum1;
time = [data1.dateNumber data2.dateNumber];
rad = [data1.Radiance; data2.Radiance];
rad = rad([1:56 64:210],:);  % Eliminates bad measurement sequence.
[m,n] = size(rad);

figure
subplot(131)
i1 = find(wn > 1123 & wn < 1136);
bt1123_1136 = [];
for k = 1:m
   bt1123_1136 = [bt1123_1136 mean(brittemp(wn(i1),rad(k,i1)'))];
end
pcolor(data1.sceneMirrorAngle(1:7),time(4:7:m),reshape(bt1123_1136,7,m/
axis([-18 18 datenum(1998,9,14,1,0,0) datenum(1998,9,14,1,6,25)])
shading interp
axis([-18 18 datenum(1998,9,14,1,0,0) datenum(1998,9,14,1,6,25)])
set(gca,'Xtick',[-18 0 18])
tmp = [datenum(1998,9,14,1,0,0) datenum(1998,9,14,1,2,0) datenum(1998,9
set(gca,'YTick',tmp)
set(gca,'YTickLabel',datestr(tmp,15))
dateaxis('y',13)
caxis([278 300])
colorbar('hor');

subplot(132)
i2 = find(wn > 985 & wn < 990);
bt985_990 = [];
for k = 1:m
   bt985_990 = [bt985_990 mean(brittemp(wn(i2),rad(k,i2)'))];
end
pcolor(data1.sceneMirrorAngle(1:7),time(4:7:m),reshape(bt985_990,7,m/7)
axis([-18 18 datenum(1998,9,14,1,0,0) datenum(1998,9,14,1,6,25)])
shading interp
axis([-18 18 datenum(1998,9,14,1,0,0) datenum(1998,9,14,1,6,25)])
set(gca,'Xtick',[-18 0 18])
tmp = [datenum(1998,9,14,1,0,0) datenum(1998,9,14,1,2,0) datenum(1998,9
set(gca,'YTick',tmp)
set(gca,'YTickLabel',datestr(tmp,15))
dateaxis('y',13)
caxis([279 302])
colorbar('hor');

subplot(133)
i3 = find(wn > 720 & wn < 740);
```

```
bt720_740 = [];
for k = 1:m
   bt720_740 = [bt720_740 mean(brittemp(wn(i3),rad(k,i3)'))];
end
pcolor(data1.sceneMirrorAngle(1:7),time(4:7:m),reshape(bt720_740,7,m/7)
shading interp
hold on
axis([-18 18 datenum(1998,9,14,1,0,0) datenum(1998,9,14,1,6,25)])
set(gca,'Xtick',[-18 0 18])
tmp = [datenum(1998,9,14,1,0,0) datenum(1998,9,14,1,2,0) datenum(1998,9
set(gca,'YTick',tmp)
set(gca,'YTickLabel',datestr(tmp,15))
dateaxis('y',13)
caxis([270 283])
colorbar('hor');

c = colormap;
c(58:64,1:3) = [1 0 0; 1 0 0; 1 0 0; 1 0 0; 1 0 0; 1 0 0; 1 0 0];
colormap(c);
```

University of Wisconsin

FY99 Final Report

Engineering and Scientific Support for the National Polar-orbiting Operational Environmental Satellite System Airborne Sounder Testbed - Interferometer (NAST-I) Instrument

30 September 1999

Deliverables by Task:

Task 1

Comparison of spectra from NAST-I, AERI, & SHIS over Andros Island during CAMEX-3.

2.NASTI comparison with calculations from CAMEX3
URL: http://danspc.larc.nasa.gov/NAST/val_calcs2.html

http://danspc.larc.nasa.gov/NAST/val_calcs2.html

NAST-I Validation: comparison with fast model calculations. 980913 23:47-23:50 UTC

This page contains comparisons of an averaged, clear-sky, night time NAST-I spectrum with calculations done with the Strow et al. NAST-I fast model. Nadir viewing NAST-I spectra are averaged from 23:47 to 23:50 UTC for the 980913/14 CAMEX3 flight. This corresponds to a relatively homogeneous, clear sky time period over ocean just west of Andros Island. The NAST-I radiance and auxiliary information suggest that this is a fairly clear scene, although there is a possibility of high, thin cirrus and possibly some low clouds as well. The following two figures contain NAST-I radiances mapped onto the Earth's surface for all scan angles for 23:43 to 23:54 UTC. The ER-2 was traveling south-easterly during this time. Also shown in the figure in magenta is the trajectory of a Vaisala radiosonde launched from the Autec facility by UW personnel at 22:37 UTC. The sonde rose vertically to ~500 mbar and then drifted slowly to the south west, reaching 300 mbar approximately 70 minutes after launch. The chosen NAST-I averaging time period (23:47-23:50) is optimal for spatial and temporal co-location with the sonde when comparing calculations performed with the sonde to midwave NAST-I radiances sensitive to upper level water vapor.

surface channel (899-903 cm-1):
upper altitude water vapor (1585-1595 cm-1)

The first figure contains mean radiances for the 899 to 903 cm-1 channels and is therefore depicting the surface and/or low clouds. The non-uniformity of the surface is evident in the figure. The second figure contains mean radiances for the 1585 to 1595 cm-1 channels and is representing the variability of upper level water vapor. Auxiliary data also detected a gradient in upper level moisture from east to west.

Nadir NAST-I spectra were averaged using the data from 23:47 to 23:50 to produce a mean spectrum for each band. Below are plots of the mean spectra and their uncertainties, with the uncertainty in the mean radiance (sigma R) computed as the one standard deviation in the radiances divided by the square root of the number of individual spectra. These uncertainties include all sources of error including true scene variations, detector noise, and vibration-induced tilt noise. Note that the transparent channels in the long and shortwave bands have large uncertainties due primarily to true surface variation.

Brightness temperature:
channels 1-3 : gif | eps
channel 1 (shortwave) : gif | eps
channel 2 (midwave) : gif | eps
channel 3 (longwave) : gif | eps
Radiance:
channels 1-3 : gif | eps
channel 1 (shortwave) : gif | eps
channel 2 (midwave) : gif | eps
channel 3 (longwav

Using pressure, temperature, and relative humidity measured with the 22:37 UTC launch Vaisala RS-80 radiosonde, calculations have been performed using the NAST-I fast model of Strow et al. The mean NAST-I spectrum and this calculation are shown below. ASCII files of the data used to generate these plots are also available.

Mean nadir spectrum: 980913, 23:47-23:50 utc

Below are expanded views of the comparison, with the NAST-I spectra shown in red. The NAST-I spectra in these figures have been apodized to be consistent with the fast model (Kaiser Bessel #6). The calculations were performed using a scalar (spectrally independent) surface emissivity of 0.975. Note the excellent agreement obtained throughout the midwave band.

Last modified: Fri Feb 19 15:52:20 UTC 1999

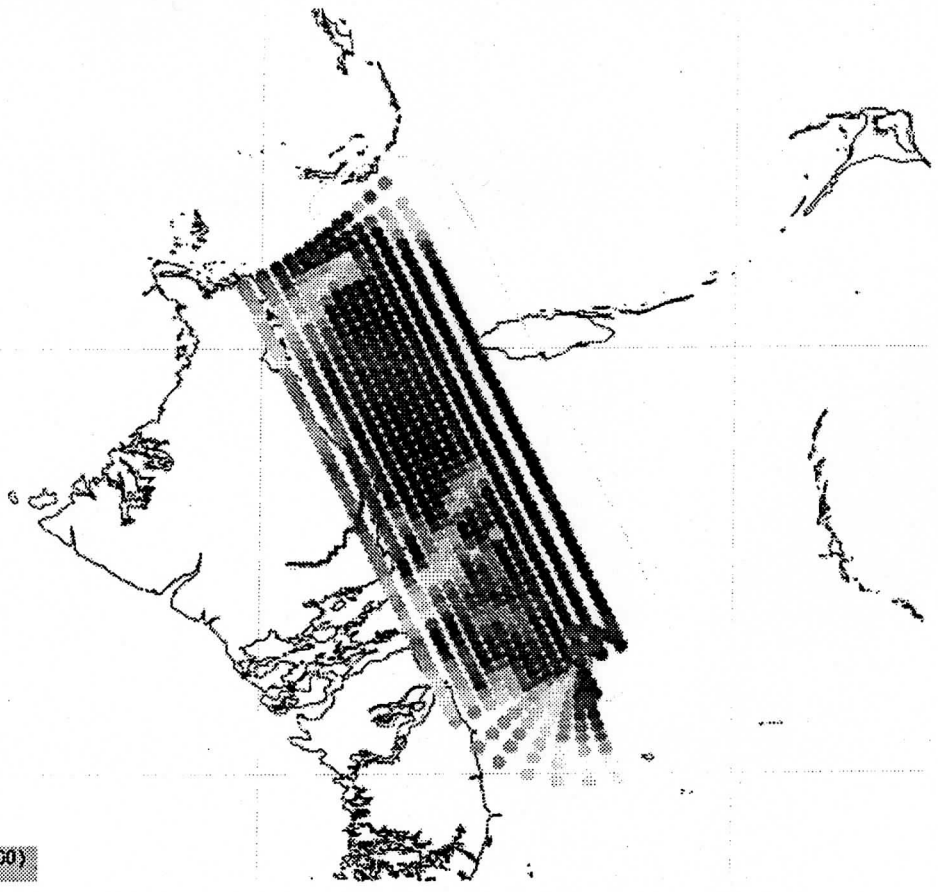
22:54:45 (-77.275, 24.160)

80

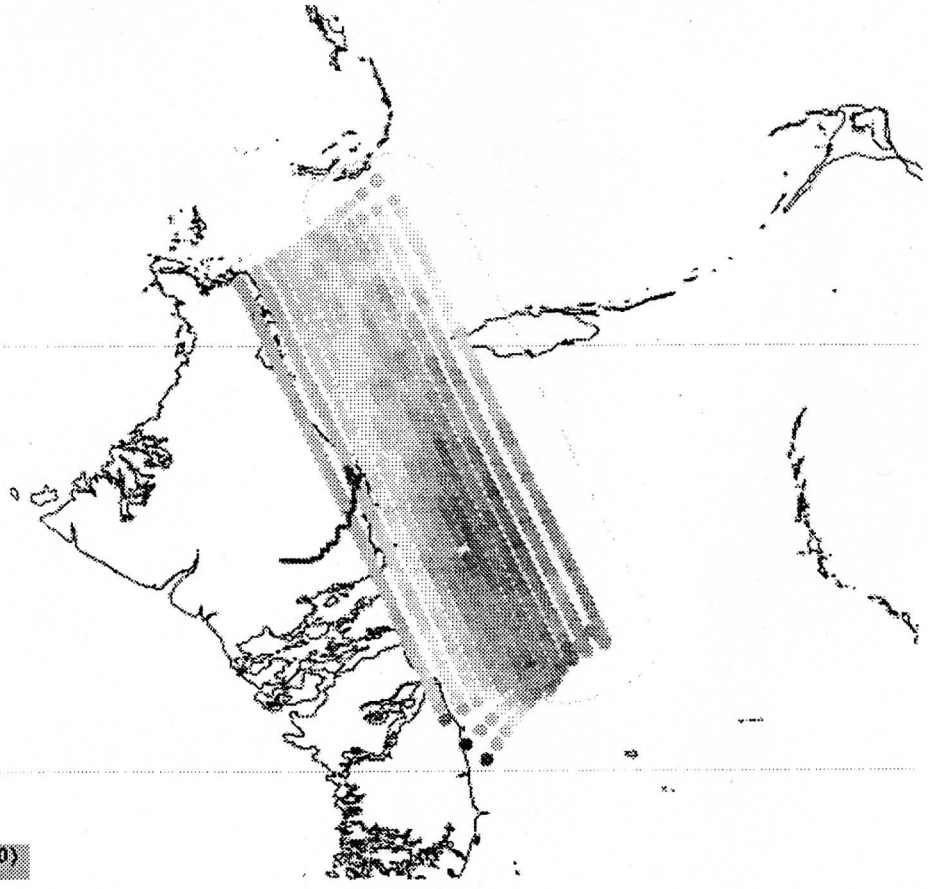

22:30:30 (-77.365, 24.170)

81

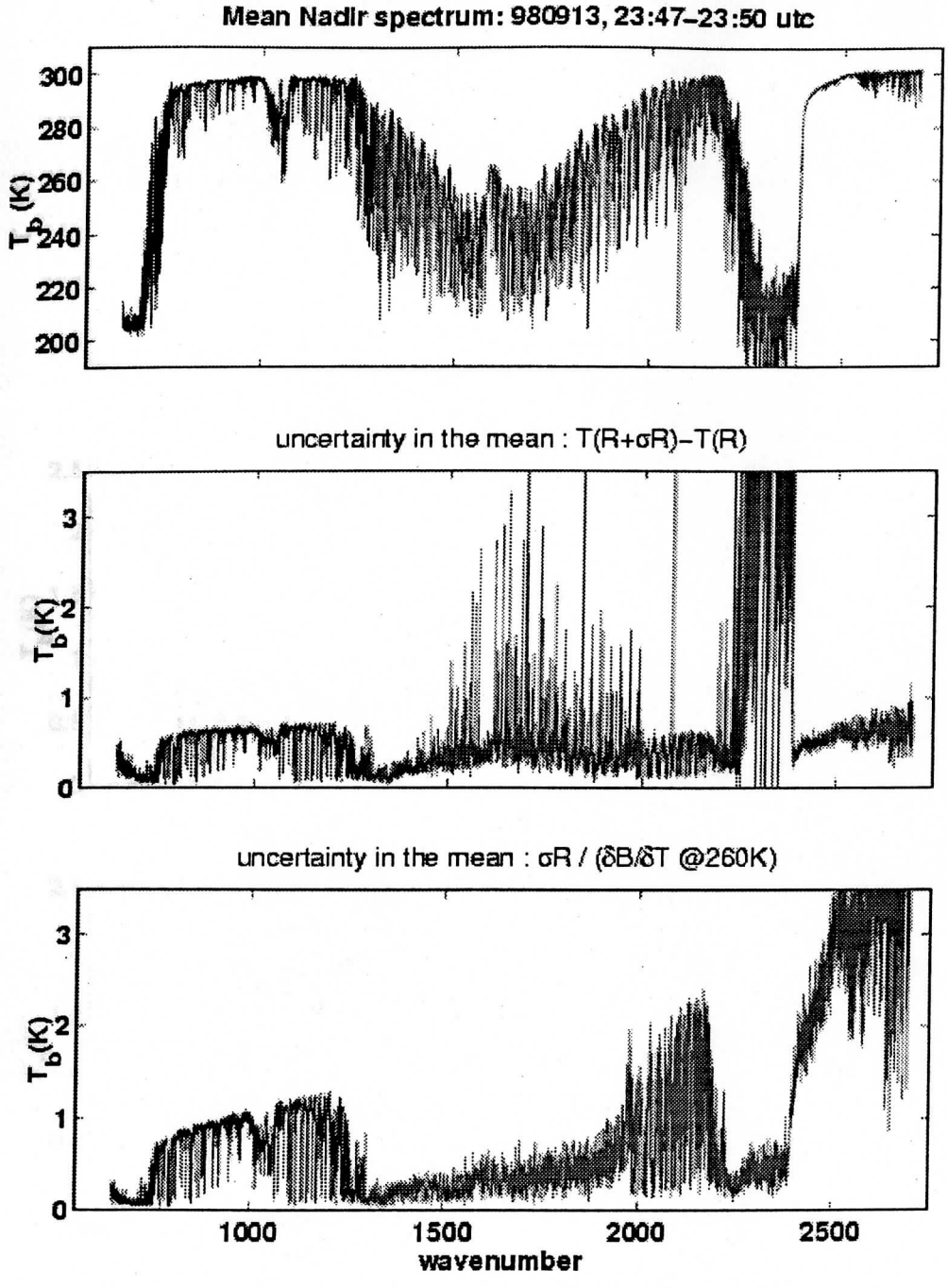
Mean Nadir spectrum: 980913, 23:47–23:50 utc
300
280
260
240
220
200
T_b (K)
uncertainty in the mean : T(R+σR)–T(R)
3
2
1
0
T_b(K)
uncertainty in the mean : σR / (δB/δT @260K)
3
2
1
0
T_b(K)
1000
1500
2000
2500
wavenumber

82

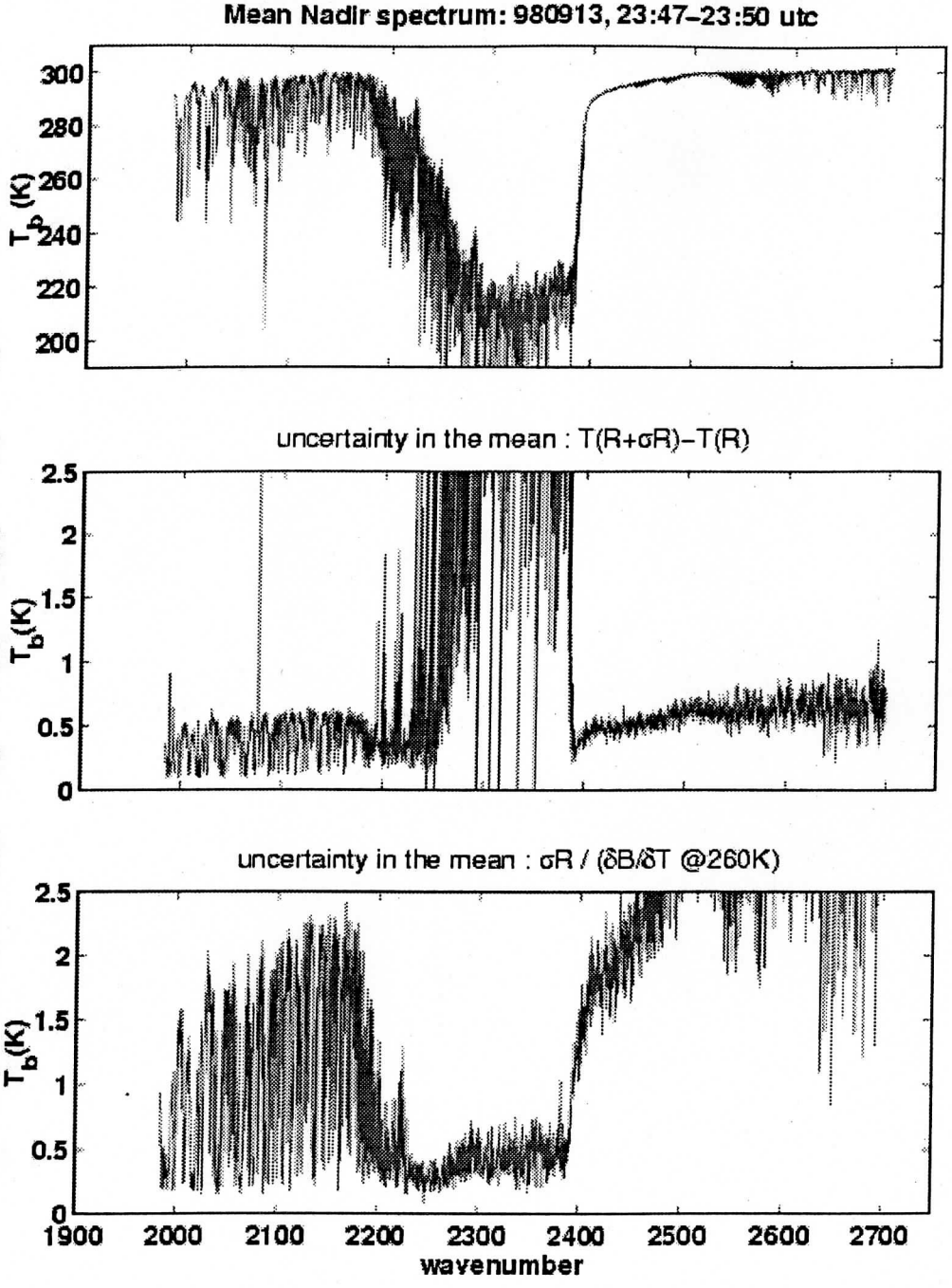
Mean Nadir spectrum: 980913, 23:47–23:50 utc
T_b (K)
300
280
260
240
220
200
uncertainty in the mean : T(R+σR)–T(R)
T_b(K)
2.5
2
1.5
1
0.5
0
uncertainty in the mean : σR / (δB/δT @260K)
T_b(K)
2.5
2
1.5
1
0.5
0
1900
2000
2100
2200
2300
2400
2500
2600
2700
wavenumber

83

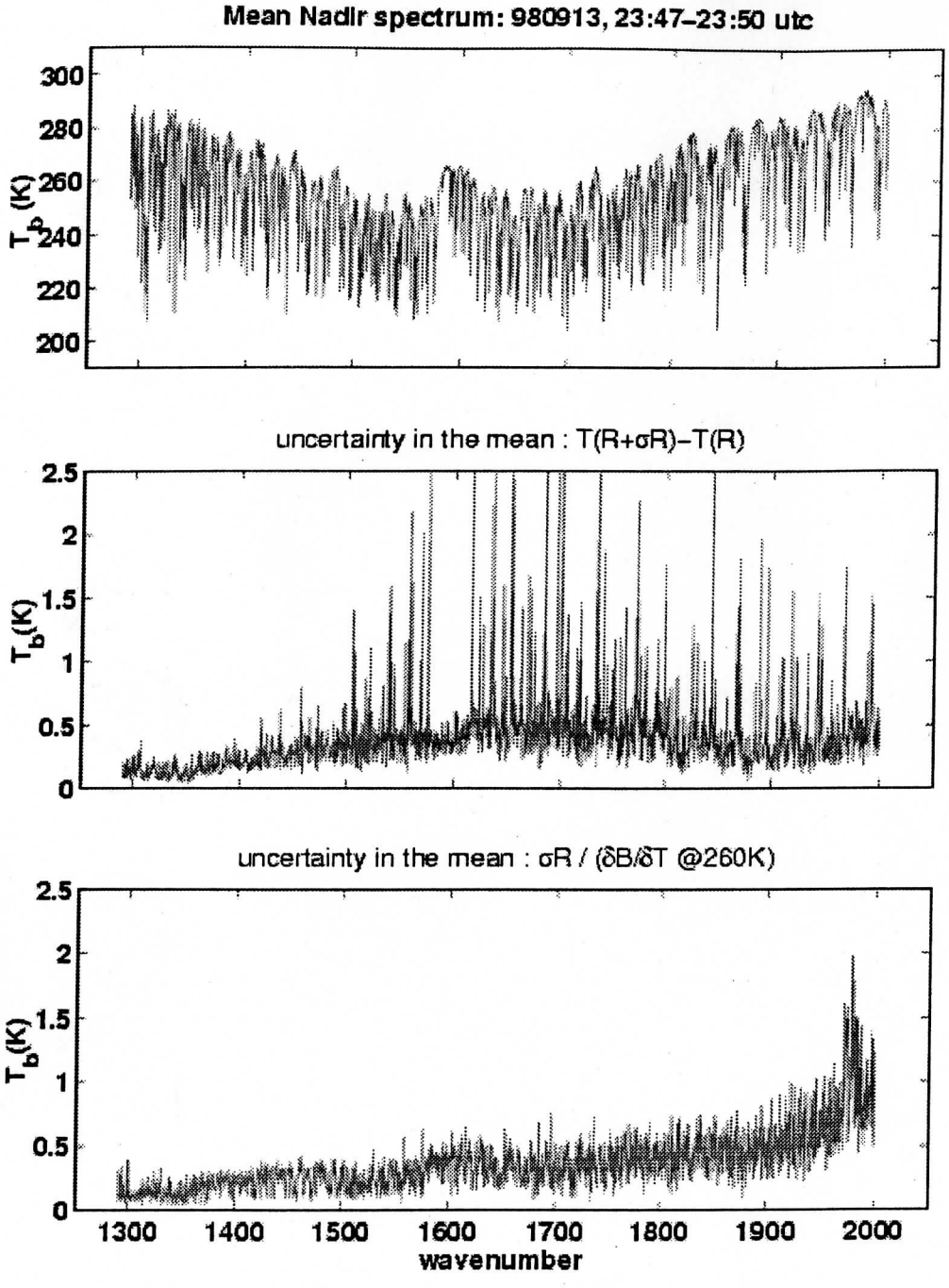
Mean Nadir spectrum: 980913, 23:47–23:50 utc
T_b (K)
300
280
260
240
220
200
uncertainty in the mean : T(R+σR)–T(R)
T_b(K)
2.5
2
1.5
1
0.5
0
uncertainty in the mean : σR / (δB/δT @260K)
T_b(K)
2.5
2
1.5
1
0.5
0
1300
1400
1500
1600
1700
1800
1900
2000
wavenumber

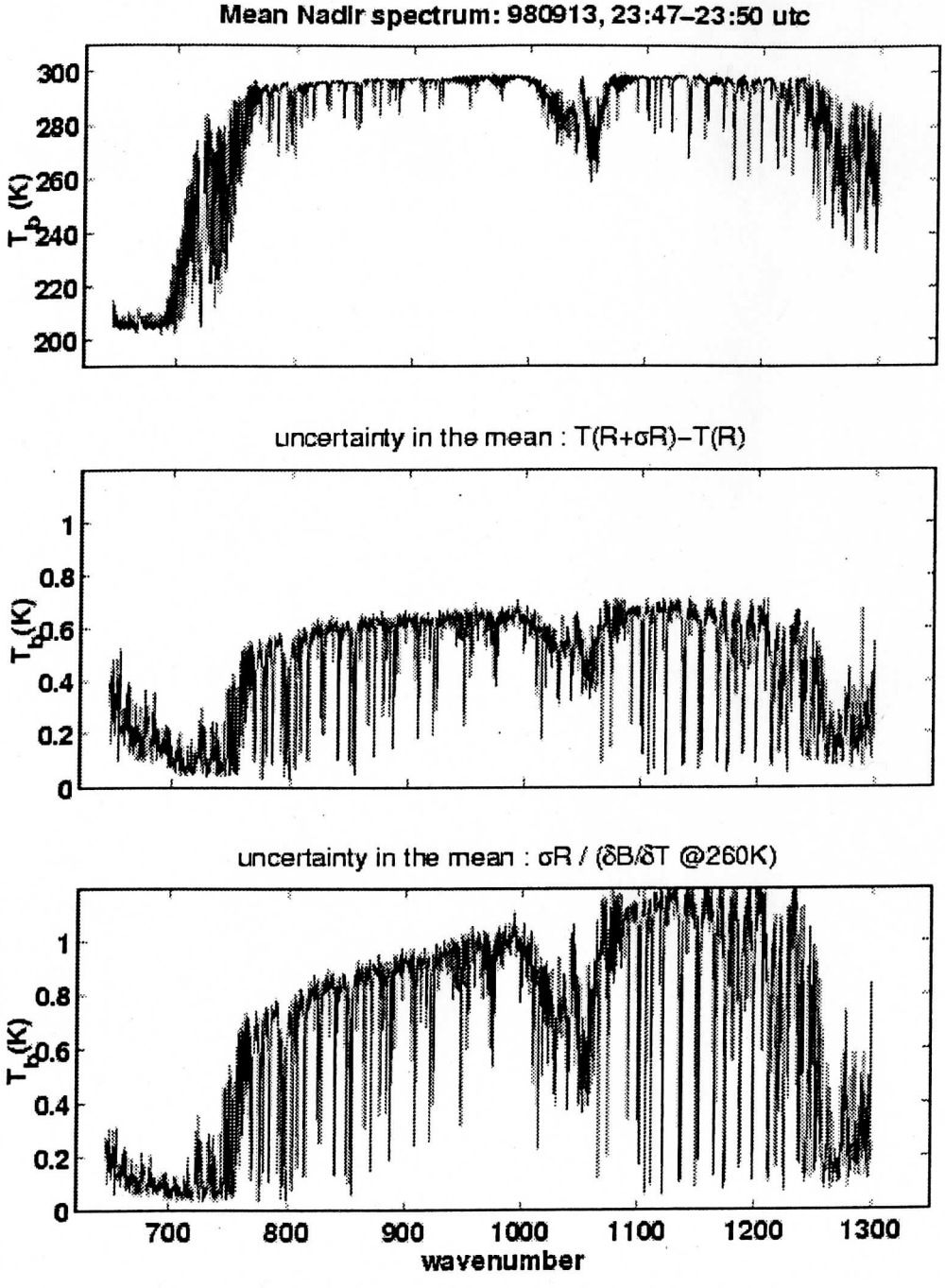
Mean Nadir spectrum: 980913, 23:47–23:50 utc
300
280
260
240
220
200
T_b (K)
uncertainty in the mean : T(R+σR)–T(R)
1
0.8
0.6
0.4
0.2
0
T_b (K)
uncertainty in the mean : σR / (δB/δT @260K)
1
0.8
0.6
0.4
0.2
0
T_b (K)
700
800
900
1000
1100
1200
1300
wavenumber

85

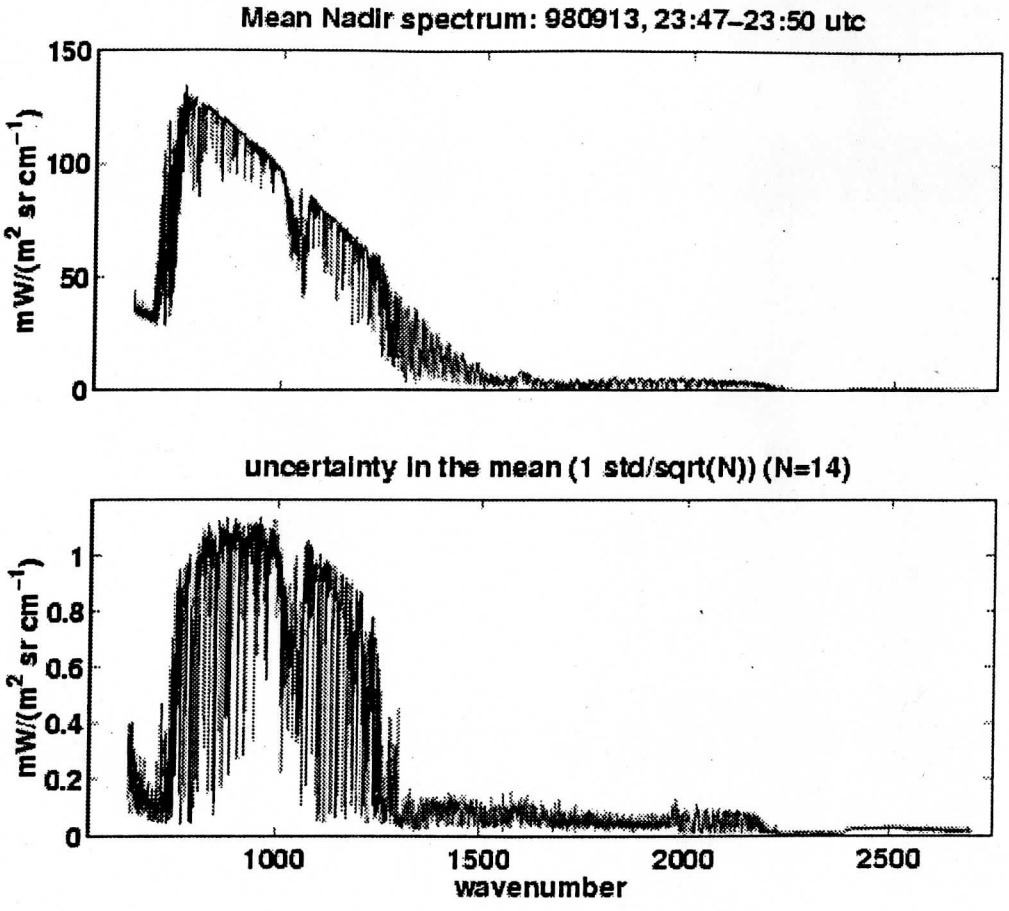
Mean Nadir spectrum: 980913, 23:47–23:50 utc
150
100
50
0
mW/(m2 sr cm-1)
uncertainty in the mean (1 std/sqrt(N)) (N=14)
1
0.8
0.6
0.4
0.2
0
mW/(m2 sr cm-1)
1000
1500
2000
2500
wavenumber

86

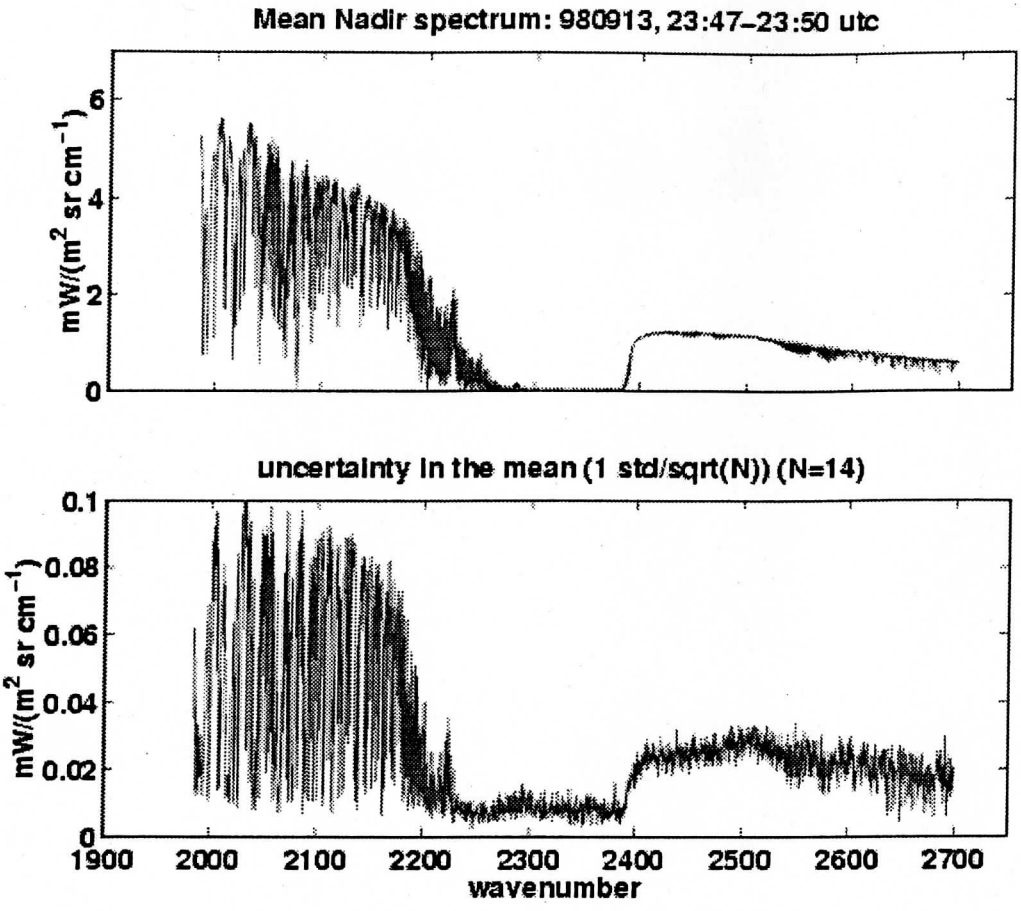
Mean Nadir spectrum: 980913, 23:47–23:50 utc
mW/(m2 sr cm-1)
0
2
4
6
uncertainty in the mean (1 std/sqrt(N)) (N=14)
mW/(m2 sr cm-1)
0
0.02
0.04
0.06
0.08
0.1
1900
2000
2100
2200
2300
2400
2500
2600
2700
wavenumber

87

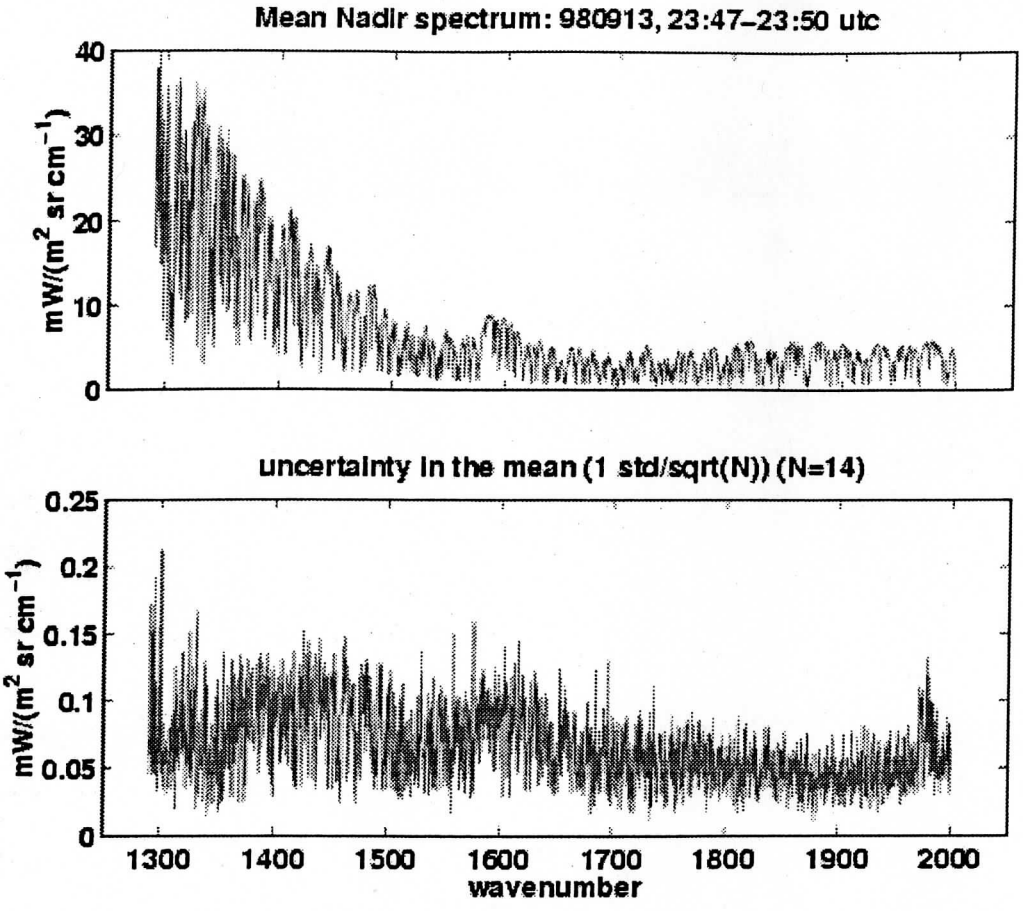
Mean Nadir spectrum: 980913, 23:47–23:50 utc
mW/(m2 sr cm-1)
40
30
20
10
0
uncertainty in the mean (1 std/sqrt(N)) (N=14)
mW/(m2 sr cm-1)
0.25
0.2
0.15
0.1
0.05
0
1300
1400
1500
1600
1700
1800
1900
2000
wavenumber

88

Index of /NAST/calc_plots2_data

Name	Last modified	Size	Description
Parent Directory	10-Nov-99 13:42	-	
fmodel_ch1.asc	18-Feb-99 17:03	1.6M	
fmodel_ch2.asc	18-Feb-99 17:03	1.6M	
fmodel_ch3.asc	18-Feb-99 17:03	1.6M	
nasti_ch1.asc	18-Feb-99 17:03	1.6M	
nasti_ch2.asc	18-Feb-99 17:03	1.6M	
nasti_ch3.asc	18-Feb-99 17:03	1.6M	

ASCII files of oversampled spectra used to make the plots
for the 980913 23:47-23:50 NASTI/Strow fastmodel comparison.
(http://danspc.larc.nasa.gov/NAST/val_calcs2.html)

for all files, the format is [wavenumber, radiance].

fmodel_ch1.asc : Strow et al. fast model, channel 1
fmodel_ch2.asc : Strow et al. fast model, channel 2
fmodel_ch3.asc : Strow et al. fast model, channel 3

nasti_ch1.asc : Averaged NASTI data, channel 1
nasti_ch2.asc : Averaged NASTI data, channel 2
nasti_ch3.asc : Averaged NASTI data, channel 3

89

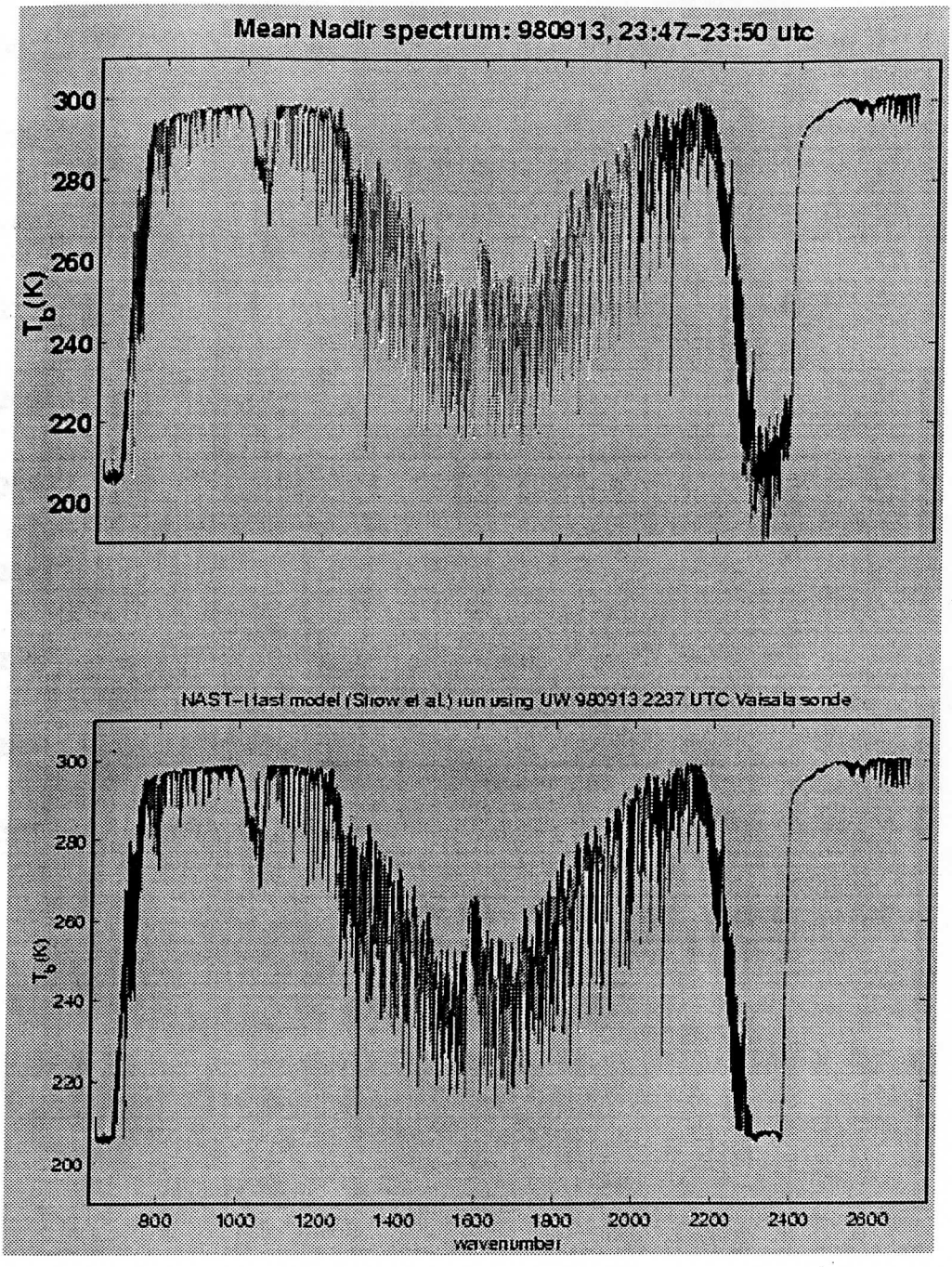
Mean Nadir spectrum: 980913, 23:47–23:50 utc
300
280
260
240
220
200
T_b(K)
NAST-I fast model (Strow et al.) run using UW 980913 2237 UTC Vaisala sonde
300
280
260
240
220
200
T_b(K)
800
1000
1200
1400
1600
1800
2000
2200
2400
2600
wavenumber

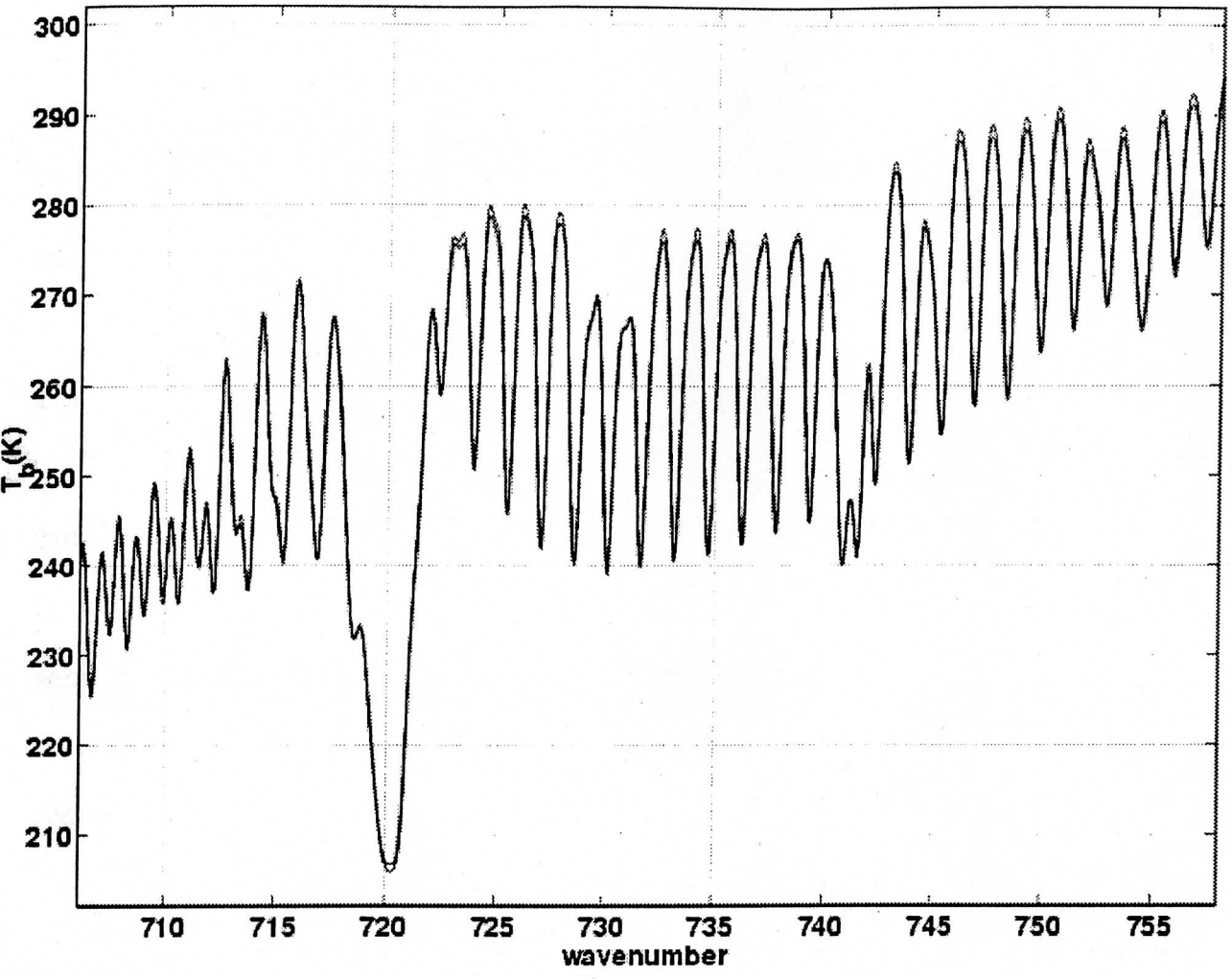
300
290
280
270
260
250
240
230
220
210
T_b(K)
710
715
720
725
730
735
740
745
750
755
wavenumber

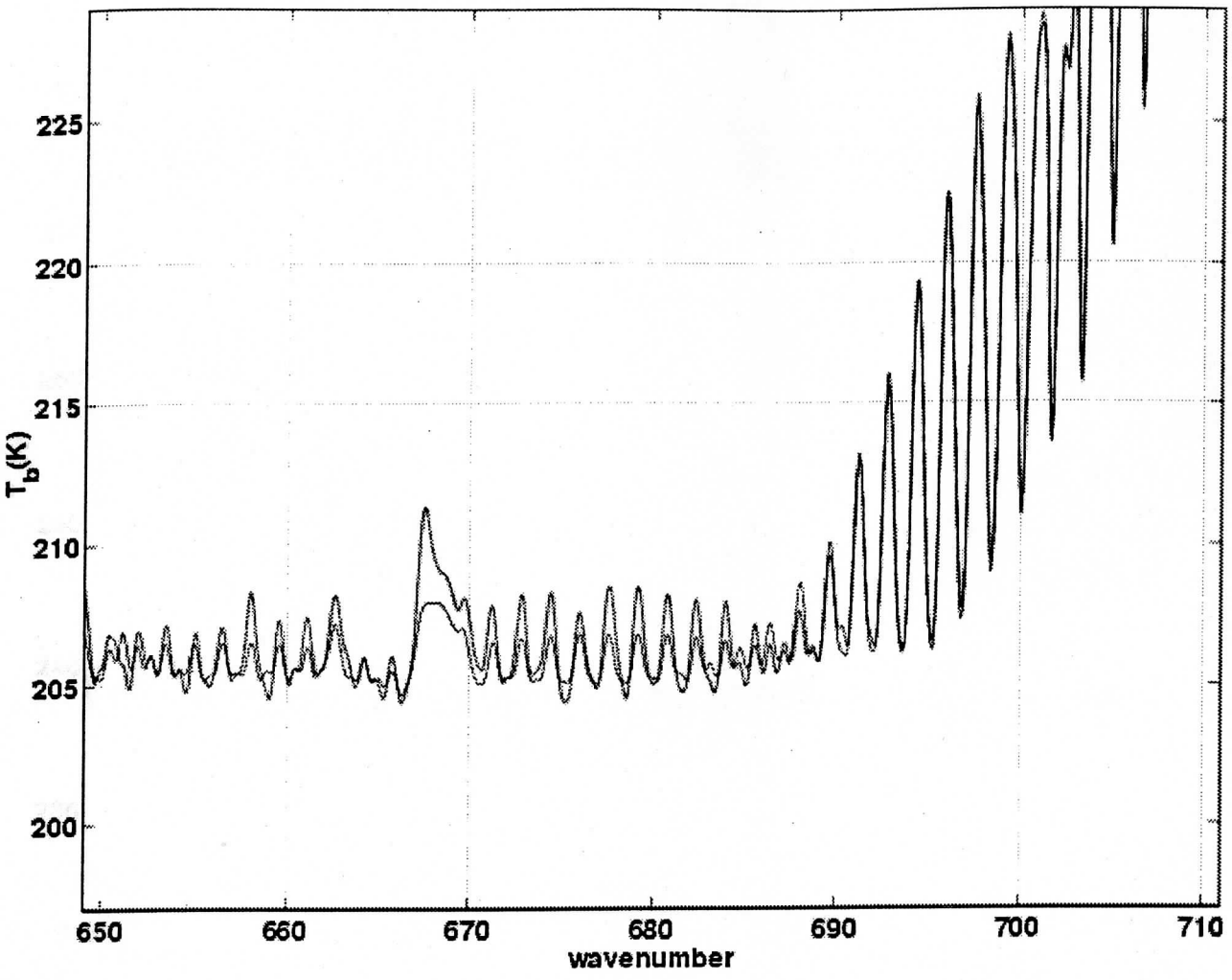
225
220
215
210
205
200
T_b(K)
650
660
670
680
690
700
710
wavenumber

92

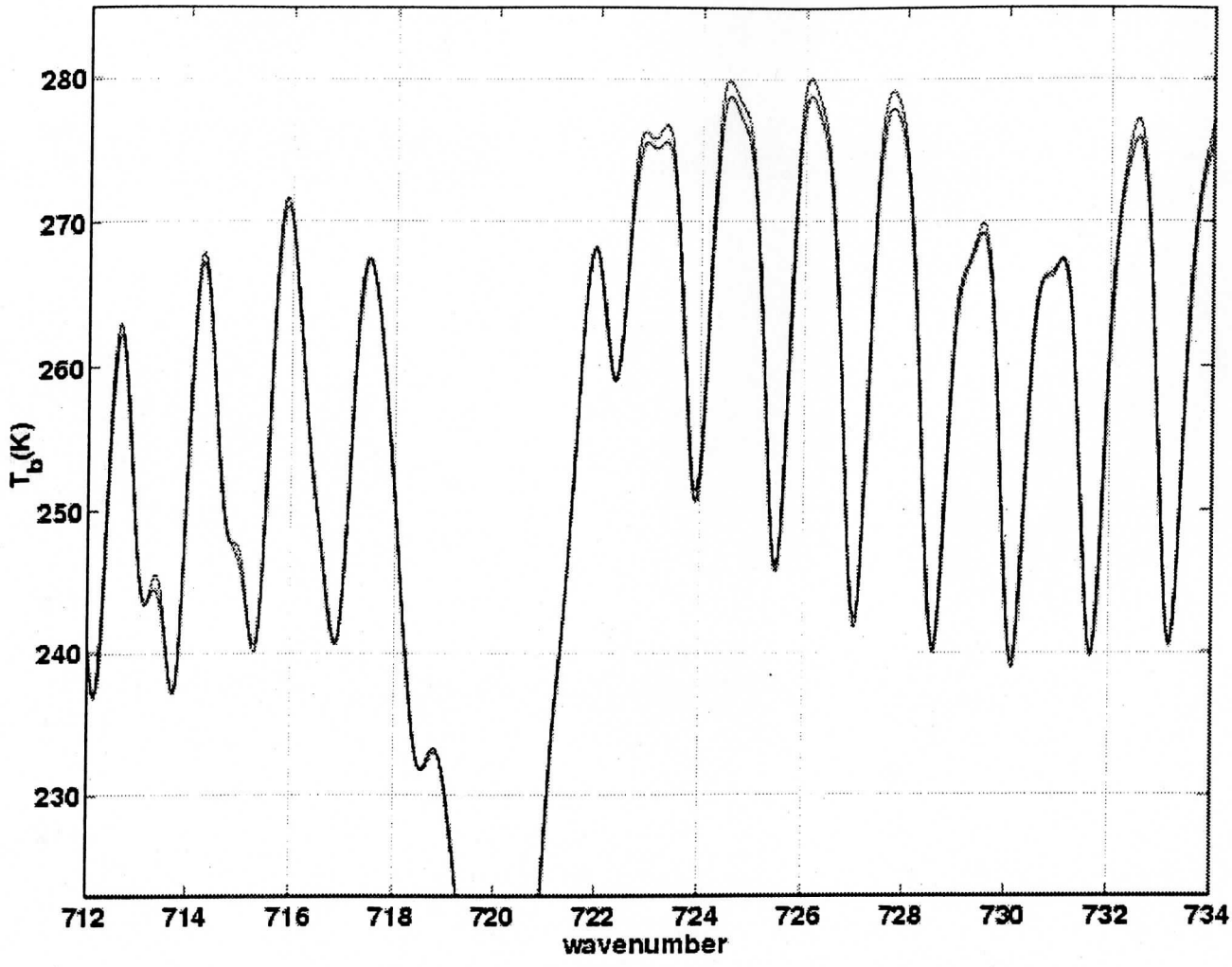
280
270
260
250
240
230
T_b(K)
712
714
716
718
720
722
724
726
728
730
732
734
wavenumber

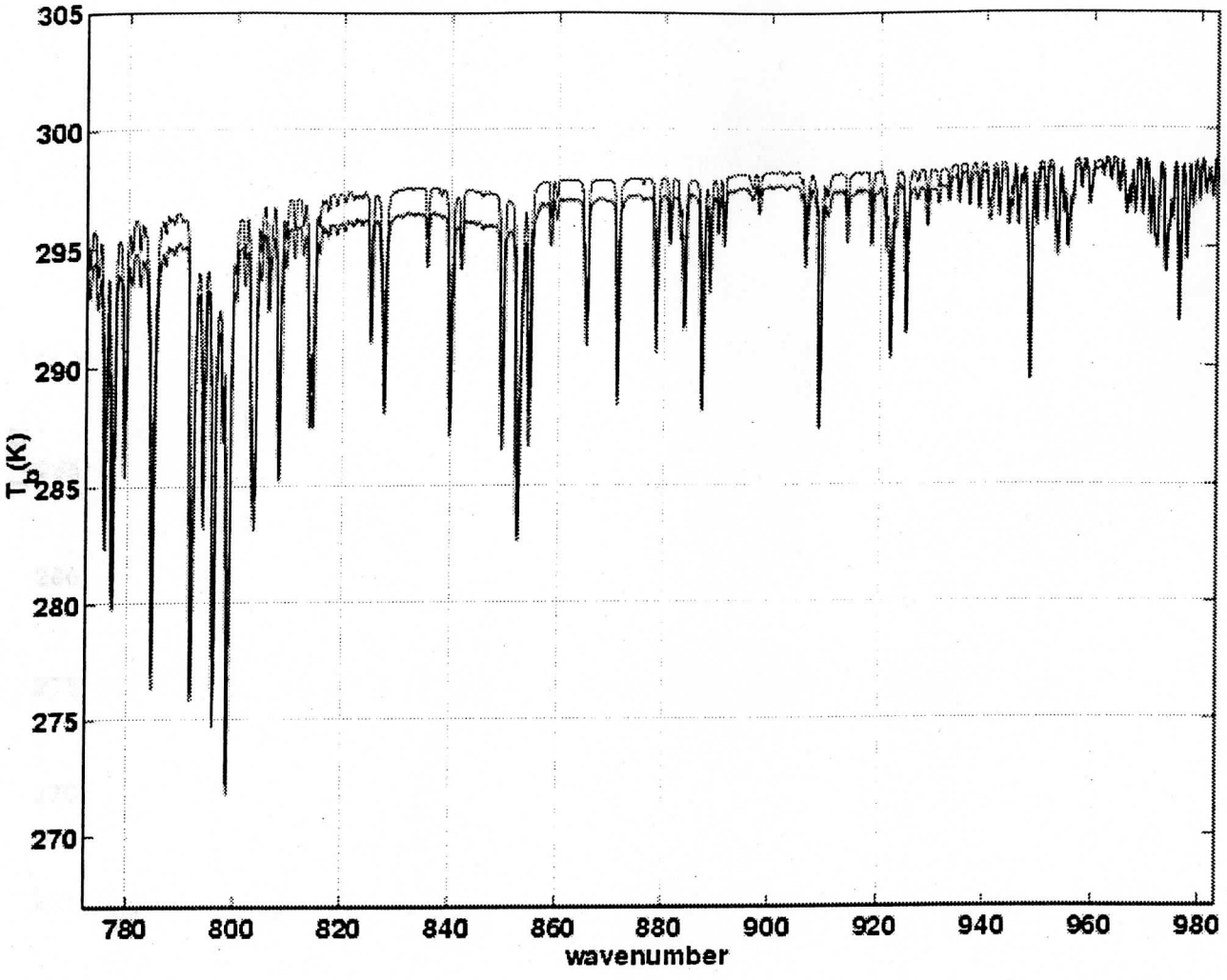
305
300
295
290
285
280
275
270
T_b(K)
780
800
820
840
860
880
900
920
940
960
980
wavenumber

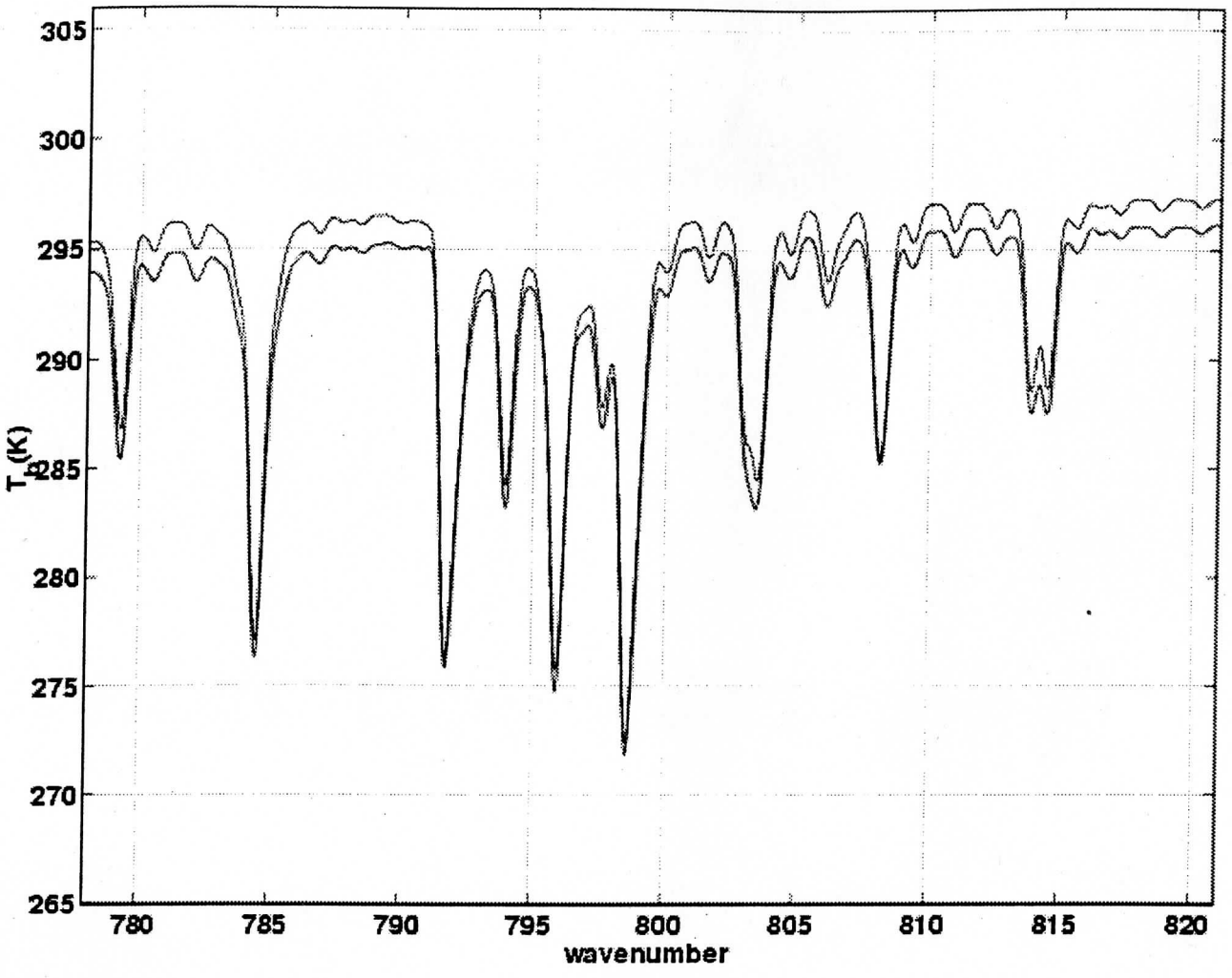
305
300
295
290
285
280
275
270
265
T_B(K)
780
785
790
795
800
805
810
815
820
wavenumber

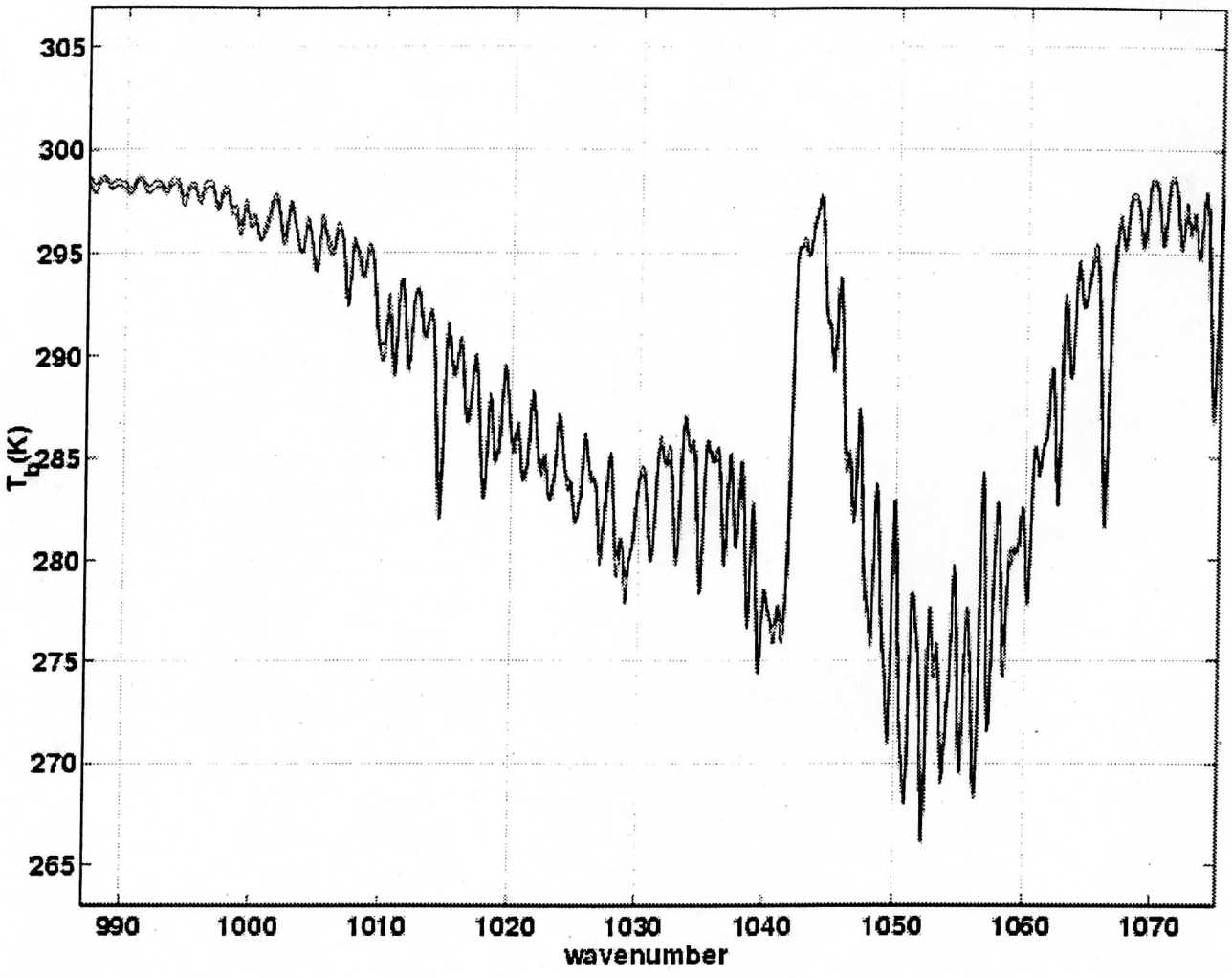
305
300
295
290
285
280
275
270
265
T_b(K)
990
1000
1010
1020
1030
1040
1050
1060
1070
wavenumber

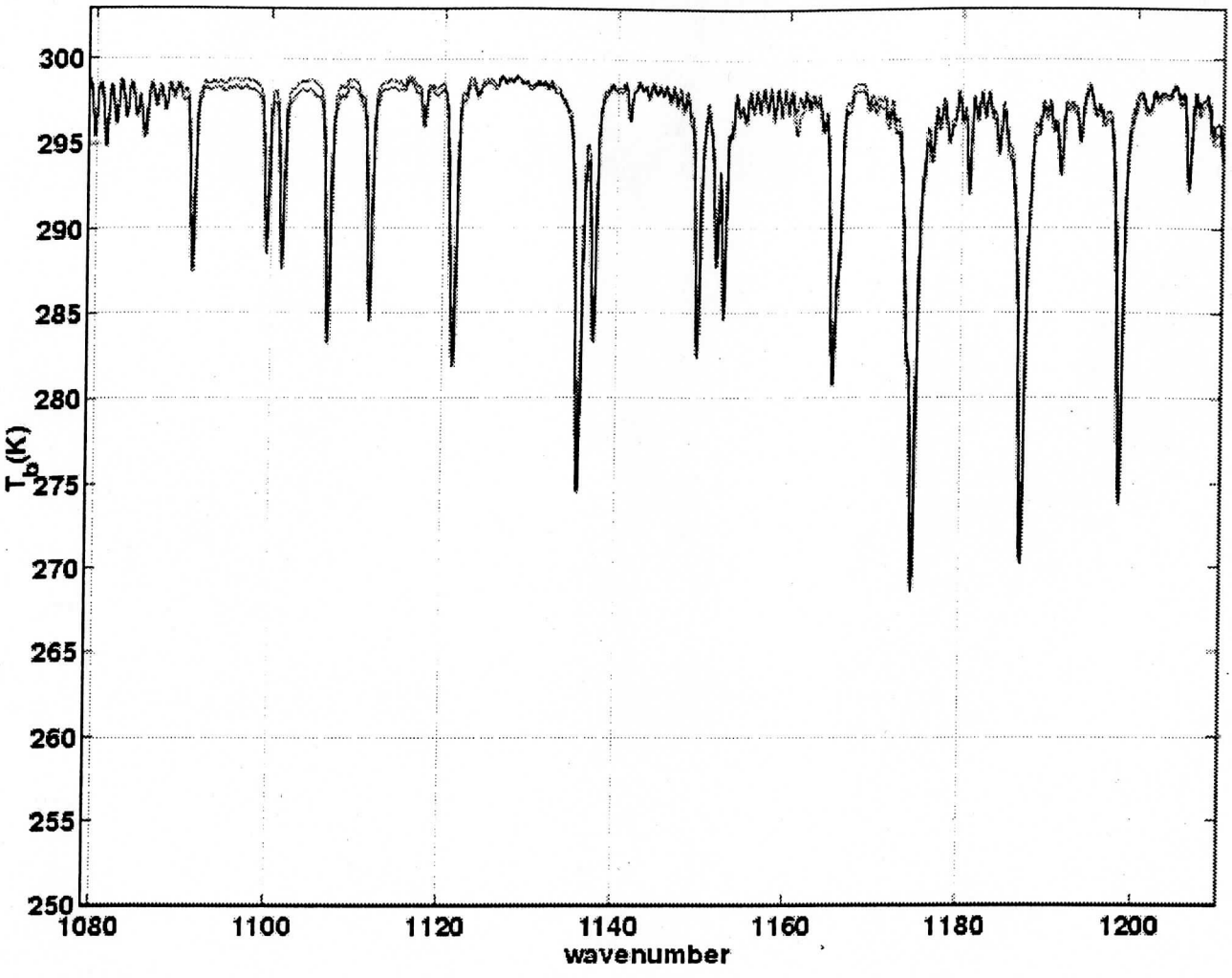
300
295
290
285
280
275
270
265
260
255
250
T_b(K)
1080
1100
1120
1140
1160
1180
1200
wavenumber

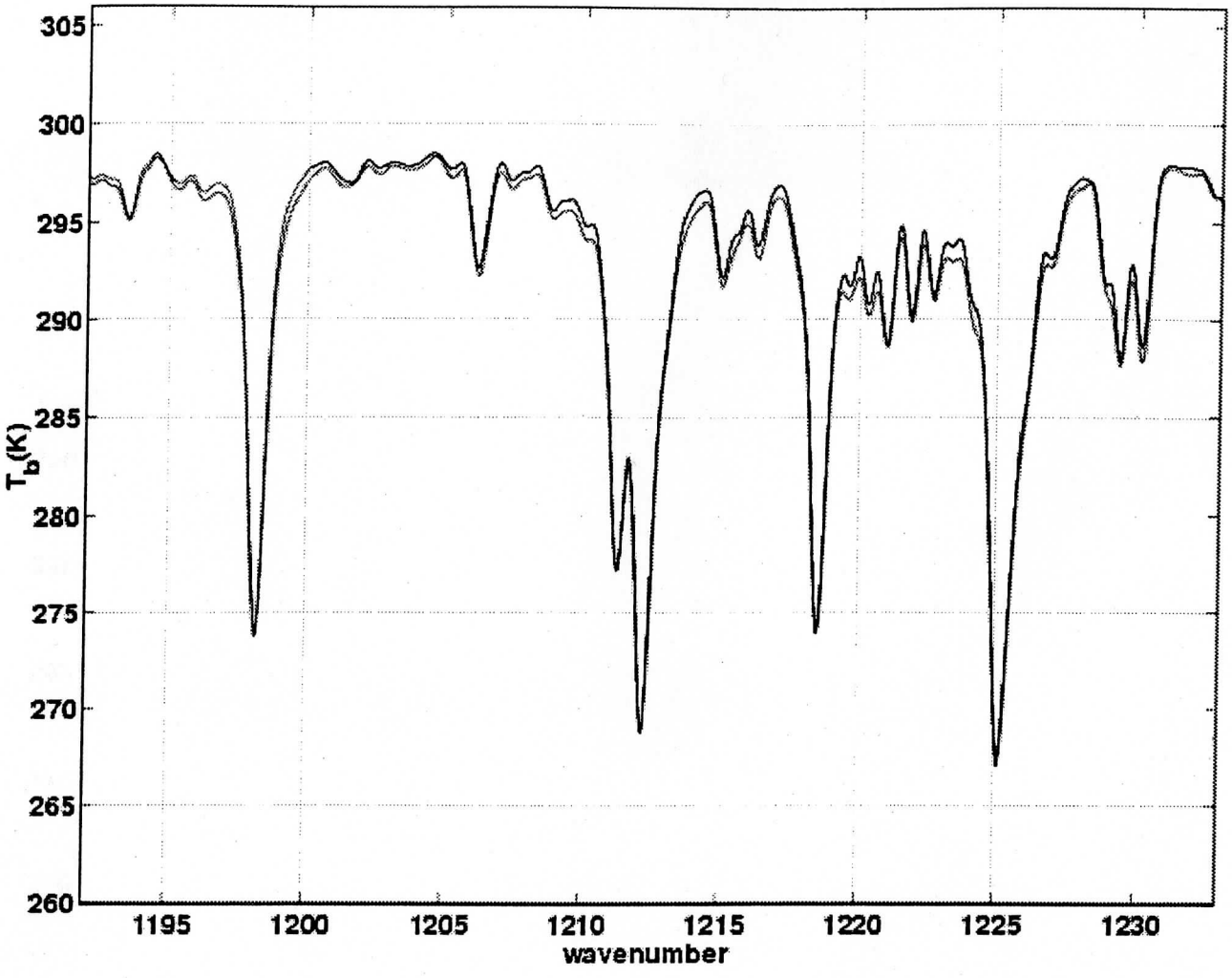
305
300
295
290
285
280
275
270
265
260
T_b(K)
1195
1200
1205
1210
1215
1220
1225
1230
wavenumber

98

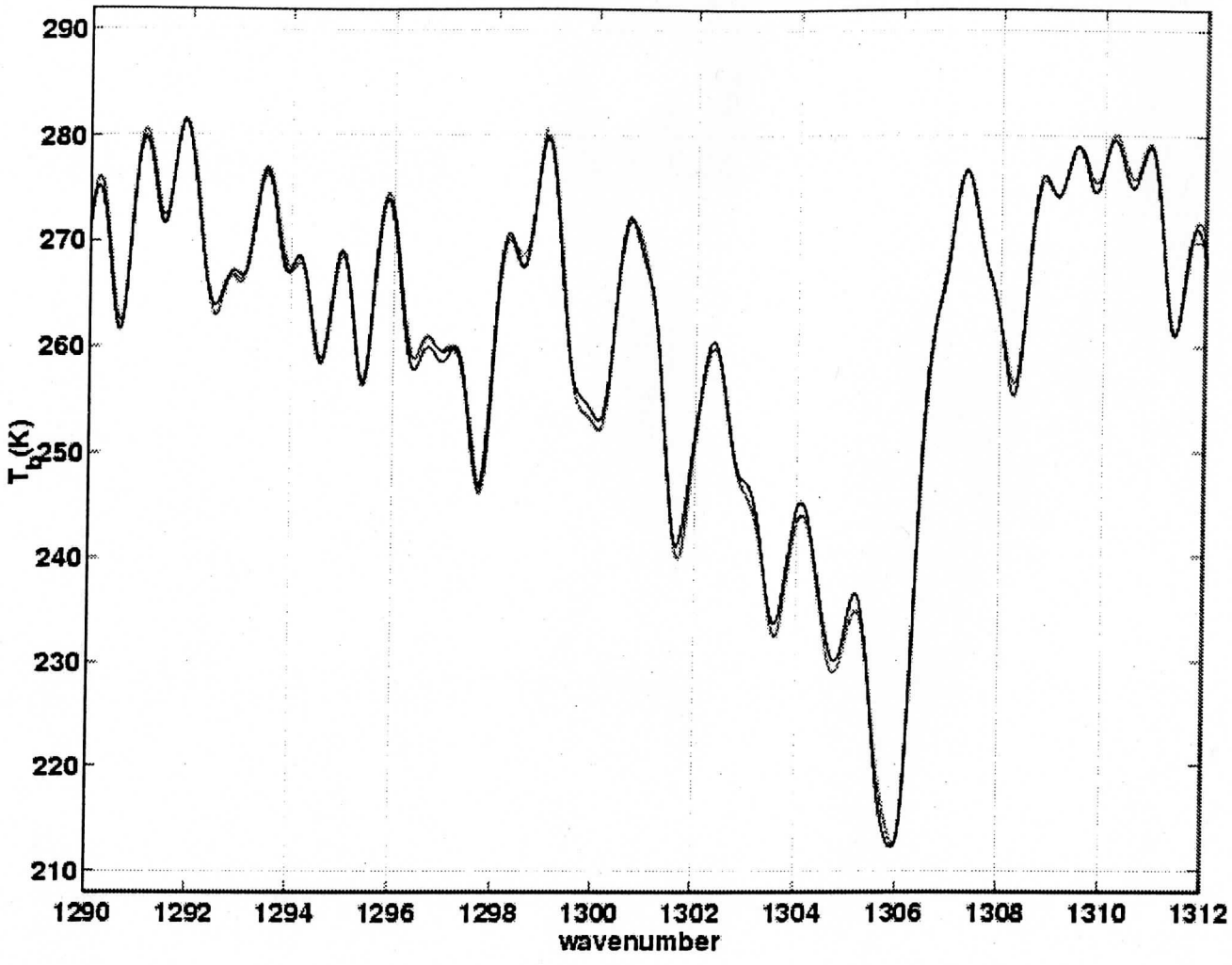
290
280
270
260
250
240
230
220
210
T_b(K)
1290
1292
1294
1296
1298
1300
1302
1304
1306
1308
1310
1312
wavenumber

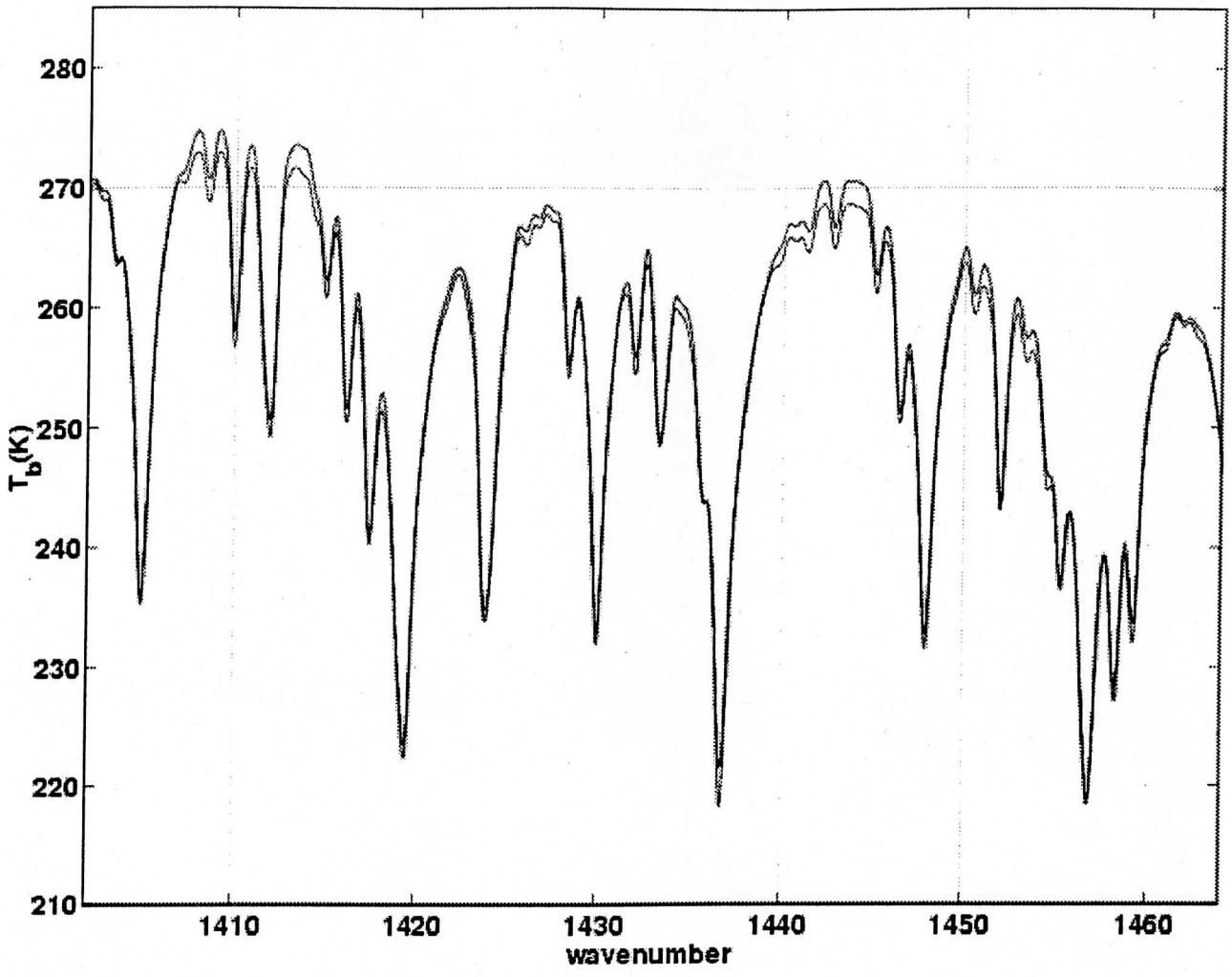
280
270
260
250
240
230
220
210
T_b(K)
1410
1420
1430
1440
1450
1460
wavenumber

100

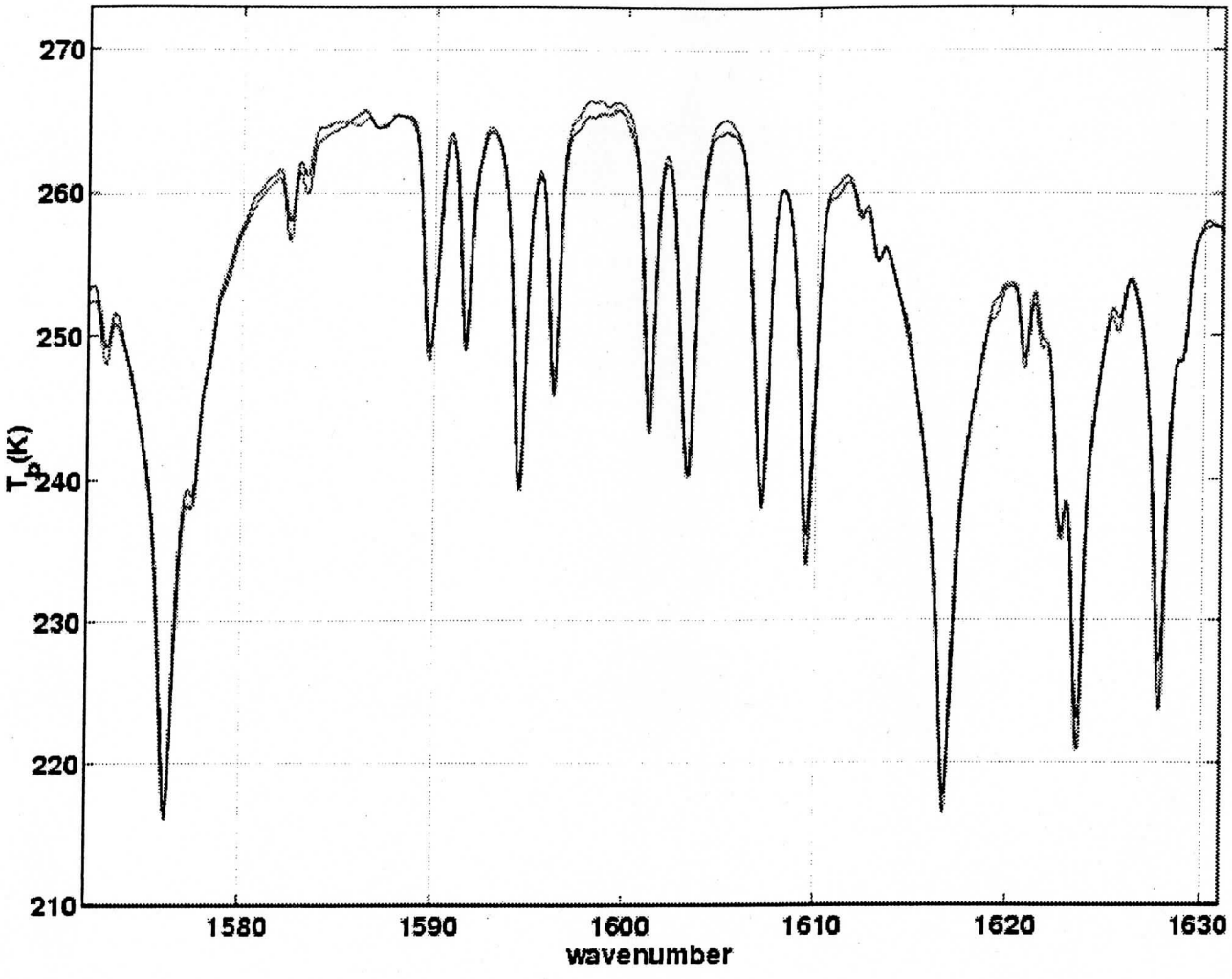
270
260
250
240
230
220
210
T_b(K)
1580
1590
1600
1610
1620
1630
wavenumber

101

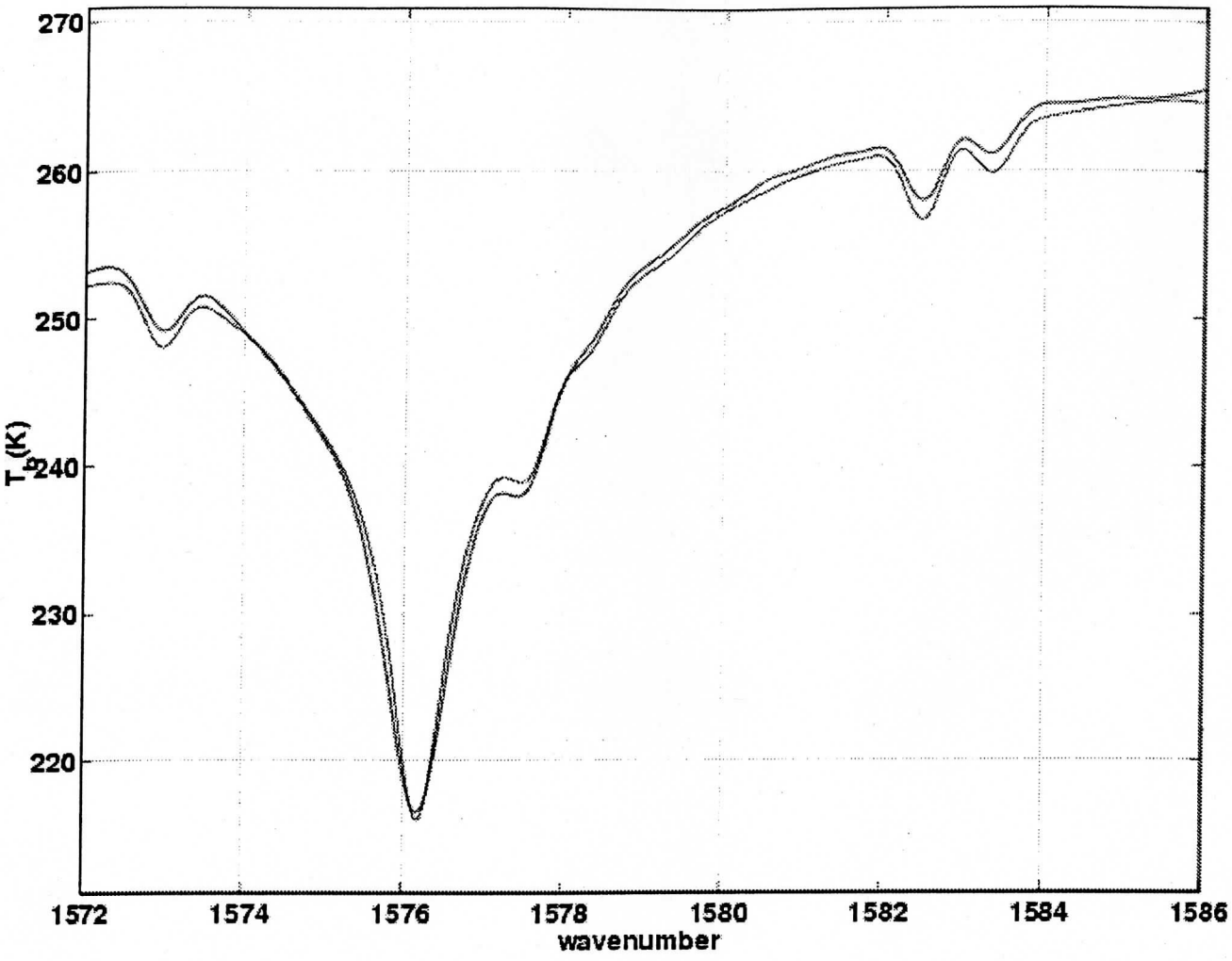
270
260
250
240
230
220
T_B(K)
1572
1574
1576
1578
1580
1582
1584
1586
wavenumber

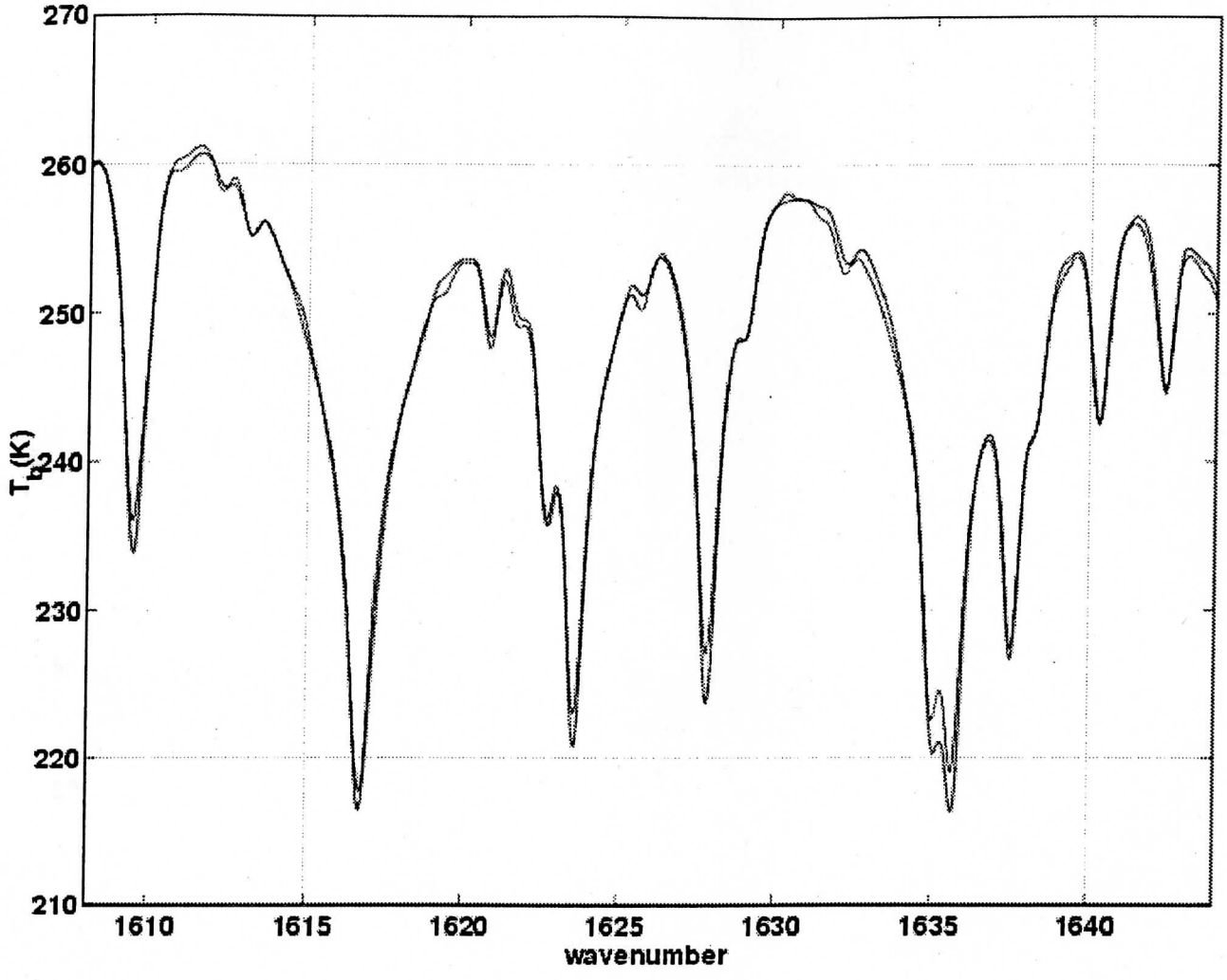
270
260
250
240
230
220
210
T_b(K)
1610
1615
1620
1625
1630
1635
1640
wavenumber

103

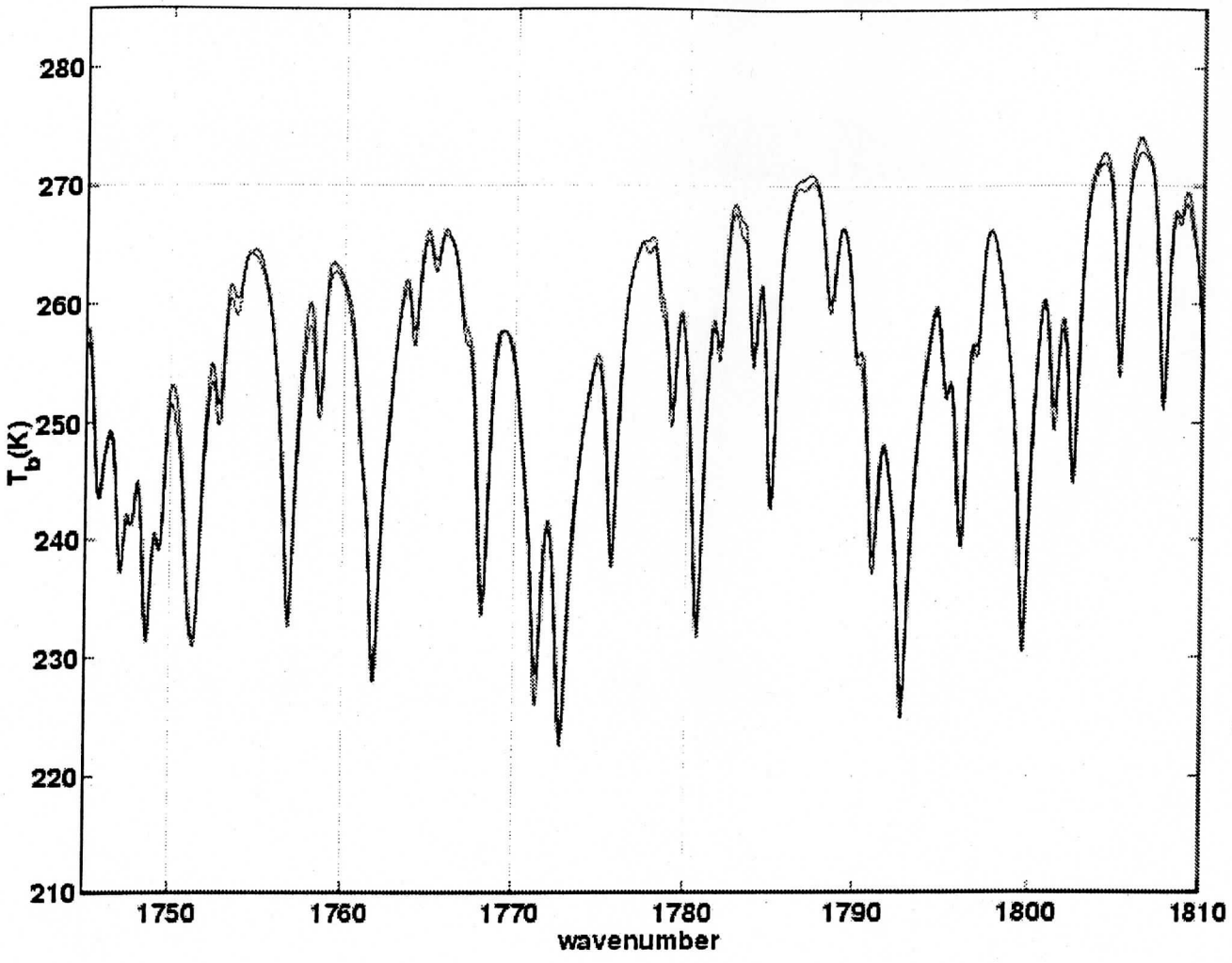
280
270
260
250
240
230
220
210
T_b(K)
1750
1760
1770
1780
1790
1800
1810
wavenumber

104

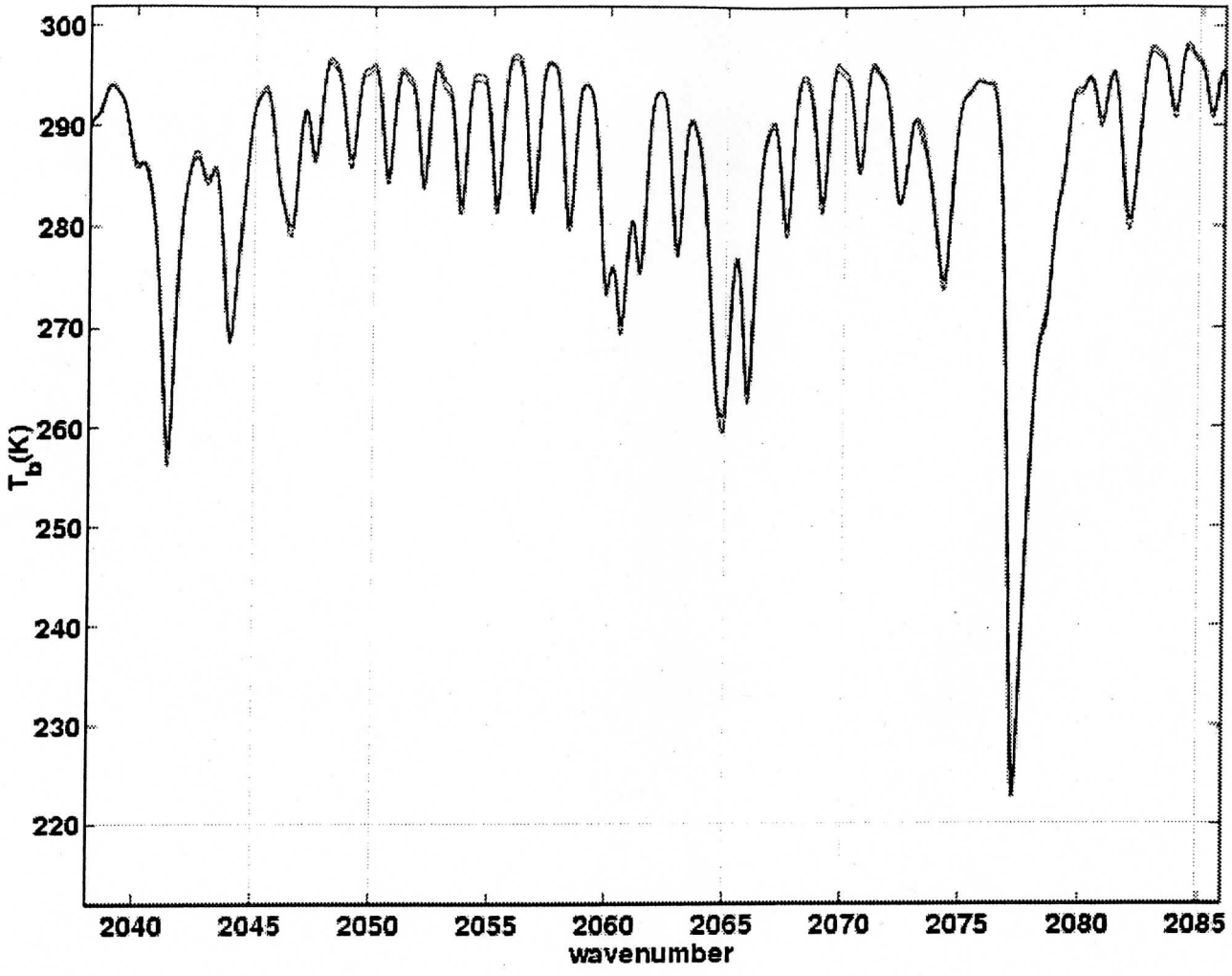
300
290
280
270
260
250
240
230
220
T_b(K)
2040
2045
2050
2055
2060
2065
2070
2075
2080
2085
wavenumber

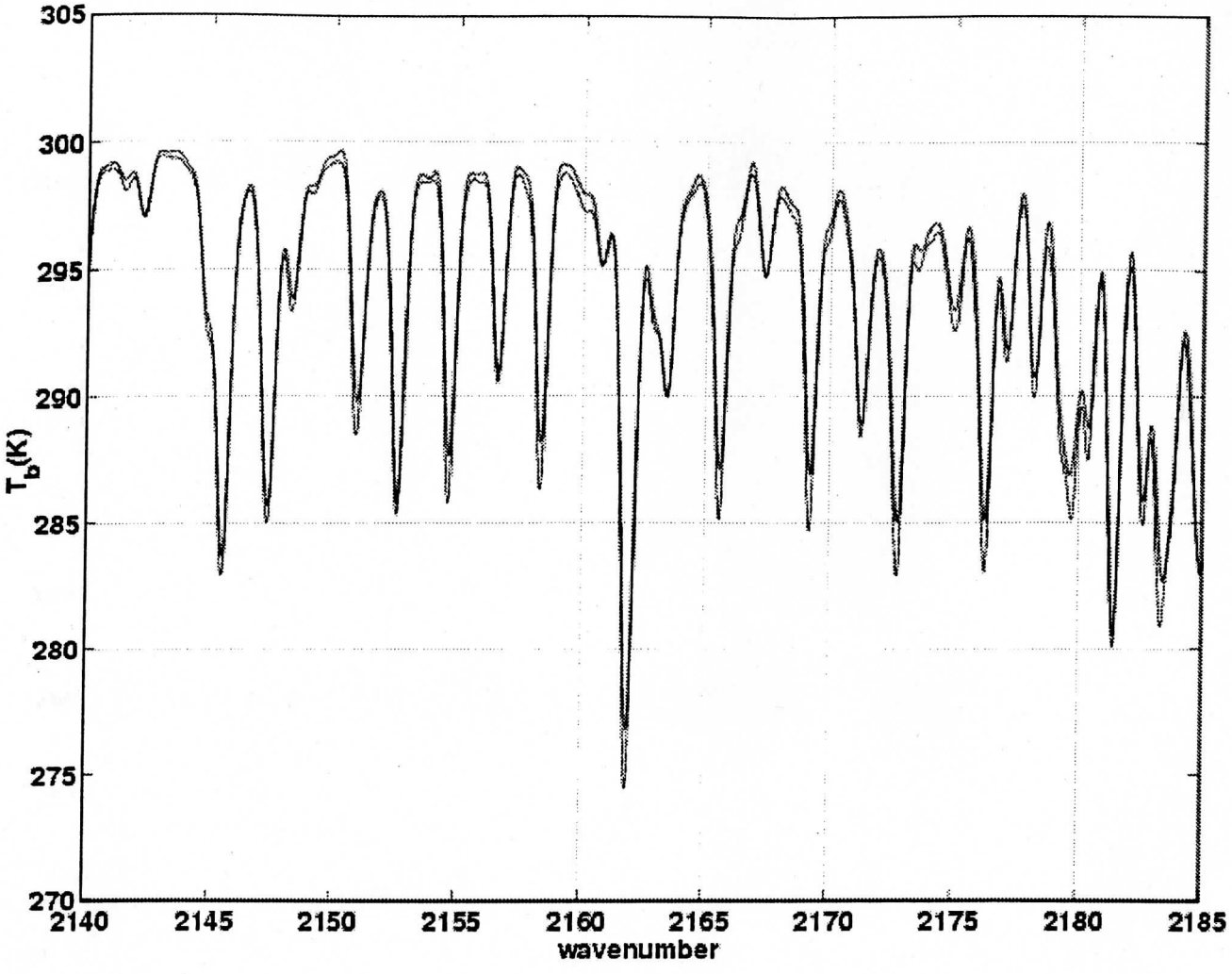
305
300
295
290
285
280
275
270
T_b(K)
2140
2145
2150
2155
2160
2165
2170
2175
2180
2185
wavenumber

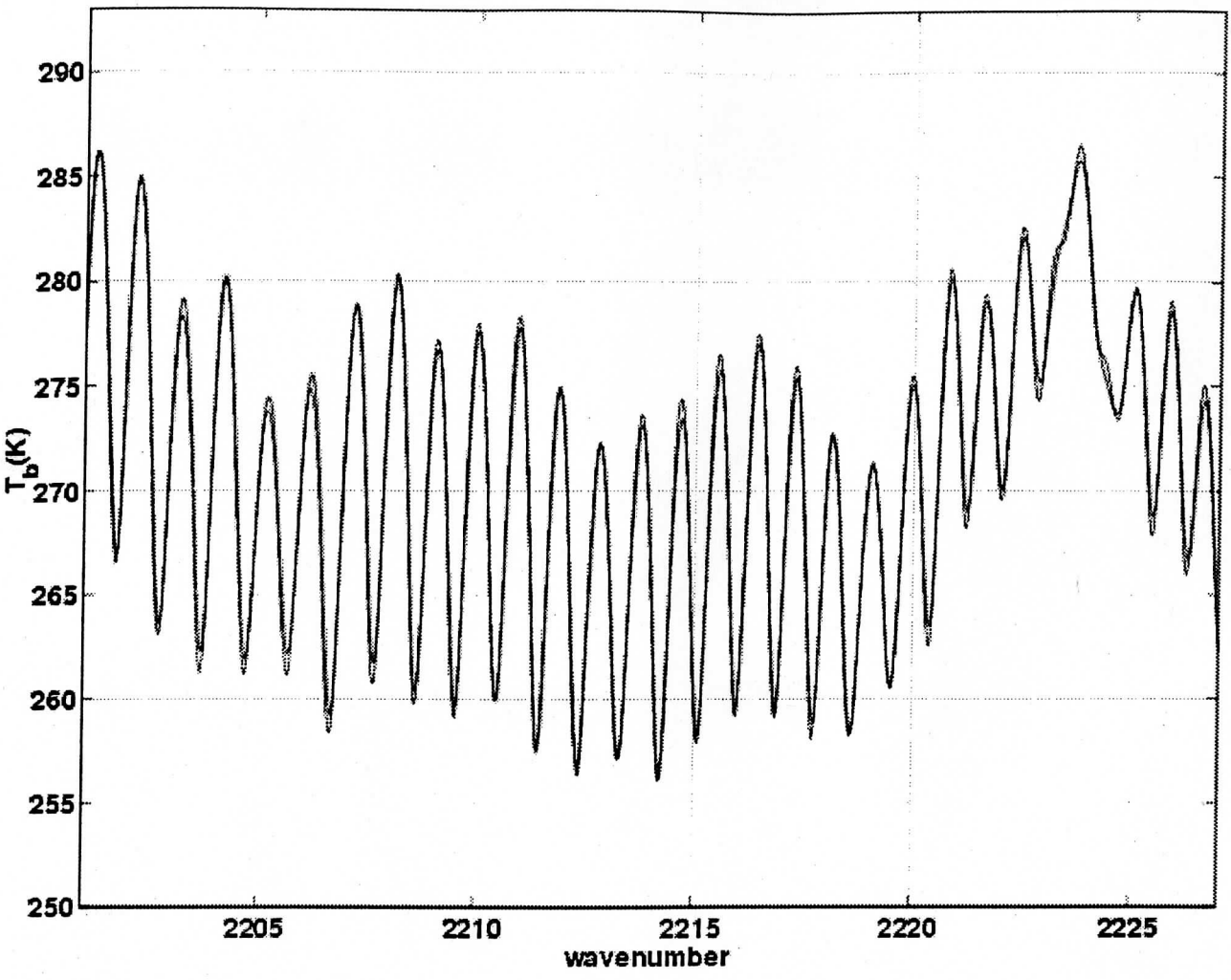
290
285
280
275
270
265
260
255
250
T_b(K)
2205
2210
2215
2220
2225
wavenumber

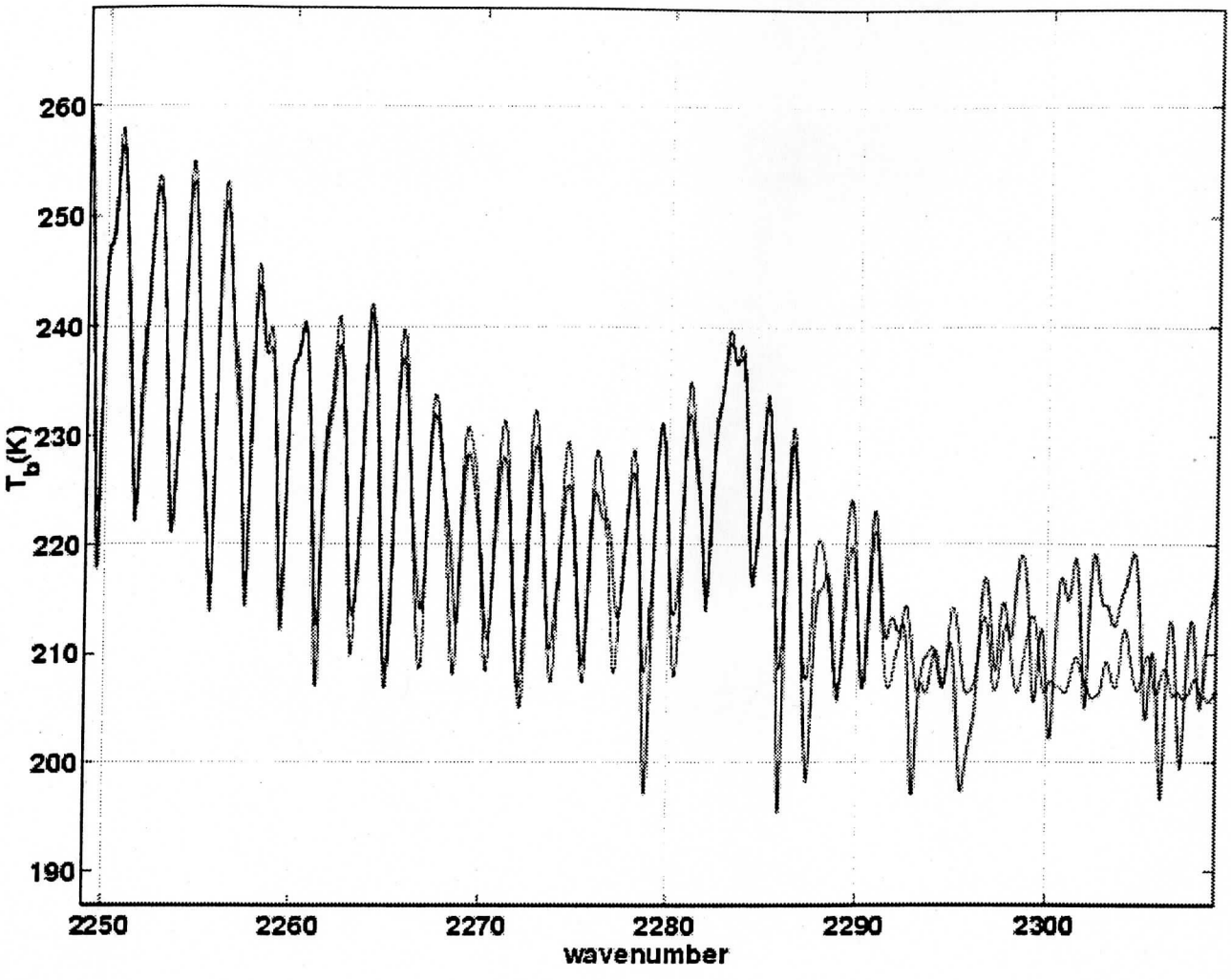
260
250
240
230
220
210
200
190
T_b(K)
2250
2260
2270
2280
2290
2300
wavenumber

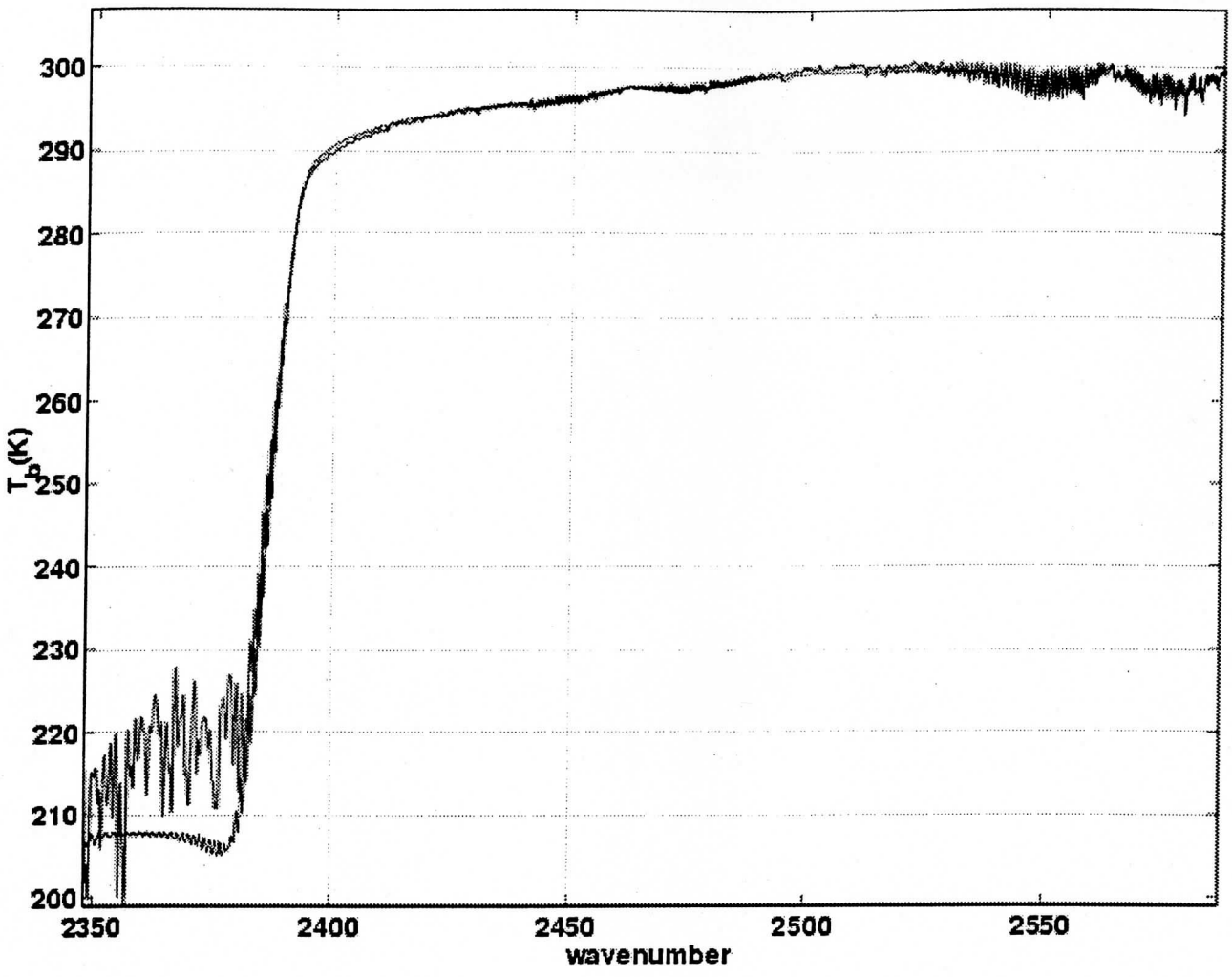
300
290
280
270
260
250
240
230
220
210
200
T_b(K)
2350
2400
2450
2500
2550
wavenumber

109

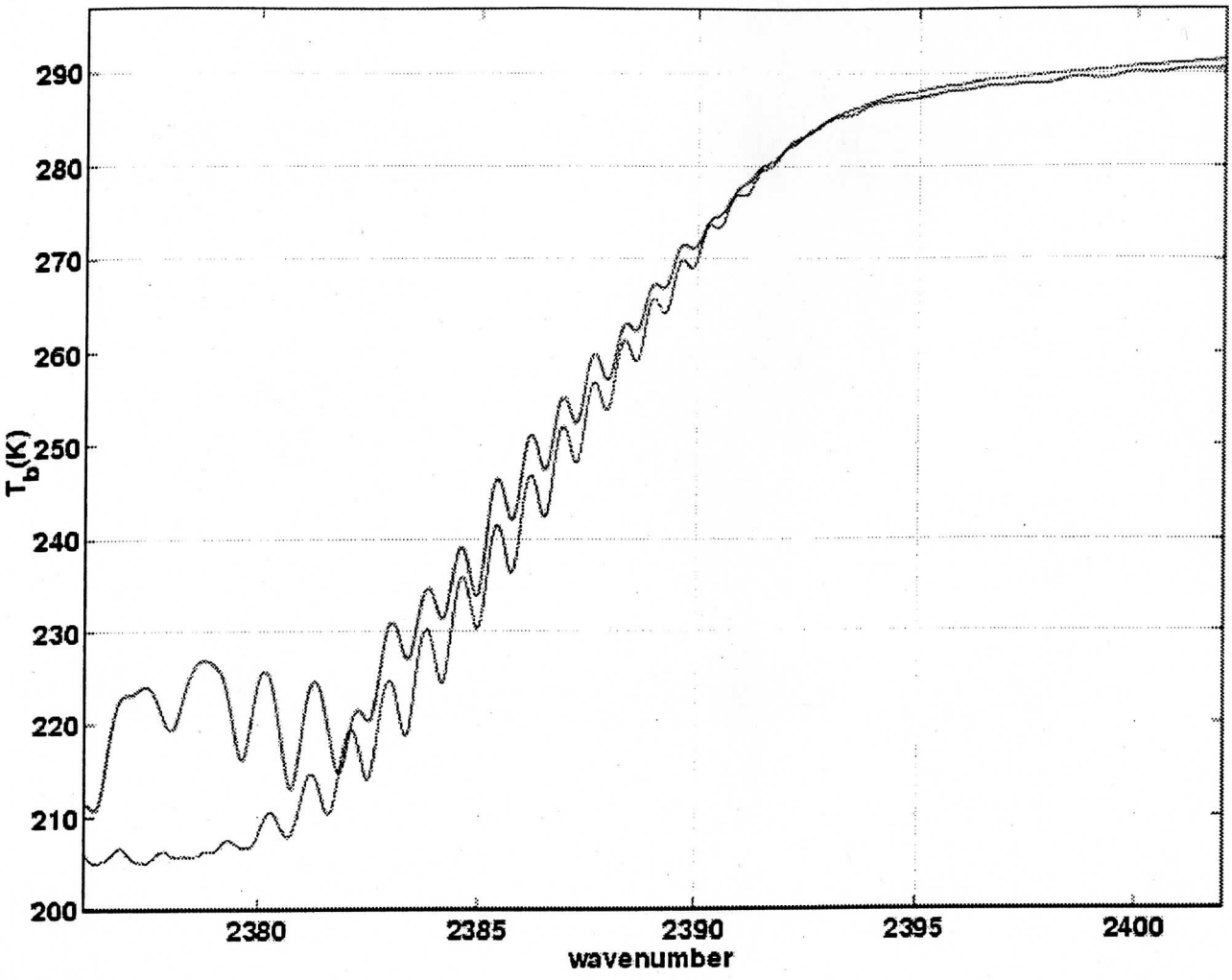
290
280
270
260
250
240
230
220
210
200
T_b(K)
2380
2385
2390
2395
2400
wavenumber

110

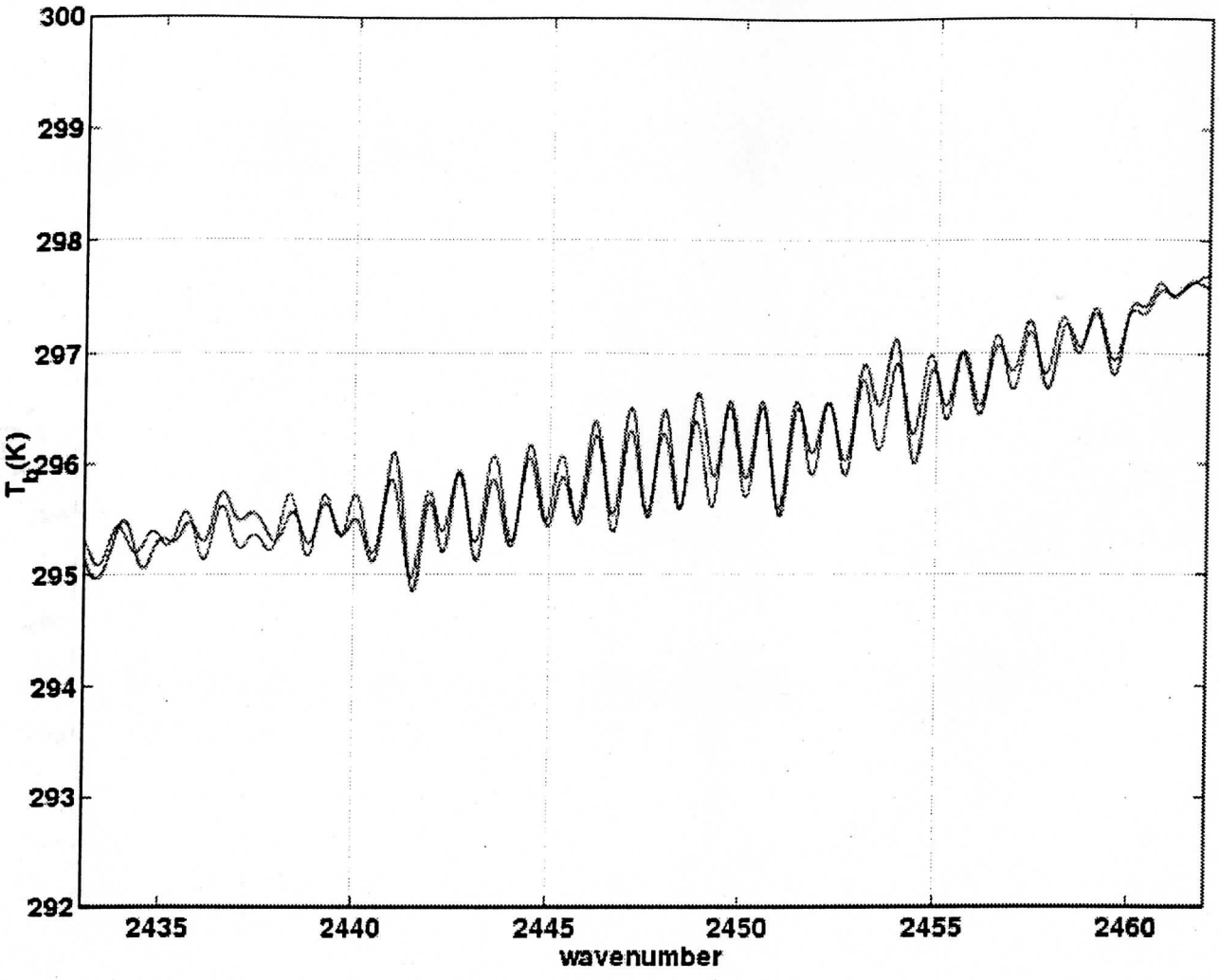
300
299
298
297
296
295
294
293
292
T_b(K)
2435
2440
2445
2450
2455
2460
wavenumber

111

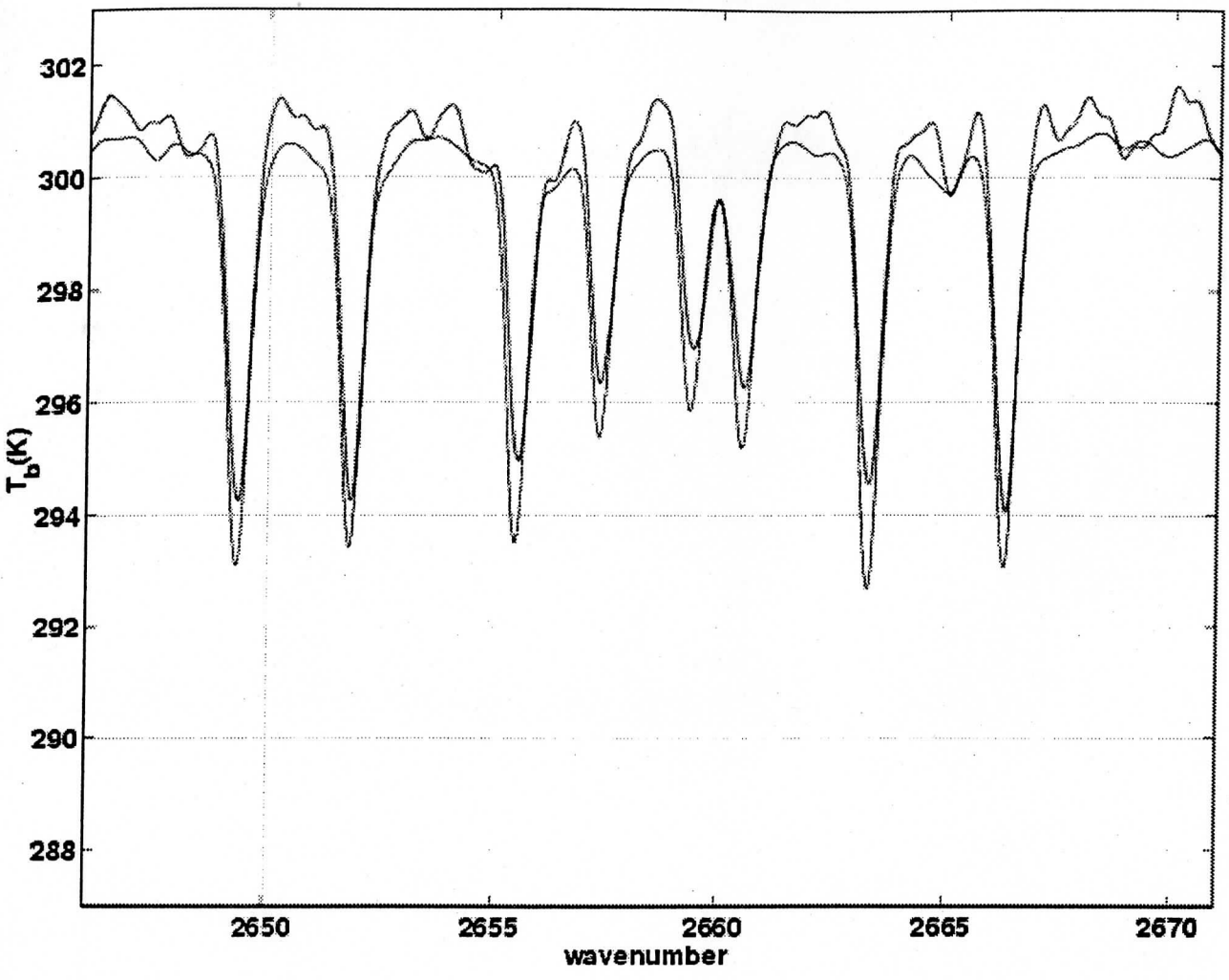
302
300
298
296
294
292
290
288
T_b(K)
2650
2655
2660
2665
2670
wavenumber

University of Wisconsin

FY99 Final Report

Engineering and Scientific Support for the National Polar-orbiting Operational Environmental Satellite System Airborne Sounder Testbed - Interferometer (NAST-I) Instrument

30 September 1999

Deliverables by Task:

Task 1

Comparison of spectra from NAST-I, AERI, & SHIS over Andros Island during CAMEX-3.

3. Comparison of Scanning HIS data with an LBLRTM calculation from CAMEX-3
URL: http://arm1.ssec.wisc.edu/~shis/Results/980913_LBLRTMcomp/shiscalc.html

113

Comparison of Scanning HIS data with an LBLRTM calculation

(CAMEX-3, 980914, 0114-0120)

This web page describes a comparison of Scanning HIS data taken during CAMEX-3 with an LBLRTM calculation. The data used as input to LBLRTM is from a dropsonde, launched on 980914 at 0114 GMT from NASA's DC-8. The vertical profile of temperature from the dropsonde is very similar to those acquired by radiosondes launched on Andros Island (by U. Wisconsin) at 2254 GMT on 980913 and 0755 GMT on 980914. A surface temperature of 301.71 K was used, which is 1 K higher than the final point in the dropsonde data.

This flight was the maiden science mission for the Scanning HIS. The measured spectra shown below are averages of nadir views from 0115 to 0120 GMT using 22 spectra. In all the plots, the red curve is the measurement, while the blue is the calculation. The measurements have been zero-filled from about 3000 points to 64K points, and are unapodized. The resolution of the calculation was degraded from 0.004 cm-1 to 0.5 cm-1, the resolution of the Scanning HIS instrument. The calculations were then zero-filled to 64K points. (Matlab mfile used to process the measurements and calculations: compare3.m)

Note that the calibrated radiances used here DO NOT have corrections for the finite field-of-view of the instrument or nonlinearities in the MCT detectors (LW and MW).

Band 1 (LW): (Radiance and Brightness Temperature)

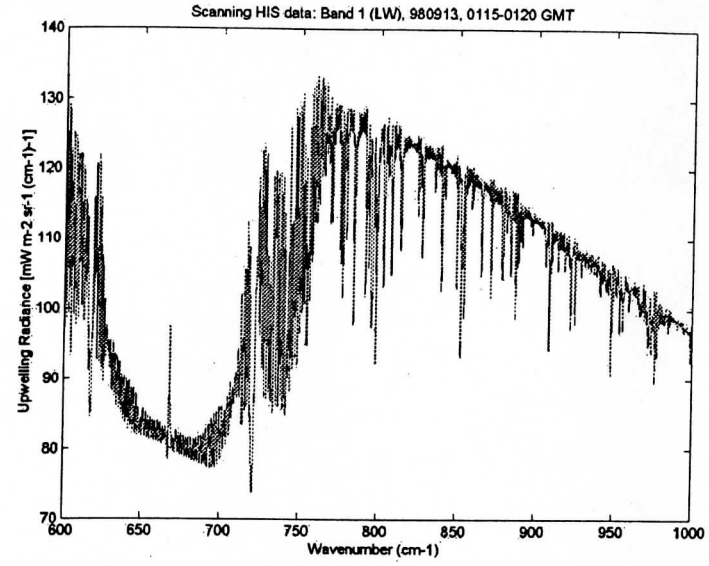

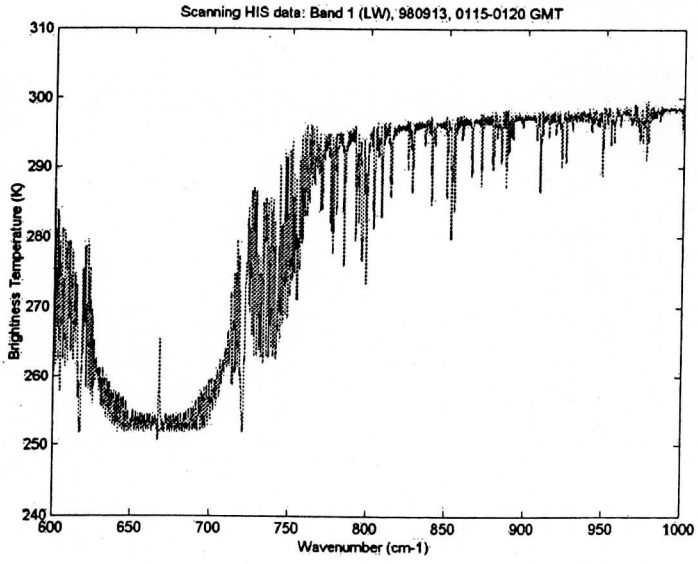

(Note: The disagreement in the central portion of the 667-cm-1 CO2 band is due to inaccurate specification of the temperature profile near the aircraft; thus, the calculated spectrum shows a larger temperature gradient than is actually measured.)

Band 2 (MW): (Radiance and Brightness Temperature)

115

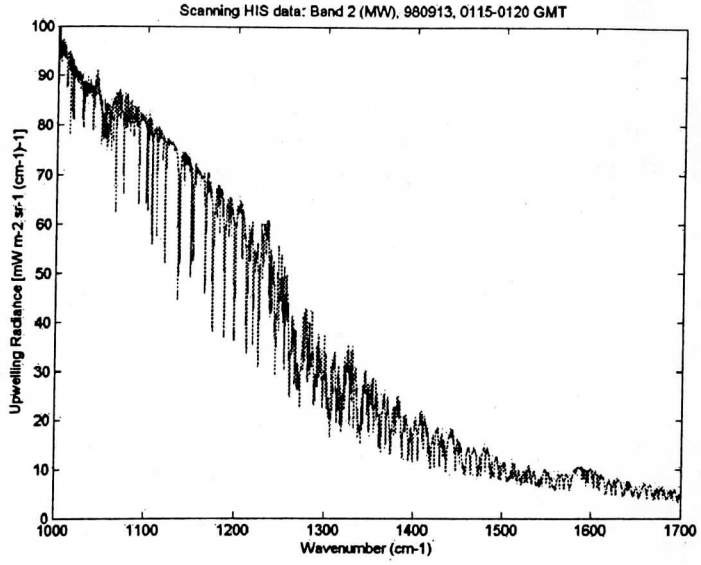

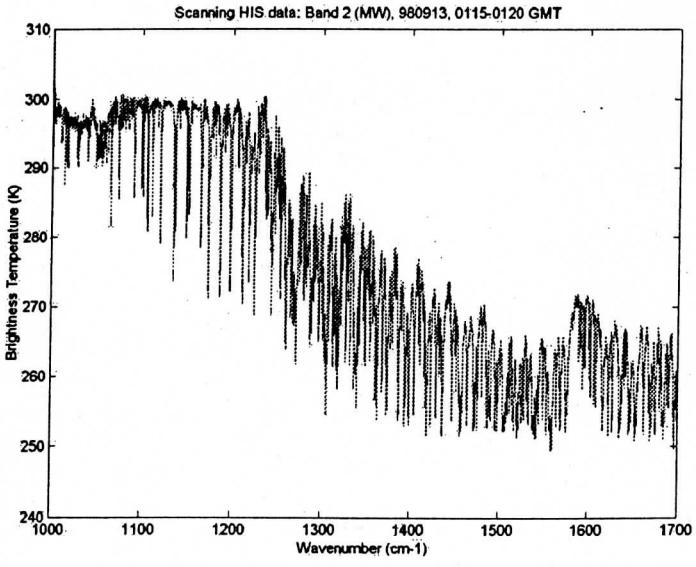

Band 3 (SW): (Radiance and Brightness Temperature)

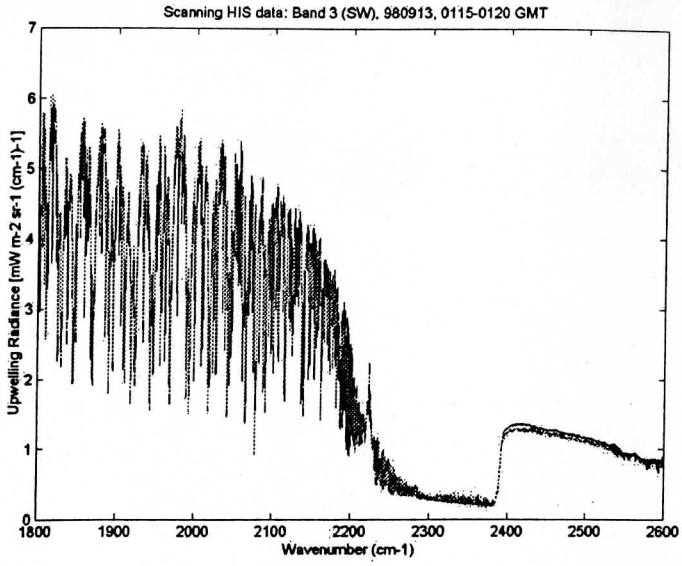

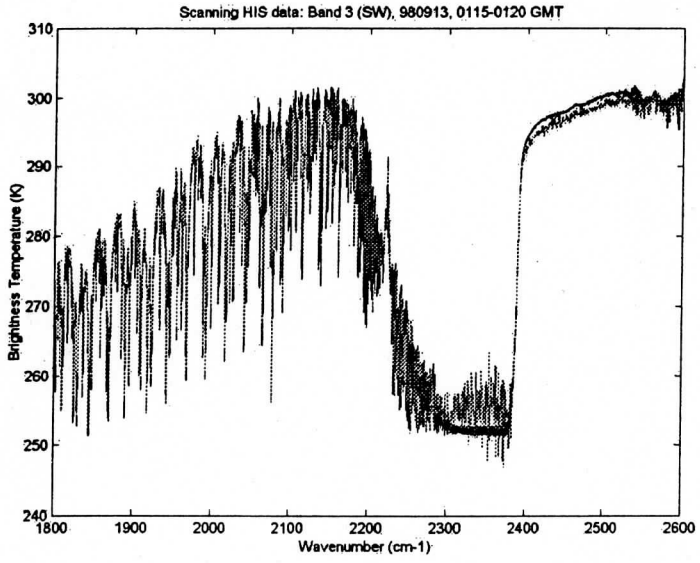

Blowups of Particular Spectral Regions

Wing of the 667-cm-1 Carbon Dioxide Band (LW)

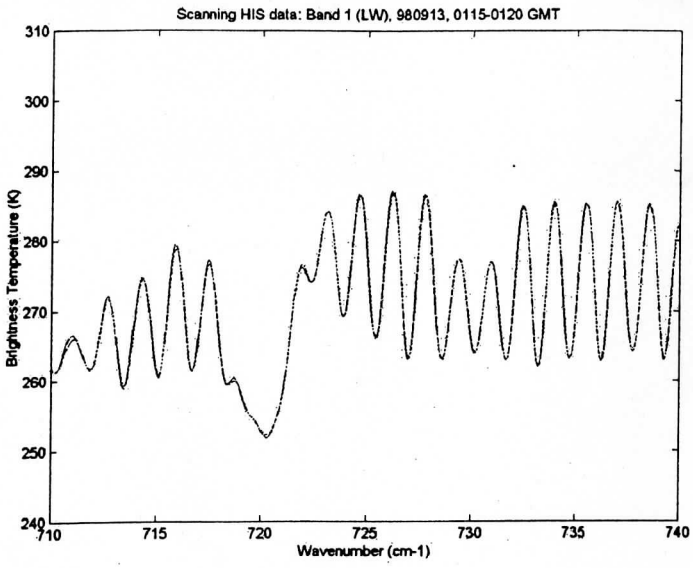

Two sides of the 1592-cm-1 Water Vapor Band (MW)

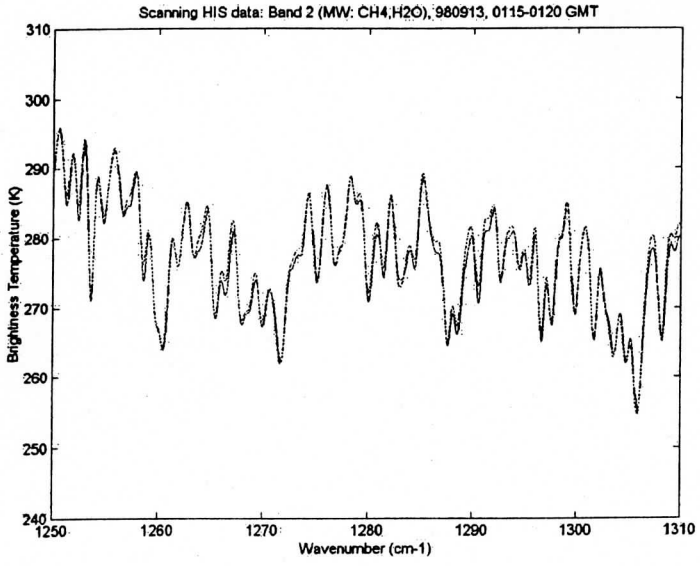

18

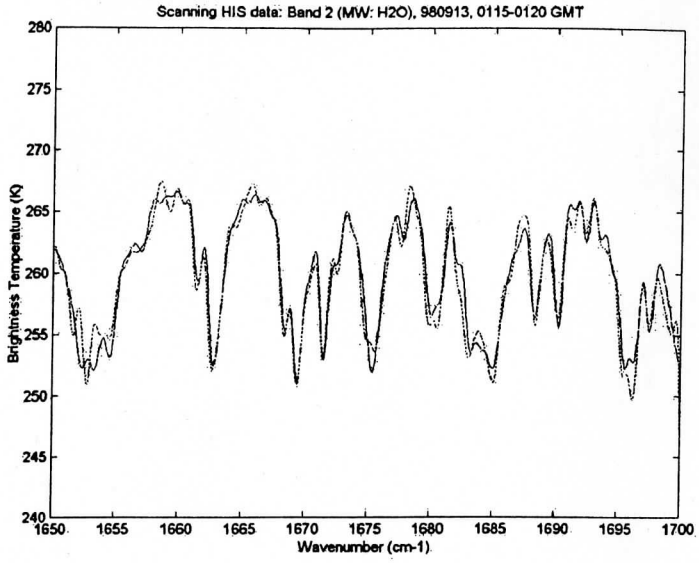

Carbon Monoxide in the Shortwave Band

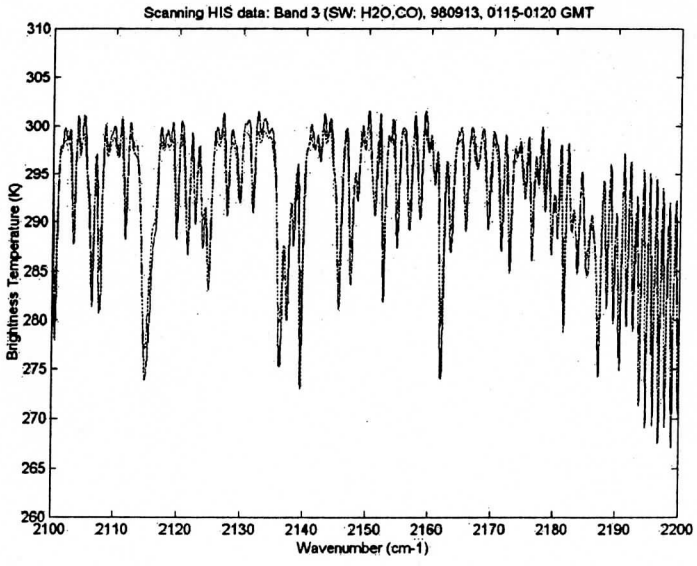

Matlab Mfile used to create plots: shiscalc.m

119

CAPE = 17.9
CIN = -173
K Index = 14
LI = 1.790
Showalter = 5.22
LCL = 872 mb
LFC = 264 mb
EL = 258 mb

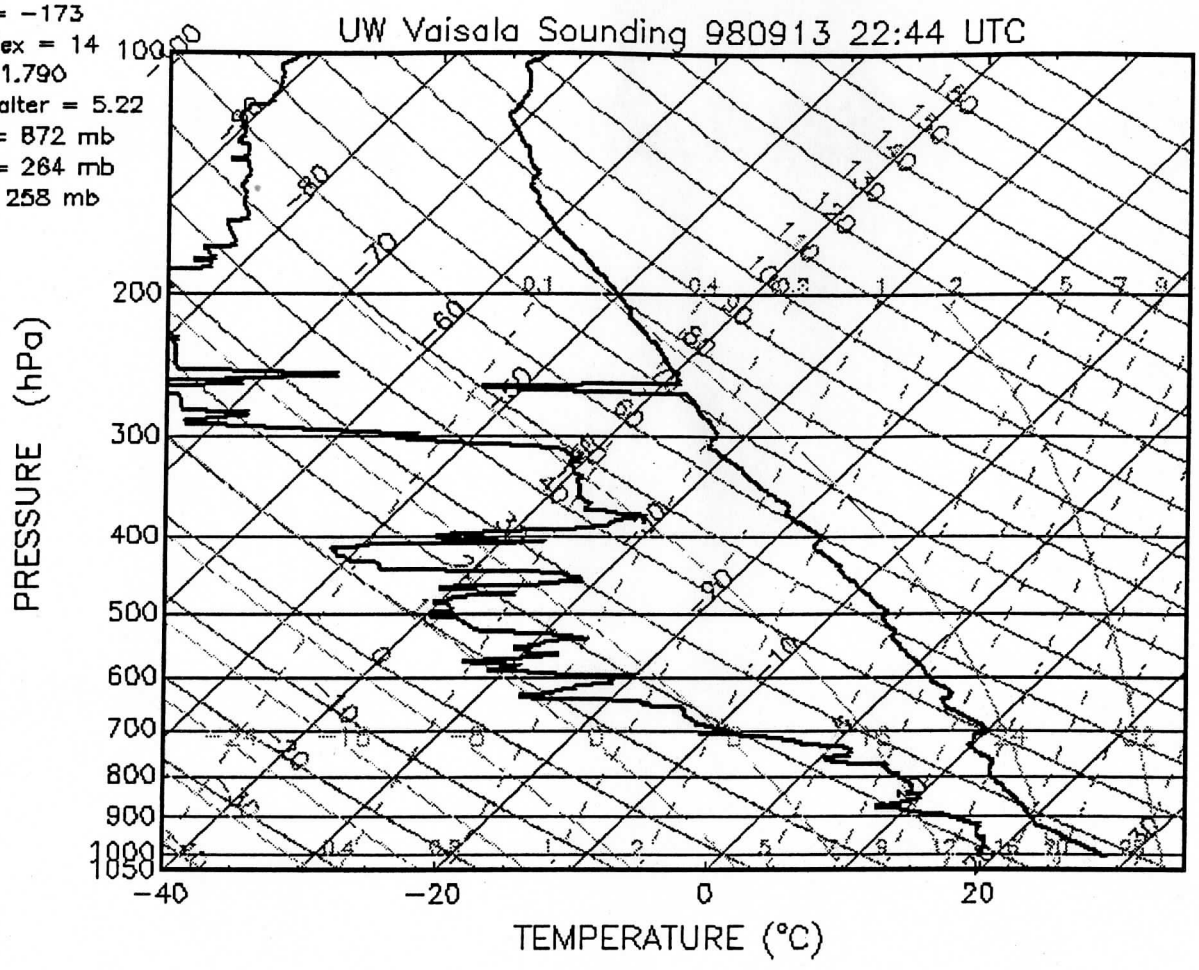

120

CAPE = 83.8
CIN = -542
K Index = 24
LI = 0.921
Showalter = 4.35
LCL = 876 mb
LFC = 653 mb
EL = 534 mb

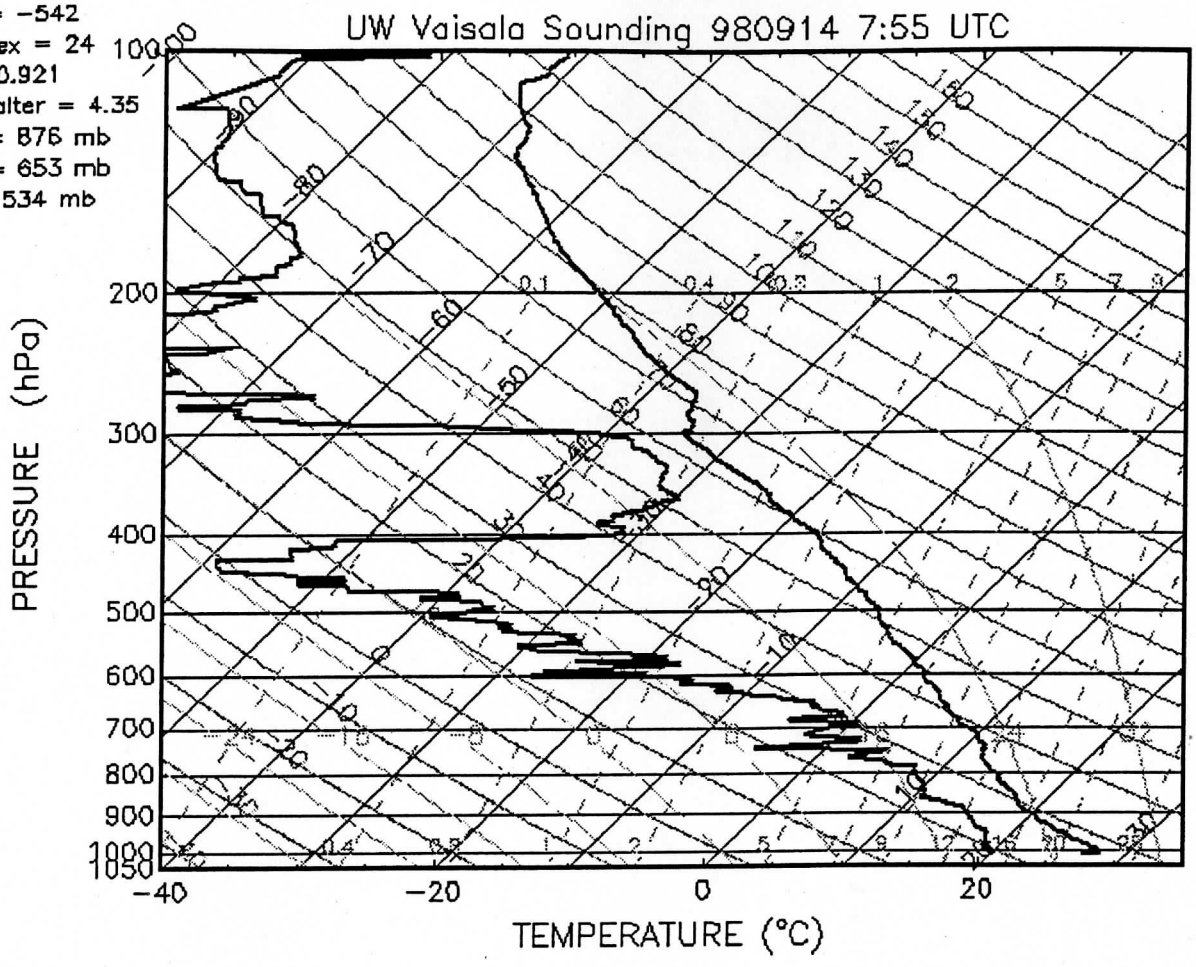

```
load /home/vonw/shis/sh980913/cal/cygbirz_11200_12100.mat

i1  = find(data.wnum1 > 600 & data.wnum1 < 1050);
Ni1 = length(i1);
i2  = find(data.wnum2 > 1000 & data.wnum2 < 1700);
Ni2 = length(i2);
i3  = find(data.wnum3 > 1800 & data.wnum3 < 2600);
Ni3 = length(i3);
mrads1 = mean(real(data.Radiance1(53:7:126,i1)));
mrads2 = mean(real(data.Radiance2(53:7:126,i2)));
mrads3 = mean(real(data.Radiance3(53:7:126,i3)));

ift_mrads1 = idct(mrads1);
ift_mrads2 = idct(mrads2);
ift_mrads3 = idct(mrads3);

%
%    ....Zero pads the interferogram to increase the number of
%        interpolated points in the subsequent spectrum.
%
N = 65536;

intfs1 = ift_mrads1;
intfs1(length(ift_mrads1)+1:N) = zeros(N-length(ift_mrads1),1);
intfs2 = ift_mrads2;
intfs2(length(ift_mrads2)+1:N) = zeros(N-length(ift_mrads2),1);
intfs3 = ift_mrads3;
intfs3(length(ift_mrads3)+1:N) = zeros(N-length(ift_mrads3),1);

%
%    ....Transform back to spectral space to yield spectrum with
%        more interpolated points.
%
dwns1 = data.wnum1(2) - data.wnum1(1);
iwns1 = data.wnum1(min(i1)) + (0:N-1)'*dwns1/(N/Ni1);
imrads1 = dct(intfs1)*sqrt(N/Ni1);
dwns2 = data.wnum2(2) - data.wnum2(1);
iwns2 = data.wnum2(min(i2)) + (0:N-1)'*dwns2/(N/Ni2);
imrads2 = dct(intfs2)*sqrt(N/Ni2);
dwns3 = data.wnum3(2) - data.wnum3(1);
iwns3 = data.wnum3(min(i3)) + (0:N-1)'*dwns3/(N/Ni3);
imrads3 = dct(intfs3)*sqrt(N/Ni3);

clear data mrads1 ift_mrads1 intfs1 dwns1;

%
%    ....Load the LBLRTM calculation
%
load /home/vonw/shis/sh980913/lblrtm/tape12.DC-8_dropsonde_980913_0114.

wnc  = tape12(:,1);
dwnc = wnc(2)-wnc(1);
rad  = tape12(:,2);
```

```
clear tape12;

N1 = floor(wnc(1)/dwnc);
N2 = N1 + length(rad);
N3 = 2^20 - N2;
radc                = zeros(N1,1);
radc(N1+1:N2)       = rad;
radc(N2+1:2^20)     = zeros(N3,1);

%
%    ....Transforms the zero-padded spectrum into an interferogram.
%
ift_radc = dct(radc);

shisconst;
dwn = SHISconst.laserWavenumber/(SHISconst.filteredInterferogramPoints.
Ni = length(ift_radc)*dwnc/dwn;
N  = 65536;
intfc(1:Ni)    = ift_radc(1:Ni);
intfc(Ni+1:N) = zeros(N-Ni,1);

%
%    ....Transform back to spectral space to yield spectrum with
%        more interpolated points.
%
iwnc  = (0:N-1)'*(2^20/65536)*(wnc(2)-wnc(1));
iradc = idct(intfc)/sqrt(2^20/65536);

clear radc ift_radc intfc;
```

123

```
load shiscalc_compare

figure
plot(iwnc,iradc,iwns1,imrads1,'r')
axis([600 1000 70 140])
xlabel('Wavenumber (cm-1)')
ylabel('Upwelling Radiance [mW m-2 sr-1 (cm-1)-1]')
title('Scanning HIS data: Band 1 (LW), 980913, 0115-0120 GMT')
print -djpeg rad1.jpg

figure
plot(iwnc,brittemp(iwnc,iradc'),iwns1,brittemp(iwns1,imrads1'),'r')
axis([600 1000 240 310])
xlabel('Wavenumber (cm-1)')
ylabel('Brightness Temperature (K)')
title('Scanning HIS data: Band 1 (LW), 980913, 0115-0120 GMT')
print -djpeg bt1.jpg

figure
plot(iwnc,iradc,iwns2,imrads2,'r')
axis([1000 1700 0 100])
xlabel('Wavenumber (cm-1)')
ylabel('Upwelling Radiance [mW m-2 sr-1 (cm-1)-1]')
title('Scanning HIS data: Band 2 (MW), 980913, 0115-0120 GMT')
print -djpeg rad2.jpg

figure
plot(iwnc,brittemp(iwnc,iradc'),iwns2,brittemp(iwns2,imrads2'),'r')
axis([1000 1700 240 310])
xlabel('Wavenumber (cm-1)')
ylabel('Brightness Temperature (K)')
title('Scanning HIS data: Band 2 (MW), 980913, 0115-0120 GMT')
print -djpeg bt2.jpg

figure
plot(iwnc,iradc,iwns3,imrads3,'r')
axis([1800 2600 0 7])
xlabel('Wavenumber (cm-1)')
ylabel('Upwelling Radiance [mW m-2 sr-1 (cm-1)-1]')
title('Scanning HIS data: Band 3 (SW), 980913, 0115-0120 GMT')
print -djpeg rad3.jpg

figure
plot(iwnc,brittemp(iwnc,iradc'),iwns3,brittemp(iwns3,imrads3'),'r')
axis([1800 2600 240 310])
xlabel('Wavenumber (cm-1)')
ylabel('Brightness Temperature (K)')
title('Scanning HIS data: Band 3 (SW), 980913, 0115-0120 GMT')
print -djpeg bt3.jpg

% Blowup
figure
plot(iwnc,brittemp(iwnc,iradc'),iwns1,brittemp(iwns1,imrads1'),'r')
```

```
axis([710 740 240 310])
xlabel('Wavenumber (cm-1)')
ylabel('Brightness Temperature (K)')
title('Scanning HIS data: Band 1 (LW: CO2), 980913, 0115-0120 GMT')
print -djpeg co2_710-740.jpg

figure
plot(iwnc,brittemp(iwnc,iradc'),iwns2,brittemp(iwns2,imrads2'),'r')
axis([1250 1310 240 310])
xlabel('Wavenumber (cm-1)')
ylabel('Brightness Temperature (K)')
title('Scanning HIS data: Band 2 (MW: CH4,H2O), 980913, 0115-0120 GMT')
print -djpeg h2o_1250-1310.jpg

figure
plot(iwnc,brittemp(iwnc,iradc'),iwns2,brittemp(iwns2,imrads2'),'r')
axis([1650 1700 240 280])
xlabel('Wavenumber (cm-1)')
ylabel('Brightness Temperature (K)')
title('Scanning HIS data: Band 2 (MW: H2O), 980913, 0115-0120 GMT')
print -djpeg h2o_1650-1700.jpg

figure
plot(iwnc,brittemp(iwnc,iradc'),iwns3,brittemp(iwns3,imrads3'),'r')
axis([2100 2200 260 310])
xlabel('Wavenumber (cm-1)')
ylabel('Brightness Temperature (K)')
title('Scanning HIS data: Band 3 (SW: H2O,CO), 980913, 0115-0120 GMT')
print -djpeg co_2100-2200.jpg
```

```
$ Andros Cal/Val CAMEX3 flight; 19980914 01:13:53 DC-8 dropsonde
 HI=1 F4=1 CN=1 AE=0 EM=1 SC=0 FI=0 PL=0 TS=0 AM=1 MG=0 LA=0 MS=0 XS=1
   600.000  2600.000
   301.710     1.000
    0    2   53    1    1    7    1 0  1     0.000     0.000  1600.000
     8.069     0.000   180.000
     0.000     0.100     0.200     0.300     0.400     0.500     0.600
     0.800     0.900     1.000     1.100     1.200     1.300     1.400
     1.600     1.700     1.800     1.900     2.000     2.100     2.200
     2.400     2.500     2.600     2.700     2.800     2.900     3.000
     3.400     3.600     3.800     4.000     4.200     4.400     4.600
     5.000     5.200     5.400     5.600     5.800     6.000     6.500
     7.500     7.636     7.787     7.945     8.069
 433 19980914 01:13:53 DC-8 dropsonde
     0.000  1012.930   300.710     AA   HA11111
    65.440   360.000
     0.025  1010.040   300.640     AA   HA11111
    65.450   360.000
     0.039  1008.480   300.600     AA   HA11111
    65.840   360.000
     0.069  1005.100   300.270     AA   HA11111
    67.630   360.000
     0.087  1003.090   300.200     AA   HA11111
    67.700   360.000
     0.092  1002.460   300.140     AA   HA11111
    68.210   360.000
     0.106  1000.870   300.030     AA   HA11111
    67.620   360.000
     0.116   999.810   299.930     AA   HA11111
    67.830   360.000
     0.124   998.870   299.840     AA   HA11111
    68.630   360.000
     0.153   995.630   299.570     AA   HA11111
    69.640   360.000
     0.181   992.500   299.240     AA   HA11111
    70.230   360.000
     0.191   991.330   299.000     AA   HA11111
    71.450   360.000
     0.220   988.080   298.810     AA   HA11111
    72.250   360.000
     0.245   985.300   298.540     AA   HA11111
    73.290   360.000
     0.270   982.480   298.410     AA   HA11111
    73.890   360.000
     0.278   981.560   298.110     AA   HA11111
    75.710   360.000
     0.289   980.440   298.010     AA   HA11111
    75.510   360.000
     0.329   975.900   297.850     AA   HA11111
    76.930   360.000
     0.338   974.940   297.750     AA   HA11111
    77.140   360.000
     0.350   973.590   297.680     AA   HA11111
```

```
 77.350   360.000
  0.353   973.250   297.560     AA   HA11111
 77.550   360.000
  0.370   971.380   297.520     AA   HA11111
 77.760   360.000
  0.378   970.470   297.400     AA   HA11111
 78.160   360.000
  0.389   969.340   297.200     AA   HA11111
 78.190   360.000
  0.404   967.670   297.070     AA   HA11111
 78.800   360.000
  0.444   963.250   296.710     AA   HA11111
 80.230   360.000
  0.457   961.850   296.640     AA   HA11111
 80.650   360.000
  0.463   961.200   296.330     AA   HA11111
 81.680   360.000
  0.492   958.020   296.240     AA   HA11111
 81.880   360.000
  0.533   953.510   295.930     AA   HA11111
 83.770   360.000
  0.543   952.430   295.840     AA   HA11111
 84.190   360.000
  0.552   951.480   295.710     AA   HA11111
 84.190   360.000
  0.569   949.600   295.550     AA   HA11111
 85.230   360.000
  0.580   948.410   295.460     AA   HA11111
 85.030   360.000
  0.583   948.020   295.390     AA   HA11111
 85.230   360.000
  0.606   945.600   295.290     AA   HA11111
 85.660   360.000
  0.611   945.040   295.200     AA   HA11111
 85.670   360.000
  0.620   944.020   295.140     AA   HA11111
 86.070   360.000
  0.628   943.210   295.080     AA   HA11111
 86.070   360.000
  0.636   942.360   294.880     AA   HA11111
 86.920   360.000
  0.675   938.090   294.810     AA   HA11111
 86.930   360.000
  0.677   937.920   294.780     AA   HA11111
 87.150   360.000
  0.690   936.490   294.780     AA   HA11111
 86.950   360.000
  0.695   935.940   294.780     AA   HA11111
 86.130   360.000
  0.706   934.820   294.780     AA   HA11111
 81.210   360.000
  0.721   933.180   294.710     AA   HA11111
 80.620   360.000
```

127

```
  0.730    932.140    294.680      AA    HA11111
 79.600    360.000
  0.746    930.490    294.550      AA    HA11111
 79.210    360.000
  0.758    929.200    294.510      AA    HA11111
 79.210    360.000
  0.765    928.460    294.430      AA    HA11111
 77.790    360.000
  0.795    925.220    294.400      AA    HA11111
 77.590    360.000
  0.814    923.190    294.310      AA    HA11111
 78.230    360.000
  0.842    920.280    294.280      AA    HA11111
 77.010    360.000
  0.853    919.070    294.220      AA    HA11111
 75.600    360.000
  0.862    918.110    294.150      AA    HA11111
 75.210    360.000
  0.879    916.370    294.120      AA    HA11111
 74.000    360.000
  0.886    915.550    294.060      AA    HA11111
 74.010    360.000
  0.900    914.080    294.000      AA    HA11111
 74.010    360.000
  0.913    912.760    293.930      AA    HA11111
 74.220    360.000
  0.962    907.590    293.670      AA    HA11111
 71.040    360.000
  0.972    906.590    293.610      AA    HA11111
 70.250    360.000
  0.988    904.920    293.420      AA    HA11111
 70.860    360.000
  1.003    903.360    293.280      AA    HA11111
 69.890    360.000
  1.031    900.340    293.190      AA    HA11111
 70.500    360.000
  1.053    898.150    293.140      AA    HA11111
 70.500    360.000
  1.083    895.010    292.880      AA    HA11111
 70.940    360.000
  1.085    894.830    292.850      AA    HA11111
 71.140    360.000
  1.086    894.710    292.760      AA    HA11111
 71.350    360.000
  1.090    894.250    292.720      AA    HA11111
 71.550    360.000
  1.123    890.800    292.660      AA    HA11111
 71.560    360.000
  1.132    889.880    292.570      AA    HA11111
 71.780    360.000
  1.144    888.670    292.530      AA    HA11111
 70.980    360.000
  1.153    887.740    292.470      AA    HA11111
```

128

```
 70.390   360.000
  1.177   885.320   292.430     AA   HA11111
 67.810   360.000
  1.217   881.170   292.490     AA   HA11111
 67.210   360.000
  1.257   877.070   292.570     AA   HA11111
 65.030   360.000
  1.267   876.090   292.600     AA   HA11111
 58.940   360.000
  1.294   873.360   292.540     AA   HA11111
 54.680   360.000
  1.311   871.660   292.510     AA   HA11111
 54.490   360.000
  1.317   870.990   292.410     AA   HA11111
 53.740   360.000
  1.349   867.760   292.380     AA   HA11111
 53.740   360.000
  1.366   866.020   292.400     AA   HA11111
 54.130   360.000
  1.375   865.190   292.340     AA   HA11111
 47.470   360.000
  1.407   861.940   291.960     AA   HA11111
 49.390   360.000
  1.435   859.090   291.740     AA   HA11111
 52.290   360.000
  1.460   856.590   291.710     AA   HA11111
 52.670   360.000
  1.554   847.300   291.090     AA   HA11111
 52.540   360.000
  1.563   846.430   291.000     AA   HA11111
 53.320   360.000
  1.577   845.060   290.760     AA   HA11111
 54.500   360.000
  1.603   842.490   290.610     AA   HA11111
 55.480   360.000
  1.612   841.520   290.450     AA   HA11111
 54.920   360.000
  1.637   839.150   290.350     AA   HA11111
 54.570   360.000
  1.647   838.170   290.260     AA   HA11111
 53.030   360.000
  1.657   837.190   290.200     AA   HA11111
 52.460   360.000
  1.659   836.930   290.160     AA   HA11111
 52.090   360.000
  1.679   835.000   290.040     AA   HA11111
 52.300   360.000
  1.685   834.360   289.970     AA   HA11111
 51.160   360.000
  1.700   832.900   289.910     AA   HA11111
 50.780   360.000
  1.713   831.710   289.820     AA   HA11111
 51.170   360.000
```

```
 1.718   831.140   289.700     AA   HA11111
51.390   360.000
 1.740   829.000   289.450     AA   HA11111
52.000   360.000
 1.750   828.030   289.300     AA   HA11111
51.820   360.000
 1.789   824.290   289.190     AA   HA11111
52.400   360.000
 1.798   823.400   289.060     AA   HA11111
52.810   360.000
 1.808   822.380   288.880     AA   HA11111
53.210   360.000
 1.816   821.680   288.800     AA   HA11111
53.790   360.000
 1.828   820.470   288.650     AA   HA11111
54.010   360.000
 1.853   818.100   288.550     AA   HA11111
54.600   360.000
 1.861   817.280   288.450     AA   HA11111
55.220   360.000
 1.863   817.070   288.370     AA   HA11111
55.810   360.000
 1.877   815.780   288.220     AA   HA11111
57.370   360.000
 1.883   815.180   287.950     AA   HA11111
64.110   360.000
 1.912   812.400   287.820     AA   HA11111
65.330   360.000
 1.916   812.060   287.520     AA   HA11111
70.800   360.000
 1.943   809.440   287.460     AA   HA11111
71.210   360.000
 1.964   807.460   287.350     AA   HA11111
72.230   360.000
 1.970   806.890   287.110     AA   HA11111
73.680   360.000
 2.013   802.790   286.940     AA   HA11111
74.740   360.000
 2.027   801.410   286.870     AA   HA11111
75.170   360.000
 2.042   799.990   286.770     AA   HA11111
75.600   360.000
 2.048   799.410   286.660     AA   HA11111
75.820   360.000
 2.055   798.800   286.570     AA   HA11111
76.450   360.000
 2.085   795.890   286.450     AA   HA11111
76.880   360.000
 2.091   795.320   286.390     AA   HA11111
76.690   360.000
 2.097   794.810   286.300     AA   HA11111
77.530   360.000
 2.113   793.280   286.180     AA   HA11111
```

130

```
 78.570   360.000
  2.118   792.850   286.030     AA   HA11111
 80.260   360.000
  2.124   792.290   285.860     AA   HA11111
 80.290   360.000
  2.146   790.230   285.810     AA   HA11111
 79.870   360.000
  2.168   788.160   285.750     AA   HA11111
 79.060   360.000
  2.172   787.760   285.660     AA   HA11111
 79.090   360.000
  2.179   787.060   285.430     AA   HA11111
 79.760   360.000
  2.214   783.790   285.360     AA   HA11111
 80.190   360.000
  2.219   783.390   285.070     AA   HA11111
 81.490   360.000
  2.259   779.630   285.010     AA   HA11111
 82.120   360.000
  2.269   778.730   284.930     AA   HA11111
 82.350   360.000
  2.285   777.240   284.860     AA   HA11111
 82.160   360.000
  2.288   776.940   284.810     AA   HA11111
 82.380   360.000
  2.300   775.850   284.720     AA   HA11111
 82.400   360.000
  2.317   774.270   284.660     AA   HA11111
 82.630   360.000
  2.322   773.820   284.570     AA   HA11111
 83.060   360.000
  2.325   773.480   284.400     AA   HA11111
 83.920   360.000
  2.335   772.600   284.340     AA   HA11111
 84.160   360.000
  2.367   769.630   284.130     AA   HA11111
 84.830   360.000
  2.413   765.450   283.900     AA   HA11111
 85.510   360.000
  2.452   761.840   283.850     AA   HA11111
 86.140   360.000
  2.461   761.030   283.610     AA   HA11111
 86.020   360.000
  2.499   757.530   283.580     AA   HA11111
 86.030   360.000
  2.514   756.230   283.460     AA   HA11111
 85.240   360.000
  2.531   754.640   283.400     AA   HA11111
 85.250   360.000
  2.541   753.810   283.300     AA   HA11111
 84.440   360.000
  2.560   752.030   283.260     AA   HA11111
 83.830   360.000
```

```
 2.591   749.220   283.030     AA   HA11111
84.530   360.000
 2.607   747.840   282.970     AA   HA11111
84.130   360.000
 2.618   746.790   282.910     AA   HA11111
83.950   360.000
 2.628   745.930   282.800     AA   HA11111
83.140   360.000
 2.642   744.650   282.730     AA   HA11111
82.330   360.000
 2.651   743.900   282.650     AA   HA11111
81.950   360.000
 2.666   742.570   282.510     AA   HA11111
81.770   360.000
 2.691   740.340   282.420     AA   HA11111
82.000   360.000
 2.703   739.210   282.250     AA   HA11111
82.250   360.000
 2.721   737.630   282.160     AA   HA11111
82.300   360.000
 2.739   736.030   282.100     AA   HA11111
82.100   360.000
 2.742   735.790   282.020     AA   HA11111
82.120   360.000
 2.746   735.370   281.830     AA   HA11111
81.740   360.000
 2.776   732.760   281.680     AA   HA11111
81.590   360.000
 2.807   730.040   281.600     AA   HA11111
81.610   360.000
 2.816   729.220   281.540     AA   HA11111
81.430   360.000
 2.836   727.500   281.420     AA   HA11111
81.670   360.000
 2.839   727.190   281.360     AA   HA11111
81.900   360.000
 2.855   725.830   281.340     AA   HA11111
82.110   360.000
 2.858   725.520   281.280     AA   HA11111
80.470   360.000
 2.903   721.590   281.170     AA   HA11111
76.160   360.000
 2.911   720.860   281.110     AA   HA11111
75.980   360.000
 2.924   719.720   281.030     AA   HA11111
76.210   360.000
 2.938   718.580   280.970     AA   HA11111
76.430   360.000
 2.946   717.840   280.890     AA   HA11111
77.680   360.000
 2.955   717.020   280.830     AA   HA11111
79.160   360.000
 2.994   713.680   280.760     AA   HA11111
```

```
 75.080   360.000
  3.034   710.220   280.710     AA   HA11111
 74.070   360.000
  3.062   707.820   280.650     AA   HA11111
 71.210   360.000
  3.076   706.610   280.600     AA   HA11111
 68.980   360.000
  3.098   704.760   280.650     AA   HA11111
 67.760   360.000
  3.103   704.280   280.640     AA   HA11111
 51.300   360.000
  3.106   704.060   280.590     AA   HA11111
 47.830   360.000
  3.138   701.340   280.470     AA   HA11111
 54.870   360.000
  3.160   699.470   280.420     AA   HA11111
 56.450   360.000
  3.171   698.530   280.200     AA   HA11111
 69.930   360.000
  3.203   695.830   280.140     AA   HA11111
 68.930   360.000
  3.225   693.940   279.940     AA   HA11111
 58.150   360.000
  3.239   692.810   279.720     AA   HA11111
 58.190   360.000
  3.275   689.770   279.670     AA   HA11111
 58.600   360.000
  3.285   688.890   279.640     AA   HA11111
 59.420   360.000
  3.300   687.680   279.580     AA   HA11111
 61.430   360.000
  3.316   686.290   279.490     AA   HA11111
 65.690   360.000
  3.334   684.770   279.330     AA   HA11111
 68.370   360.000
  3.346   683.810   279.250     AA   HA11111
 69.610   360.000
  3.353   683.190   279.060     AA   HA11111
 76.430   360.000
  3.384   680.600   279.030     AA   HA11111
 79.150   360.000
  3.397   679.530   279.000     AA   HA11111
 81.650   360.000
  3.414   678.140   278.970     AA   HA11111
 81.450   360.000
  3.424   677.330   278.940     AA   HA11111
 73.390   360.000
  3.474   673.210   278.880     AA   HA11111
 74.230   360.000
  3.484   672.360   278.860     AA   HA11111
 72.390   360.000
  3.493   671.670   278.830     AA   HA11111
 70.750   360.000
```

```
 3.502   670.870   278.660     AA   HA11111
68.570   360.000
 3.528   668.760   278.600     AA   HA11111
67.980   360.000
 3.538   667.990   278.520     AA   HA11111
66.170   360.000
 3.549   667.050   278.440     AA   HA11111
66.590   360.000
 3.565   665.740   278.360     AA   HA11111
66.200   360.000
 3.573   665.120   278.300     AA   HA11111
64.830   360.000
 3.592   663.600   278.220     AA   HA11111
64.850   360.000
 3.597   663.190   278.140     AA   HA11111
63.860   360.000
 3.636   659.990   277.840     AA   HA11111
61.720   360.000
 3.648   659.000   277.600     AA   HA11111
67.860   360.000
 3.681   656.330   277.460     AA   HA11111
74.900   360.000
 3.723   653.000   277.440     AA   HA11111
72.840   360.000
 3.744   651.270   277.400     AA   HA11111
68.550   360.000
 3.780   648.470   277.340     AA   HA11111
63.090   360.000
 3.822   645.070   277.310     AA   HA11111
61.500   360.000
 3.829   644.540   277.340     AA   HA11111
60.890   360.000
 3.833   644.260   277.540     AA   HA11111
48.410   360.000
 3.880   640.540   277.650     AA   HA11111
27.890   360.000
 3.891   639.660   277.670     AA   HA11111
15.690   360.000
 3.896   639.290   277.640     AA   HA11111
12.590   360.000
 3.916   637.710   277.640     AA   HA11111
11.630   360.000
 3.919   637.440   277.560     AA   HA11111
11.800   360.000
 3.941   635.730   277.510     AA   HA11111
11.790   360.000
 3.955   634.670   277.460     AA   HA11111
11.960   360.000
 3.960   634.250   277.320     AA   HA11111
12.310   360.000
 3.968   633.640   277.240     AA   HA11111
12.470   360.000
 3.991   631.800   277.160     AA   HA11111
```

```
 12.330   360.000
  4.003   630.880   277.130     AA   HA11111
 12.170   360.000
  4.042   627.860   276.890     AA   HA11111
 11.240   360.000
  4.047   627.460   276.780     AA   HA11111
 11.240   360.000
  4.059   626.540   276.700     AA   HA11111
 11.250   360.000
  4.079   625.000   276.570     AA   HA11111
 11.260   360.000
  4.087   624.410   276.510     AA   HA11111
 11.280   360.000
  4.094   623.850   276.250     AA   HA11111
 11.940   360.000
  4.110   622.630   276.170     AA   HA11111
 11.790   360.000
  4.149   619.640   276.040     AA   HA11111
 11.650   360.000
  4.160   618.780   275.930     AA   HA11111
 11.650   360.000
  4.161   618.700   275.830     AA   HA11111
 11.660   360.000
  4.168   618.200   275.570     AA   HA11111
 11.520   360.000
  4.216   614.520   275.330     AA   HA11111
 11.390   360.000
  4.243   612.420   274.990     AA   HA11111
 12.230   360.000
  4.266   610.680   274.730     AA   HA11111
 14.060   360.000
  4.291   608.810   274.310     AA   HA11111
 28.600   360.000
  4.342   604.970   274.200     AA   HA11111
 28.990   360.000
  4.349   604.440   274.090     AA   HA11111
 29.190   360.000
  4.356   603.920   273.810     AA   HA11111
 28.530   360.000
  4.381   601.990   273.560     AA   HA11111
 32.020   360.000
  4.389   601.420   273.410     AA   HA11111
 35.210   360.000
  4.437   597.840   273.200     AA   HA11111
 39.190   360.000
  4.461   596.000   272.990     AA   HA11111
 40.770   360.000
  4.473   595.170   272.860     AA   HA11111
 43.690   360.000
  4.479   594.680   272.790     AA   HA11111
 47.790   360.000
  4.512   592.240   272.640     AA   HA11111
 50.780   360.000
```

```
 4.519   591.710   272.590     AA   HA11111
50.000   360.000
 4.536   590.430   272.440     AA   HA11111
47.480   360.000
 4.568   588.110   272.370     AA   HA11111
47.300   360.000
 4.591   586.430   272.310     AA   HA11111
41.120   360.000
 4.606   585.310   272.290     AA   HA11111
34.120   360.000
 4.617   584.540   272.230     AA   HA11111
20.810   360.000
 4.638   582.950   272.200     AA   HA11111
18.740   360.000
 4.658   581.540   272.130     AA   HA11111
18.750   360.000
 4.670   580.660   272.060     AA   HA11111
19.270   360.000
 4.683   579.670   272.030     AA   HA11111
20.670   360.000
 4.692   579.040   271.950     AA   HA11111
21.020   360.000
 4.704   578.190   271.900     AA   HA11111
20.160   360.000
 4.710   577.690   271.870     AA   HA11111
20.340   360.000
 4.737   575.750   271.820     AA   HA11111
19.490   360.000
 4.740   575.520   271.810     AA   HA11111
16.750   360.000
 4.752   574.720   271.750     AA   HA11111
15.750   360.000
 4.784   572.390   271.620     AA   HA11111
15.770   360.000
 4.792   571.810   271.550     AA   HA11111
16.280   360.000
 4.809   570.570   271.480     AA   HA11111
16.630   360.000
 4.826   569.370   271.350     AA   HA11111
16.810   360.000
 4.841   568.320   271.280     AA   HA11111
18.010   360.000
 4.856   567.240   271.150     AA   HA11111
19.580   360.000
 4.870   566.200   271.060     AA   HA11111
19.770   360.000
 4.884   565.190   271.010     AA   HA11111
19.950   360.000
 4.896   564.380   270.880     AA   HA11111
19.970   360.000
 4.899   564.160   270.780     AA   HA11111
19.810   360.000
 4.923   562.440   270.710     AA   HA11111
```

136

```
 19.810   360.000
  4.928   562.080   270.510     AA   HA11111
 18.980   360.000
  4.931   561.900   270.440     AA   HA11111
 18.130   360.000
  4.955   560.200   270.330     AA   HA11111
 16.100   360.000
  4.986   558.000   270.260     AA   HA11111
 14.940   360.000
  4.999   557.080   270.180     AA   HA11111
 14.440   360.000
  5.006   556.580   270.110     AA   HA11111
 14.110   360.000
  5.025   555.230   269.750     AA   HA11111
 14.650   360.000
  5.061   552.730   269.680     AA   HA11111
 15.160   360.000
  5.085   551.040   269.610     AA   HA11111
 15.510   360.000
  5.091   550.590   269.340     AA   HA11111
 15.370   360.000
  5.133   547.690   269.270     AA   HA11111
 16.400   360.000
  5.157   546.010   269.200     AA   HA11111
 17.080   360.000
  5.190   543.750   268.930     AA   HA11111
 17.980   360.000
  5.197   543.240   268.780     AA   HA11111
 19.220   360.000
  5.234   540.720   268.710     AA   HA11111
 19.400   360.000
  5.265   538.590   268.660     AA   HA11111
 19.250   360.000
  5.289   536.920   268.580     AA   HA11111
 18.050   360.000
  5.304   535.930   268.520     AA   HA11111
 17.530   360.000
  5.320   534.850   268.430     AA   HA11111
 16.670   360.000
  5.327   534.340   268.380     AA   HA11111
 16.340   360.000
  5.351   532.700   268.330     AA   HA11111
 16.170   360.000
  5.373   531.250   268.260     AA   HA11111
 15.680   360.000
  5.387   530.270   268.160     AA   HA11111
 14.330   360.000
  5.431   527.330   268.120     AA   HA11111
 14.170   360.000
  5.465   525.080   268.050     AA   HA11111
 13.490   360.000
  5.482   523.910   267.970     AA   HA11111
 13.680   360.000
```

```
 5.498   522.880   267.900     AA   HA11111
13.530   360.000
 5.503   522.540   267.870     AA   HA11111
13.360   360.000
 5.511   522.000   267.810     AA   HA11111
13.190   360.000
 5.534   520.480   267.680     AA   HA11111
11.890   360.000
 5.538   520.170   267.620     AA   HA11111
11.720   360.000
 5.580   517.420   267.570     AA   HA11111
11.060   360.000
 5.598   516.190   267.550     AA   HA11111
10.730   360.000
 5.606   515.710   267.420     AA   HA11111
 9.940   360.000
 5.636   513.700   267.350     AA   HA11111
 9.780   360.000
 5.648   512.930   267.290     AA   HA11111
 9.620   360.000
 5.665   511.800   267.100     AA   HA11111
 8.980   360.000
 5.699   509.580   267.020     AA   HA11111
 8.350   360.000
 5.703   509.360   266.870     AA   HA11111
 8.510   360.000
 5.730   507.570   266.750     AA   HA11111
 9.010   360.000
 5.734   507.320   266.630     AA   HA11111
 9.190   360.000
 5.789   503.790   266.540     AA   HA11111
 9.040   360.000
 5.800   503.030   266.370     AA   HA11111
 9.060   360.000
 5.815   502.060   266.280     AA   HA11111
 9.050   360.000
 5.825   501.450   266.190     AA   HA11111
 8.900   360.000
 5.831   501.030   266.070     AA   HA11111
 8.760   360.000
 5.847   500.030   265.980     AA   HA11111
 8.600   360.000
 5.860   499.160   265.870     AA   HA11111
 8.440   360.000
 5.880   497.910   265.770     AA   HA11111
 8.290   360.000
 5.883   497.690   265.710     AA   HA11111
 8.120   360.000
 5.919   495.420   265.500     AA   HA11111
 7.980   360.000
 5.943   493.920   265.420     AA   HA11111
 7.980   360.000
 5.946   493.670   265.370     AA   HA11111
```

```
 7.820   360.000
 5.948   493.550   265.250     AA   HA11111
 7.510   360.000
 5.976   491.810   265.210     AA   HA11111
 7.510   360.000
 5.985   491.250   265.160     AA   HA11111
 7.360   360.000
 6.002   490.170   265.110     AA   HA11111
 7.360   360.000
 6.018   489.130   265.070     AA   HA11111
 6.880   360.000
 6.028   488.530   265.020     AA   HA11111
 6.890   360.000
 6.032   488.270   264.950     AA   HA11111
 6.580   360.000
 6.052   487.010   264.880     AA   HA11111
 6.590   360.000
 6.070   485.900   264.790     AA   HA11111
 6.590   360.000
 6.082   485.120   264.730     AA   HA11111
 6.750   360.000
 6.089   484.690   264.650     AA   HA11111
 6.920   360.000
 6.091   484.570   264.540     AA   HA11111
 6.780   360.000
 6.125   482.420   264.470     AA   HA11111
 6.780   360.000
 6.140   481.490   264.250     AA   HA11111
 6.620   360.000
 6.177   479.180   264.170     AA   HA11111
 6.460   360.000
 6.201   477.740   263.870     AA   HA11111
 6.160   360.000
 6.247   474.890   263.740     AA   HA11111
 6.010   360.000
 6.269   473.540   263.650     AA   HA11111
 5.850   360.000
 6.278   472.950   263.630     AA   HA11111
 5.680   360.000
 6.290   472.250   263.560     AA   HA11111
 5.540   360.000
 6.310   471.040   263.510     AA   HA11111
 5.390   360.000
 6.314   470.760   263.320     AA   HA11111
 5.240   360.000
 6.319   470.480   263.210     AA   HA11111
 5.230   360.000
 6.346   468.790   262.960     AA   HA11111
 5.090   360.000
 6.413   464.750   262.740     AA   HA11111
 5.110   360.000
 6.434   463.480   262.650     AA   HA11111
 5.110   360.000
```

```
 6.456   462.170   262.590     AA   HA11111
 5.120   360.000
 6.467   461.480   262.450     AA   HA11111
 5.130   360.000
 6.472   461.210   262.360     AA   HA11111
 5.130   360.000
 6.491   460.050   262.300     AA   HA11111
 4.970   360.000
 6.507   459.100   262.170     AA   HA11111
 4.980   360.000
 6.524   458.080   262.100     AA   HA11111
 5.140   360.000
 6.538   457.270   262.000     AA   HA11111
 4.980   360.000
 6.570   455.320   261.740     AA   HA11111
 4.510   360.000
 6.582   454.610   261.670     AA   HA11111
 4.520   360.000
 6.604   453.320   261.580     AA   HA11111
 4.370   360.000
 6.630   451.780   261.300     AA   HA11111
 4.070   360.000
 6.655   450.330   261.130     AA   HA11111
 3.910   360.000
 6.674   449.220   261.040     AA   HA11111
 3.770   360.000
 6.742   445.210   260.930     AA   HA11111
 3.920   360.000
 6.768   443.710   260.760     AA   HA11111
 3.770   360.000
 6.788   442.570   260.660     AA   HA11111
 3.920   360.000
 6.826   440.330   260.380     AA   HA11111
 4.100   360.000
 6.846   439.180   260.120     AA   HA11111
 3.960   360.000
 6.862   438.240   259.910     AA   HA11111
 4.130   360.000
 6.891   436.620   259.800     AA   HA11111
 4.130   360.000
 6.912   435.420   259.660     AA   HA11111
 4.290   360.000
 6.948   433.340   259.450     AA   HA11111
 4.300   360.000
 6.967   432.230   259.350     AA   HA11111
 4.140   360.000
 6.983   431.350   259.240     AA   HA11111
 4.150   360.000
 6.987   431.100   259.130     AA   HA11111
 4.160   360.000
 7.001   430.340   259.030     AA   HA11111
 4.320   360.000
 7.023   429.070   258.930     AA   HA11111
```

```
 4.160   360.000
 7.035   428.420   258.850     AA   HA11111
 4.000   360.000
 7.049   427.580   258.810     AA   HA11111
 3.990   360.000
 7.080   425.860   258.650     AA   HA11111
 4.020   360.000
 7.085   425.550   258.590     AA   HA11111
 3.860   360.000
 7.124   423.380   258.570     AA   HA11111
 3.850   360.000
 7.143   422.320   258.470     AA   HA11111
 3.860   360.000
 7.148   422.020   258.340     AA   HA11111
 3.700   360.000
 7.172   420.720   258.220     AA   HA11111
 3.540   360.000
 7.201   419.090   258.200     AA   HA11111
 3.540   360.000
 7.226   417.710   258.060     AA   HA11111
 3.380   360.000
 7.247   416.580   258.000     AA   HA11111
 3.540   360.000
 7.252   416.260   257.920     AA   HA11111
 3.540   360.000
 7.275   415.020   257.900     AA   HA11111
 3.370   360.000
 7.302   413.520   257.820     AA   HA11111
 3.530   360.000
 7.323   412.380   257.740     AA   HA11111
 3.370   360.000
 7.349   410.940   257.530     AA   HA11111
 3.370   360.000
 7.369   409.880   257.430     AA   HA11111
 3.700   360.000
 7.432   406.430   257.150     AA   HA11111
 4.350   360.000
 7.460   404.920   257.110     AA   HA11111
 4.520   360.000
 7.477   404.040   256.940     AA   HA11111
 4.690   360.000
 7.497   402.980   256.800     AA   HA11111
 4.700   360.000
 7.503   402.620   256.400     AA   HA11111
 4.710   360.000
 7.546   400.340   256.290     AA   HA11111
 4.720   360.000
 7.556   399.780   256.220     AA   HA11111
 4.550   360.000
 7.565   399.300   256.140     AA   HA11111
 4.710   360.000
 7.588   398.110   256.000     AA   HA11111
 4.560   360.000
```

```
     7.597    397.610    255.890      AA    HA11111
     4.570    360.000
     7.614    396.710    255.820      AA    HA11111
     4.560    360.000
     7.636    395.550    255.720      AA    HA11111
     4.560    360.000
     7.684    392.900    255.250      AA    HA11111
 4.500e+00    360.000      0.000      0.000      0.000      0.000      0.000
     7.720    391.000    254.950      AA    HA11111
 4.500e+00    360.000      0.000      0.000      0.000      0.000      0.000
     7.753    389.300    254.750      AA    HA11111
 4.500e+00    360.000      0.000      0.000      0.000      0.000      0.000
     7.787    387.500    254.450      AA    HA11111
 4.500e+00    360.000      0.000      0.000      0.000      0.000      0.000
     7.819    385.900    254.150      AA    HA11111
 4.500e+00    360.000      0.000      0.000      0.000      0.000      0.000
     7.851    384.300    253.850      AA    HA11111
 4.500e+00    360.000      0.000      0.000      0.000      0.000      0.000
     7.882    382.600    253.550      AA    HA11111
 4.500e+00    360.000      0.000      0.000      0.000      0.000      0.000
     7.914    381.000    253.250      AA    HA11111
 4.500e+00    360.000      0.000      0.000      0.000      0.000      0.000
     7.945    379.400    252.950      AA    HA11111
 4.500e+00    360.000      0.000      0.000      0.000      0.000      0.000
     7.976    377.800    252.750      AA    HA11111
 4.500e+00    360.000      0.000      0.000      0.000      0.000      0.000
     8.008    376.200    252.450      AA    HA11111
 4.500e+00    360.000      0.000      0.000      0.000      0.000      0.000
     8.037    374.700    252.150      AA    HA11111
 4.500e+00    360.000      0.000      0.000      0.000      0.000      0.000
     8.069    373.100    251.950      AA    HA11111
 4.500e+00    360.000      0.000      0.000      0.000      0.000      0.000
    3    0    0  The following cross-sections were selected:
CCL4       F11        F12
    2    0  Using 1995 UNEP values
     0.000     AAA
 1.105e-04 2.783e-09 5.027e-04
     8.069     AAA
 1.105e-04 2.783e-09 5.027e-04
%
```

University of Wisconsin

FY99 Final Report

Engineering and Scientific Support for the National Polar-orbiting Operational Environmental Satellite System
Airborne Sounder Testbed - Interferometer (NAST-I) Instrument

30 September 1999

Deliverables by Task:

Task 1

Comparison of spectra from NAST-I, AERI, & SHIS over Andros Island during CAMEX-3.

4. Validation data from Andros Island (AERI, Sondes, GPS, ...)
URL: http://cimss.ssec.wisc.edu/camex3/camexiii.html

143

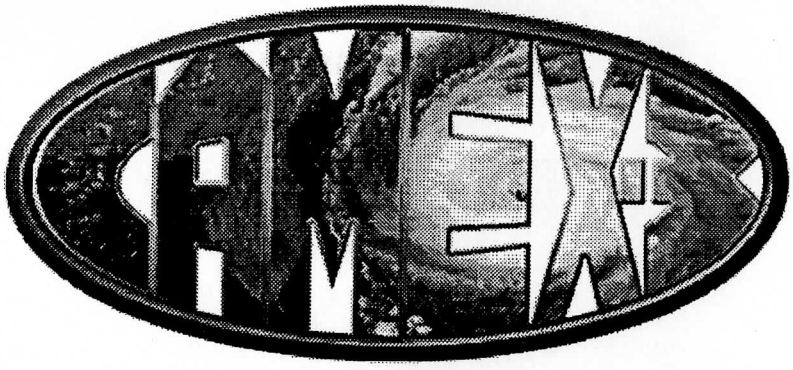

WISCONSIN CAMEX-III ANDROS ISLAND HOMEPAGE

Instrumentation | Weather Information | Daily Quicklook / Data Archive

Andros Pictures | Other CAMEX III Links

The purpose of this homepage is to organize the ground based dataset collected by the University of Wisconsin team at Andros Island for quick distribution. Quick looks and data sets will be organized by instrument type and date of collection under the daily quick look and data archive section. To view any other CAMEX III information please go to the official CAMEX III Homepage (http://ghrc.msfc.nasa.gov/camex3/) .

Important Messages: Last updated 10/08/98

- Moved homepage to CIMSS main web server
- Updated all quicklooks and data through 980920 (through end of field experiment)

Last Updated: October 8, 1998

Send corrections or suggestions for the Wisconsin CAMEX III Homepage to: wayne.feltz@ssec.wisc.edu

University of Wisconsin Instrumentation at the CAMEX-III Ground Truth Site

AUTEC Facility, FASCO Bldg
(24 deg 41.985 min N, 77 deg 46.102 min W)
Andros Island, Bahamas

The University of Wisconsin is responsible for the deployment and operation of several advanced meteorological instruments at the CAMEX-III ground truth site on Andros Island in the Bahamas. The focus of the ground-based observations is on the accurate measurement of atmospheric water vapor in the column of atmosphere above the ground truth site. Analysis of this data in conjunction with coincident observations from NASA aircraft and weather satellites will contribute to the improvement of hurricane prediction by providing validation of the algorithms and models used in the interpretation of the aircraft and satellite data. The University of Wisconsin ground-based observations on Andros Island are being made in close coordination with the Goddard Space Flight Center Scanning Raman Lidar (SRL) and the Wallops Island Flight Facility (WFF) upper air balloon sounding teams.

Several state-of-the-art sensors were deployed by the University of Wisconsin on Andros Island,

- an Atmospheric Emitted Radiance Interferometer (AERI) for continuous boundary layer profiling of temperature and water vapor,
- a water vapor GPS for accurate continuous total column measurements,
- a surface weather station featuring an accurate dewpoint (chilled mirror) hygrometer provided by Scott Richardson of the University of Oklahoma,
- an upper air balloon sounding system (CLASS) for measurement of temperature and water vapor profiles using Vaisala RS80 radiosondes.

The equipment is based in and around the University of Wisconsin research vehicle which was transported by barge to the island at end of July 1998. Photo images of the instrument setup on Andros Island are given below (photos courtesy of John Short, U.Wisc).

- AUTEC facility (main street, barge dock, the beach)
- Experiment site (FASCO building)
- Wisconsin Research vehicle (the AERIBAGO)
- AERI system inside AERIBAGO,
- Water vapor GPS antennae,
- CLASS radiosonde tracking antennae and location of chilled mirror surface sensor
- GSFC SRL (Lidar van, scanning direction)
- Wallops Island balloon setup (personnel, tracking antennae)

Related Links:

OFFICIAL CAMEX III Homepage

Wisconsin CAMEX III NAST-I Homepage (ER-2 instrument)

Wisconsin CAMEX III Scanning-HIS Homepage (DC-8 instrument)

University of Wisconsin Cooperative Institute for Meteorological Satellite Studies

University of Wisconsin Space Science and Engineering Center

Send corrections or suggestions for the Homepage to: wayne.feltz@ssec.wisc.edu

Last revised 8/14/98 r. knuteson (robert.knuteson@ssec.wisc.edu)

University of Wisconsin

FY99 Final Report

Engineering and Scientific Support for the National Polar-orbiting Operational Environmental Satellite System Airborne Sounder Testbed - Interferometer (NAST-I) Instrument

30 September 1999

Deliverables by Task:

Task 1

Comparison of spectra from NAST-I and SHIS during WINTEX

1.S-HIS/NAST-I Comparison from WINTEX
URL: http://arm1.ssec.wisc.edu/~shis/wintex/results/shisnastcomp.html

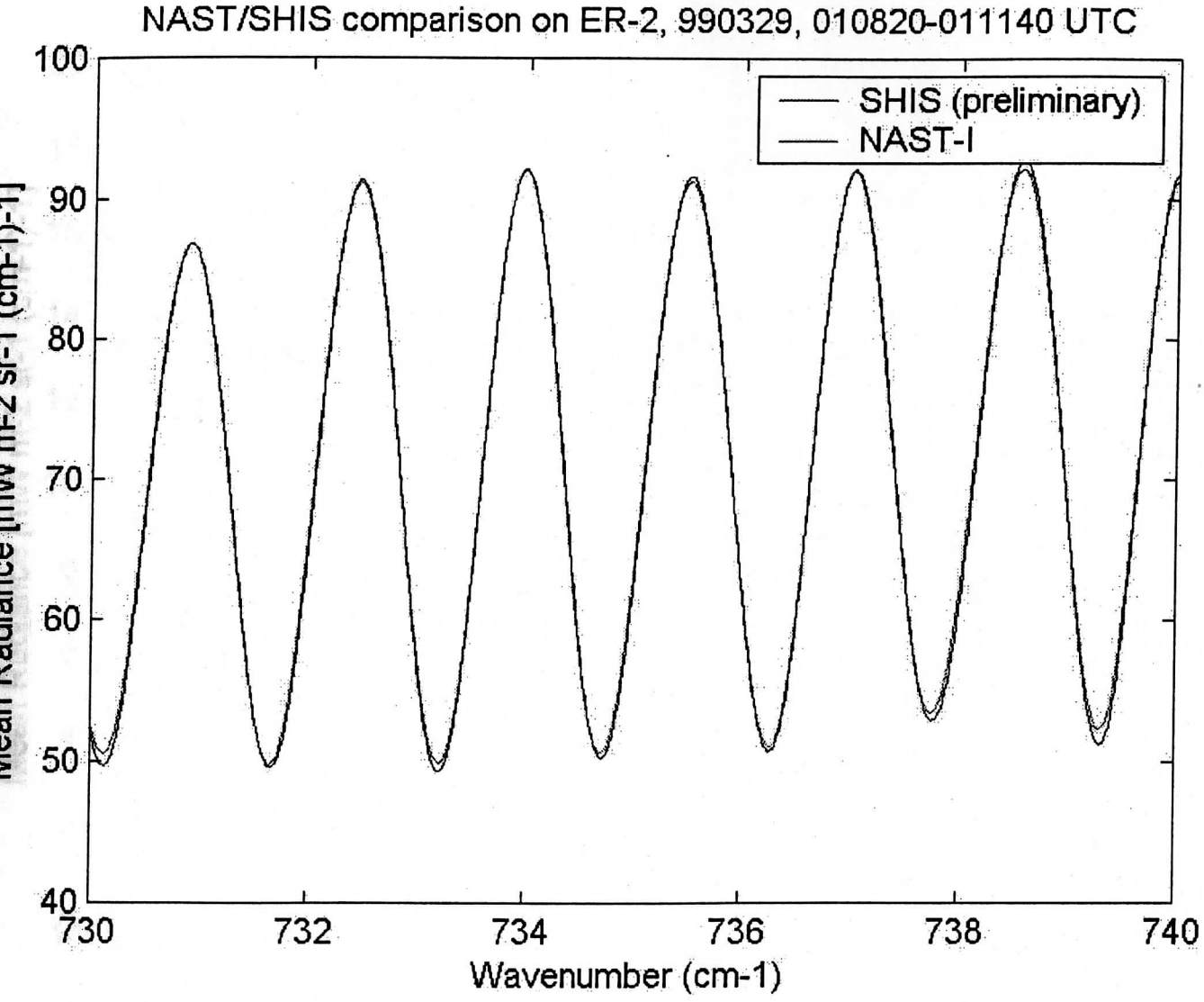
NAST/SHIS comparison on ER-2, 990329, 010820-011140 UTC
SHIS (preliminary)
NAST-I
Mean Radiance [mW m-2 sr-1 (cm-1)-1]
100
90
80
70
60
50
40
730
732
734
736
738
740
Wavenumber (cm-1)

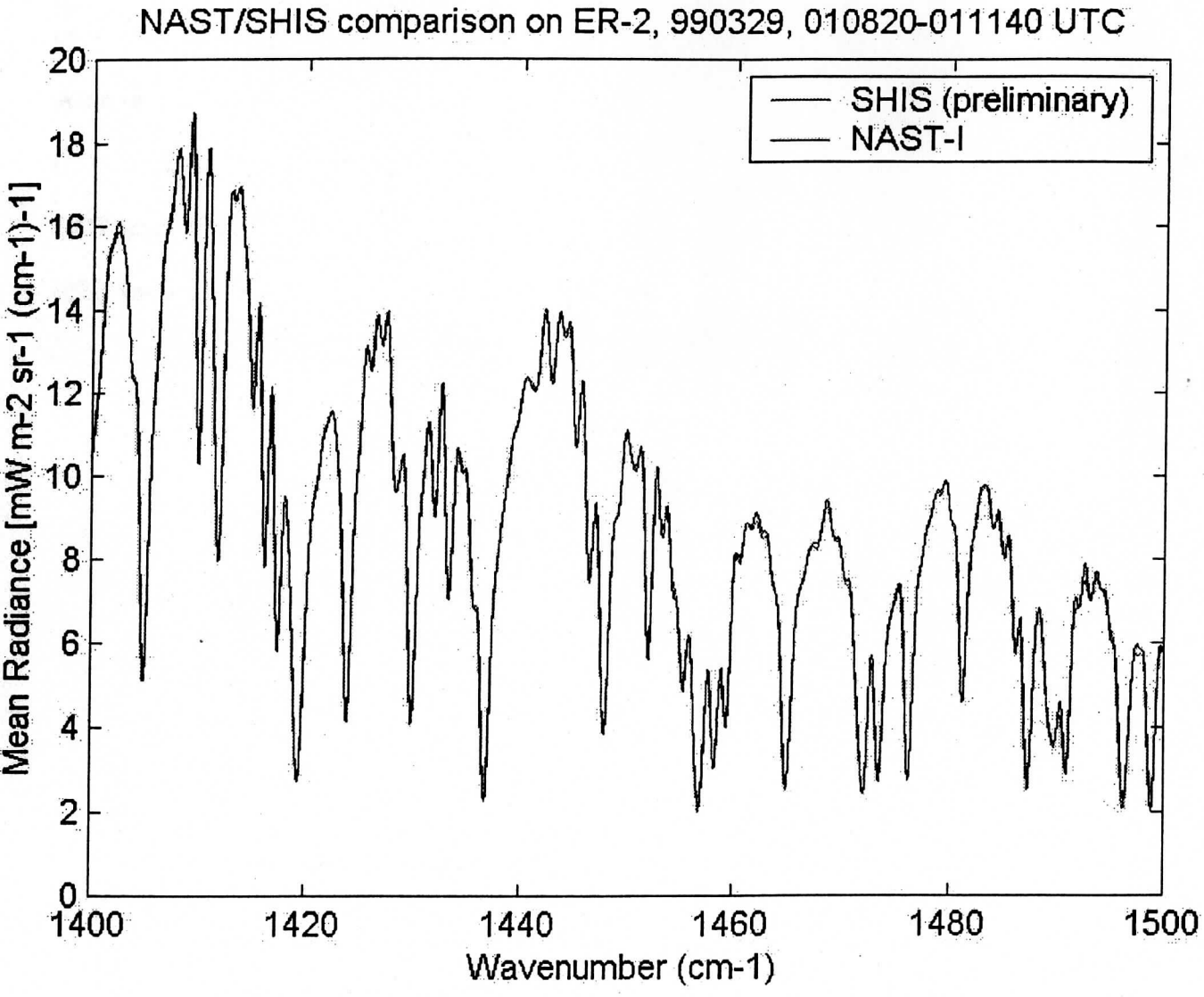
NAST/SHIS comparison on ER-2, 990329, 010820-011140 UTC
SHIS (preliminary)
NAST-I
Mean Radiance [mW m-2 sr-1 (cm-1)-1]
Wavenumber (cm-1)
0
2
4
6
8
10
12
14
16
18
20
1400
1420
1440
1460
1480
1500

149

S-HIS / NAST-I Comparison from ER-2 Flight #99-057, 29 March 1999

The following links show comparisons between infrared spectra measured by the Scanning HIS and the NAST-I instruments. These spectra were taken over Lake Michigan on 29 March 1999 (flight track). The spectral resolution of the NAST-I data were reduced to the resolution of the Scanning HIS data, then padded with zeros. The Scanning HIS data were also padded with zeros. The calibration of the Scanning HIS data is preliminary; refinements to the longwave and midwave detector nonlinearity corrections will be made in the future, along with the application of a tilt-error correction.

All bands [jpg, ps]

CO2 band (690-780 cm-1) [jpg, ps]

CO2 lines (730-740 cm-1) [jpg, ps]

H2O lines (1400-1500 cm-1) [jpg, ps]

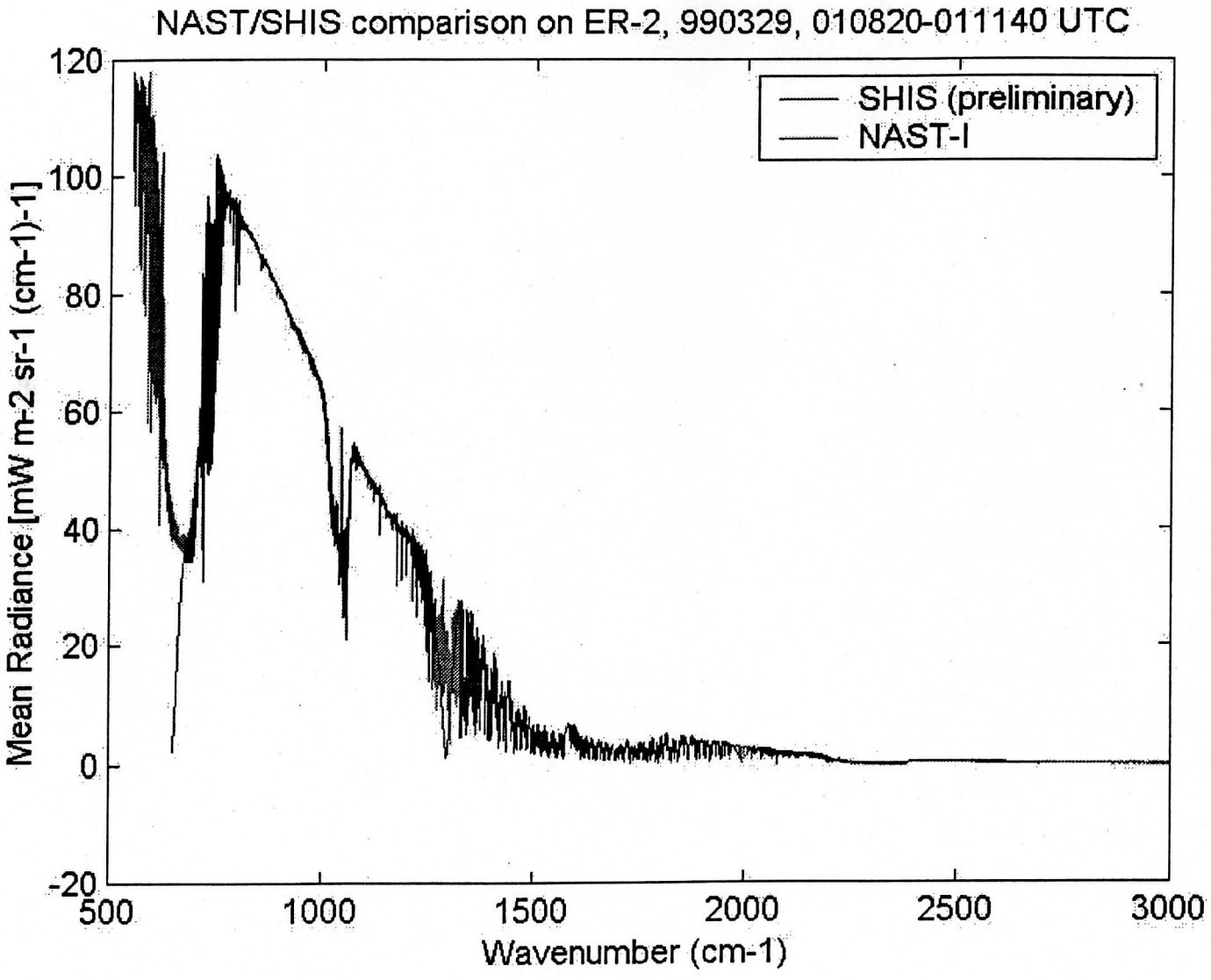
NAST/SHIS comparison on ER-2, 990329, 010820-011140 UTC
SHIS (preliminary)
NAST-I
Mean Radiance [mW m-2 sr-1 (cm-1)-1]
Wavenumber (cm-1)
120
100
80
60
40
20
0
-20
500
1000
1500
2000
2500
3000

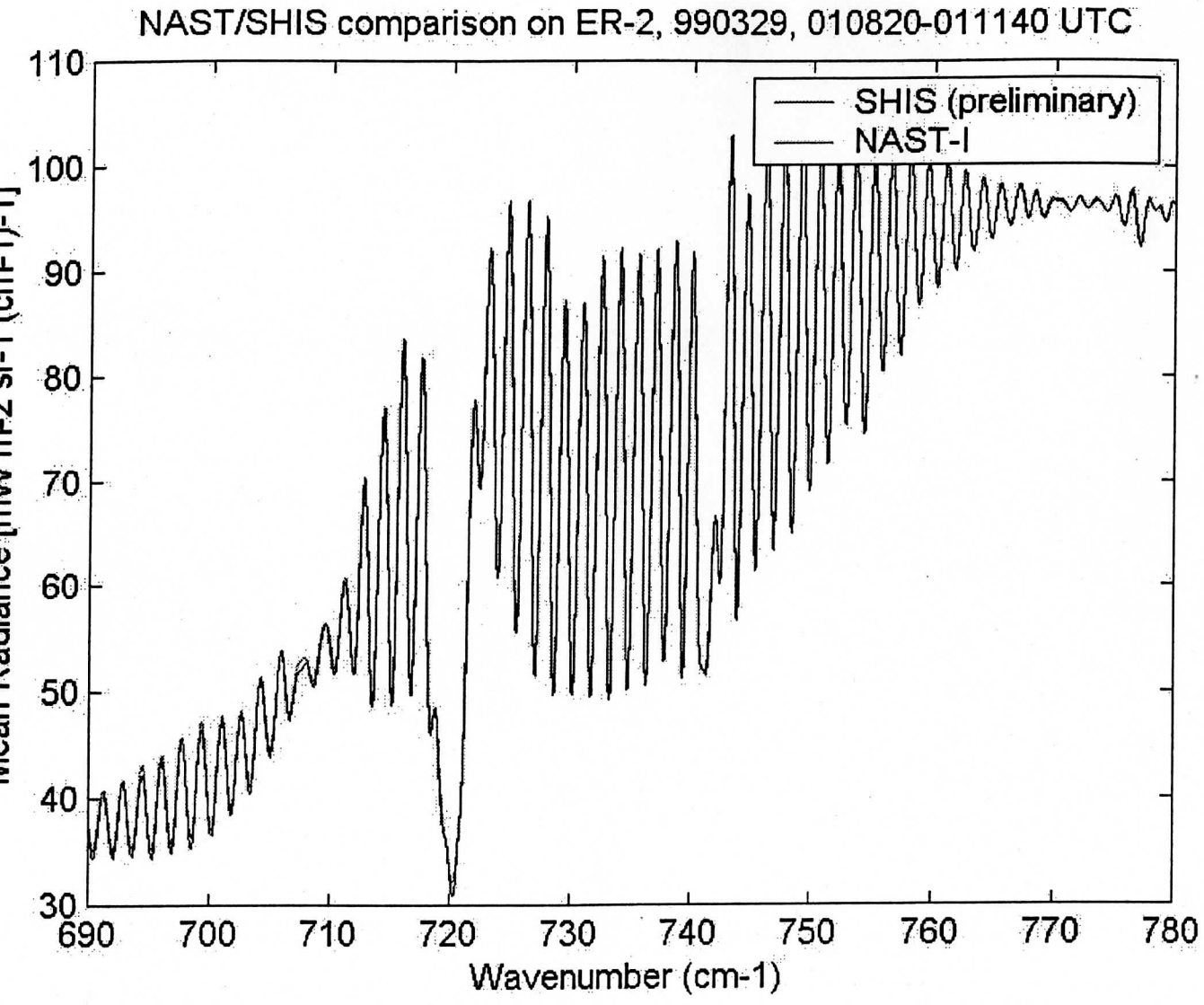
NAST/SHIS comparison on ER-2, 990329, 010820-011140 UTC
SHIS (preliminary)
NAST-I
110
100
90
80
70
60
50
40
30
690
700
710
720
730
740
750
760
770
780
Wavenumber (cm-1)

University of Wisconsin

FY99 Final Report

Engineering and Scientific Support for the National Polar-orbiting Operational Environmental Satellite System Airborne Sounder Testbed - Interferometer (NAST-I) Instrument

30 September 1999

Deliverables by Task:

Task 1

Comparison of spectra from NAST-I and SHIS during WINTEX

2.NASTI comparison with calculations from WINTEX:
- Case Description (URL: http://danspc.larc.nasa.gov/NAST/wintexa/wintexa.html)
- Comparison Summary (postscript file Wintex_NASTI_Obscalc.ps)

WINTEX Clear Sky Case Study: 30 March 1999 over Lake Michigan

This page contains the compilation of NASTI and radiosonde data for clear-sky radiative transfer calculation validation studies. This case is taken from the WINTEX field campaign, on March 30, 1999 over Lake Michigan. Relevant facts and data files are given in the table below.

Case-ID	WINTEX(a)
Campaign	WINTEX
Location	southern Lake Michigan (upper Midwest, US)
Date	03-30-99
Time	00:50-00:53 UTC
Radiance Observations	NASTI (ER-2), SHIS (ER-2), AERI (ground-based, AERI-bago)
ER-2 altitude	19.713 +- 0.020 km from 00:50 to 00:53 UTC
Atmospheric State Observations	UW Vaisala RS-80 launched from Sheboygan, WI at 00:15 UTC: ASCII | NetCDF | GIF
Averaged Radiances	NASTI Mean and 1 standard deviation of 15 individual nadir spectra from 00:50 to 00:53 UTC. channel 1: ASCII | PS; channel 2: ASCII | PS; channel 3: ASCII | PS.

General Description:

Very clear, stable, homogeneous case over southern Lake Michigan as part of a NOAA-K over-pass validation mission during WINTEX. The NASTI and SHIS were both aboard the ER-2 and collected good data as three coincident race-track patterns were conducted. The AERI-bago was deployed to Sheboygan, WI where the AERI scanned Lake Michigan from a cliff overlooking the lake making surface emissivity measurements, zenith spectra were collected, and a sonde was launched. For more general information on this day, read the flight summary on the UW Wintex page for this day. The following figure shows the average 899-903 1/cm NAST-I brightness temperatures mapped to the surface for a portion of the flight. The time series of the nadir values is shown in the top panel. In the map, the outline of Lake Michigan is in red, nadir NASTI footprints at 00:50 and 00:53 are circled, and the sonde flight track is shown in magenta. From 00:50 to 00:53 UTC, the NASTI collected 15 individual nadir spectra as the ER-2 went from (-87.2116,43.1988) to (-87.3257,43.5076), approximately 35 km along a north westerly flight track. During this time (00:50-00:53), the sonde, which was launched at 00:15 UTC, drifted south easterly and was at an altitude of approximately 12 km (~200 mbar) above sea level and at a range of ~16 km from the ER-2.

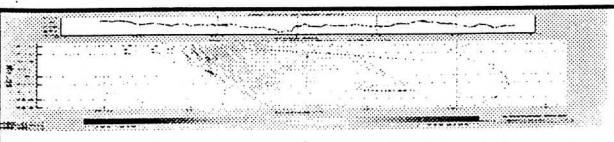

Click to enlarge

Other Comments/Info:

1. Lake Michigan is fresh water and its southern portion was unfrozen during the over-pass.
2. The 00:15 sonde is a Vaisala sonde of serial # 908257005 (YWWDXXXXX --> calibrated/packaged on 2/23/99) and was therefore approximately one month old when launched.
3. sonde to ~50 mbar, but RHs are zeroed out above ~200 mbar. Upper altitude temperatures are also suspect.
4. 00:00 UTC is 6 pm local time.
5. sample sea water emissivity data

[NAST Home]

155

WINTEX 1999

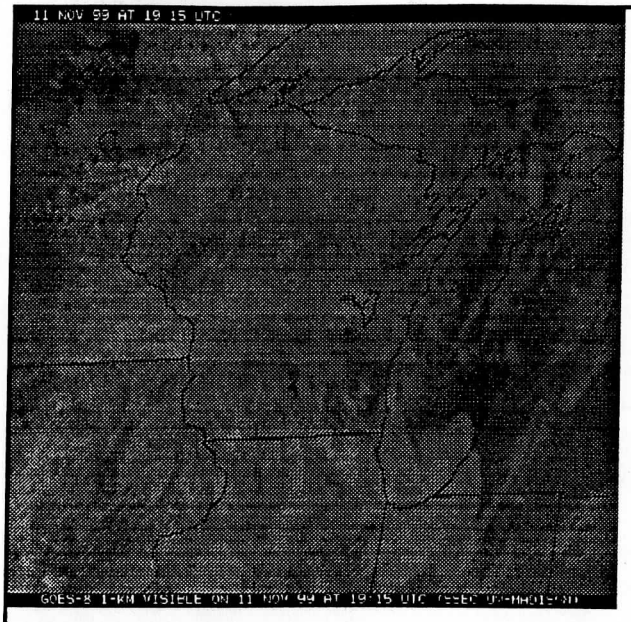

Overview | Logistics | Instrumentation | Objectives

Mission Planning | Weather Information | Daily Quicklook / Data Archive

Maps and Hotel Links | Outreach | Photo Gallery

Important Messages: Last updated 4/09/99 11:30 AM CDT

- **MAS data Quicklooks are now available for all flights (including ferry flight) on the Daily Quicklook / Data Archive section of the WINTEX page.**

Send corrections or suggestions for the WINTEX Homepage to: wayne.feltz@ssec.wisc.edu

156

CAPE = −999
CIN = −999
K Index = −2
LI = 8.946
Showalter = 8.94
LCL = 665 mb
LFC = −99 mb
EL = −99 mb
TPW = 0.44 cm

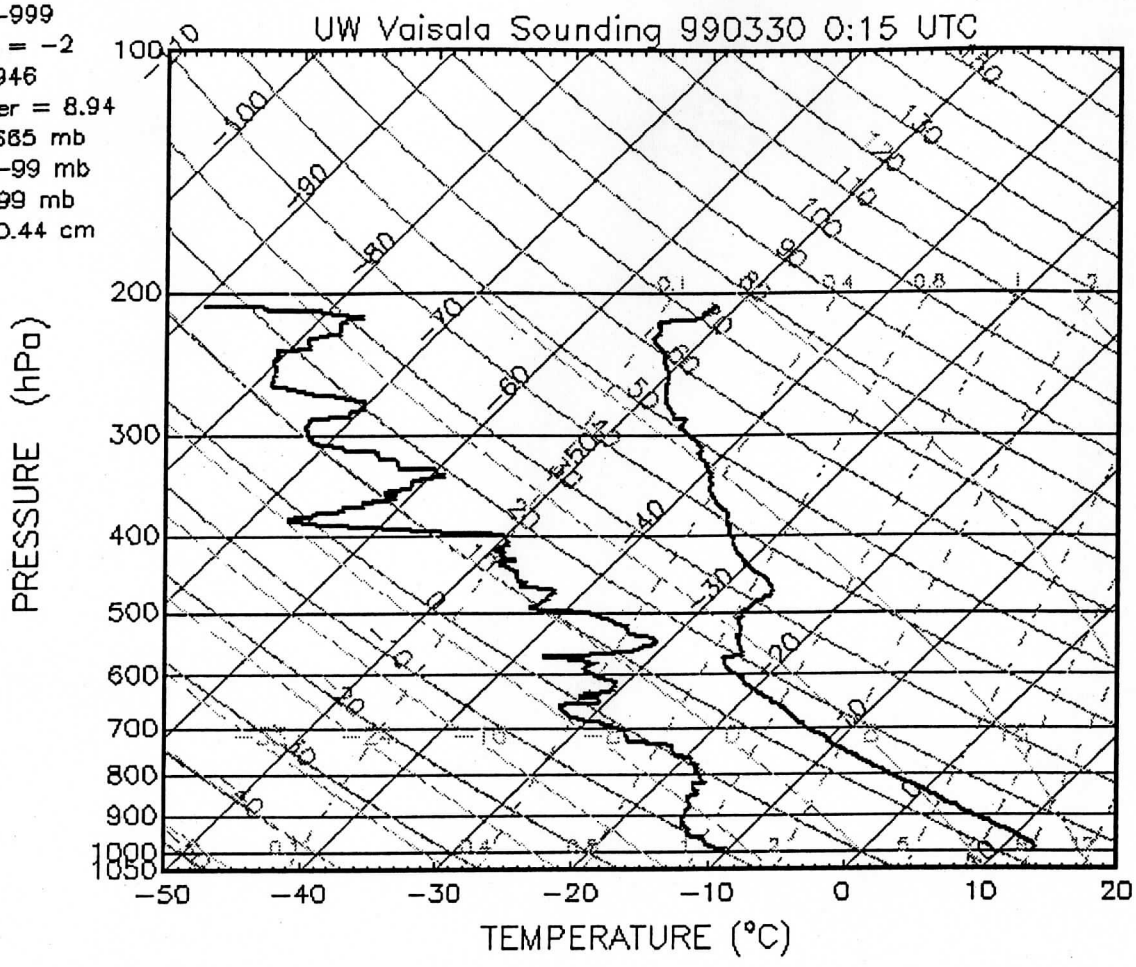

157

WINTEX QUICKLOOKS

March 29, 1999

Aircraft

- ER-2 Flight summary
- ER-2 flight track
- ER-2 flight track overlaid on GOES-8 Infrared image 3.9 um | 6.7 um | 11 um
- MAS Quicklooks
  - Flight Lines 1 | 2 | 3 | 4 | 5 | 6 |7 | 8 | 9 | 10 | 11 | 12 | 13 | 14 | 15 | 16 | 17 |
  - Flight Lines (IR) 1 | 2 | 3 | 4 | 5 | 6 |7 | 8 | 9 | 10 | 11 | 12 | 13 | 14 | 15 | 16 | 17 |
- NOAA-15 Overpass Quicklook 0049 UTC: Gif 1 | Gif 2

Ground-Based

- AERI on SSEC Rooftop :
  - Radiance Summary
  - AERI+GOES Retrievals: Temperature Gif | Moisture Gif | Retrievals (Netcdf)
- AERI in AERIBAGO: (at Sheboygan)
  - Radiance Summary
  - Data (Lake Michigan Radiances included) Channel 1 | Channel 2
- GOES Netcdf Physical Retrievals (3 X 3 Centered on Madison)
- SSEC Radiosonde (launched in near Sheboygan):
  - 990330 01:03 UTC SKEWT | ASCII | NETCDF
- NWS 00 UTC Radiosondes
  - Green Bay, WI Gif | Txt

This page is being maintained by WINTEX/CIMSS personnel. Please refer questions to Steve Ackerman at steve.ackerman@ssec.wisc.edu.

158

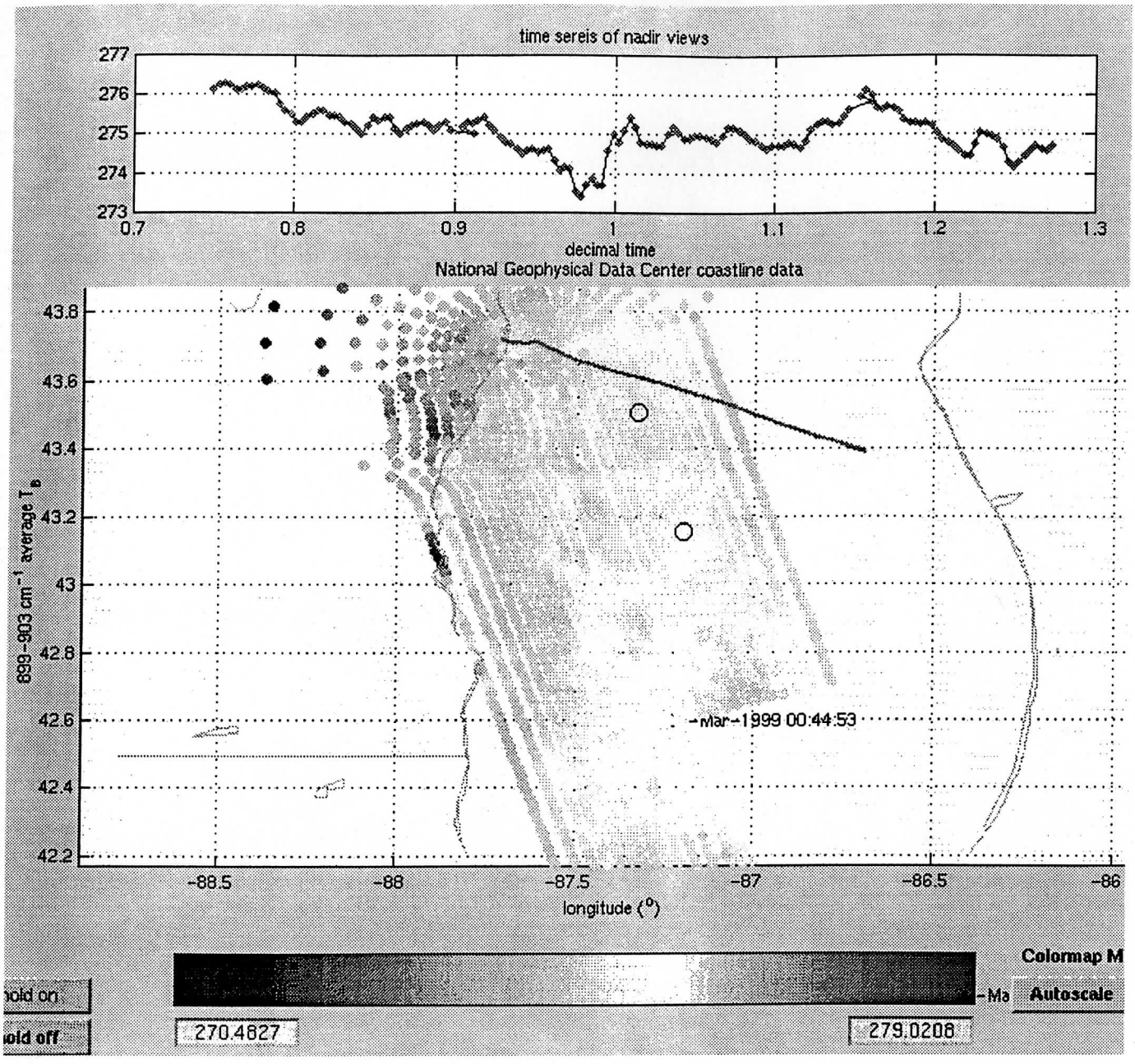
time sereis of nadir views
277
276
275
274
273
0.7
0.8
0.9
1
1.1
1.2
1.3
decimal time
National Geophysical Data Center coastline data
43.8
43.6
43.4
43.2
43
42.8
42.6
42.4
42.2
899-903 cm-1 average TB
-Mar-1999 00:44:53
-88.5
-88
-87.5
-87
-86.5
-86
longitude (°)
Colormap M
Autoscale
270.4627
279.0208

University of Wisconsin

FY99 Final Report

Engineering and Scientific Support for the National Polar-orbiting Operational Environmental Satellite System Airborne Sounder Testbed - Interferometer (NAST-I) Instrument

30 September 1999

Deliverables by Task:

Task 1

Papers submitted to trade journals or conferences concerning NAST-I performance.
(click here to see the list of papers)

160

Papers Referencing NAST-I

through September 30, 1999

1. Revercomb, H. E., V.P. Walden, J. Anderson, F.A. Best, N.C. Ciganovich, R.G. Dedecker, T. Dirkx, S.C. Ellington, R.K. Garcia, R. Herbsleb, R.O. Knuteson, D. LaPorte, D. McRae, D.C. Tobin, and M. Werner (1998): *Recent results from two new aircraft-based Fourier transform interferometers: The Scanning High-resolution Interferometer Sounder and the NPOESS Atmospheric Sounder Testbed Interferometer.* Proceedings of the 8th International Workshop on Atmospheric Science from Space using Fourier Transform Spectrometry (ASSFTS8), Toulouse, France, 16-18 November, 1998. (shisextabs.ps)

2. Smith, W. L., A. Larar, H. Howell, H. Revercomb, C. A. Sisko, D. H. DeSlover, D. C. Tobin, D. Cousins, D. Mooney, M. Gazarik, and S. Mango (1999): *Remote sensing of surface and atmospheric properties using imaging FTS observations.* In Fourier Transform Spectroscopy: New Methods and Applications. OSA Optical Remote Sensing of the Atmosphere, Santa Barbara, CA, June 22-24, 1999. (OSA_99_Smith.ps)

3. DeSlover, D. H., C. A. Sisko, D. C. Tobin, and W. L. Smith (1999): *Data visualization tools demonstrated with NPOESS Aircraft Sounder Testbed-Interferometer (NAST-I) data.* In Fourier Transform Spectroscopy: New Methods and Applications. OSA Optical Remote Sensing of the Atmosphere, Santa Barbara, CA, June 22-24, 1999. (OSA_99_DeSlover.ps)

4. Revercomb, Hank E., R. O. Knuteson, F. A. Best, D.D. LaPorte, S. A. Ackerman, N.N. Ciganovich, R.G. Dedecker, T.P. Dirkx, S.D. Ellington, W.F. Feltz, R.A. Herbsleb, H.B. Howell, R.K. Garcia, J.F. Short, D.C. Tobin, P. van Delst, V.P. Walden, M. Werner, and H.M. Woolf, 1999: *UW High Spectral Resolution Emission Observations for Climate and Weather Research: Part I Airborne.* Conference on Atmospheric Radiation, 10th, Madison, WI, 28 June-2 July 1999. Boston, MA, American Meteorological Society.

5. Smith, W. L., A. Larar, D. Hinton, H.B. Howell, H.E. Revercomb, D.H. DeSlover, C.A. Sisko, D.C. Tobin, D. Cousins, D. Mooney, M. Gazarik, and S. Mango, 1999: *Remote Sensing at High Spectral Resolution.* Conference on Atmospheric Radiation, 10th, Madison, WI, 28 June-2 July 1999. Boston, MA, American Meteorological Society.

6. Sisko, C. A., H. E. Revercomb, D. C. Tobin, W. L. Smith, A. M. Larar, D. K. Zhou, D. H. DeSlover, B. Huang, and N. Nalli (1999): *NAST-I: High spectral resolution measurements from an across-track scanning infrared sounder and future implications for infrared sounders.* In Remote Sensing of Clouds and the Atmosphere, EOS/SPIE Symposium on Remote Sensing, Florence, Italy, 20-24 September. (http://its.ssec.wisc.edu/nast/papers/eos-spie.html)

Contact: robert.knuteson@ssec.wisc.edu

Last Updated: 27 October 1999

161

NAST-I: High spectral resolution measurements from a cross-track scanning infrared sounder and future implications for infrared sounders.

Christopher A. Sisko[a], William L. Smith[b], David C. Tobin[a], Daniel K. Zhou[b], Henry E. Revercomb[a], Daniel H. DeSlover[a], Allen L. Larar[b], Bormin Huang[a], Nicholas R. Nalli[a], and Paolo B. Antonelli[a]

[a]Cooperative Institute for Meteorological Satellite Studies, University of Wisconsin,
1225 West Dayton Street, Madison, WI , USA 53706
[b]NASA Langley Research Center, Hampton, VA, USA

The National Polar orbiting Operational Satellite System (NPOESS) Aircraft Sounder Testbed - Interferometer (NAST-I) is one of two airborne infrared sounder systems currently being used to evaluate future spaceborne advanced sounder designs. The NAST-I instrument is a cross-track scanning Fourier Transform Spectrometer (FTS) that measures the upwelling radiation in the infrared spectrum between 645-2700 1/cm (15.5 - 3.7 microns) at a high spectral resolution of 0.25 1/cm. Each observation has a spatial resolution of 2.6 km from NASA's ER-2 high-altitude aircraft, which operates 20 km above the surface. Measurements from this instrument in its first year of operation have not only contributed to risk reduction studies for future IR sounders but have also provided valuable datasets from three different climate regimes. The spatial coverage, 40 km swath width, has facilitated evaluation of non-linear retrieval algorithms using high spectral resolution information content and provided a means for further validation of infrared radiative transfer models. The capabilities of the NAST-I instrument have already been tested under varied field conditions such as tropical, mid-latitude summer, and mid-latitude winter regimes. Preliminary results from these field campaigns have demonstrated favorable sounding capability under such conditions, including intensive tropical cyclone environments (Hurricane Bonnie, August 1998 and Hurricane Georges, September 1998). In addition, repeated observations over the same geographic location near Andros Island in the Bahamas have provided additional information on the temporal change and spatial distribution of water vapor responding to complex mesoscale and large-scale dynamic processes. The framework for future spaceborne IR sounders will be well established by current and future observations made by the NAST-I instrument with its capability to remotely sense atmospheric state variables and cloud radiative properties.

Keywords: infrared sounder, retrieval, high-spectral resolution, infrared radiative transfer, atmospheric profiling

EOS/SPIE Symposium on Remote Sensing: 20-24 September 1999
University of Florence, Italy

Section: Remote Sensing of Clouds and the Atmosphere.
New Sensors and Data Processing.

Paper Number: 3867-20

Paper presented by: Christopher Sisko (UW-CIMSS)
21 September 1999

University of Wisconsin

FY99 Final Report

Engineering and Scientific Support for the National Polar-orbiting Operational Environmental Satellite System Airborne Sounder Testbed - Interferometer (NAST-I) Instrument

30 September 1999

Deliverables by Task:

Task 2

Specific recommendations made to LaRC for the operation of NAST-I (click here to view the recommendations)

Specific Recommendations for the Improvement of NAST-I Performance

through September 30, 1999

1. **Detector Nonlinearity**: Based on the analysis of the NAST-I data during CAMEX-III (Aug/Sept 1998), the University of Wisconsin recommended that the on-board hot blackbody set point temperature be changed from 330K to about 305K in order to reduce the importance of the detector nonlinearity on the calibrated spectra in the longwave and midwave bands. This was successfully implemented in time for WINTEX and subsequent experiments.

2. **Knowledge of Instrument View Angle**: Analysis of several of the NAST-I flights has shown an apparent offset in the instrument view angle, that is asymmetrical brightness temperatures are observed in a cross-track scan at wavelengths where the scene is expected to be uniform. The sounding retrieval is sensitive to this problem and the only way to correct for this currently is by assuming the offset angle is constant and making an estimate of the amount of the offset based on the cross-track temperature gradient. The specific recommendation in the operation of the NAST-I by LaRC is to identify the source of the angular offset in instrument view and either correct for it in the hardware or if not correctable then to fly an inclinometer sensor with the instrument to measure the instrument orientation independently of the aircraft pitch and roll.

3. **Vibration-induced Tilt Noise Reduction**: While the first series of NAST flights on the ER2 during 1998 (Wallops '98, CAMEX-III) demonstrated extremely good radiometric performance, they also demonstrated that the instrument noise performance was not dominated by detector noise alone (a design goal). The source of the extra noise contribution has been characterized and is referred to as vibration-induced tilt noise (VT noise), because it is caused by subtle wavefront tilts forced from aircraft vibrations (and to some degree from the detector cooler generated vibrations). The evaluation of this noise source, efforts to correct 1998 flight data to minimize its effects, and the definition of instrument modifications to reduce the extraneous noise were major UW tasks during this reporting period. A brief summary of the effort is enumerated below.
   --Identification of the source as amplitude modulation from variable wavefront tilts was accomplished by demonstrating the expected wavenumber correlation and dependence of the noise amplitude on the signal level and on the wavenumber squared.
   --Correction algorithms based on a mathematical model of the VT noise were developed and applied to the flight data. These correction algorithms have met with some success in reducing the effects of this noise source for many applications of existing data.
   --Hardware corrections to reduce the size of VT noise were investigated. The primary success to date has been related to recommendation #1 above, the reduction of the inflight hot blackbody temperature. Although mainly motivated by reducing the effect of detector non-linearities, it also substantially reduced the effect of the tilt errors by reducing the largest signals associated with calibrating atmospheric views. The other changes that were expected to reduce the noise by factors of 3-5 by reducing static tilts (bi-refringent replacement and matched clocking of beamsplitter/compensator wedges) have not been successful and require further investigation.

Contact: robert.knuteson@ssec.wisc.edu

Last Updated: 9 November 1999

University of Wisconsin

FY99 Final Report

Engineering and Scientific Support for the National Polar-orbiting Operational Environmental Satellite System Airborne Sounder Testbed - Interferometer (NAST-I) Instrument

30 September 1999

Deliverables by Task:

Task 3

Meteorological sounding products from selected datasets as directed by the LaRC NAST-I Principal Investigator
URL: http://its.ssec.wisc.edu/nast/retrieval/products/

165

NAST-I (NPOESS Aircraft Sounder Testbed-Interferometer)

High-spectral resolution Infrared Retrieval Algorithm Development

(joint University of Wisconsin / NASA Langley Center Project)

NAST-I Meteorological Sounding Products:

- **NAST-I sounding products derived from non-linear retrieval algorithm research development.**
- **All cases represented here were derived from: pre-CAMEX-III (Wallops-98), CAMEX-III, and WINTEX NAST-I field experiment datasets.**
- **All cases represented here do *not* include any radiosonde bias corrections.**
- **All cases generated using calibrated NAST-I spectra and noise datasets that are *not* final calibration datasets and available at the time.**
- **All retrievals presented here are derived from varying degrees of retrieval code development.**
- **Retrieval products derived from UW 40-level retrieval algorithm and NASA-LaRC (UW modified base code) 66-level retrieval algorithm.**
- **All products shown here are NOT allowed for use in any publications, meetings, or conferences without prior written consent from the NAST P.I. to the requesting agency.**

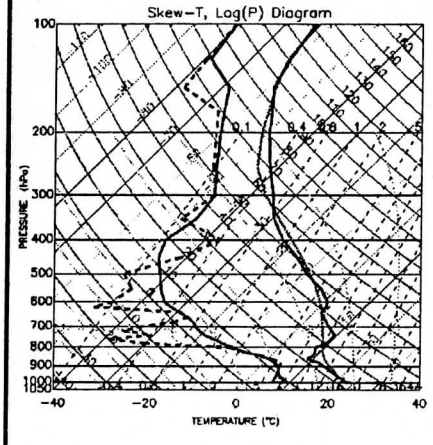

Date: July 11, 1998
Field Experiment: pre CAMEX-III (Wallops-98, AVIRIS mission)
Location: NASA/WFF

Description: First NAST-I retrieved temperature and water vapor profile from a single in-the-field preliminary calibrated radiance spectrum. NAST-I retrieved temperature (red) and retrieved water vapor (blue). Solid black is UW Vaisalla radiosonde temperature profile and dashed black is radiosonde water vapor profile (launched July 11, 1998)

Notes: Using USAF SkewT-Log P type thermodynamic diagram for sounding plot. Used pre-CAMEX-III (July-1998) in-the-field preliminary calibration spectrum and noise spectrum, and since superceded by other releases. Using 1st working version 40-Level (UW) physical retrieval algorithm (July-1998) and regression retrieval as 1st guess profile, and since has been superceded with other revisions.

166

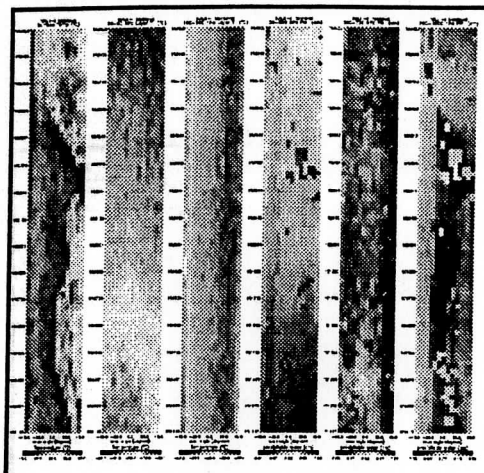

Date: July 11, 1998

Field Experiment: pre CAMEX-III (Wallops-98, AVIRIS mission)

Location: Virginia Coastline

Description: Mean layer NAST-I retrieved temperature (degrees C) and column precipitable water (cm) derived from NAST-I retrieved water vapor in the across-track and along-track direction over the Virgina coastline - top of image is southern-most direction and bottom is northern-most direction.

Notes: Used CAMEX-III (Sep-1998) preliminary calibration spectrum and noise spectrum, and since superceded by other releases. Using 2nd version of initial 40-Level (UW) physical retrieval algorithm (Sep-1998) and regression retrieval as 1st guess profile, and since has been superceded with other revisions.

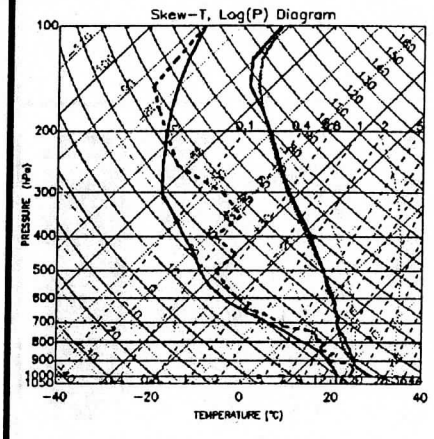

Date: September 13, 1998

Field Experiment: CAMEX-III (Andros Island Cal/Val Flight)

Location: Andros Island, Bahamas

Description: NAST-I retrieved temperature and water vapor profile from single in-the-field preliminary calibrated radiance spectrum. NAST-I retrieved temperature (red) and retrieved water vapor (blue). Solid black is UW Vaisalla radiosonde temperature profile and dashed black is radiosonde water vapor profile (launched September 13, 1998 from Andros Island)

Notes: Used CAMEX-III (Sep-1998) preliminary calibration spectrum and noise spectrum, and since superceded by other releases. Using 2nd version of initial 40-Level (UW) physical retrieval algorithm (Sep-1998) and regression retrieval as 1st guess profile, and since has been superceded with other revisions.

167

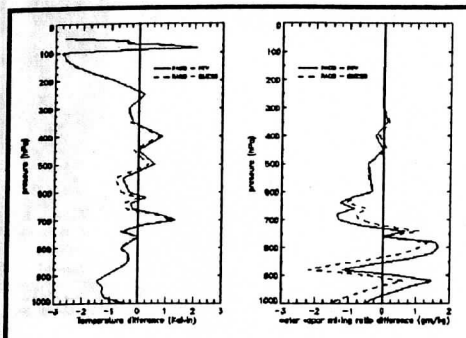

Date: September 13, 1998
Field Experiment: CAMEX-III (Andros Island Cal/Val Flight)
Location: Andros Island, Bahamas

Description: NAST-I retrieved temperature and water vapor profile from single in-the-field preliminary calibrated radiance spectrum and UW Vaisalla sonde differences between regression retrieval (listed as "guess") and physical retrieval (listed as "RTV"). UW Vaisalla radiosonde temperature and water vapor profile interpolated to 40 level retrieval pressure coordinate system for comparison (launched September 13, 1998).

Notes: Used CAMEX-III (Sep-1998) preliminary calibration spectrum and noise spectrum, and since superceded by other releases. Using 2nd version of initial 40-Level (UW) physical retrieval algorithm (Sep-1998) and regression retrieval as 1st guess profile, and since has been superceded with other revisions. Limitations: sonde launched over land and observation 26 km over marine boundary layer, and sonde package contamination also encountered.

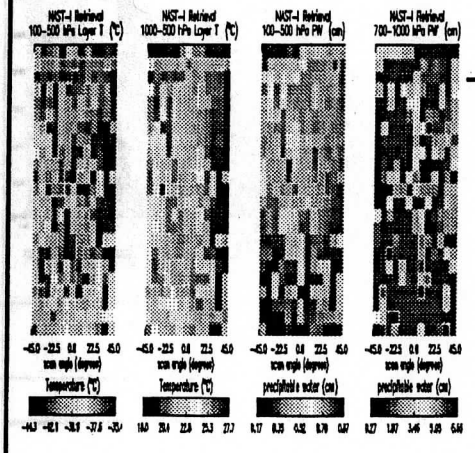

Date: September 14, 1998
Field Experiment: CAMEX-III (Andros Island)
Location: Andros Island, Bahamas (map)

Description: Mean layer NAST-I retrieved temperature (degrees C) and column precipitable water (cm) derived from NAST-I retrieved water vapor in the across-track and along-track direction. Retrievals performed using single observation NAST-I spectra - retrieval mesoscale sensitivity study.

Notes: Used post CAMEX-III (Dec-1998) preliminary calibration spectrum and noise spectrum, and since superceded by other releases. Using 3rd version of initial 40-Level (UW) physical retrieval algorithm (Dec-1998) and regression retrieval as 1st guess profile, and since has been superceded with other revisions.

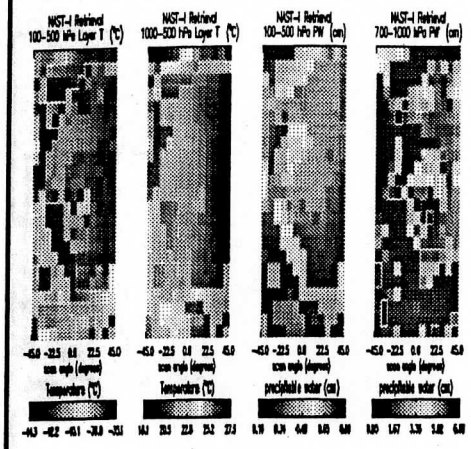

Date: September 14, 1998
Field Experiment: CAMEX-III (Andros Island)
Location: Andros Island, Bahamas (map)

Description: Mean layer NAST-I retrieved temperature (degrees C) and column precipitable water (cm) derived from NAST-I retrieved water vapor in the across-strack and along-track direction. Retrievals performed using 3x3 NAST-I averaged spectra (test-set for evaluation of 3x3 algorithm performance - algorithm test-set evaluation and retrieval performance.

Notes: Used post CAMEX-III (Dec-1998) preliminary calibration spectrum and noise spectrum, and since superceded by other releases. Using 3rd version of initial 40-Level (UW) physical retrieval algorithm (Dec-1998) and regression retrieval as 1st guess profile, and since has been superceded with other revisions.

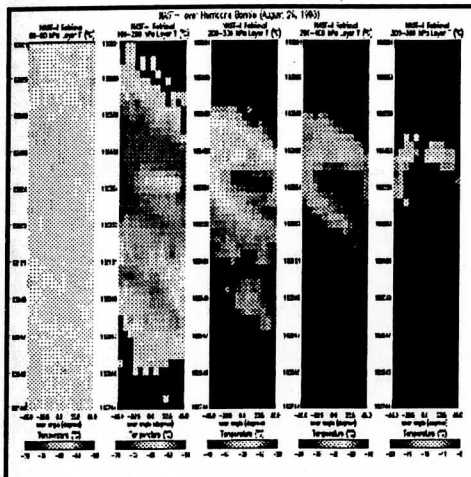

Date: August 26, 1998
Field Experiment: CAMEX-III (Hurricane Bonnie Landfall)
Location: North Carolina, USA

Description: Mean layer NAST-I retrieved temperature (degrees C) from NAST-I in the across-track and along-track direction. Sample of retrieval down to cloud top level using maximum departure from coincident sonde measurements - black indicates cloud level reached or exceeded.

Notes: Used CAMEX-III (Sep-1998) preliminary calibration spectrum and noise spectrum, and since superceded by other releases. Using 2nd version of initial 40-Level (UW) physical retrieval algorithm (Sep-1998) and regression retrieval as 1st guess profile, and since has been superceded with other revisions.

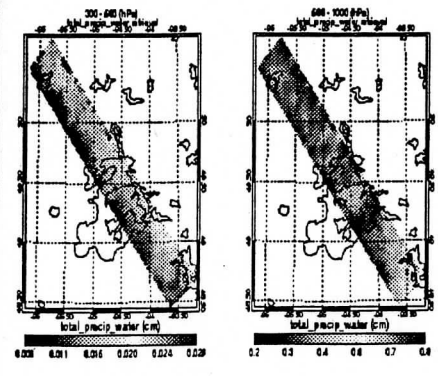

Date: March 26, 1999
Field Experiment: WINTEX (Madison, WI) NPOESS EDRs

Location: International Falls, MN / Southwest Ontario

Description: Column precipitable water (cm) derived from NAST-I retrieved water vapor in the across-strack and along-track direction. Retrievals performed using single spectra and observations navigated to Mercator map projection.

Notes: Used preliminary WINTEX (Mar-1999) preliminary calibration spectrum and noise spectrum. Using 4th version of initial 40-Level (UW) physical retrieval algorithm (Mar-1999) and regression retrieval as 1st guess profile.

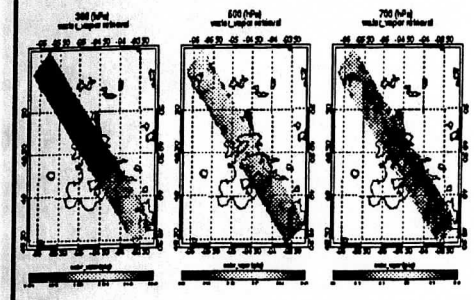

Date: March 26, 1999
Field Experiment: WINTEX (Madison, WI) NPOESS EDRs

Location: International Falls, MN / Southwest Ontario

Description: NAST-I retrieved water vapor (g/kg) in the across-strack and along-track direction. Retrievals performed using single spectra and observations navigated to Mercator map projection.

Notes: Used preliminary WINTEX (Mar-1999) preliminary calibration spectrum and noise spectrum. Using 4th version of initial 40-Level (UW) physical retrieval algorithm (Mar-1999) and regression retrieval as 1st guess profile.

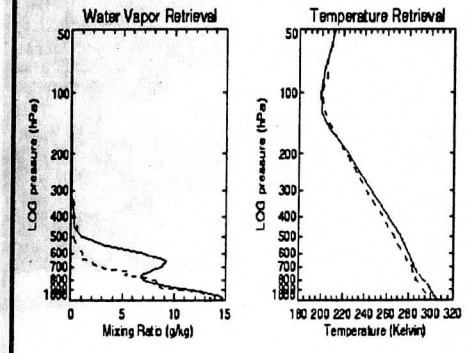

Date: March 30, 1999
Field Experiment: WINTEX (Madison, WI) NOAA-15 Validation Flight
Location: (Lake Michigan race-track pattern)

Description: Single NAST-I temperature and water vapor profile derived from in-the-field calibrated radiance spectrum and noise spectrum plotted against Vaisalla sonde temperature and water vapor profile. Solid line is NAST-I retrieval and dashed line is radiosonde profile.

Notes: Used preliminary WINTEX (Mar-1999) preliminary calibration spectrum and noise spectrum. Using 4th version of initial 40-Level (UW) physical retrieval algorithm (Mar-1999) and regression retrieval as 1st guess profile. Limitations: radiosonde launched over land while NAST-I observations and retrieval are taken over Lake Michigan during NOAA-15 underflight.

170

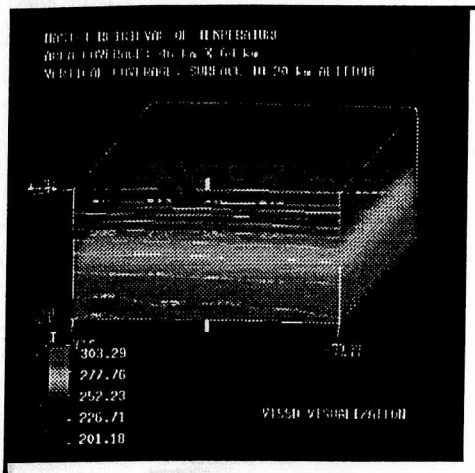

Date: September 13/14, 1999
Field Experiment: CAMEX-III (Andros Island Cal/Val Flight)
Location: Andros Island, Bahamas

Description: NAST-I retrieved temperature (Kelvin) 3-D volume derived from the NASA-LaRC (UW base code) - surface to ER-2 level.

Notes: Used CAMEX-III (May-1999) preliminary calibration spectrum and noise spectrum. Using NASA-LaRC 66-Level (UW base code) regression retrieval algorithm. Using VIS-5D version 5.0 for volume rendering of temperature

.

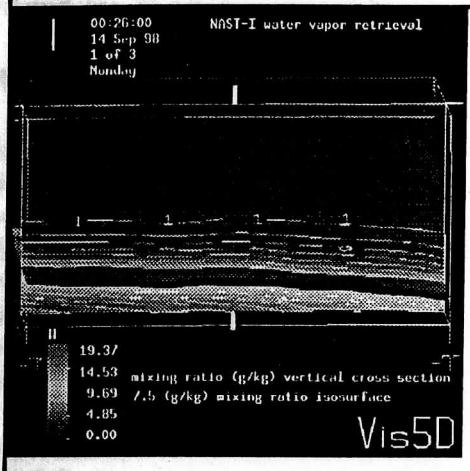

Date: September 13/14, 1999
Field Experiment: CAMEX-III (Andros Island Cal/Val Flight)
Location: Andros Island, Bahamas

Description: NAST-I retrieved water vapor mixing ratio (g/kg) cross-section across and water vapor iso-surface derived from the NASA-LaRC (UW base code) - surface to ER-2 level and across entire swath-width.

Notes: Used CAMEX-III (May-1999) preliminary calibration spectrum and noise spectrum. Using NASA-LaRC 66-Level (UW base code) regression retrieval algorithm. Using VIS-5D version 5.0 for rendering vertical cross-section and iso-surface.

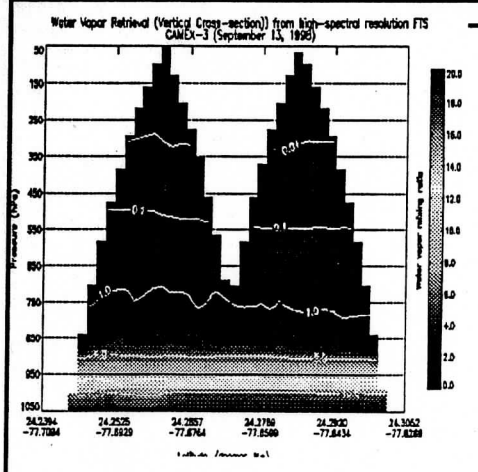

Date: September 13, 1999
Field Experiment: CAMEX-III (Andros Island Cal/Val Flight)
Location: Andros Island, Bahamas

Description: NAST-I retrieved water vapor (g/kg) vertical cross-section, NASA-LaRC (UW base code) 66-Level retrieval. Applied a 3-D irregular grid to regular grid mapping reconstruction method using 2 separate ER-2 passes near Andros Island.

Notes: Used CAMEX-III (May-1999) preliminary calibration spectrum and noise spectrum. Using NASA-LaRC 66-Level (UW base code) regression retrieval algorithm.

171

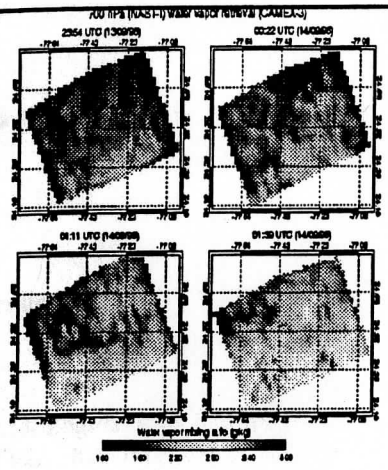

Date: September 13/14, 1999
Field Experiment: CAMEX-III (Andros Island Cal/Val Flight)
Location: Andros Island, Bahamas

Description: NAST-I retrieved water vapor (g/kg) horizontal slices derived from the NASA-LaRC (UW base code) 66-Level retrieval - 700 hPa pressure level. Applied a **4-D** irregular grid to regular grid mapping reconstruction using 4 separate ER-2 race-track patterns near Andros Island.

Notes: Used CAMEX-III (May-1999) preliminary calibration spectrum and noise spectrum. Using NASA-LaRC 66-Level (UW base code) regression retrieval algorithm.

Last update: 28-OCT-1999 (CAS)

Credits:

UW Retrieval programming specialist:	Christopher Sisko (UW-CIMSS)
UW 40-Level retrieval algorithm maintenance / development:	Christopher Sisko (UW-CIMSS)
NASA-LaRC 66-Level retrieval algorithm maintenance / development:	Dr. Daniel Zhou (NASA-LaRC)
UW 40-Level and NASA-LaRC 66-Level retrieval visual development:	Christopher Sisko (UW-CIMSS)
Initial non-linear retrieval algorithm design:	Dr. Jun Li (UW-CIMSS), and Dr. William Smith (NASA-LaRC)
NAST Principal Investigator:	Dr. William Smith (NASA-LaRC)
NAST Co-Investigator:	Dr. Henry Revercomb (UW-SSEC/CIMSS)
NAST-I 40-Level Fast Transmittance Code:	Hal Woolf (UW-CIMSS)
NAST-I 66-Level Fast Transmittance Code (IPO release):	Dr. Larrabee Strow (UMBC) and Scott Hannon (UMBC)

University of Wisconsin

FY99 Final Report

Engineering and Scientific Support for the National Polar-orbiting Operational Environmental Satellite System
Airborne Sounder Testbed - Interferometer (NAST-I) Instrument

30 September 1999

Deliverables by Task:

Task 3

Meteorological sounding products from selected datasets as directed by the LaRC NAST-I Principal Investigator
URL: http://its.ssec.wisc.edu/nast/retrieval/products/

173

NPOESS Aircraft Sounder Testbed-Interferometer (NAST-I)

P.I.: William L. Smith, NASA LaRC, 757-864-5914
bill.l.smith@larc.nasa.gov

This page will serve as the official link to the NAST-I data archival site.

Please contact the NAST PI if you encounter any problems with the use of these data. It is our desire to keep the entire NAST data user community fully informed regarding data characteristics including any abnormalities discovered through the use of these data. We therefore ask that each user who feels that they have discovered a characteristic which impacts the use of these data communicate this finding to the NAST PI for investigation. Important new information about NAST data characteristics will be communicated through the NAST web page.

General NAST Information

NAST-I Data

NAST-I Data Processing Information

NAST-I Data Readers:
Common NetCDF IDL GUI Reader (Chris Sisko: UW)

NAST-I Experiment Quicklink

NAST-I Talks and Papers

NAST-I Visualization Tools:
IDL (Chris Sisko: UW)
Matlab (Dave Tobin: UW)

Radiative Transfer Calculations (Bormin Huang: UW)
For comparisons against NAST-I data, see NAST-I Data Processing Information (above)

Dan DeSlover, Web Author
deslover@ssec.wisc.edu

NAST-I PI: William L. Smith
bill.l.smith@larc.nasa.gov

Significant contributions by Ben Howell, Bormin Huang, Hank Revercomb, Chris Sisko, and Dave Tobin.

174

http://danspc.larc.nasa.gov/NAST-data/index.html
This page was last updated 27 March 1999.

University of Wisconsin

FY99 Final Report

Engineering and Scientific Support for the National Polar-orbiting Operational Environmental Satellite System
Airborne Sounder Testbed - Interferometer (NAST-I) Instrument

30 September 1999

Deliverables by Task:

Task 4

Retrieval algorithm development summary
URL: http://its.ssec.wisc.edu/nast/retrieval/description/

176

NAST-I (NPOESS Aircraft Sounder Testbed-Interferometer)

High-spectral resolution Infrared Retrieval Algorithm Development

(joint University of Wisconsin / NASA Langley Center Project).

Non-linear Retrieval Algorithm Description:

The NAST-I non-linear retrieval algorithm uses a single NAST-I FOV brightness temperature spectra (referred henceforth as channel) and a regression first guess of atmospheric state, temperature and water vapor, to simultaneously determine an optimal solution for the surface skin temperature Ts, the atmospheric temperature profile T(p) and the atmospheric moisture profile q(p). When given any single NAST-I channel, the clear radiative transfer equation written in a linearized form as a variation from a first guess will take the following form:

$$(1)\ \delta T_b = W_{Ts}\,\delta T_s + \int_0^{p_s} W_T\,\delta T(p)\,dp + \int_0^{p_s} W_{\ln q}\,\delta \ln q(p)\,dp$$

where delta denotes the difference between the observation and calculation from the first guess state, Tb is the NAST-I brightness temperature, the delta quantities of Ts, Tp , and ln q(p) are unknown quantities of surface skin temperature, atmospheric temperature profile and water vapor mixing ratio profile (water vapor profile is expressed by the logarithm of the mixing ratio). W is the linear model of the NAST-I Radiative Transfer Equation (RTE) which is the derivative of brightness temperature with respect to the following variables (Ts, T(p), or ln q(p)).

A hybrid Newtonian iteration scheme initially developed by Levenberg and Marquardt that incorporates the inverse Hessian and steepest descent method for use in obtaining a solution of equation (1). The Levenberg-Marquardt approach is formulated as:

$$(2)\ X_{n+1} = X_n - [\nabla^2 J(X) + \gamma I]^{-1} \nabla J(X)$$

where X is the solution vector of Ts, T(p), and ln q(p), gama is a parameter used to control the rate of convergence (a key element in this unique approach), J(X) is a cost function to be minimized and n and n+1 are the previous and current iterative state. The cost function stated before takes the following form:

$$(3)\ J(X) = (X - X^0)^T C^{-1} (X - X^0) + [Y^m - Y(X)] E^{-1} [Y^m - Y(X)]$$

where X0 is the first guess of X, Ym is the vector of brightness temperature measurements, and Y(X) is the vector of brightness temperature calculated from the atmospheric state X. E is the NAST-I measurement error covariance matrix, C is the estimated first guess error covariance matrix, superscripts T and -1 represent matrix transpose and inverse. The parameter gama is adjusted in each iteration of equation (2). If the iteration converges, then decrease the gama value, otherwise increase the gama value. Finally, an optimal solution is obtainable through use of this non-linear iteration method. The resultant non-linear retrieval algorithm can use a high number of NAST-I observations that span important absorption regions such as CO2, H2O, and O3 to provide temperature profile information or concentration profile information.

Non-linear Retrieval Algorithm Approach Outline:

The following outline summarizes the development of the NAST-I retrieval algorithm and the components required

177

to complete this task. The outline below is the documented approach to meeting the objective of delivering a viable research retrieval algorithm.

Retrieval Training

- **Fast Transmittance Code (FTC)**
  - 40-Level FTC Model and transmittance coefficients (UW)
  - 66-Level FTC Model and transmittance coefficients (UMBC / IPO)
- **Atmospheric Profile Training Database**
  - Regional sonde database of temperature and water vapor
  - Climate ozone database used for Ozone regression
  - TIGR profile database
  - EOFs of temperature, water vapor, and ozone derived from sonde database
  - profile filtering / cloud detection
  - profile adjustment at cloud top level (experimental) for cloudy retrieval training
  - local zenith angle extensions, skin temperature uncertainty, and profile uncertainty adjustments
- **Optimal channel selection**
  - CO2, H2O (vapor), O3, and CO
- **Eigenvector Calculations**
  - clear sky spectrum derived from FTC models
  - variable zenith angle effects
  - clear + cloudy sky effects
  - least squares regression of eigenvectors versus temperature and water vapor

Pre-processing

- apodization of calibrated datasets (Kaisser-Bessel #6, Strong Beer apodization functions)
- read / write to native data ingestion format
  - noise spectrum
  - radiance spectrum
  - instrument and aircraft metadata
  - coincident sonde information
- radiosonde bias adjustment (optional)

Retrieval Algorithm (Physical and Regression)

- **Input options**
  - trace gas model (AFGL) usage
  - simulated noise spectrum or real noise spectrum plus noise factor
  - gamaT (temperature), gamaW(water vapor) or gamaTs(skin temperature)
  - channel region selection:
    - longwave infrared region only
    - longwave + midwave infrared region
    - longwave + midwave + shortwave infrared region
    - midwave + shortwave infrared region
  - bias correction or exclude bias correction
  - simulation or real datasets
  - regression or alternate profile fisrt guess (physical only)
  - comparison profile (performance tuning)
  - emissivity
  - single selection or multiple selection processing
- **internal processing**
  - optimal channel selection

178

- supplemental channel selection
- conditional noise selection
- conditional radiance selection
- topography / ecosystem determination (database)
- internal statistical accounting
- scan geometry correction - platform deviations from level flight mode
- cloud detection scheme (experimental)
- bias adjustment (optional)
- non-physical exclusion check sequences
- non fixed gama approach
- status log and error log reporting

- **Post-retrieval processing**
  - retrieval statistic output generation
  - unit conversion of atmospheric parameters
  - file output
    - detailed: all supplemental data included (netCDF)
    - non-detailed: retrievals only (netCDF or native)
- **Post-processing**
  - re-navigation based on peak weighting functions (optional)
  - irregular grid to regular grid transformation (optional)
    - triangulation surface reconstruction (implemented and best approach)
    - 2-D Krigging
    - thin-plate spline (MIN curve surface fitting)
- **Evaluation**
  - strict comparisons
  - single - multiple vertical sounding display
  - track surface display - utilizing any post-processing technique
  - vertical cross-section display - utilizing any post-processing technique
  - navigated display (various projections) - utilizing any post-processing technique
  - VIS-5D visualization or VIS-AD visualization and analysis tool

---

Last update: 29-OCT-1999 (CAS)

Credits:

UW Retrieval programming specialist:	Christopher Sisko (UW-CIMSS)
UW 40-Level retrieval algorithm maintenance / development:	Christopher Sisko (UW-CIMSS)
NASA-LaRC 66-Level retrieval algorithm maintenance / development:	Dr. Daniel Zhou (NASA-LaRC)
UW 40-Level and NASA-LaRC 66-Level retrieval visual development:	Christopher Sisko (UW-CIMSS)
Initial non-linear retrieval algorithm design:	Dr. Jun Li (UW-CIMSS), and Dr. William Smith (NASA-LaRC)
NAST Principal Investigator:	Dr. William Smith (NASA-LaRC)
NAST Co-Investigator:	Dr. Henry Revercomb (UW-SSEC/CIMSS)
NAST-I 40-Level Fast Transmittance Code:	Hal Woolf (UW-CIMSS)
NAST-I 66-Level Fast Transmittance Code (IPO release):	Dr. Larrabee Strow (UMBC) and Scott Hannon (UMBC)

University of Wisconsin

FY99 Final Report

Engineering and Scientific Support for the National Polar-orbiting Operational Environmental Satellite System
Airborne Sounder Testbed - Interferometer (NAST-I) Instrument

30 September 1999

Deliverables by Task:

Task 4

Retrieval algorithm delivery schedule
URL: http://its.ssec.wisc.edu/nast/retrieval/delivery/
NOTE -- delivery made to NASA-LaRC as per P.I. request, future / ongoing work declared. No general public release of retrieval code allowed, only delivery to NASA-LaRC permitted.

180

NAST-I (NPOESS Aircraft Sounder Testbed-Interferometer)

High-spectral resolution Infrared Retrieval Algorithm Development

(joint University of Wisconsin / NASA Langley Center Project).

Initial Retrieval Deliverables requested by NAST-LaRC P.I.)

1. Fortran 77 source code (retrieval)
2. retrieval-related databases and coefficient databases
3. Fortran 77 source and IDL source for retrieval utilities
4. IDL Graphical User Interface (GUI) visualization source
5. special request development source
6. user support
7. training set profiles for past and future deployment schedules

Initial NAST Retrieval Beta Code Delivery (40-Level Release) - direct delivery to NASA-LaRC only

- **40-Level transmittance coefficient database**
  - 1st version of transmittance coefficient database (delivered June 1998)
  - 2nd version of transmittance coefficient database (delivered January 1999)
  - future versions of transmittance coefficient database (future delivery as necessary)
- **40-Level NAST-I Fast model** (delivered June 1998, update January 1999)
- **Ozone database and ozone regression algorithm**
  - 1st release ozone database and ozone regression (delivered June 1998)
  - updates to ozone database (delivery on continuous basis as needed)
- **Regional temperature and water vapor profile information**
  - source for profiles
    - read / write utilities (delivered June 1998)
    - conversion utilities (delivered June 1998)
    - profile check sequence routine (delivered June 1998, updates March/May 1999)
    - clear + cloudy profile check sequence and adjustment routines (delivered May 1999)
  - Wallops-98 / CAMEX-3 training profiles (delivered July 1998)
  - WINTEX training profiles (delivered March 1999)
  - CAMEX-3 area extended tropical training profiles (delivered Sep 1999)
- **Training dataset applications**
  - temperature, water vapor, and ozone optimal channel selection (delivered June 1998)
  - temperature, water vapor and ozone EOF routines (delivered June 1998)
  - NAST-I spectral eigenvector routines (delivered June 1998)
  - NAST-I regression coefficient generation routines (delivered June 1998)
- **Retrieval applications**
  - eigenvector regression applications (delivered June 1998)
  - bias correction routines (delivered June 1998)
  - internal read / write routines (delivered June 1998)
  - noise spectrum ingestion routines - real and simulated (delivered June 1998)
  - physical retrieval (delivered June 1998)
  - planck function routines (delivered June 1998, revised versions delivered January 1999)
  - water vapor conversion routines (delivered June 1998)
- **Retrieval-related utilities**

- calibrated dataset read / write utilities (netCDF) (delivered January 1999)
- calibrated dataset read (netCDF) to binary direct retrieval format converters (delivered June 1998, update release May 1999)
- calibrated dataset extraction routines (delivered January 1999)
- calibrated dataset apodization routines (netCDF to netCDF) (delivered May 1999)
- calibrated dataset Graphical User Interface (GUI) visualization routine (delivered May 1999)
- common netCDF Graphical User Interface (GUI) read utility (delivered May 1999)
- radiance level track image display quicklook generators (delivered May 1999)
- user requested 66-Level retrieval display
  - horizontal retrieval image color display (delivered May 1999)
  - navigated retrieval image display with pressure coordinate adjustment (delivered May 1999)
  - vertical retrieval cross-section display (delivered May 1999)
- NAST flight track mapping routine (delivered May 1999)

Future Retrieval Code Development

Purpose: Provide a *new* retrieval design specification that will focus on evolution of a retrieval algorithm that is independent of the instrument specifications. In turn, the demanding nature of scanning geometry sounders requires a modular design concept that will facilitate combined use of other instrument co-located data (Lidar, Microwave, ground-based, etc) within the retrieval algorithm process.

Design considerations:

- High-level program language considerations
  - migrate Fortran 77 retrieval code to Fortran 90, advantages: <-- Current work
    - enhanced operation features
    - modular design capabilities
    - variable derived typing (structure usage)
    - dynamic array allocation
    - simplified matrix manipulation
    - pointers and overloaded operations permitted
    - simplified access to netCDF
    - improved optimization
  - retrieval code development in C++, advantages: <-- Future work
    - object orientated
    - data encapsulation
    - improved optimization
- Visual retrieval interface (see below for prototype description)
  - JAVA driven visual interface (interface front-end to the retrieval)
    - direct radiance to retrieval interaction
    - direct tolerance interaction
    - first guess visual profile adjustment
    - band, channel re-adjustments
    - automatic and manual scaling and zoom capability
- Multi-instrument usage (Synergistic datasets) such as microwave, imager, lidar, radar, etc
  - supplemental retrieval information
  - direct retrieval information
- Revision control enforcement
  - provide multi-stage development tracking

Completed development:

JAVA interface Prototype:

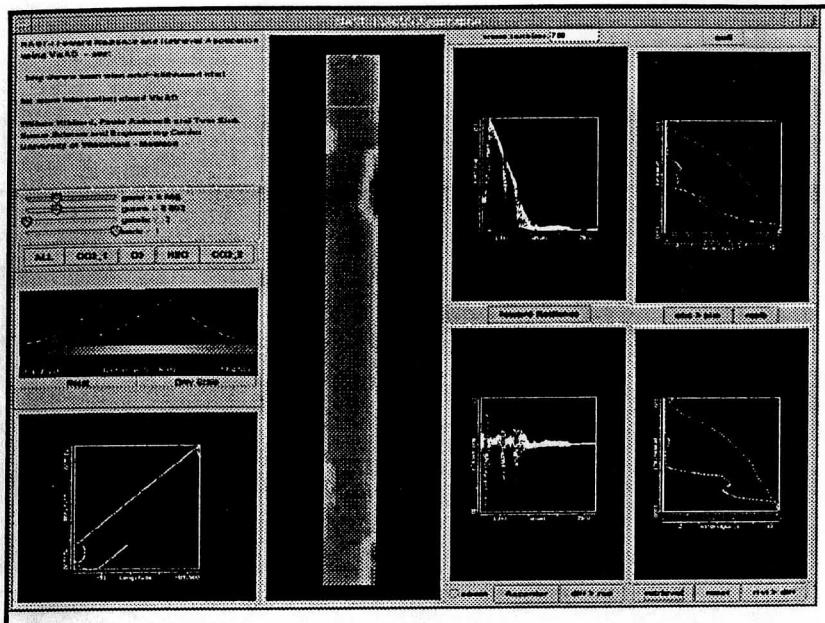

NAST-I VIS-AD JAVA prototype retrieval interface

Description: JAVA VIS-AD interface front-end for the NASTI retrieval

Features:

- access to NAST calibrated datasets
  - bandpass imagery
  - flight track information
- forward model / retrieval / calibrated data / linkage
  - NAST observed spectrum display
  - forward model / calibrated spectrum residuals
  - input interaction controls
    - input profile sensitivity adjustments (first guess)
    - gamaT, gamaW, gamaTs tolerance selection
    - manual atmospheric constituent overrides
  - retrieval output profile display
  - mouse interactive scaling and zoom capability on all panels
- Compatibility (Fortran 77 initial retrieval algorithm), will alter to latest versions

Future Direction: Implement latest stable version of retrieval code with future design features included and allow for inclusion of multi-instrument external dataset (synergistic approach)

Multi-instrument incorporation (synergistic approach):

183

Description: Merge external instrument datasets into the retrieval algorithm to provide improved performance with direct or in-direct measurement information. Sample depicted here is MAS high-spatial imager data and MASK cloud mask information co-located within the NAST-I Field-of-View (FOV).

Features:

- high-spatial visible and infrared information (broad-band)
  - mean and standard deviation of radiances within NASTI FOV
- reliable cloud detection scheme within the NASTI FOV
  - cloud detection confidence indicators
  - thin cirrus detection schemes
  - 1km ecosystem and topography information (North America only)
  - group and individual test error indicators
  - spatial texture cloud group tests
  - aerosol detection
  - sun glint, and snow / ice flags

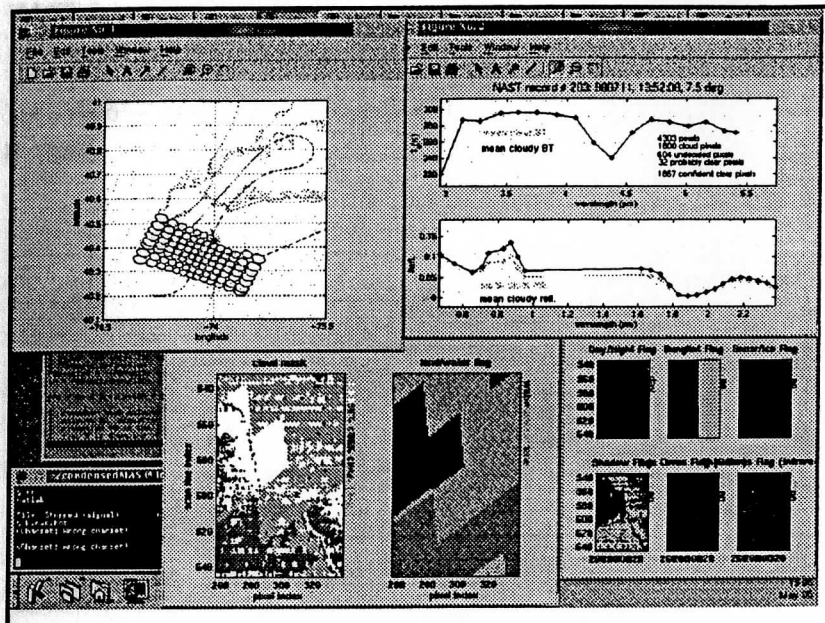

NAST-I / MAS Combined Product

Synergistic Uses:

- cloud detection
  - clear sky retrieval decision
  - clear sky retrieval to cloud top level decision
  - cloud cleared retrieval decision
- cloud clearing
  - use imager to derive cloud clearing parameters
  - apply imager cloud clearing parameters to sounder spectrum
  - use cloud cleared spectrum in retrieval

Last update: 29-OCT-1999 (CAS)

Credits:

UW Retrieval programming specialist:	Christopher Sisko (UW-CIMSS)
UW 40-Level retrieval algorithm maintenance / development:	Christopher Sisko (UW-CIMSS)
NASA-LaRC 66-Level retrieval algorithm maintenance / development:	Dr. Daniel Zhou (NASA-LaRC)
UW 40-Level and NASA-LaRC 66-Level retrieval visual development:	Christopher Sisko (UW-CIMSS)
Initial non-linear retrieval algorithm design:	Dr. Jun Li (UW-CIMSS), and Dr. William Smith (NASA-LaRC)
VIS-AD JAVA Development team	Bill Hibbard, Tom Rink, and Paolo Antonelli (UW-SSEC/CIMSS)
MAS/NAST Combined product development:	Dave Tobin (UW-SSEC/CIMSS)
MAS Cloud mask development:	Steve Ackerman, Rich Frey, and Liam Gumley (UW-SSEC/CIMSS)
NAST Principal Investigator:	Dr. William Smith (NASA-LaRC)
NAST Co-Investigator:	Dr. Henry Revercomb (UW-SSEC/CIMSS)
NAST-I 40-Level Fast Transmittance Code:	Hal Woolf (UW-CIMSS)
NAST-I 66-Level Fast Transmittance Code (IPO release):	Dr. Larrabee Strow (UMBC) and Scott Hannon (UMBC)

University of Wisconsin

FY99 Final Report

Engineering and Scientific Support for the National Polar-orbiting Operational Environmental Satellite System Airborne Sounder Testbed - Interferometer (NAST-I) Instrument

30 September 1999

Deliverables by Task:

Task 4

Accurate 3-D representation of NAST-I derived atmospheric parameters
URL: http://its.ssec.wisc.edu/nast/retrieval/3-D/

186

NAST-I (NPOESS Aircraft Sounder Testbed-Interferometer)

High-spectral resolution Infrared Retrieval Algorithm Development

(joint University of Wisconsin / NASA Langley Center Project)

Accurate 3-D representation of NAST-I derived atmospheric parameters:

Presented here is the current approach (#3, in below table) used to accurately represent 3-D distributions of temperature, water vapor, and ozone profiles derived from the NAST-I non-linear retrieval algorithm.

CURRENT REPRESENTATION and POSSIBLE SOLUTION EXAMPLES:

Current 2-D representation:

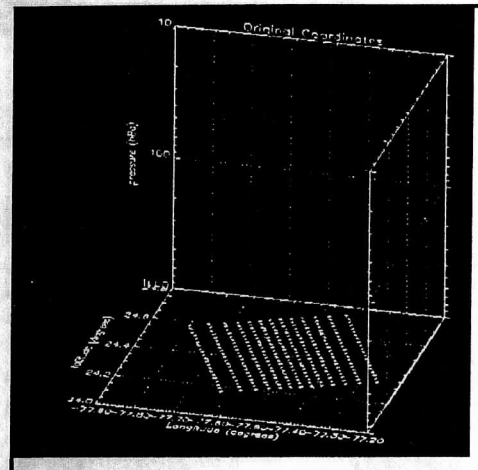

2-D FOV coordinate information (provided in the calibrated dataset)

~~(1) ORIGINAL 2-D Coordinate Representation- No~~ **Coordinate Adjustment**

Description: 3-D Plot depicting NAST-I FOV observation latitude and longitude coordinates projected onto the surface.

- roll effects included.
- represents the navigation information provided within the calibrated dataset
- swath width coverage at surface represented corrected, no other level coordinate information available.
- only channels where max weighting functions peak at surface are accurately represented.

Notes: Coordinates provided in the final calibration data file is the 2-D surface projected. This plot represents the minimum amount of recoverable information.

3-D variant representation:

187

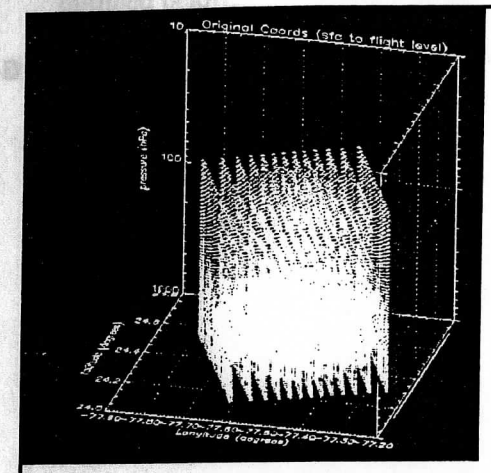

3-D FOV coordinate information (sfc to flight level)
(replicated from provided surface coordinates)

(2) ORIGINAL 3-D Coordinate "surface to flight level extrapolation" No Coordinate Adjustment

Description: 3-D Plot depicting NAST-I FOV observation latitude and longitude coordinates projected from the surface to the flight level of the instrument platform (ER-2).

- roll effects included.
- swath width coverage at surface represented correctly
- swath width coverage at other levels is incorrectly represented.
- all channels with peak weighting functions through the depth of the atmosphere are accurately represented.

Notes: This type of representation is only used when deriving along-track and along-track flat horizontal imagery or vertical profile information in which actual geo-location of the data is unnecessary.

3-D variant representation *(with coordinate adjustments)*:

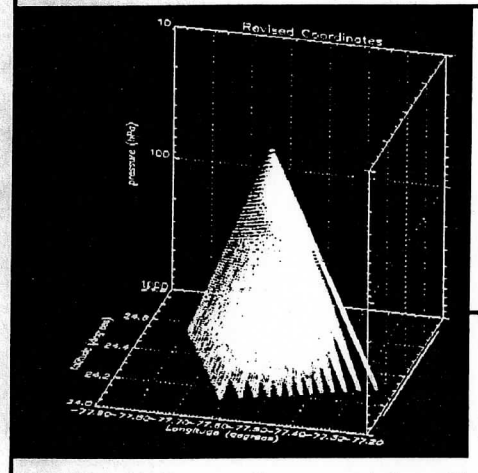

3-D FOV coordinate adjustment (sfc to flight level)
(derived from surface coordinates and pressure levels)

(3) CORRECT 3-D Representation (sfc to flight level) Coordinate Adjustment

Description: 3-D Plot depicting NAST-I FOV observation latitude and longitude coordinates projected from the surface to the flight level of the instrument platform (ER-2) with latitude and longitude coordinates computed at each level of the retrieval - either 40 level (UW) or 66 level (IPO).

- roll effects included.
- swath width coverage at surface represented correctly
- swath width coverage at other levels is correctly represented.
- all channels with peak weighting functions through the depth of the atmosphere are accurately represented.

Notes: accurate depicts the level and location of the measurement. Used as means of depicting either A) horizontal retrieval slices on a map projection, B) vertical cross-sections, or C) 3-D atmospheric parameter volume rendering.
Method discussed below as ACCURATE 3-D ATMOSPHERIC PARAMETER REPRESENTATION APPROACH.

ACCURATE 3-D ATMOSPHERIC PARAMETER REPRESENTATION APPROACH:

Summary of CORRECT 3-D Representation (#3) Approach:

Our approach in representing accurate coordinate information derived from the non-linear retrieval or the measured radiance observations is outlined below:

1. obtain the latitude / longitude coordinates from the on-board NAST-I GPS receiver
2. compute the surface latitude / longitude positions for each observation as a function of view angle and platform flight characteristics (roll, pitch, yaw, etc.)
3. using the surface based latitude / longitude coordinates (which are dimensioned by time); recompile new coordinates at individual pressure levels (expansion to dimensions of time, levels) - using the algorithm

outlined below:

2-D to 3-D Coordinate Expansion Algorithm:

Equation (1) $$\kappa = \frac{L_o - L_{sa}}{\ln\left(\frac{p_{k0}}{p_o}\right)}$$

Equation (2) $$L_a = L_{sa} + \kappa \ln\left(\frac{p_k}{p_0}\right)$$

Variable Description

$L_0 \equiv$ nadir latitude / longitude coordinate position

$L_{sa} \equiv$ nadir latitude / longitude coordinate position at a fixed angle from platform to su

$p_k \equiv$ pressure at some level $_k$ above the surface to platform level

$p_{k0} \equiv$ pressure at uppermost platform flight level

$p_o \equiv$ surface pressure $(p_k \neq p_0)$

$L_a \equiv$ derived latitude / longitude coordinate position at p_k

---

SOURCE:

2-D to 3-D Coordinate Expansion Algorithm Source:

Language type: IDL (Interactive Data Language, RSI)
Platform dependency: None

Online documentation: help info
Sources: nasti_coord_adjustment.pro

EXAMPLES:

Application of the 2-D to 3-D Coordinate Expansion Algorithm to Retrievals:

Vertical cross-section example with a 3-D coordinate algorithm expansion applied to the retrieval data

189

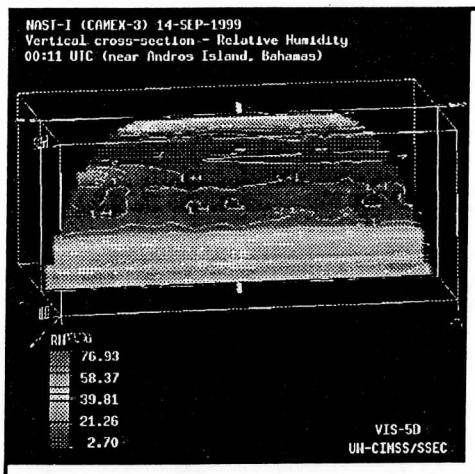

Date: September 13, 1999
Field Experiment: CAMEX-III (Andros Island Cal/Val Flight)
Location: Andros Island, Bahamas

Description: NAST-I retrieved water vapor, depicted as relative humidity (%), vertical cross-section (vertical color slice and contour), NASA-LaRC (UW base code) 66-Level retrieval. Applied a **3-D** irregular grid to regular grid mapping reconstruction (transforming the 2-D supplied coordinates into 3-D representative coordinates) method using 2 separate ER-2 passes near Andros Island.

Notes: Used CAMEX-III (May-1999) preliminary calibration spectrum and noise spectrum. Using NASA-LaRC 66-Level (UW base code) regression retrieval algorithm. Using the CORRECT 3-D representation (#3) approach.
Visualization completed using VIS5D, version 5.0 (UW).

Vertical cross-section example with a 3-D coordinate algorithm expansion applied to the retrieval data

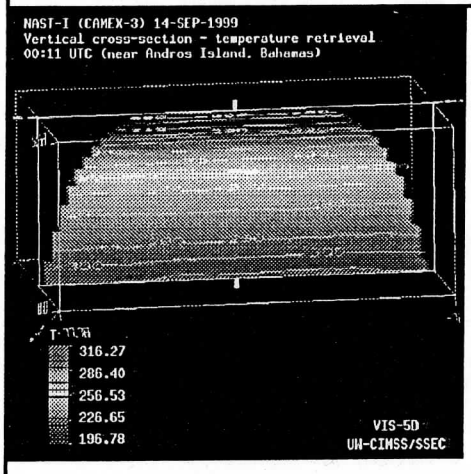

Date: September 14, 1999
Field Experiment: CAMEX-III (Andros Island Cal/Val Flight)
Location: Andros Island, Bahamas

Description: NAST-I retrieved temperature (Kelvin) vertical cross-section (vertical color slice and contour), NASA-LaRC (UW base code) 66-Level retrieval. Applied a **3-D** irregular grid to regular grid mapping reconstruction (transforming the 2-D supplied coordinates into 3-D representative coordinates) method using 2 separate ER-2 passes near Andros Island.

Notes: Used CAMEX-III (May-1999) preliminary calibration spectrum and noise spectrum. Using NASA-LaRC 66-Level (UW base code) regression retrieval algorithm. Using the CORRECT 3-D representation (#3) approach.
Visualization completed using VIS5D, version 5.0 (UW).

Vertical cross-section example with a 3-D coordinate algorithm expansion applied to the retrieval data

190

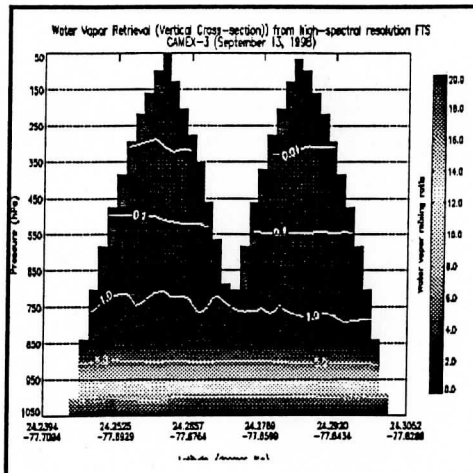

Date: September 13, 1999
Field Experiment: CAMEX-III (Andros Island Cal/Val Flight)
Location: Andros Island, Bahamas

Description: NAST-I retrieved water vapor (g/kg) vertical cross-section, NASA-LaRC (UW base code) 66-Level retrieval. Applied a **3-D** irregular grid to regular grid mapping reconstruction (transforming the 2-D supplied coordinates into 3-D representative coordinates) method using 2 separate ER-2 passes near Andros Island.

Notes: Used CAMEX-III (May-1999) preliminary calibration spectrum and noise spectrum. Using NASA-LaRC 66-Level (UW base code) regression retrieval algorithm. Using the CORRECT 3-D representation (#3) approach.
IDL developed vertical cross-section code (UW).

Vertical cross-section example with a 3-D coordinate algorithm expansion applied to the retrieval data in 4-D:

The four panels depicted below are retrieved water vapor derived from the NASA-LaRC 66-Level (UW base code) taken during the 1998 CAMEX-3 field experiment (Sep 13/14, 1998). During this time, the ER-2 completed four ~~circuits (4 race track patterns) off the coast of Andros Island, Bahamas. The reconstructed~~ retrieval images provided below as examples were generated in the following manner (brief outline):

- each grid includes 2 swath width passes of a NW to SE run, and a parallel SE to NW run (depicted nicely in the 200 hPa panel).
- extraction process of relevant observations along flight track (i.e. roll exclusion, etc)
- for the entire 66 levels, new latitude / longitude coordinates were generated for each level using the CORRECT 3-D representation (#3) approach.
- a transformation from irregular grid spacing to regular grid spacing using a Delaunay triangulation of a planar set of points:
  - for each level, surfaces constructed via connections made between closest observations were implemented
  - regular grid interval spacing chosen, and each grid point is assigned a value off the reconstructed surface
  - locations outside of the measurement area but within the regular grid area are treated as data void areas
  - impact is that interpolation is based on the nearest sets of observation points, so the scale variations are preserved.

Notes: Used CAMEX-III (May-1999) preliminary calibration spectrum and noise spectrum. Using NASA-LaRC 66-Level (UW base code) regression retrieval algorithm. Using the CORRECT 3-D representation (#3) approach.

Mean grid times:	**panel 1** 23:54 UTC 13-Sep-1999 (upper left) **panel 2** 00:22 UTC 14-Sep-1999 (upper right) **panel 3** 01:11 UTC 14-Sep-1999 (lower left) **panel 4** 01:39 UTC 14-Sep-1999 (lower right)

4-D NAST-I Simulated Retrieval Reconstruction:

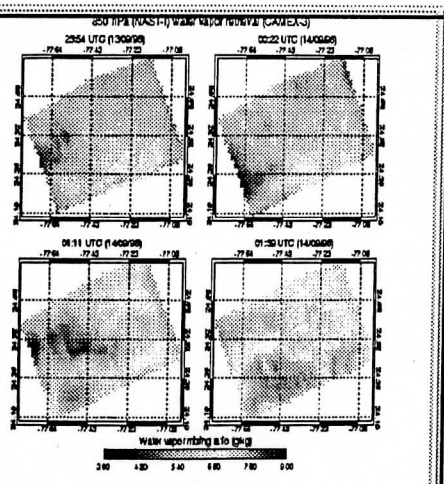

850 hPa Level
(4 reconstructed time periods)

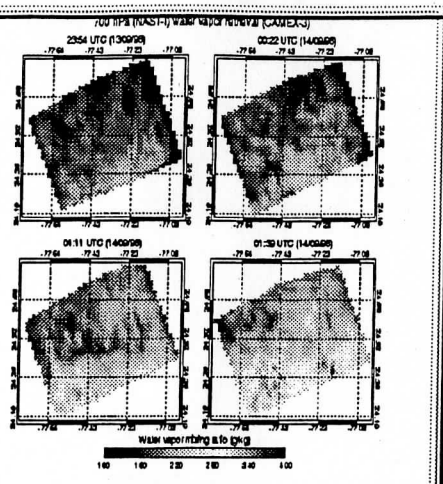

700 hPa Level
(4 reconstructed time periods)

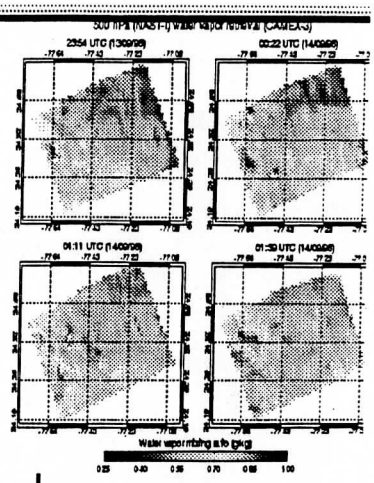

500 hPa Level
(4 reconstructed time periods)

Last update: 03-NOV-1999 (CAS)

Credits:

UW Retrieval programming specialist:	Christopher Sisko (UW-CIMSS)
UW 40-Level retrieval algorithm maintenance / development:	Christopher Sisko (UW-CIMSS)
NASA-LaRC 66-Level retrieval algorithm maintenance / development:	Dr. Daniel Zhou (NASA-LaRC)
UW 40-Level and NASA-LaRC 66-Level retrieval visual development:	Christopher Sisko (UW-CIMSS)
Initial non-linear retrieval algorithm design:	Dr. Jun Li (UW-CIMSS), and Dr. William Smith (NASA-LaRC)
NAST Principal Investigator:	Dr. William Smith (NASA-LaRC)
NAST Co-Investigator:	Dr. Henry Revercomb (UW-SSEC/CIMSS)
NAST-I 40-Level Fast Transmittance Code:	Hal Woolf (UW-CIMSS)
NAST-I 66-Level Fast Transmittance Code (IPO release):	Dr. Larrabee Strow (UMBC) and Scott Hannon (UMBC)